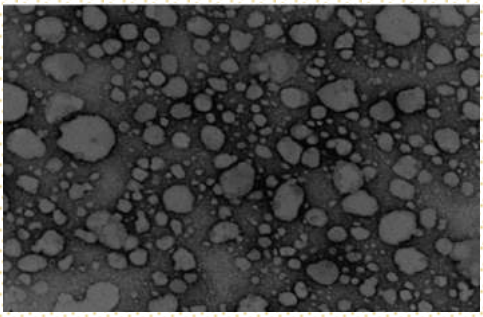

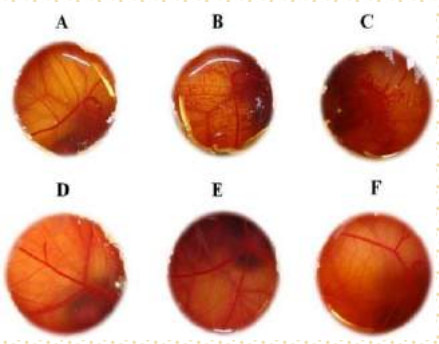

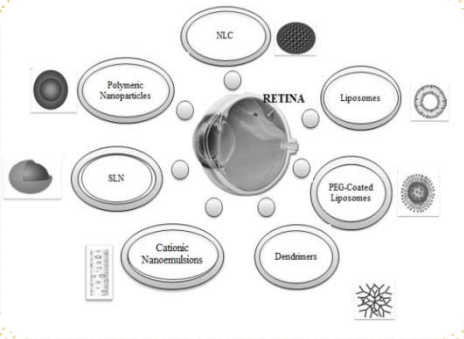

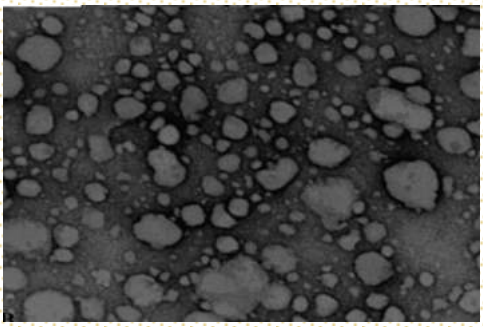

Joana Filipa Peixoto Fangueiro

CATIONIC LIPID NANOMEDICINES FOR THE TREATMENT OF DIABETIC RETINOPATHY

Tese de doutoramento em Ciências Farmacêuticas, na Especialidade de Tecnologia Farmacêutica, orientada pela Senhora Professora Doutora Eliana Maria Barbosa Souto e pela Senhora Professora Doutora Amélia Maria Lopes Dias da Silva e apresentada à Faculdade de Farmácia da Universidade de Coimbra

2015

· U C ·

Cationic lipid nanomedicines for the treatment of diabetic retinopathy

Faculdade de Farmácia da Universidade de Coimbra

Joana Filipa Peixoto Fangueiro

2015

Doctoral thesis submitted to the Pharmacy Faculty of University of Coimbra, in fulfillment of the requirements for the degree of Doctor of Philosophy in Pharmacy, specializing in Pharmaceutical Technology.

Tese de Doutoramento para obtenção do grau de Doutor em Ciências Farmacêuticas, especialidade de Tecnologia Farmacêutica e apresentada à Faculdade de Farmácia da Universidade de Coimbra.

The work presented in this thesis has been developed at the Department of Pharmaceutical Technology, Faculty of Pharmacy, University of Coimbra (Portugal), at the University Fernando Pessoa, at the Department of Biology and Environment of the University of Trás-os-Montes e Alto-Douro (UTAD) and at the Department of Physical Chemistry of the University of Barcelona, and has been granted by the *Fundação para a Ciência e Tecnologia* (FCT, Lisboa, Portugal), as individual PhD fellowship under the reference SFRH/BD/80335/2011.

O trabalho apresentado nesta tese foi desenvolvido no Laboratório de Tecnologia Farmacêutica da Faculdade de Farmácia da Universidade de Coimbra (Portugal), na Universidade Fernando Pessoa, no Departamento de Biologia e Ambiente da Trás-os-Montes e Alto-Douro (UTAD) e no Departamento de Física e Química da Universidade de Barcelona e suportado financeiramente pela Fundação para a Ciência e Tecnologia (FCT, Lisboa, Portugal), pela bolsa individual de doutoramento com a referência SFRH/BD/80335/2011.

According to the provisions of No. 2 of Art.8 of Decree-Law No. 388/70, the results of scientific publications and literature reviews have been used to write the present thesis. In compliance with the Decree-Law, the author of this work declares to be a major player in the design and implementation of experimental work, in interpreting the results and writing of the manuscripts published under the name of **Joana F. Fangueiro**:

[1] Eliana B. Souto, **Joana F. Fangueiro**, Rainer H. Müller, "Solid Lipid Nanoparticles (SLN^{TM})", in "Fundamentals of Pharmaceutical Nanoscience" from Springer, by Ijeoma Uchegbu, Andreas Schatzlein, Woei Ping Cheng, Aikaterini Lalatsa (Eds), Chapter 5, 91-116, 2014 (http://link.springer.com/book/10.1007%2F978-1-4614-9164-4)

[2] **Joana F. Fangueiro**, Alexander Parra, Amélia M. Silva, Eliana B. Souto, Maria L. Garcia and Ana C. Calpena, Validation of a high performance liquid chromatography method for the stabilization of epigallocatechin gallate, International Journal of Pharmaceutics (2014) 475 (1-2): 181-190.

[3] **Joana F. Fangueiro**, Tatiana Andreani, Lisete Fernandes, Maria L. Garcia, Maria A. Egea, Amélia M. Silva, Eliana B. Souto, Physicochemical characterization of epigallocatechin gallate lipid nanoparticles (EGCG-LNs) for ocular instillation, Colloids and Surface B: Biointerfaces (2014) 123: 452-460.

[4] **Joana F. Fangueiro**, Tatiana Andreani, Maria A. Egea, Maria L. Garcia, Selma B. Souto, Amélia M. Silva, Eliana B. Souto. Design of cationic lipid nanoparticles for ocular delivery: development, characterization and cytotoxicity, International Journal of Pharmaceutics (2014) 461(1-2): 64-73.

[5] **Joana F. Fangueiro**, Amélia M. Silva, Maria L. Garcia, Eliana B. Souto. Current nanotechnology approaches for the treatment and management of diabetic retinopathy, European Journal of Pharmaceutics and Biopharmaceutics (2015) 95: 307–322.

Dedicatory

"As coisas vulgares que há na vida
Não deixam saudades
Só as lembranças que doem
Ou fazem sorrir

Há gente que fica na história
da história da gente
e outras de quem nem o nome
lembramos ouvir

São emoções que dão vida
à saudade que trago
Aquelas que tive contigo
e acabei por perder

Há dias que marcam a alma
e a vida da gente
e aquele em que tu me deixaste
não posso esquecer"

Mariza, in "A Chuva"

To my dearest daddy, thank you for all the support you have given me and for always telling me that family is the most important thing that we have. If I am a force of the nature, it is because you have taught me so. Eternal miss you.

Acknowledgments

Throughout this five-years journey, I faced periods of many emotions as encompassing joy and happiness, but also periods of grief, despair and uncertainty. Thus, I reserve this page to thank all the people with whom I shared emotions, and who helped me to overcome the many difficulties I encountered during my academic career to pursue this Doctoral Degree.

Firstly, I would like to thank my family all the support and persistence they always provided me throughout my life, to pursue my dreams and my ambitions. Without the support of my parents, husband and brother, none of this dream would be possible. Thank you for being my pillar when I needed, for all the patience, and for understanding the entire time away from you. In particular, to my Father, thank you for always believed me, and had always been the first to encourage and to captivate my goals.

Not less important, I would like to thank my advisor Prof. Dr[a]. Eliana Souto for all the help provided during my academic career. Thanks for your dedication, professionalism and above all, the friendship that always welcomed me. I have a great admiration and friendship for you. All your experience, constructive criticism and all availability have made everything more easily. To you, I owe much of my professional training and personal motivation for joining the PhD.

I would like to my express my gratitude to my friend and confident during this journey, Tatiana Andreani. Thank you for everything, for your friendship and love, and for hearing me countless hours during these five years. All your help and scientific discussion assisted the development of this project and many publications associated with it.

I would like to thank to Prof. Dr[a]. Amelia Silva, from University of Trás -os- Montes and Alto Douro (UTAD) for all the support and kindness she always offered me, and for receiving me in her lab. Your co-orientation was essential for the development of this project. From UTAD, I also would like to thank Prof. Dr. Dario Santos for the contribution in the antioxidant studies and Lisete Fernandes for all the logistic support with the x-ray analysis. Additionally, I would like to thank to Dr[a]. Slavomira Doktorovova for all the support, friendship and scientific brainstorming.

From the University of Barcelona, where I spent one research year I would like to thank to Prof. Dr[a]. Maria Luísa Garcia, Prof. Dr[a]. Ana C. Calpena and Prof. Dr[a]. Maria Antónia Egea for welcoming me in their institution and laboratory. It was an extreme pleasure working with you, and I appreciate all the dedication that you have offered to my project. Thanks to all my laboratory colleagues, Guadalupe, Helen, Mireia, Elena, Martha, Alexander, Elizabeth, Gladys, who contributed to my pleasant and unforgettable journey, fostering my personal and professional growth.

I also would like to thank to Dr[a]. Beatriz Clares from the University of Granada, thank you for your help during my secondment in Barcelona, without your technical and scientific support much of the results would have been more difficult to achieve.

I would like to thank to Dr[a]. Patrícia Severino from the University Tiradentes, Brazil, for being a great friend I gained in this journey, for all the wisdom she passed on me and for all the good times we spent together.

Thanks to all my laboratory colleagues of the University Fernando Pessoa and Faculty of Pharmacy from University of Coimbra (FFUC). Specially, I am very grateful to Mrs. Regina Vieira from the Laboratory of Pharmaceutical Technology of FFUC for the technical support provided during my stay in the lab and for her endless kindness.

Thanks to all my close friends for their support and presence during this journey, for never leaving me and for always sharing my dedication to this project.

I also would like to thank to the Director of the FFUC, Prof. Dr. Francisco Veiga and Prof. Carlos Cavaleiro for the support and promptness in responding to all the requests and applications submitted, thank you for your concern and administrative assistance in the elaboration of this project.

Finally, I would like to acknowledge the *Fundação para a Ciência e Tecnologia* of *Ministério da Ciência e Tecnologia* (FCT, Portugal) for the financial support with a doctoral fellowship under the following reference SFRH/BD/80335/20111.

Contents

List of Figures

Chapter 1 - General Introduction

Chapter 1.1. Solid Lipid Nanoparticles (SLN^{TM})

Chapter 1.2. Current nanotechnology approaches for the treatment and management of Diabetic Retinopathy

Chapter 5 - Evaluation of cytotoxicity and the antioxidant activity of Epigallocatechin gallate loaded cationic lipid nanoparticles in Y-79 human retinoblastoma cells

List of Tables

Chapter 4 - Biopharmaceutical evaluation of epigallocatechin gallate loaded cationic lipid nanoparticles (EGCG-LNs): in vivo, in vitro and ex vivo studies

Chapter 5 - Evaluation of cytotoxicity and the antioxidant activity of Epigallocatechin gallate loaded cationic lipid nanoparticles in Y-79 human retinoblastoma cells

Abbreviations and symbols

ACE	Angiotensin-I converting enzyme
AFM	Atomic force microscopy
AGEs	Advanced glycation end-products
AGT	Angiotensinogen
AGTR1	Angiotensin II type 1 receptor
AIC	Akaike Information Criteria
AMD	Age-related macular degeneration
ANOVA	One-way analysis of variance
AR	Aldose reductase
ARPE	Arising retinal pigment epithelia
ARVO	Association for Research in Vision and Ophthalmology
ATP	Adenosine triphosphate
AUC	Area under the curve
BHT	2,6-di-tert-butyl-4-methylphenol/ butylatedhydroxytoluene
BRB	Blood-retinal barrier
BS	Backscattering
BSA	Bovine serum albumin
BSS	Balanced salt solution
CAT	Catalase
CDNB	1-chloro- 2,4-dinitrobenzene
CTAB	Cetyl trimethylammonium bromide
CTAB-LN	Cetyl trimethylammonium bromide based lipid nanoparticles
CV	Coefficient of variation
DCF-DA	Dichlorofluorescein-diacetate
DDAB	Dimethyldioctadecylammonium bromide
DDAB-LN	Dimethyldioctadecylammonium bromide based lipid nanoparticles

DLS	Dynamic light scattering
DME	Diabetic macular edema
DNA	Deoxyribonucleic acid
DODAB	Dioctadecyldimethyl ammonium bromide
DOTAP	1,2-dioleoyl-3-trimethylammonium-propane
DR	Diabetic retinopathy
DSC	Differential scanning calorimetry
DTA	Differential thermal analysis
DTNB	5,5'-ditiobis(2-nitrobenzoate)
EE	Encapsulation efficiency
EGCG	Epigallocatechin gallate
EGCG-CTAB LN	Epigallocatechin gallate cetyl trimethylammonium bromide based lipid nanoparticles
EGCG-DDAB LN	Epigallocatechin gallate dimethyldioctadecylammonium bromide based lipid nanoparticles
ELS	Electrophoretic light scattering
EPO	Erythropoietin
E_R%	Release efficiency
FBS	Fetal bovine serum
FDA	Food and Drug Administration
FPD	Freezing point depression
FTIR	Fourier transform infrared
GCG	Gallocatechin gallate
GH	Growth hormone
GHIH	Growth hormone-inhibiting hormone
GIT	Gastrointestinal tract
GLUT1	Glucose transporter 1
Gpx	Glutathione peroxidase
GR	Glutathione reductase

GRAS	Generally regarded as safe
GSH	Reduced glutathione
GSSG	Glutathione oxidized
HEPES	4-(2-hydroxyethyl)-1-piperazineethanesulfonic acid
HET-CAM	Hen's Egg Test Chorioallantoic Membrane
HL	Hydration level
HLB	Hydrophilic-Lipophilic Balance
HPH	High pressure homogenization
HPLC	High performance liquid chromatography
ICH	International Conference on Harmonisation
IgG	Immunoglobulin G
IGF	Insulin-like growth factor
IOP	Intraocular pressure
IRMA	Intra-retinal microvascular abnormalities
K5	Plasminogen kringle 5
LC	Loading capacity
LD	Laser diffraction
LN	Lipid nanoparticles
LOD	Detection limit
LOQ	Quantification limit
MDA	Malondialdehyde
MnSOD	Manganese superoxide dismutase
mRNA	messenger ribonucleic acid
MRT	Mean release time
MTS	Mean total score
NAD^+	Reduced nicotinamide adenine dinucleotide
NADPH	Nicotinamide adenine dinucleotide phosphate
NBT	3,30-(3,30-dimethoxy [1,10-biphenyl]-4,40-diyl) bis [2- (4-nitrophenyl)]-2H-tetrazolium dichloride

NISA	Non-peptide imidazolidine-2,4-dione
NLC	Nanostructured lipid carriers
NOS	Nitric oxide synthases
NPDR	Non-proliferative diabetic retinopathy
OII	Ocular irritation index
P188	Poloxamer 188
PAMAM	Polyamidoamine
PBS	Phosphate buffered saline
PCS	Photon correlation spectroscopy
PDGFs	Platelet-derived growth factors
PDR	Proliferative diabetic retinopathy
PEDF	Pigment epithelium derived factor
PEGs	Polyethyleneglycols
PEG-PCL	Poly(ethylene glycol)-β-polycaprolactone
PI	Polydispersity index
PKC	Protein kinase C
PLA	Poly(lactic acid*)*
PLGA	Poly(lactic-co-glycolic acid*)*
PMMA	Poly(methyl methacrylate)
PVA	Polyvinyl alcohol
RAGEs	Receptor for advanced glycation end-products
REDOX	Oxidation-reduction
RES	Reticulo-endothelial system
rHLB	required Hydrophilic-Lipophilic Balance
RNS	Reactive nitrogen species
ROS	Reactive oxygen species
RP-HPLC	Reverse phase high performance liquid chromatography
RPE	Retinal pigment epithelia

RSD	Relative standard deviation
RVO	Retinal vein occlusion
S	Calibration curve
S100	Softisan® 100
SAXS	Small angle x-ray scattering
SD	Standard deviation
SDS	Sodium dodecyl sulfate
SEM	Scanning electronic microscopy
SI	Silicate
SLN	Solid Lipid Nanoparticles
SOD	Superoxide dismutase
SRIF	Somatotropin release-inhibiting factor
SSTR	Somatostatin receptor
STZ	Streptozotocin
T	Transmission
TAGs	Triacylglycerols
TBA	Thiobarbituric acid
TBARS	Thiobarbituric acid reactive substances
TEM	Transmission electronic microscopy
TiO_2	Titanium dioxide
TGFbeta	Transforming growth factor beta
TGA	Thermogravimetric analysis
TMA	Thermomechanical analysis
UDP	Uridine diphosphate
UV-Vis	Ultraviolet-visible
VEGFs	Vascular endothelial growth factors
VEGFR	Vascular endothelial growth factors receptors
WAXS	Wide angle x-ray scattering

Z-Ave	Mean particle size
ZP	Zeta potential

Abstract

The present work is focused on the development and understanding of the applications of novel lipid-based systems for ocular drug delivery in the treatment of Diabetic Retinopathy (DR). The use of cationic lipid nanoparticles encapsulating an antioxidant drug, epigallocatechin gallate (EGCG), is innovative and has been firstly proposed by our research group for ocular administration.

Solid lipid nanoparticles (SLN) are novel drug delivery systems. The chemical structure, production methodology and physicochemical characterization (e.g. particle size, distribution, polymorphic behavior, and crystallization) are widely described along with the biopharmaceutical stability and profile. DR, is the major ocular consequence of diabetes, and the biochemical and anatomic abnormalities that induces in the microvasculature of the retina affect the eye, leading to vision loss, and contributing to the decrease of patient's life quality. The conventional treatments, including surgical and pharmaceutical strategies, are discussed and also the new strategies involving nanomedicines based on nanoparticles. Despite the multifactorial nature of DR, targeting approaches to reach the posterior segment of the eye have been considered and seem to achieve promising results. The development of cationic lipid nanoparticles (LNs) for ocular delivery based on a 3^3 full factorial design was carried out to optimize their composition. Three different variables and their influence on the physicochemical properties of the produced LNs were analyzed. The cationic lipid, cetyltrimethylammonium bromide (CTAB), was further added to the lipid matrix of the optimal LN dispersion for physical and chemical evaluation, crystallization and polymorphism, and stability. The best formulation with respect to physiochemical stability and safety, was obtained with 4.5 wt% of Softisan®100, 0.5 wt% of CTAB, 0.5 wt % of Lipoid®S75, 37.5 wt % of glycerol and 1.0 wt % of Poloxamer 188. The study of EGCG stability in HEPES and in a mimetic biological medium was performed regarding the pH dependency, storage temperature and in the presence of ascorbic acid, a reducing agent. After stabilization of EGCG, a validation method based on RP-HPLC with UV-Vis detection was carried out for two media: water and a biocompatible physiological medium composed of Transcutol®P, ethanol and ascorbic acid. The encapsulation of EGCG in LNs was obtained using two distinct cationic lipids, namely,

CTAB and dimethyldioctadecylammonium bromide (DDAB). The results show that different lipids lead to different characteristics mainly associated with the acyl chain composition, i.e. double tail lipid shows to have influence in the crystallization and stability. Despite the recorded differences between CTAB and DDAB, they both seem to fit the appropriate physicochemical parameters for ocular drug delivery, namely, particle size and size distribution, pH, osmolarity and viscosity. The biopharmaceutical study of EGCG LNs was assessed *in vitro* with the release of EGCG by dialysis bag following the analysis by a validated RP-HPLC method. The results showed a prolonged EGCG release following a Boltzmann sigmoidal profile. Also, the *ex vivo* transcorneal and transscleral permeation assay in Franz diffusion cells revealed the capacity of EGCG to permeate ocular tissues. The pharmacokinetic study of the corneal permeation showed a first order kinetics for both cationic formulations, while EGCG-CTAB LNs followed a Boltzmann sigmoidal profile and EGCG-DDAB-LNs a first order profile for transscleral permeation. Thus, the developed EGCG-LNs revealed to be non-irritant and safe for ocular delivery, as demonstrated by HET-CAM and Draize tests. The influence of the LNs developed and EGCG in the cell viability and antioxidant enzymatic activity was evaluated in Y-79 retinoblastoma cells. The activity of superoxide dismutase, catalase, glutathione reductase and glutathione-S-transferase seems to decrease, indicating the inability to neutralize the ROS formation and thus, leading to oxidative stress. Also, the lipids and proteins oxidation was increased which is related to the decreased enzymatic activity. The DDAB-LNs was the only formulation with improved enzymatic protection regarding the cell viability, antioxidant enzymatic activity and protection against lipids and proteins oxidation. It is therefore possible to associate the EGCG chelating effect with lower availability of the drug for exerting their proven antioxidant effects. Also, the EGCG was found not prevent lipid peroxidation but has been more efficient in preventing proteins oxidation.

This thesis is finalized with the general conclusions obtained by the curation of the data presented and discussed in the previous chapters.

Keywords: Cationic lipid nanoparticles; Diabetic retinopathy; Nanomedicines; Nanotechnology; Ocular delivery.

Resumo

O presente trabalho relata o desenvolvimento e compreensão da aplicação de inovadores sistemas terapêuticos lipídicos para a entrega de fármacos por administração ocular no tratamento da Retinopatia Diabética (RD). O uso de nanopartículas de lípidos catiónicas encapsulando um fármaco anti-oxidante, galato de epigalocatequina (EGCG), é inovadora e foi proposta pela primeira vez, para fins oculares, pelo nosso grupo de investigação.

As nanopartículas de lípidos sólidos (SLN) são novos sistemas terapêuticos. A estrutura química, metodologia de produção e caraterização físico-química (por exemplo, tamanho de partícula, distribuição, comportamento polimórfico, e cristalização) são descritos, assim como a sua estabilidade e perfil biofarmacêutico. A RD é a principal consequência da diabetes a nível ocular. As alterações bioquímicas e anatómicas induzidas na microvasculatura da retina afeta os olhos, levando à perda da visão, e contribuindo para a diminuição da qualidade de vida dos pacientes diabéticos. São abordados os tratamentos convencionais, incluindo estratégias cirúrgicas e farmacêuticas, assim como as novas estratégias que envolvem nanopartículas. Apesar da natureza multifatorial da RD, novas estratégias para o direcionamento ativo ao segmento posterior do olho, têm sido consideradas com a obtenção de resultados promissores. O desenvolvimento de nanopartículas lipídicas (NLs) catiónicas para administração ocular foi realizado através de um desenho fatorial completo 3^3. Foram avaliadas três variáveis e a sua influência sobre as propriedades físico-químicas das NLs. Um lípido catiónico, o brometo de cetiltrimetilamónio (CTAB), foi adicionado à matriz lipídica da NL otimizada para avaliação das propriedades físico-químicas. A formulação produzida mais adequada relativamente à sua estabilidade físico-química e segurança foi obtida com 4,5 p/p % Softisan®100, 0,5 p/p % CTAB, 0,5 p/p % Lipoid®S75, 37,5 p/p % glicerol e 1,0 p/p % poloxâmero 188. O estudo de estabilidade de EGCG em HEPES e num meio biológico mimético foi realizado relativamente à dependência do pH, temperatura de armazenamento e na presença ou não de um agente redutor, o ácido ascórbico. Após a estabilização da EGCG, foi desenvolvido um método de validação por cromatografia líquida de alta resolução de fase reversa (RP-HPLC) com deteção ultravioleta-vísivel (UV-Vis) em dois meios: em água e num meio

fisiológico biocompatível composto por Transcutol®P, etanol e ácido ascórbico. Realizou-se a encapsulação de EGCG em NLs como um sistema inovador para administração ocular e para o futuro tratamento de várias doenças, tais como RD. Foram utilizados dois lípidos catiónicos distintos, o CTAB e o brometo de dimetildioctadecilamónio (DDAB), e os resultados demonstram que diferentes lípidos conduzem a caraterísticas diferentes, principalmente associados com a composição da cadeia de acilo, a cauda dupla mostra ter maior influência na cristalização e estabilidade das NLs. Apesar das diferenças registadas, ambas as formulações parecem adequar-se aos parâmetros para administração ocular no que respeita ao tamanho de partícula e distribuição, pH, osmolaridade e viscosidade. O estudo biofarmacêutico das NLs encapsuladas com EGCG foi realizado através do perfil de libertação *in vitro* da EGCG pela técnica do saco de diálise e posteriormente analisado por RP-HPLC. Os resultados demosntraram uma libertação prolongada seguindo um perfil sigmoidal de Boltzmann. A permeação transcorneal e transscleral *ex vivo* em células de difusão de Franz revelou a capacidade da EGCG em permear os tecidos oculares. A nível transcorneal, observou-se uma cinética de primeira ordem para ambas as formulações, enquanto a nível transscleral as EGCG-CTAB NLs obedeceram um perfil sigmoidal de Boltzmann e as EGCG-DDAB-NLs um perfil de primeira ordem. Através dos testes de HET-CAM e Draize, as EGCG-NLs demonstraram ser seguras e não irritantes para administração ocular. A avaliação da viabilidade celular e da atividade enzimática foi avaliada em células Y-79 de retinoblastoma humano. Verificou-se que a atividade da superóxido dismutase, catalase, glutationa-redutase e glutationa-S-transferase diminuiu, indicando a incapacidade para neutralizar a formação de espécies reativas de oxigénio (ROS) e, assim, conduzindo a um ambiente de *stress* oxidativo. Além disso, aumentou a oxidação de lípidos e proteínas, fenómeno que está relacionado com a diminuição da atividade enzimática. A DDAB-NLs foi a única formulação que revelou maior protecção enzimática ao nível da viabilidade celular, da atividade enzimática antioxidante e da oxidação lípidos e proteínas. É, pois, possível associar o efeito quelante ao EGCG, o que poderá reduzir a sua disponibilidade para exercer os seus efeitos antioxidantes comprovados. Além disso, o EGCG parece não impedir a peroxidação lipídica, mas parece ser mais eficiente evitando a oxidação de proteínas.

Esta tese finaliza com as conclusões gerais resultantes do tratamento dos dados apresentados e discutidos nos capítulos antecedentes.

Palavras-chave: Administração ocular; Nanomedicinas; Nanopartícluas lipídicas catiónicas; Nanotecnologia; Retinopatia diabética.

Aims

The general aim of this work was focused in the design, characterization and evaluation of cationic lipid nanomedicines encapsulating an antioxidant drug to avoid the oxidative stress present in the diabetic retinopathy.

The thesis is organized as a collection of chapters, each one with a scientific paper format and with a specific aim. The first chapter is a bibliographic review of the state-of-the-art of the solid lipid nanoparticles and their applications in drug delivery and also the diabetic retinopathy and its innovative treatments. The following chapters are composed by scientific and original work covering (1) the design of cationic lipid nanoparticles regarding its composition, (2) the physicochemical characterization of the developed formulations, (3) the stabilization of EGCG in a medium able to protect it for its encapsulation in LNs and also for the biopharmaceutical studies, (4) the biopharmaceutical assessment of the formulations regarding the *in vitro* release, *ex vivo* ocular permeation, *in vitro* HET-CAM test and *in vivo* Draize test, (5) the toxicological studies and enzymatic activity in the principal antioxidant enzymes of the defense system was assessed in Y-79 human retinoblastoma cells. The cellular viability was determined by the Alamar Blue assay.

CHAPTER 1 - General introduction

CHAPTER 1.1

Solid Lipid Nanoparticles (SLN)TM

CHAPTER 1.2

Current nanotechnology approaches for the treatment and management of Diabetic Retinopathy

CHAPTER 1.1. - SOLID LIPID NANOPARTICLES (SLN™)

Eliana B. Souto[1,2*], **Joana F. Fangueiro[1]**, Rainer H. Müller[3]

[1]Faculty of Health Sciences, Fernando Pessoa University (FCS-UFP), Rua Carlos da Maia, 296, P-4200-150 Porto, Portugal

[2]Institute of Biotechnology and Bioengineering, Centre of Genomics and Biotechnology, University of Trás-os-Montes and Alto Douro (CGB-UTAD/IBB), P-5001-801, Vila Real, Portugal

[3]Freie Universität Berlin, Department of Pharmacy, Pharmaceutical Technology, Biopharmaceutics & NutriCosmetics, Kelchstraße 31, 12169 Berlin, Germany

Published in Fundamentals of Pharmaceutical Nanoscience" from Springer, Chapter 5, 91-116, 2014

CHAPTER 1.1 - Solid Lipid Nanoparticles (SLN™)

Abstract

Solid lipid nanoparticles (SLN™) are a new generation of drug delivery systems being exploited for several drugs since the nineties. These particles can be composed of different types of solid lipids, such as acylglycerols, waxes, and fatty acids, and stabilized by a wide range of surfactants. In the present chapter, the chemical structure, production methodology and physicochemical characterization are systematically discussed. Parameters such as particle size, distribution, polymorphic behavior, and crystallization are required to characterize SLN and may predict their *in vitro* stability and *in vivo* profile, therefore structural parameters can influence the biopharmaceutical properties. The use of SLN for drug delivery is discussed addressing the key points that may limit their clinical use.

1.1.1. Introduction

Nanotechnology applied to drug delivery emerged in the last decade as the high-tech of science. Nanosciences and Nanotechnologies were defined by the Royal Society and Royal Academy of Engineering "*as the study of phenomena and manipulation of materials at atomic, molecular and macromolecular scales, and the design, characterization, production and application of structures, devices and systems by controlling shape and size at nanometer scale"* (Ann P, 2004; Dowling et al., 2004). Lipid nanoparticles are being developed for drug delivery to overcome the limitations of traditional therapies providing endless opportunities in this area. Since the nineties that Solid Lipid Nanoparticles (SLN™) capture attention of several researchers because they combine innovation and versatility, and also show major advantages for various application routes (parenteral, oral, dermal, ocular, pulmonary, rectal). The main features of SLN include their suitability to optimize drug loading and release profiles, long shelf life and low chronic toxicity, protection of incorporated labile drugs, site-specific targeting and excellent physical stability (Fangueiro et al., 2011b; Souto and Muller, 2010; Wissing et al., 2004). However, some limitations may also be pointed out, such as the insufficient loading capacity, the risk of drug expulsion after polymorphic transitions

during storage, and the high amount of water (70-99.9%) required in their composition. SLN typically consist of three essential components, i.e. solid lipid, surfactant and water. These lipid particles are composed only of solid lipids at body and room temperature, having a mean particle size between 50-1000 nm (Fangueiro et al., 2011b; Souto and Doktorovova, 2009; Souto and Muller, 2011). They have the potential to load both hydrophilic and hydrophobic drugs. Depending on the location of the drug, i.e., if the drug is entrapped inside the lipid matrix, encapsulated or adsorbed onto the surface of particles, they can exist in three different morphological types. The SLN Type I is composed of a homogenous matrix which the drug is molecularly dispersed within the lipid core or it is present in the form of amorphous clusters, also homogenously dispersed in the lipid core. The SLN Type II or drug-enriched shell model occurs when the lipid concentration is low relatively to the drug, and a drug-free (or drug reduced) lipid core is formed when the drug reaches its saturation solubility in the remaining melt. An outer shell will solidify containing both drug and lipid, being the drug mainly onto the surface of the particles. The SLN Type III or drug-enriched core model is formed when the drug concentration is relatively close to or at its saturation solubility in the lipid melt. The drug forms a core surrounded by a lipid enriched shell. Types I and III are those reported to provide prolonged or/and controlled release profile.

The present chapter reviews the lipid nanoparticles chemistry, production techniques, physicochemical characterization, and their developments in drug delivery.

1.1.2. Nanomaterials

The characteristic of nanomaterials used for the production of SLN is their size, which falls in the transitional zone between individual atoms or molecules and the corresponding bulk materials. Size reduction can modify the physical and chemical properties of nanomaterials distinctively from their bulk and molecular counterparts. Independently of the particle size, the materials present in the nanoparticles in contact with cell membranes and the chemical reactivity of those materials, play a dominant role when the particles react with other substances or tissues (Yang et al., 2008). Colloidal dispersed lipids are interesting carrier systems for bioactive substances, particularly for lipophilic drugs. By definition, SLN are colloidal dispersions, since they are neither a

suspension nor an emulsion (Heike, 2011). Lipid compounds (of animal or vegetable resources) are generally regarded as safe (GRAS) and proved their biocompatible and biodegradability, since they are physiological lipids that occur naturally in the organism. The most common used lipids are listed in Table 1.1.1. The general lipid composition (e.g. fatty acids, waxes) will have different crystallinity and capacity for accommodation of drug molecules. In addition, the organization of lipid molecules after recrystallization could adapt three possible forms, mainly, an amorphous α form, an orthorhombic perpendicular β' form, and a triclinic parallel β polymorphic form. The crystanillity is crescent from α to β' and to β (Westesen et al., 1993). Lipids usually show high crystanillity during storage time, and not immediately after SLN production. This could lead to a problem related to drug expulsion from the lipid matrix, since less space is left for the accommodation of drug molecules with the creation of a perfect crystal lattice. The metastable form β' is usually related to a controlled drug release profile (Wiechers and Souto, 2010).

Triacylglycerols (TAGs) are widely used in pharmaceuticals as matrix materials. Physical properties, such as polymorphism, melting and solidification, density, and molecular flexibility, are influenced by the crystalline phases of TAGs. The structural properties of TAG crystals are sensitive and influenced by their molecular properties, such as saturation/unsaturation of the fatty acid moieties, glycerol conformations, symmetry/asymmetry of the fatty acid compositions connected to the glycerol groups. Fats may be represented by TAGs, despite diacyl- and monoacylglycerols may be categorized as fats. The physical properties of TAGs depend on their fatty acid compositions (Kaneko, 2001). TAGs mostly used in SLN are trilaurin, trimyristin, tripalmitin and tristearin (Souto et al., 2011). These types of lipids are reported to be safe for use as colloidal carriers. Tripalmitin and tristearin showed to be biodegradable by lipases (Olbrich et al., 2002). However, some disadvantages are associated with the use of pure TAGs, since immediately after recrystallization α modification is formed, and more drug is incorporated due to the less ordered crystal structure. During storage, other polymorphic modifications may happen (β and β') and organization does not leave space enough for the loaded drug molecules, leading to their expulsion from the lipid matrix (Souto et al., 2011). Nevertheless, their use should not be discarded, since studies of long-

term stability of SLN-based TAGs have also been reported (Souto and Muller, 2006). Mono- and diacylglycerols are also broadly used in SLN production. Despite having higher solubilization capacity than TAGs, their use in lipid matrices has the advantage of forming less ordered crystal structures leaving more space for drug accommodation (Souto et al., 2011).

Fatty acids are also used for SLN production since these also figure in the membranes and fat tissues (Kaneko, 2001). The main advantages of their applications are the acyl chains that provide flexibility and consequently leading to a molecular conformation and lateral packing. The crystal structure mainly depends on the physical properties, such as the presence of long chains, melting point, heat capacity, and elasticity (Kaneko, 2001).

Depending on the chain length of the fatty acid, fatty alcohols are suitable to be used in lipid matrices, since they show good biotolerability as the other lipids mentioned above for dermal delivery. They could be useful as skin permeation enhancers due to the disturbance in the lipid packing order (Sanna et al., 2010). For parenteral administration, these type of lipids also showed to be biodegradable and safe, since they are metabolized in the body via endogenous alcohol dehydrogenase enzyme systems (Dong and Mumper, 2006).

Hard fats could compromise the feasibility of several types of SLN. They can be a mixture of acylglycerols based on saturated fatty acids. Their use in SLN proved to form a lipid matrix able to load proteins and peptides safety for parenteral administration (Almeida et al., 1997; Fangueiro et al., 2011b; Sarmento et al., 2011).

Waxes are a group of lipids comprising esters of fatty acids and fatty alcohols. In opposition to acylglycerols, the alcohol represented is not glycerol. Waxes may contain free hydroxyl groups within the molecule (e.g. hydroxyoctanosyl, hydroxystearate) or free fatty acid functions (e.g. beeswax). Their polymorphism is mainly an orthorhombic form that prevails, and the polymorphic transition rate is low (Jenning and Gohla, 2000). They have proven to load drugs with limited solubility, and also to provide a release profile depending on the amount of wax in the lipid matrix (Kheradmandnia et al., 2010).

Cationic lipids are been recently applied mainly for gene therapy (Tabatt et al., 2004), and in particular for negatively surface mucosas, such as the ocular mucosa (del Pozo-Rodríguez et al., 2008). Their chemical composition is mainly quaternary ammonium salts. In SLN, they are reported to be useful for monoclonal antibodies adsorption and/or deoxyribonucleic acid (DNA) onto the surface of the particles and for specific targeting (Carbone et al., 2012). These lipids can be used as lipid matrices along with the other lipids already described. The anti-inflammatory effects of cationic lipids have also been reported (Filion and Phillips, 1997) and they may be useful for some administration routes. A list of most used solid lipids for the production of SLN is shown in Table 1.1.1.

Table 1.1.1. Examples of common solid lipids for the production of SLN.

	Trade Name	Chemical Terminology	Reference(s)
TAGs	Precirol®ATO5	Mixture of monoacylglycerols (8-22 %), diacylglycerols (40-60 %) and triacylglycerols (25-35 %) of palmitic and stearic acid	(Das et al., 2011; Sivaramakrishnan et al., 2004)
	Compritol®888ATO	Glyceryl dibehenate	(Blasi et al., 2011; Das et al., 2011; Doktorovova et al., 2011; Kuo and Chen, 2009; Kuo and Chung, 2011; Rahman et al., 2010; Sivaramakrishnan et al., 2004)
	Dynasan®114	Glyceryl Trimyristate	(Aditya et al., 2010; Martins et al., 2012; Noack et al., 2011; Petersen et al., 2011)
	Dynasan®116	Glyceryl Tripalmitate	(Cengiz et al., 2006; Kuo and Chung, 2011; Kuo and Lin, 2009)
	Dynasan®118	Glyceryl Tristearate	(Noack et al., 2011; Petersen et al., 2011)
	Imwitor®900K	Mono- and diacylglycerols based or hydrogenated fats with a glyceryl monostearate content of 40-55 %	(Doktorovova et al., 2011; Sivaramakrishnan et al., 2004)
	Softisan®100	Blends of TAGs Composed by fatty acids with a chain length of C_{10}-C_{18}	(Fangueiro et al., 2011b; Zhang et al., 2008)
	Softisan®142	Blends of TAGs Composed by fatty acids with a chain length of C_{10}-C_{18}	(Blasi et al., 2011; Nassimi et al., 2010)
Fatty acids	Stearic acid	Saturated C_{18} fatty acid	(Ghadiri et al., 2012; Severino et al., 2011; Zhang et al., 2000)

Fatty alcohols	Cetyl alcohol		(Sanna et al., 2010)
	Stearyl alcohol		(Sanna et al., 2010; Souto et al., 2004a)
	Witepsol®E85	Mixtures of hard fats	(Kuo and Chen, 2009; Martins et al., 2012; Sarmento et al., 2011)
Waxes	Cacao butter		(Kim et al., 2005; Kuo and Chung, 2011; Kuo and Lin, 2009)
	Carnauba wax		(Kheradmandnia et al., 2010)
	Beeswax		(Attama and Müller-Goymann, 2008; Kheradmandnia et al., 2010)
	Cetyl palmitate	Ester of palmitic acid and cetyl alcohol	(Blasi et al., 2011; Carbone et al., 2012; Fangueiro et al., 2011a; Ghadiri et al., 2012; Martins et al., 2012)
Cationic Lipids	CTAB	Cetyl trimethylammonium bromide	(Carbone et al., 2012; Doktorovova et al., 2012)
	DDAB	Dimethyldioctadecylammonium bromide	(Carbone et al., 2012)
	DOTAP	1,2-dioleoyl-3-trimethylammonium-propane	(Carbone et al., 2012; del Pozo-Rodríguez et al., 2010; Tabatt et al., 2004)
	DODAB	Dioctadecyldimethyl ammonium bromide	(Kuo and Chen, 2009; Kuo and Wang, 2010)

Emulsifiers have amphiphilic structure that are used to reduce the surface tension and facilitate the particle partition, i.e., their hydrophilic groups oriented towards the aqueous phase and the hydrophobic groups oriented to the lipid (Rosen, 2004). The selection of the emulsifiers mainly depends on the chosen lipid, since they need to be qualitatively and quantitatively compatible (Severino et al., 2012). The hydrophilic-lipophilic balance (HLB) is directly related to the solubility, i.e. it is the balance of the size and strength of the lipophilic and hydrophilic groups of the emulsifier and it is mandatory to form an emulsion. Thus, the required HLB (rHLB) of a final dispersion should be calculated according to the HLB of the lipid and HLB of the emulsifier (and co-emulsifier, if needed), using the following equation (Vieira et al., 2012):

$$rHLB = \lfloor \%_{Lipid}\, xHLB_{Lipid} \rfloor = \lfloor \%_{Emulsifier}\, xHLB_{Emulsifier} \rfloor + \lfloor \%_{Co-Emulsifier}\, xHLB_{Co-Emulsifier} \rfloor$$

This equation could be useful to predict the quantities required to form an emulsion, and it is highly applied in fluid emulsions, such as SLN. However, for cream type emulsions and w/o/w emulsions it is not sufficient. Nevertheless, calculating the rHLB is extremely relevant, since the selection of the ideal chemical emulsifier compromises the stability of the entire formulation. The blend of the emulsifier should adjust to the tails of the lipid chains in the interface to allow the co-existence of the oil droplets in a continuous aqueous phase. The interactions between lipids and emulsifiers are mainly electrostatic, since hydrophobic moieties have attractive forces to lipid molecules. Emulsifiers are physically adsorbed onto the surface or loaded within the lipid matrix. The hydrophilic groups of the emulsifier give rise to repulsive forces, depending on the volume size and chemical nature of the hydrophilic moieties of emulsifiers (Rosen, 2004).

The emulsifiers typically used in the production of SLN could be selected according to their nature (i.e. HLB) and also to the nature of the hydrophilic group. Apparently, the non-ionic emulsifiers do not show ionic charge (e.g. $RCOOCH_2CHOHCH_2OH$, monoacylglycerol of long-chain fatty acid). The most used are the polyoxyethylene sorbitan fatty acid esters (Tween® 20, 40, 60, 80), sorbitan fatty acid esters (Span®20, 40, 60, 80), polyoxyethylene sorbitol esters (Mirj® 45, 52, 53, 59), alkyl aryl polyether

alcohols (Tyloxapol), and the triblock copolymers composed of polyoxypropylene (poloxamer, pluronic or Lutrol®F68, F127). Sugar esters could also be employed. This type of emulsifiers includes esters of stearic, palmitic, oleic, and lauric acids.

Polyoxyethylene sorbitan fatty acid esters and triblock copolymers composed of polyoxypropylene are hydrophilic amphiphilic molecules that are dissolved in the aqueous phase of emulsions, and their lipophilic moiety is adsorbed onto the particles surface and the long polyoxypropylene chains allows the stabilization and aggregation with other particles. Sorbitan fatty acid esters are lipophilic amphiphilic molecules that are better adsorb onto particles surface and easily dissolved with melted lipids (Kaneko, 2001).

The use of anionic or cationic emulsifiers could be important to improve the zeta potential (ZP), and thus input an electrostatic charge to avoid particle aggregation/sedimentation. The cationic emulsifiers have a molecule moiety with positive charge (e.g. salt of a long-chain amine $RNH_3^+Cl^-$, or a quaternary ammonium salt, $RN(CH_3)_3^+Cl^-$). Stearylamine (Kuo and Chen, 2009; Pedersen et al., 2006; Vighi et al., 2010), cationic lipids (quaternary ammonium salts) (Doktorovova et al., 2012; Doktorovova et al., 2011; Tabatt et al., 2004) and Esterquat 1 (N,N-di-(b-stearoylethyl)-N,N-dimethyl-ammonium chloride) (Vighi et al., 2007, 2010) are examples used in SLN. Anionic emulsifiers have a negative moiety in the molecule (e.g. $RCOO^-Na^+$, sodium salt) and the most applied are bile salts (e.g. sodium cholate and sodium taurocholate), which improve the absorption of particles in the gastrointestinal tract (GIT). Other types of emulsifiers often applied are the phospholipids. Phospholipids derived from soy or egg phosphatidyl choline have a variable fatty chain composition. Generally, soybean phosphatidyl choline contains more saturated fatty acyl chains than egg phosphatidyl choline (Souto et al., 2011). Its use is reported to improve the emulsions stability and may also be applied as permeation enhancer for topical administration (Cui et al., 2006; Dreher et al., 1997). Also, its use was proven to decrease particle size due to the amphiphilic properties (Schubert et al., 2006; Schubert and Muller-Goymann, 2005).

1.1.3. Production methods of SLN

The classical production methods of SLN are very well described in the literature (Fangueiro et al., 2011b; Müller et al., 2000; Souto and Muller, 2011) and include those not requiring organic solvents and those requiring the use of solvents to solubilize the lipid materials. The selection of the ideal method mainly depends on the properties of the required drug, such as solubility, chemistry, molecular weight, and thermal stability. The most applied and simple method is the High Pressure Homogenization (HPH), either hot HPH or/and cold HPH (Müller et al., 2000). For both, the drug is dispersed or solubilized in the melted lipids. In hot HPH, an aqueous surfactant solution at the same temperature is added to the lipid phase and homogenized by high shear homogenization 1 min at 8.000 rpm. Then, this pre-emulsion is processed by HPH to obtain a desirable particle size. Usually, 3-5 homogenization cycles at 500 bar are sufficient. After this process a nanoemulsion is obtained, following a temperature decrease leading to lipid recrystallization, and consequently to the formation of SLN. The cold HPH has a small change in comparison to the hot HPH. After drug dispersion or solubilization in the melted lipid, this mixture is cooled using nitrogen liquid or dry ice. The obtained solid lipid mixture is ground using a mortar milling, producing microparticles which are suspended in an aqueous surfactant solution. Nanoparticles are formed when this microparticle suspension is homogenized by HPH at room temperature or below. The shear forces and cavitation forces in the homogenizer are able to break the microparticles into nanoparticles (Mishra et al., 2010). The main difference of these two techniques is the temperature, because cold HPH is applied when the drug is labile or heat sensitive. The cold HPH was also developed to overcome some failures of hot HPH, such as drug distribution in the aqueous phase during homogenization and complexity of the crystallization step, which could lead to supercooled melts. However, hot HPH is the most applied process due to scale-up facilities (Sinha et al., 2011).

Production of SLN by sonication or by high shear homogenization is applied less frequently. The lipid phase and aqueous phase are heated up to the same temperature and emulsified by mechanical stirring (high shear homogenization) or sonication. The main disadvantage of these techniques is the presence of both nanostructures, i.e. micro- ad nanoparticles in the final dispersion (Sinha et al., 2011).

The microemulsion technique was developed by Gasco (Gasco, 1997) and since then, it is being developed and modified by different research groups (Fontana et al., 2005; Ghadiri et al., 2012; Patel and Patravale, 2011; Pedersen et al., 2006). The lipid and aqueous phase are heated and homogenized at temperature above the melting point of lipid. This microemulsion in diluted with cooled water, which leads to the breaking of the microemulsion into a nanoemulsion. The obtained nanoemulsion is cooled leading to the formation of SLN. During stirring, the control of the temperature is an important factor to keep the lipid in the melted state (Sinha et al., 2011).

The double emulsion method is another alternative method for producing SLN described by Garcia-Fuentes and co-workers. (Garcia-Fuentes et al., 2002). This method is appropriate for the incorporation of hydrophilic or/and labile drugs, such as proteins and peptides, since these are loaded in an inner aqueous phase avoiding chemical or enzymatic degradation. Briefly, the hydrophilic drug is solubilized in an inner aqueous phase and added to the lipid phase containing a suitable emulsifier to form a primary w/o emulsion under high shear homogenization. The second step involves the dispersion of this primary w/o emulsion in an external aqueous surfactant phase to form the final w/o/w emulsion (Fangueiro et al., 2011b).

The solvent emulsification-evaporation method was described by Sjöström and Bergensåhl (Sjöström and Bergenstahl, 1992) being applied when the drug is not soluble in the lipid. In this case, an organic solvent, non-miscible with water (e.g. cyclohexane, chloroform) but soluble in the lipid, is dispersed in an aqueous surfactant solution to produce an o/w emulsion. The organic solvent is evaporated during stirring. This method is useful for hydrophilic drugs, such as proteins and peptides.

The solvent displacement method (also named as nanoprecipitation method) was initially described for polymeric nanoparticles (Quintanar-Guerrero et al., 1999) and adapted for SLN production (Dong et al., 2012; Hu et al., 2002; Videira et al., 2002). This method requires a semi-polar water-miscible solvent (e.g. acetone, ethanol, or methanol) that is used to dissolve the lipid phase consisting in the lipid material and drug. This lipid phase is added by injection to an aqueous surfactant phase already prepared under magnetic stirring. Lipid particles are formed after complete removal of

the solvent by diffusion or by distillation leading to nanoparticles precipitation (Souto and Müller, 2007).

In the emulsification-diffusion method, a solution of a semi-polar organic solvent previously saturated with water to ensure thermodynamic equilibrium, is used to dissolve the lipid. This solution is added to an aqueous surfactant solution obtaining a w/o emulsion. The saturated solution prevents the diffusion of the solvent from the droplets into the water phase**.** Formation of SLN is obtained by adding an excess of water to the emulsion, which facilitates the diffusion of solvent from the droplets (Sinha et al., 2011; Wissing et al., 2004).

The phase inversion-based method has been described by Heurtault and co-workers (Heurtault et al., 2002). This method involves two steps. First, all components are melted and magnetically stirred using a temperature program (e.g. 25–85°C) and cooled down to lower temperature (e.g. 60°C). Three temperature cycles (85–60–85–60–85°C) are applied to reach the inversion process defined by a temperature range. In the second step, an irreversible shock is applied by adding cold water. This process leads to the formation of stable nanoparticles.

More recently a new method has been described for the production of SLN. This method developed by Battaglia and co-workers (Battaglia et al., 2010) produces SLN by coacervation in a controlled way, starting from fatty acids alkaline salts. The basis of the method is the interaction of micellar solution of sodium salts of fatty acids (e.g. sodium stearate, sodium palmitate, sodium myristate, sodium behenate) and an acid solution (coacervating solution) in the presence of an amphiphilic polymeric stabilizing agent (Battaglia et al., 2010; Corrias and Lai, 2011). With the decrease of pH, the SLN can be precipitated. It is a very simple, inexpensive and thermosensitive method that allows the incorporation of drugs and also can be applied from the laboratorial scale to the industrial scale (Battaglia and Gallarate, 2012).

The different methods described here have been classified as those not using organic solvents (Figure 1.1.1.) and those using organic solvents (Figure 1.1.2).

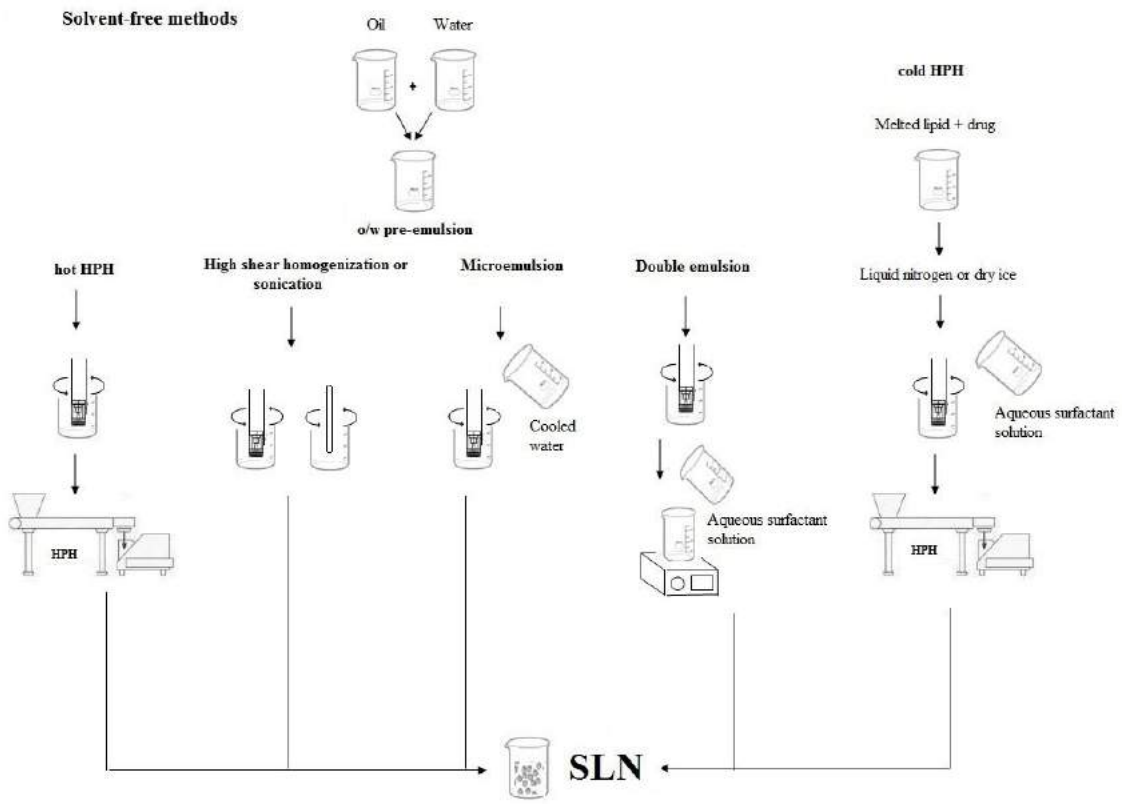

Figure 1.1.1. Schematic representation of the classical methods by solvent-free methods applied for the production of SLN.

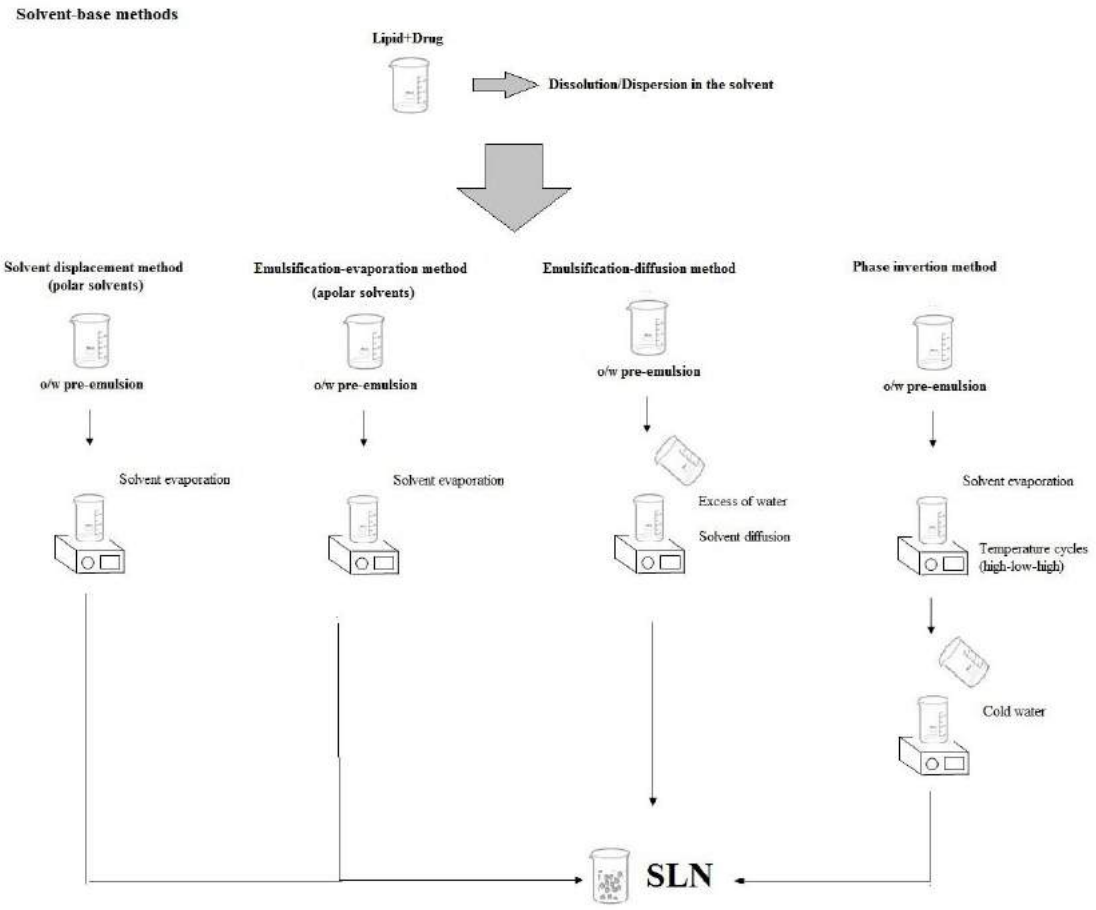

Figure 1.1.2. Schematic representation of the classical methods by solvent methods applied for the production of SLN.

1.1.4.Characterization and evaluation of SLN

The physicochemical characterization of SLN is crucial to evaluate their stability, safety, and suitability of these particles for drug delivery. The physicochemical properties of SLN may compromise the administration route, but also the toxicological profile. A major parameter is the colloidal stability of SLN in aqueous dispersions, and also the crystallization and polymorphic behavior of the lipid matrix. The most commonly applied methods for the characterization of SLN are described in this section.

1.1.4.1. Mean particle size, distribution and electrical charge

After SLN production, the first parameter to assess should be the mean particle size and size distribution, since it is desirable to have monodispersed populations in the nanometer range. The most common techniques are the dynamic light scattering (DLS), also known as photon correlation spectroscopy (PCS), and the laser diffraction (LD). DLS is able of determining the particle size in the submicron range based on the Brownian movement of the spherical particles in suspension. A monochromatic light beam, such as a laser, hits the moving particle, changing the wavelength of the incoming light. This change is related to the size of the particle (Berne and Pecora, 2000). The frequency shifts, the angular distribution, the polarization, and the intensity of the scattered light, are determined by the size, shape and molecular interactions in the scattering material (Gethner and Gaskin, 1978). It is possible to compute the spherical size distribution, and give a description of the particle's motion in the medium, measuring its diffusion coefficient and using the autocorrelation function (Berne and Pecora, 2000).

LD is another technique that could be applied based on the principle that particles passing through a laser beam will scatter light at an angle that it is directly related to their size. The observed scattering angle is dependent on the shape and size of the particles and increases logarithmically with the increase of the particle size. The scattering intensity is high for larger particles and low for smaller particles (Eshel et al., 1991; Ma et al., 2000). Both techniques are broadly applied because of the advantages they show, e.g. fast data collection, relatively inexpensive, good reproducibility, low volume of samples and automated for routine measurements. In addition, extensive experience in the technique is not required. The main differences between DLS and LD are the collected data. DLS reports the mean particle size of the entire population, whereas LD usually reports the mean particle size of 10% (LD_{10}), 50% (LD_{50}), and 90% (LD_{090}) of the population of the particles. Another difference is the detection limit; DLS is not able to detect particles above 3 µm, while LD is.

Each particle develops a net charge at the surface affecting the distribution of ions in the surrounding interfacial region, resulting in an increased concentration of counter ions (ions of opposite charge to that of the particle) close to the surface. Thus, an electrical

double layer is formed. In the inner region, there is the Stern layer, the ions are strongly bound, and in the outer diffuse region they are less firmly attached. The zeta potential (ZP) refers the electrical charge at the surface of the hydrodynamic shear surrounding the colloidal particles. The magnitude of the ZP gives an indication about the long-term stability of the colloidal system (Hiemenz and Rajagopalan, 1997). Thus, if all the particles in suspension have a high negative or positive value of ZP then they will tend to repulse each other and there is no tendency to flocculate. However, if the particles have low ZP values then there is no force to prevent the particles coming together and flocculating (Shchukin et al., 2001). The limiting values between stable and unstable suspensions is generally taken at either +30mV or -30mV. DLS is a current technique that also allows determining the ZP, however other techniques exist, such as electrophoretic light scattering (ELS), acoustic and electroacoustic. DLS for determining ZP is the most sensitive and versatile technique, however it does not directly measure the ZP. The analysis is carried out in a cell with electrodes in each end to which a potential is applied. When the voltage is applied, the particles move towards the electrode of opposite charge, and their velocity is measured and expressed as ZP **(**Figure 1.1.3). The mobility of the particles is commonly determined by laser Doppler anemometry, which is based on the evaluation of a frequency (Doppler) shift that is observed for the light scattered from the particles motion in the electric field. DLS converts this signal directly in ZP through the Helmholtz-Smoluchowski equation (Bunjes, 2005):

$$\mu = \frac{\varepsilon\zeta}{\eta}$$

where μ is the electrophoretic mobility, ε is the permittivity, ζ is the zeta potential, and η is the viscosity of the dispersion medium.

Unlike other parameters, such as particle size, ZP is affected by the surrounding environment, e.g., pH, ionic strength, and consequently the type of ions in the suspension. Therefore, the measurements should be conducted after dilution to avoid multiple scattering and for better resolution (Renliang, 2008).

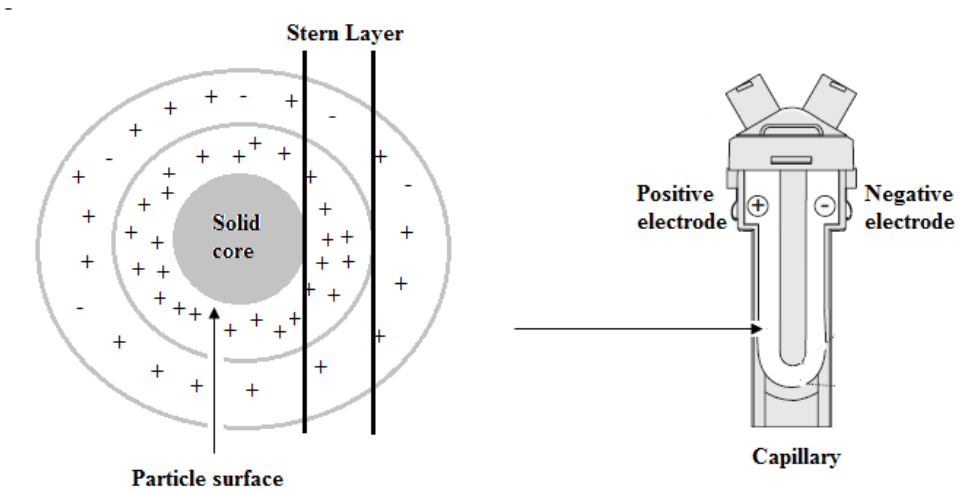

Figure 1.1.3. Illustration of the ZP in the surface of particles and the schematic representation of a capillary and the electrodes.

1.1.4.2. Microscopy

Microscopy is a technique used to verify the surface, morphology of the particles, their size, distribution, and shape, and other potential species that may have been produced simultaneously. Particle shape is a very important factor, since particles are preferentially required to be spherical. For controlled release, the particles should provide protection of loaded drugs, where the contact with the aqueous environment should be minimal (Bunjes, 2005). The most applied techniques are the scanning electron microscopy (SEM), transmission electron microscopy (TEM) and atomic force microscopy (AFM). Usually, these sophisticated techniques require a sample treatment, (e.g. freeze-drying) previously to imaging, thus particles are not observed in their native state (i.e. as liquid dispersions). The major difference between TEM and SEM is the electron incidence in the sample. In SEM, electrons are scanned over the surface of the sample and can produce very high-resolution images of a sample surface, revealing details less than 1 nm in size. In TEM, electrons are transmitted through the sample providing information about the thickness and composition (crystal structure) of samples (Dubes et al., 2003). In SEM, a chemical fixation to preserve and stabilize particle structure is required. Fixation is usually performed by incubation in a buffer solution, such as glutaraldehyde, sometimes in combination with formaldehyde and

other fixatives, and optionally followed by post-fixation with osmium tetroxide (Muller-Goymann, 2004).

TEM is relatively fast and simple with negative staining (Friedrich et al., 2010). Samples for TEM need to be as thick as possible to allow the electron beams interacting rapidly with the sample. This technique requires a drying process and yields additional information about the internal structure of the nanoparticles. The samples are fixed with a solution containing heavy metal salts which provide high contrast in the electron microscope (e.g. uranyl acetate or phosphotungstic acid) (Kuntsche et al., 2011). Unfortunately, the resulting images have low resolution and since the freeze-drying of samples is required, they are not observed in the original state, leading to artifacts in the images (Bunjes, 2005). Cryogenic microscopy is very useful for lipids, requiring low temperatures. Cryofixation may be used and low-temperature SEM/TEM performed on the cryogenically fixed samples.

AFM utilizes the force acting between a surface and a probing tip resulting in a spatial resolution of up to 0.01 nm for imaging (Mühlen et al., 1996). This technique allows imaging under hydrated conditions without pre-treatment of the samples, however samples need to be fixed e.g. by adsorption (Muller-Goymann, 2004). AFM provides a three-dimensional profile surface, which leads to a higher resolution and gives more information about the particles` surface. However, AFM requires longer time for analysis than SEM or TEM (Geisse, 2009; Mühlen et al., 1996; Olbrich et al., 2001; Shahgaldian et al., 2003).

1.1.4.3. Thermal analysis

During the recrystallization process, lipid materials could exist in a well-defined crystal, or as a mixture of different internal lattice structure. Thermal analysis could provide information about the polymorphic modifications of lipid materials, crystallization and thermal behavior. The polymorphic behavior and crystallinity of SLN can be checked by differential scanning calorimetry (DSC), thermogravimetric analysis (TGA), thermomechanical analysis (TMA), and the differential thermal analysis (DTA). Phase

transitions are followed by free energy changes, associated with changes in the enthalpy or entropy of the system. Enthalpy changes of samples require an endothermic or exothermic reaction that it is translated in a signal, depending on the consumption of energy (e.g. melting of a solid), or a release of energy (e.g. recrystallization of an isotropic melt). The transition from the crystalline to amorphous phase usually requires a high energy input. Therefore, care has to be taken to ensure that the measuring device is sensitive enough to give a sufficiently low detection limit. Entropy changes can be recognized by a change in the baseline slope, due to a change in the specific heat capacity (Ford and Mann, 2011).

DSC is the most applied thermal analysis in SLN that evaluates the physical and chemical properties of the lipids as a function of time and temperature (McElhaney, 1982). Two samples are usually analyzed, namely SLN sample and the bulk material (i.e. the solid lipid used), and temperature of both samples are raised identically over time in different containers (Gill et al., 2010). The difference in the input energy required to match both temperatures would be the amount of excess heat absorbed (endothermic) or released (exothermic) by the lipid in the SLN. During a change in temperature, DSC measures the heat quantity needed for the transition to occur, which is released or absorbed excessively by the sample on the basis of a temperature difference between the sample and the bulk material. In DSC, the amount of heat put into the systems is exactly equivalent to the amount of heat absorbed or released during a transition (Christian and O´Reilly, 1986). The main advantages shown by this technique are the detection of polymorphism, the small sample size (e.g. 2-3 mg (solid) or ml (liquid)) relatively fast, sensitive and versatile. TGA is also very similar to DSC, being the major difference the continuous analysis of sample and bulk material, and it is based on the thermobalance. It measures the mass variation of a sample when subjected to temperature. The source of heat is an infra-red lamp, and the atmosphere is controlled by addition of inert gases (e.g. nitrogen, helium) or reactive gases (e.g. oxygen, hydrogen). The decomposition of effluent material can be characterized, also by coupling gas chromatograph or mass spectrometer (McCauley and Brittain, 1995). DTA is similar to DSC, however it is more accurate of all thermal analyses, because the thermocouple is inserted into the sample (McCauley and Brittain, 1995). TMA

measures the deformation of the sample under non-oscillating stress subjected to temperature. The sample usually is placed in a small tube connected by a quartz probe to a differential exchanger. The movements of the sample are monitored by the displacement of the exchanger. This technique enables the measurement of several characteristics, such as tensile strength, volume expansion, penetration or elasticity (McCauley and Brittain, 1995).

Figure 1.1.4 shows the typical DSC profiles of a solid bulk lipid, analyzed before tempering the material for 1 hour at 100ºC. The differences between the two heating runs (A and B) allow the detection between different polymorphic forms in the same material. In Figure 1.1.4A, the difffractogram clearly shows a sharp peak representing the β-form of the tested bulk lipid (i.e. Dynasan®116) (Souto and Muller, 2006). In the second heating run (Figure 1.1.4B) it is also possible to detect the metastable α-form. This type of analysis mimics the thermals tress of the lipid, since for production of SLN it is necessary to melt the lipid first and then cool the pre-emulsion for SLN formation. Analysis of SLN represents the second heating run. This explains the different polymorphic forms between bulk materials and the lipid particles (Souto and Muller, 2006).

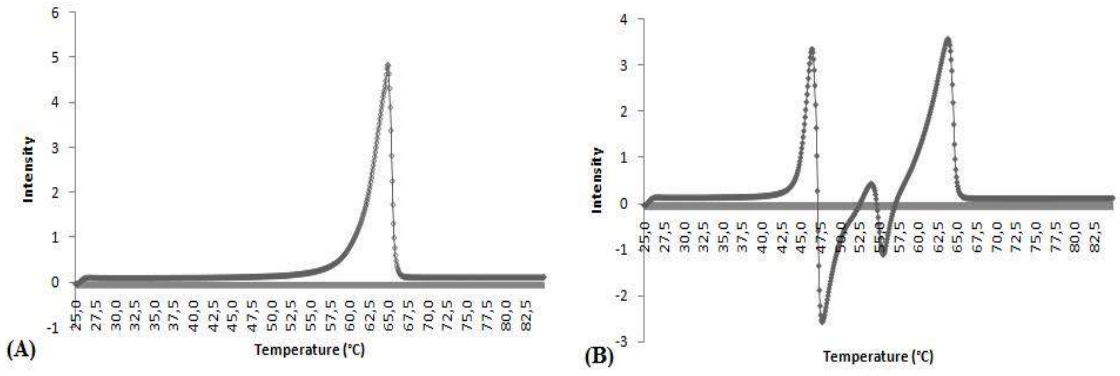

Figure 1.1.4. DSC analysis of bulk lipid (A) First heating run before tempering and (B) Second heating run before tempering (modified after Souto and Muller, 2006).

1.1.4.4. Crystallinity and Polymorphism

X-ray is a widely used method for the evaluation of crystallinity, since it applies wavelengths of the same magnitude as the distance between the atoms or molecules of crystal. Thus, it allows the determination of the arrangement of molecules within a crystal, i.e. the macromolecular structure of the particles (Heurtault et al., 2003). This method is based on a beam of X-rays that reaches a crystal and causes the spread of light into many specific directions. This energetic radiation may arise from the removal of inner orbital electrons. These transitions are followed by the emission of a X-ray photon having energy equal to the energy difference between the two states (Kratky, 1982). From the angles and intensities of these diffracted beams, a crystallographer can produce a three-dimensional picture of the density of electrons within the crystal, as shown in Figure 1.1.5. From this electron density, the mean positions of the atoms in the crystal can be determined, as well as their chemical bonds, their disorder and various other factors (Jenknins, 2000). This technique can be carried out using the small angle x-ray scattering (SAXS) or the wide angle x-ray scattering (WAXS), both widely applied in the evaluation of SLN crystallinity (Aji Alex et al., 2011; Heurtault et al., 2003; Müller et al., 2008; Schubert et al., 2006). The only difference between both methods is the range of scattering angles 2θ. While standard diffractometers cover angles between about 5° and 180°, the range between 0.01° and 3° is typical for small angle instruments. These techniques are specific for studying structural features of colloidal size in bulk materials and particles loaded with drug, determining their polymorphic transitions and the quantitative determination of crystalline components in the formulation (Bunjes and Unruh, 2007). It is also important to confirm the presence of the drug in the systems, i.e. if the drug is molecularly dispersed in the lipid matrix, or if it is in the amorphous state. Studies with this technique pointed differences in the polymorphism of particles composed of acylglycerols (Bunjes et al., 2003; Westesen et al., 1997) and also in the bulk materials (Souto et al., 2006).

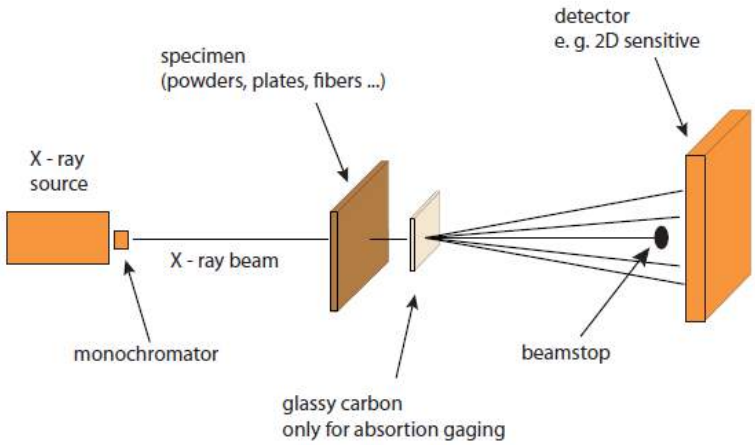

Figure 1.1.5. Illustration of the x-ray instrumentation and methodology.

This technique is applied to differentiate between the crystalline and amorphous material. A typical example is shown in Figure 1.1.6. The X-ray study confirms the transition rates of both liquid and solid lipids used in the lipid particles. The use of higher amounts of oil in the particles (Figure 1.1.6B), decreases the crystanillity, and consequently decreases the peaks intensity in X-ray diffractogram.

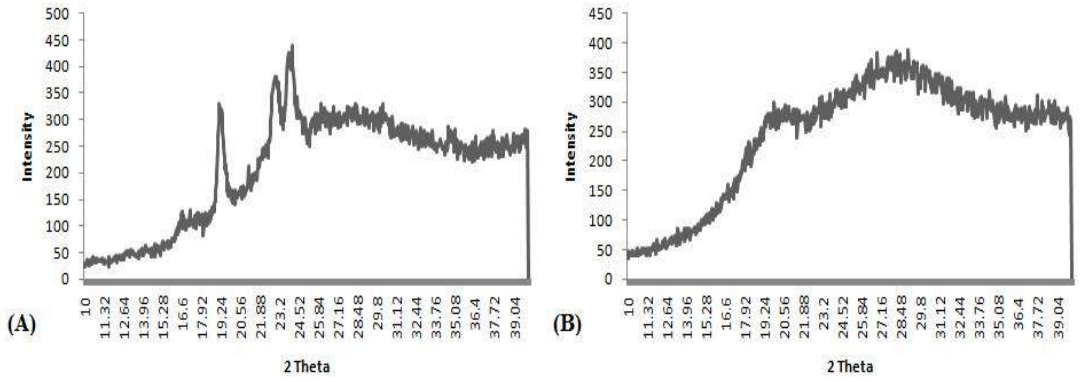

Figure 1.1.6.. X-ray analysis of lipid particles. (A) Lipid particles made of solid lipid and (B) Lipid particles made of liquid and solid lipids (modified after Souto et al., 2004b).

1.1.4.5. Infra-red spectroscopy

Infra-red spectroscopy is applied to characterize SLN at molecular level. Each molecule absorbs at a specific wavelength that is related to its molecular and chemical structure.

The usefulness of Fourier transform infrared (FTIR) imaging in the characterization of drug delivery systems was demonstrated by Coutts-Lendon and co-workers (Coutts-Lendon et al., 2003). FTIR could be useful to identify the lipid composition and also the presence of drug contaminants and degradants in the lipid matrix. For bulk materials, FTIR could also provide information about the functional groups. In general, this technique is very sensitive, non-destructive, and the amount of sample required for analysis is about a few nanograms. The particles are isolated by microneedle and transferred to a circular salt plate placed on the instrument. The recorded data is a three-dimensional spectra image, with spacial information in the x- and y- directions and spectral information in the z- direction (Barber, 1993; Bhargava and Levin, 2001).

1.1.5. Applications of SLN in drug delivery

SLN play an important role in the delivery of a variety of drugs, poorly water-soluble drugs, hydrophilic drugs, such as peptides and proteins (Almeida and Souto, 2007). The many advantages already mentioned are mainly related with their nanometer size, but also with the protection of the dug from chemical and enzymatic degradation. In addition, the improvement on the bioavailability is also a reason for selecting SLN independently on the administration route. SLN changes the pharmacokinetic and biodistribution profiles of the loaded drug, and may offer a targeted delivery (Mrsny, 2012).

Depending on the administration route, SLN can overcome the many barriers for the absorption of the majority of drugs. For oral delivery, the GIT could compromise the activity of several drugs (e.g. peptides and proteins) due to the harsh environment, as well as the transcelular pathway that particles take, that leads to the uptake via M cells to the transport of the particles to the lymph (Mrsny, 2012). However, some strategies to overcome these barriers are been exploited, such as the use of permeation enhancers, modification of drug solubilization/permeability, the use of protease inhibitors to avoid proteolytic degradation and also the encapsulation techniques (Souto et al., 2013).

In the ocular delivery, the anatomy and physiology of the eye is an interesting challenging for drug delivery. For the anatomic point of view, the blood-retina barrier

for delivering drugs into the post-segment of the eye is one of the most difficult barriers to overcome. In addition, the physiologic characteristics of the eye also limit the drug delivery, due to the short drug residence time in the eye (Araújo et al., 2009). For these reasons, new drug delivery systems based on solid lipids are required for ocular purposes to facilitate drug penetration through the corneal epithelium. Strategies including positively charged SLN are been investigated due to the slightly anionic characteristics of the ocular mucosa above its isoelectric point (Araújo et al., 2009; Başaran et al., 2010; Sandri et al., 2010). This could increase particles´ adhesion onto the ocular mucosa surface and increasing drug residence time (Araújo et al., 2009).

For intravenous delivery, there are also some features, e.g. the particle size and size distribution need to be optimized to allow the circulation of particles through the vasculature. The main problem is the activation of the reticulo-endothelial system (RES), responsible for the uptake of the particles to the spleen and kidney (Yoo et al., 2011). Many strategies to overcome the particles recognition by the immune system include the use of polyethyleneglycols (PEGs) recovering the particles' surface to extend their residence time circulation in the bloodstream. This strategy also named as "stealth technology" results in long circulating particles loading active molecules with high target efficiency and activity (Cavadas et al., 2011; Moghimi et al., 2001). For brain delivery and targeting the particles have been tested, where the blood-brain barrier limits the passage of drugs. Furthermore, the surface of SLN can easily be modified offering drug targeting to tumors, the liver and the brain with many ligands (e.g. monoclonal antibodies, DNA) (Blasi et al., 2007; Harms and Müller-Goymann, 2011).

Dermal and transdermal delivery are an area of great interest for delivering drugs. The main advantages that SLN offers by this route are (i) chemical protection of drugs, (ii) modulation of release profile and, (iii) occlusive effect provided by SLN due to a formation of an occlusive adhesive lipid film (Battaglia and Gallarate, 2012). One the major barrier of the skin is the stratum corneum, which offers a protective and effective barrier to microorganisms (Neubert, 2011), and also avoids SLN permeation. SLN show good biocompatibility and biodegradability, since they are composed of lipids that figure on skin´ structure (Souto et al., 2011).

Table 1.1.2 summarizes examples of SLN formulations with respect to their therapeutic effect and administration route.

Table 1.1.2. Examples of drugs loaded in SLN and their therapeutic effect, type of lipid used in the lipid matrix, surfactants and respective administration route.

Drug	Therapeutic applications	Solid lipid	Surfactant(s)	Administration route	References
Artemether	Antimalaria	Dynasan®114	Tween® 80	Oral	(Aditya et al., 2010)
Carvedilol	Antihypertensive	Imwitor®900K	Pluronic® F 68 and , soybean phospatidylcholine	Intraduodenal	(Venishetty et al., 2012)
Clotrimazole	Antifungic	Dynasan®116	Tyloxapol	Dermal	(Souto and Müller, 2005)
Clozapine	Antipsychotic	Dynasan®114, 116 and 118	Pluronic® F 68, soybean phospatidylcholine and stearylamine	Intravenous Intraduodenal	(Manjunath and Venkateswarlu, 2005)
Cyclosporine A	Immune suppressor	Imwitor®900	Tagat S and sodium cholate	Oral	(Müller et al., 2008)
		Compritol® 888 ATO	Pluronic® F 68 and Tween® 80	Ocular	(Gokce et al., 2008)
Diazepam	Sedative, anticonvulsivant	Cetyl palmitate	Plantacare	Rectal	(Sznitowska et al., 2001)
Fluticasone	Corticosteroid anti-inflammatory	Precirol® ATO 5	Tween® 80 and soybean phosphatidylcholine	Dermal	(Doktorovova et al., 2010)
Gatifloxacin	Antibiotic	Stearic acid and Compritol® 888 ATO	Pluronic® F 68	Ocular	(Kalam et al., 2010)
Insulin	Diabetes mellitus	Softisan®100	Lipoid® S75 Pluronic® F 68	Oral	(Fangueiro et al., 2011b)

		Stearic acid and palmitic acid	Soybean phosphatidylcholine and sodium cholate	Pulmonary	(Liu et al., 2008)
Ketoconazole	Antifungic	Compritol® 888 ATO	Pluronic® F 68 and sodium deoxycholate	Dermal	(Souto and Müller, 2005)
Ketoprofen	Nonsteroidal anti-inflammatory	Beeswax and carnauba wax	Tween® 80 and egg phosphatidylcholine	n.a.	(Kheradmandnia et al., 2010)
Lopinavir	HIV infection	Compritol® 888 ATO	Pluronic® F 127	Intravenous	(Aji Alex et al., 2011)
Paclitaxel	Chemotherapeutic	Precirol® ATO 5	Tween® 80	Pulmonar	(Videira et al., 2011)
Paromomycin	Antimicrobial	Cetyl palmitate and stearic acid	Tween® 80, Span® 85	Dermal	(Ghadiri et al., 2012)
Rifampicin, isoniazid and pyrazinamide	Antitubercular	Stearic acid	PVA	Pulmonary	(Pandey and Khuller, 2005)
Saquinavir, Stavudine and Delavirdine	HIV infection	Compritol® 888 ATO, Dynasan® 116, and cacao butter	Phospatidylcholine, cholesteryl hemisuccinate, and taurocholate	n.a.	(Kuo and Chung, 2011)
Taspine	Acetylcholinesterase inhibitor	Compritol® 888	Pluronic® F 68	Intravenous	(Lu et al., 2008)
Timolol	Non-selective beta-adrenergic receptor blocker	Phospholipon 90G®	Tween®80	Ocular	(Attama et al., 2009)
Titanium dioxide	Sunscreen	Dynasan® 116	Tyloxapol®	Dermal	(Cengiz et al., 2006)
Tobramycin	Antibiotic	Stearic acid	Sodium taurocholate and Cremophor® EL	Ocular	(Cavalli et al., 2002)
Tretinoin	Potential anti-cancer drug	Precirol® ATO 5 Compritol® 888 ATO	Tween® 80	Oral	(Das et al., 2011)

		Dynasan® 114 Dynasan® 118			
Vitamin E or α-tocopherol	Anti-aging	Cetyl Palmitate	Tego Care® 450	Dermal	(Fangueiro et al., 2011a)

1.1.6.Conclusion

SLN emerged in the last decade as innovative and versatile drug delivery systems due to the many advantages they show relatively to other traditional therapies. From a physicochemical point of view, SLN are simple delivery systems based on solid lipids that could allow the delivery of many problematic drugs, such as peptides and proteins, and poorly water-soluble drugs. However, knowledge about the physicochemical parameters is important due to their influence on biopharmaceutical parameters. Even this knowledge has increased considerably, it is very important the evaluation of the interactions of drugs with the systems and the prediction of their pharmaceutical profile for the introduction of new nanocarriers. Intensive structural investigations are required to functionalize and accept SLN as new generation drugs.

1.1.7.Bibliographic References

Aditya, N. P., Patankar, S., Madhusudhan, B., Murthy, R. S. R., and Souto, E. B. (2010). Arthemeter-loaded lipid nanoparticles produced by modified thin-film hydration: Pharmacokinetics, toxicological and in vivo anti-malarial activity. *European Journal of Pharmaceutical Sciences,* 40(5), 448-455.

Aji Alex, M. R., Chacko, A. J., Jose, S., and Souto, E. B. (2011). Lopinavir loaded solid lipid nanoparticles (SLN) for intestinal lymphatic targeting. *European Journal of Pharmaceutical Sciences,* 42(1–2), 11-18.

Almeida, A. J., Runge, S., and Müller, R. H. (1997). Peptide-loaded solid lipid nanoparticles (SLN): Influence of production parameters. *International Journal of Pharmaceutics,* 149(2), 255-265.

Almeida, A. J., and Souto, E. (2007). Solid lipid nanoparticles as a drug delivery system for peptides and proteins. *Advanced Drug Delivery Reviews,* 59(6), 478-490.

Ann P, D. (2004). Development of nanotechnologies. *Materials Today,* 7(12, Supplement), 30-35.

Araújo, J., Gonzalez, E., Egea, M. A., Garcia, M. L., and Souto, E. B. (2009). Nanomedicines for ocular NSAIDs: safety on drug delivery. *Nanomedicine: Nanotechnology, Biology and Medicine,* 5(4), 394-401.

Attama, A. A., and Müller-Goymann, C. C. (2008). Effect of beeswax modification on the lipid matrix and solid lipid nanoparticle crystallinity. *Colloids and Surfaces A: Physicochemical and Engineering Aspects,* 315(1-3).

Attama, A. A., Reichl, S., and Muller-Goymann, C. C. (2009). Sustained Release and Permeation of Timolol from Surface-Modified Solid Lipid Nanoparticles through Bioengineered Human Cornea. *Current Eye Research,* 34, 698-705.

Barber, T. A. (1993). *Pharmaceutical Particulate Matter: Analysis and Control*. Buffalo Grove, III., USA: Interpharm Press, Inc.

Başaran, E., Demirel, M., Sırmagül, B., and Yazan, Y. (2010). Cyclosporine-A incorporated cationic solid lipid nanoparticles for ocular delivery. *Journal of Microencapsulation,* 27(1), 37-47.

Battaglia, L., and Gallarate, M. (2012). Lipid nanoparticles: state of the art, new preparation methods and challenges in drug delivery. *Expert Opinion in Drug Delivery*, 9(5):497-508

Battaglia, L., Gallarate, M., Cavalli, R., and Trotta, M. (2010). Solid lipid nanoparticles produced through a coacervation method. *Journal of Microencapsulation,* 27(1), 78-85.

Berne, B. J., and Pecora, R. (2000). *Dynamic light scattering: with applications to chemistry, biology, and physics*. Mineola, USA: John Wiley and Sons.

Bhargava, R., and Levin, I. W. (2001). Fourier transform infrared imaging: theory and practice. *Analytical Chemistry.,* 73, 5157-5167.

Blasi, P., Giovagnoli, S., Schoubben, A., Puglia, C., Bonina, F., Rossi, C., and Ricci, M. (2011). Lipid nanoparticles for brain targeting I. Formulation optimization. *International Journal of Pharmaceutics,* 419(1–2), 287-295.

Blasi, P., Giovagnoli, S., Schoubben, A., Ricci, M., and Rossi, C. (2007). Solid lipid nanoparticles for targeted brain drug delivery. *Advanced Drug Delivery Reviews,* 59(6), 454-477.

Bunjes, H. (2005). Characterization of Solid Lipid Nano- and Microparticles. In C. Nastruzzi (Ed.), *Lipospheres in Drug Targets and Delivery*. Florida, USA: CRC Press.

Bunjes, H., Koch, M. H. J., and Westesen, K. (2003). Influence of emulsifiers on the crystallization of solid lipid nanoparticles. *Journal of Pharmaceutical Sciences,* 92(7), 1509-1520.

Bunjes, H., and Unruh, T. (2007). Characterization of lipid nanoparticles by differential scanning calorimetry, X-ray and neutron scattering. *Advanced Drug Delivery Reviews,* 59(6), 379-402.

Carbone, C., Tomasello, B., Ruozi, B., Renis, M., and Puglisi, G. (2012). Preparation and optimization of PIT solid lipid nanoparticles via statistical factorial design. *European Journal of Medicinal Chemistry*, 49, 110-117.

Cavadas, M., González-Fernández, Á., and Franco, R. (2011). Pathogen-mimetic stealth nanocarriers for drug delivery: a future possibility. *Nanomedicine: Nanotechnology, Biology and Medicine,* 7(6), 730-743.

Cavalli, R., Gasco, M. R., Chetoni, P., Burgalassi, S., and Saettone, M. F. (2002). Solid lipid nanoparticles (SLN) as ocular delivery system for tobramycin. *International Journal of Pharmaceutics,* 238(1–2), 241-245.

Cengiz, E., Wissing, S. A., Muller, R. H., and Yazan, Y. (2006). Sunblocking efficiency of various TiO(2)-loaded solid lipid nanoparticle formulations. *International Journal of Cosmetic Science,* 28(5), 371-378.

Christian, G. D., and O´Reilly, J. E. (1986). *Instrumental Analysis* (2nd Edition ed.). Boston, USA: Allyn and Bacon.

Corrias, F., and Lai, F. (2011). New methods for lipid nanoparticles preparation. *Recent Patents on Drug Delivery and Formulation,* 5(3), 212-213.

Coutts-Lendon, C. A., Wright, N. A., Mieso, E. V., and Koenig, J. L. (2003). The use of FT-IR imaging as an analytical tool for the characterization of drug delivery systems. *Journal of Controlled Release,* 93(3), 223-248.

Cui, Z., Qiu, F., and Sloat, B. R. (2006). Lecithin-based cationic nanoparticles as a potential DNA delivery system. *International Journal of Pharmaceutics,* 313(1-2), 206-213.

Das, S., Ng, W. K., Kanaujia, P., Kim, S., and Tan, R. B. H. (2011). Formulation design, preparation and physicochemical characterizations of solid lipid nanoparticles containing a hydrophobic drug: Effects of process variables. *Colloids and Surfaces B: Biointerfaces,* 88(1), 483-489.

del Pozo-Rodríguez, A., Delgado, D., Solinís, M. A., Gascón, A. R., and Pedraz, J. L. (2008). Solid lipid nanoparticles for retinal gene therapy: Transfection and intracellular trafficking in RPE cells. *International Journal of Pharmaceutics,* 360(1–2), 177-183.

del Pozo-Rodríguez, A., Delgado, D., Solinís, M. Á., Pedraz, J. L., Echevarría, E., Rodríguez, J. M., and Gascón, A. R. (2010). Solid lipid nanoparticles as potential tools for gene therapy: In vivo protein expression after intravenous administration. *International Journal of Pharmaceutics,* 385(1–2), 157-162.

Doktorovova, S., Araujo, J., Garcia, M. L., Rakovsky, E., and Souto, E. B. (2010). Formulating fluticasone propionate in novel PEG-containing nanostructured lipid carriers (PEG-NLC). *Colloids and Surfaces B: Biointerfaces,* 75(2), 538-542.

Doktorovova, S., Shegokar, R., Martins-Lopes, P., Silva, A. M., Lopes, C. M., Müller, R. H., and Souto, E. B. (2012). Modified Rose Bengal assay for surface hydrophobicity

evaluation of cationic solid lipid nanoparticles (cSLN). *European Journal of Pharmaceutical Sciences,* 45(5), 606-612.

Doktorovova, S., Shegokar, R., Rakovsky, E., Gonzalez-Mira, E., Lopes, C. M., Silva, A. M., Souto, E. B. (2011). Cationic solid lipid nanoparticles (cSLN): Structure, stability and DNA binding capacity correlation studies. *International Journal of Pharmaceutics,* 420(2), 341-349.

Dong, X., and Mumper, R. J. (2006). The metabolism of fatty alcohols in lipid nanoparticles by alcohol dehydrogenase. *Drug Development* and *Industrial Pharmacy,* 32(8), 973-980.

Dong, Y., Ng, W. K., Shen, S., Kim, S., and Tan, R. B. H. (2012). Solid lipid nanoparticles: Continuous and potential large-scale nanoprecipitation production in static mixers. *Colloids and Surfaces B: Biointerfaces,* 94, 68-72.

Dowling, A., Clift, R., Grobert, N., Hutton, D., Oliver, R., O'neill, O., Whatmore, R. (2004). Nanoscience and Nanotechnologies: Opportunities and Uncertainties. *The Royal Society and the Royal Academy of Engineering.*

Dreher, F., Walde, P., Walther, P., and Wehrli, E. (1997). Interaction of a lecithin microemulsion gel with human stratum corneum and its effect on transdermal transport. *Journal of Controlled Release,* 45(2), 131-140.

Dubes, A., Parrot-Lopez, H. l. n., Abdelwahed, W., Degobert, G., Fessi, H., Shahgaldian, P., and Coleman, A. W. (2003). Scanning electron microscopy and atomic force microscopy imaging of solid lipid nanoparticles derived from amphiphilic cyclodextrins. *European Journal of Pharmaceutics and Biopharmaceutics,* 55(3), 279-282.

Eshel, G., Levy, G. J., Mingelgrin, U., and Singer, M. J. (1991). Critical Evaluation of the Use of Laser Diffraction for Particle-Size Distribution Analysis. *Soil Science Society of America Journal,* 68(3), 736-743.

Fangueiro, J., Macedo, A., Jose, S., Garcia, M., Souto, S., and Souto, E. (2011a). Thermodynamic behavior of lipid nanoparticles upon delivery of Vitamin E derivatives into the skin: in vitro studies. *Journal of Thermal Analysis and Calorimetry,* 108(1), 275-282.

Fangueiro, J. F., Gonzalez-Mira, E., Martins-Lopes, P., Egea, M. A., Garcia, M. L., Souto, S. B., and Souto, E. B. (2011a). A novel lipid nanocarrier for insulin delivery: production, characterization and toxicity testing. *Pharmaceutical Development and Technology,* 18(3), 545-549.

Filion, M. C., and Phillips, N. C. (1997). Anti-inflammatory activity of cationic lipids. *British Journal of Pharmacology,* 122(3), 551-557.

Fontana, G., Maniscalco, L., SchilIaci, D., Cavallaro, G., and Giammona, G. (2005). Preparation, characterization and in vitro antitumoral activity of solid lipid nanoparticles (SLN) containing tamoxifen. *Drug Delivery,* 12(6), 385-392.

Ford, J. L., and Mann, T. E. (2011). Fast-Scan DSC and its role in pharmaceutical physical form characterisation and selection. *Advanced Drug Delivery Reviews,* 64(5), 422-430.

Friedrich, H., Frederik, P. M., de With, G., and Sommerdijk, N. A. J. M. (2010). Imaging of self-assembled structures: interpretation of TEM and cryo-TEM images. *Angewandte Chemie International Edition,* 49, 7850-7858.

Garcia-Fuentes, M., Torres, M. R., and Alonso, J. M. (2002). Design of lipid nanoparticles for the oral delivery of hydrophilic macromolecules. *Colloids and Surfaces B: Biointerfaces,* 27, 159-168.

Gasco, M. R. (1997). Solid lipid nanospheres from warm microemulsion. *Pharmaceutical Technology* Europe, 9, 52-58.

Geisse, N. A. (2009). AFM and combined optical techniques. *Materials Today,* 12(7-8), 40-45.

Gethner, J. S., and Gaskin, F. (1978). Dynamic Light Scattering from solutions of microtubules. *Biophysical Journal,* 24, 505-515.

Ghadiri, M., Fatemi, S., Vatanara, A., Doroud, D., Najafabadi, A. R., Darabi, M., and Rahimi, A. A. (2012). Loading hydrophilic drug in solid lipid media as nanoparticles: Statistical modeling of entrapment efficiency and particle size. *International Journal of Pharmaceutics,* 424(1–2), 128-137.

Gill, P., Moghadam, T. T., and Ranjbar, B. (2010). Differential Scanning Calorimetry Techniques: Applications in Biology and Nanoscience. *The Journal of Biomolecular Techniques,* 21(4), 167-193.

Gokce, E. H., Sandri, G., Bonferoni, M. C., Rossi, S., Ferrari, F., Güneri, T., and Caramella, C. (2008). Cyclosporine A loaded SLNs: Evaluation of cellular uptake and corneal cytotoxicity. *International Journal of Pharmaceutics,* 364(1), 76-86.

Harms, M., and Müller-Goymann, C. C. (2011). Solid lipid nanoparticles for drug delivery. *Journal of Drug Delivery Science and Technology,* 21(1), 89-99.

Heike, B. (2011). Structural properties of solid lipid based colloidal drug delivery systems. *Current Opinion in Colloid and Interface Science,* 16(5), 405-411.

Heurtault, B., Saulnier, P., Pech, B., Proust, J.-E., and Benoit, J.-P. (2003). Physico-chemical stability of colloidal lipid particles. *Biomaterials,* 24(23), 4283-4300.

Heurtault, B., Saulnier, P., Pech, B., Proust, J. E., and Benoit, J. P. (2002). A novel phase inversion-based process for the preparation of lipid nanocarriers. *Pharmaceutical Research*, 19(6), 875-880.

Hiemenz, P. C., and Rajagopalan, R. (1997). *Principles of Colloid and Surface Chemistry* (3rd ed.). New York, USA: Marcel Dekker, Inc.

Hu, F. Q., Yuan, H., Zhang, H. H., and Fang, M. (2002). Preparation of solid lipid nanoparticles with clobetasol propionate by a novel solvent diffusion method in aqueous system and physicochemical characterization. *International Journal of Pharmaceutics*, 239(1–2), 121-128.

Jenknins, R. (2000). X-ray Techniques: Overview. In R. A. Meyers (Ed.), *Encyclopedia of Analytical Chemistry* (pp. 1-20). Chichester: John Wiley and Sons Ltd.

Jenning, V., and Gohla, S. (2000). Comparison of wax and glyceride solid lipid nanoparticles (SLN®). *International Journal of Pharmaceutics*, 196(2), 219-222.

Kalam, M. A., Sultana, Y., Ali, A., Aqil, M., Mishra, A. K., and Chuttani, K. (2010). Preparation, characterization, and evaluation of gatifloxacin loaded solid lipid nanoparticles as colloidal ocular drug delivery system. *Journal of Drug Targeting*, 18(3), 191-204.

Kaneko, F. (2001). Polymorphism and Phase Transitions of Fatty Acids and Acylglycerols. In N. Garti and K. Sato (Eds.), *Crystallization Processes in Fats and Lipid Systems* (pp. 53-98). New York, USA

Kheradmandnia, S., Vasheghani-Farahani, E., Nosrati, M., and Atyabi, F. (2010). Preparation and characterization of ketoprofen-loaded solid lipid nanoparticles made from beeswax and carnauba wax. *Nanomedicine: Nanotechnology, Biology and Medicine*, 6(6), 753-759.

Kim, B.-D., Na, K., and Choi, H.-K. (2005). Preparation and characterization of solid lipid nanoparticles (SLN) made of cacao butter and curdlan. *European Journal of Pharmaceutical Sciences*, 24(2–3), 199-205.

Kratky, O. (1982). Part I - Introduction. In O. Kratky and O. Glatter (Eds.), *Small Angle X-ray Scattering* (pp. 3-15). London, UK: Academic Press Inc.

Kuntsche, J., Horst, J. C., and Bunjes, H. (2011). Cryogenic transmission electron microscopy (cryo-TEM) for studying the morphology of colloidal drug delivery systems. *International Journal of Pharmaceutics*, 417, 120-137.

Kuo, Y.-C., and Chen, H.-H. (2009). Entrapment and release of saquinavir using novel cationic solid lipid nanoparticles. *International Journal of Pharmaceutics*, 365(1–2), 206-213.

Kuo, Y.-C., and Chung, C.-Y. (2011). Solid lipid nanoparticles comprising internal Compritol 888 ATO, tripalmitin and cacao butter for encapsulating and releasing stavudine, delavirdine and saquinavir. *Colloids and Surfaces B: Biointerfaces,* 88(2), 682-690.

Kuo, Y.-C., and Lin, C.-W. (2009). Effect of electromagnetic field and surface modification on the electrical behavior of novel solid lipid nanoparticles covered with l-arginine. *Colloids and Surfaces B: Biointerfaces,* 71(1), 45-51.

Kuo, Y.-C., and Wang, C.-C. (2010). Electrophoresis of human brain microvascular endothelial cells with uptake of cationic solid lipid nanoparticles: Effect of surfactant composition. *Colloids and Surfaces B: Biointerfaces,* 76(1), 286-291.

Liu, J., Gong, T., Fu, H., Wang, C., Wang, X., Chen, Q., Zhang, Z. (2008). Solid lipid nanoparticles for pulmonary delivery of insulin. *International Journal of Pharmaceutics,* 356(1–2), 333-344.

Lu, W., He, L. C., Wang, C. H., Li, Y. H., and Zhang, S. Q. (2008). The use of solid lipid nanoparticles to target a lipophilic molecule to the liver after intravenous administration to mice. *International Journal of Biological Macromolecules,* 43(3), 320-324.

Ma, Z., Merkus, H. G., de Smet, J. G. A. E., Heffels, C., and Scarlett, B. (2000). New developments in particle characterization by laser diffraction: size and shape. *Powder Technology,* 111(1–2), 66-78.

Manjunath, K., and Venkateswarlu, V. (2005). Pharmacokinetics, tissue distribution and bioavailability of clozapine solid lipid nanoparticles after intravenous and intraduodenal administration. *Journal of Controlled Release,* 107(2), 215-228.

Martins, S., Tho, I., Souto, E., Ferreira, D., and Brandl, M. (2012). Multivariate design for the evaluation of lipid and surfactant composition effect for optimisation of lipid nanoparticles. *European Journal of Pharmaceutical Sciences,* 45(5), 613-623.

McCauley, J. A., and Brittain, H. G. (1995). Thermal Methods of Analysis. In H. G. Brittain (Ed.), *Physical Characterization of Pharmaceutical Solids* (pp. 224-250). New York, USA: Marcel Dekker.

McElhaney, R. N. (1982). The use of differential scanning calorimetry and differential thermal analysis in studies of model and biological membranes. *Chemistry and Physics of Lipids,* 30(2–3), 229-259.

Mishra, B., Patel, B. B., and Tiwari, S. (2010). Colloidal nanocarriers: a review on formulation technology, types and applications toward targeted drug delivery. *Nanomedicine,* 6(1), 9-24.

Moghimi, S. M., Hunter, A. C., and Murray, J. C. (2001). Long-Circulating and Target-Specific Nanoparticles: Theory to Practice. *Pharmacological Reviews,* 53(2), 283-318.

Mrsny, R. J. (2012). Perspective: Oral drug delivery research in Europe. *Journal of Controlled Release,* 161(2), 247-253.

Mühlen, A. z., Mühlen, E. z., Niehus, H., and Mehnert, W. (1996). Atomic Force Microscopy Studies of Solid Lipid Nanoparticles. *Pharmaceutical Research,* 13(9), 1411-1416.

Muller-Goymann, C. C. (2004). Physicochemical characterization of colloidal drug delivery systems such as reverse micelles, vesicles, liquid crystals and nanoparticles for topical administration. *European Journal of Pharmaceutics and Biopharmaceutics,* 58(2), 343-356.

Müller, R. H., Mäder, K., and Gohla, S. (2000). Solid lipid nanoparticles (SLN) for controlled drug delivery – a review of the state of the art. *European Journal of Pharmaceutics and Biopharmaceutics,* 50(1), 161-177.

Müller, R. H., Runge, S. A., Ravelli, V., Thünemann, A. F., Mehnert, W., and Souto, E. B. (2008). Cyclosporine-loaded solid lipid nanoparticles (SLN®): Drug–lipid physicochemical interactions and characterization of drug incorporation. *European Journal of Pharmaceutics and Biopharmaceutics,* 68(3), 535-544.

Nassimi, M., Schleh, C., Lauenstein, H. D., Hussein, R., Hoymann, H. G., Koch, W., Müller-Goymann, C. (2010). A toxicological evaluation of inhaled solid lipid nanoparticles used as a potential drug delivery system for the lung. *European Journal of Pharmaceutics and Biopharmaceutics,* 75(2), 107-116.

Neubert, R. H. H. (2011). Potentials of new nanocarriers for dermal and transdermal drug delivery. *European Journal of Pharmaceutics and Biopharmaceutics,* 77(1), 1-2.

Noack, A., Hause, G., and Mäder, K. (2011). Physicochemical characterization of curcuminoid-loaded solid lipid nanoparticles. *International Journal of Pharmaceutics,* 423(2), 440-445.

Olbrich, C., Bakowsky, U., Lehr, C.-M., Müller, R. H., and Kneuer, C. (2001). Cationic solid-lipid nanoparticles can efficiently bind and transfect plasmid DNA. *Journal of Controlled Release,* 77(3), 345-355.

Olbrich, C., Kayser, O., and MÃ¼ller, R. H. (2002). Lipase degradation of Dynasan 114 and 116 solid lipid nanoparticles (SLN)â€”effect of surfactants, storage time and crystallinity. *International Journal of Pharmaceutics,* 237(1-2), 119-128.

Pandey, R., and Khuller, G. K. (2005). Solid lipid particle-based inhalable sustained drug delivery system against experimental tuberculosis. *Tuberculosis,* 85(4), 227-234.

Patel, P., A. , and Patravale, V., B. (2011). AmbiOnp: solid lipid nanoparticles of amphotericin B for oral administration. *Journal of Biomedical Nanotechnology,* 7(5), 632-639.

Pedersen, N., Hansen, S., Heydenreich, A. V., Kristensen, H. G., and Poulsen, H. S. (2006). Solid lipid nanoparticles can effectively bind DNA, streptavidin and biotinylated ligands. *European Journal of Pharmaceutics and Biopharmaceutics,* 62(2), 155-162.

Petersen, S., Steiniger, F., Fischer, D., Fahr, A., and Bunjes, H. (2011). The physical state of lipid nanoparticles influences their effect on in vitro cell viability. *European Journal of Pharmaceutics and Biopharmaceutics,* 79(1), 150-161.

Quintanar-Guerrero, D., Allémann, E., Fessi, H., and Doelker, E. (1999). Pseudolatex preparation using a novel emulsion–diffusion process involving direct displacement of partially water-miscible solvents by distillation. *International Journal of Pharmaceutics,* 188(2), 155-164.

Rahman, Z., Zidan, A. S., and Khan, M. A. (2010). Non-destructive methods of characterization of risperidone solid lipid nanoparticles. *European Journal of Pharmaceutics and Biopharmaceutics,* 76(1), 127-137.

Renliang, X. (2008). Progress in nanoparticles characterization: Sizing and zeta potential measurement. *Particuology,* 6(2), 112-115.

Rosen, M. J. (2004). *Surfactants and Interfacial Phenomena* (Third Edition ed.). New Jersey, USA: John Wiley and Sons, Inc.

Sandri, G., Bonferoni, M. C., Gökçe, E. H., Ferrari, F., Rossi, S., Patrini, M., and Caramella, C. (2010). Chitosan-associated SLN: in vitro and ex vivo characterization of cyclosporine A loaded ophthalmic systems. *Journal of Microencapsulation,* 27(8), 735-746.

Sanna, V., Caria, G., and Mariani, A. (2010). Effect of lipid nanoparticles containing fatty alcohols having different chain length on the ex vivo skin permeability of Econazole nitrate. *Powder Technology,* 201(1), 32-36.

Sarmento, B., Mazzaglia, D., Bonferoni, M. C., Neto, A. P., do Céu Monteiro, M., and Seabra, V. (2011). Effect of chitosan coating in overcoming the phagocytosis of insulin loaded solid lipid nanoparticles by mononuclear phagocyte system. *Carbohydrate Polymers,* 84(3), 919-925.

Schubert, M. A., Harms, M., and MÃ¼ller-Goymann, C. C. (2006). Structural investigations on lipid nanoparticles containing high amounts of lecithin. *European Journal of Pharmaceutical Sciences,* 27(2-3), 226-236.

Schubert, M. A., and Muller-Goymann, C. C. (2005). Characterisation of surface-modified solid lipid nanoparticles (SLN): Influence of lecithin and nonionic emulsifier. *European Journal of Pharmaceutics and Biopharmaceutics,* 61(1-2), 77-86.

Severino, P., Andreani, T., Macedo, A., Fangueiro, J. F., Santana, M., H.,, Silva, A. M., and Souto, E. B. (2012). Current State-of-Art and New Trends on Lipid Nanoparticles (SLN and NLC) for Oral Drug Delivery. *Journal of Drug Delivery,* doi: 10.1155/2012/750891.

Severino, P., Pinho, S. C., Souto, E. B., and Santana, M. H. A. (2011). Polymorphism, crystallinity and hydrophilic–lipophilic balance of stearic acid and stearic acid–capric/caprylic triglyceride matrices for production of stable nanoparticles. *Colloids and Surfaces B: Biointerfaces,* 86(1), 125-130.

Shahgaldian, P., Quattrocchi, L., Gualbert, J., Coleman, A. W., and Goreloff, P. (2003). AFM imaging of calixarene based solid lipid nanoparticles in gel matrices. *European Journal of Pharmaceutics and Biopharmaceutics,* 55(1), 107-113.

Shchukin, E. D., Pertsov, A. V., and Amelina, E. A. (2001). *Colloid and Surface Chemistry*. Amsterdam, The Netherlands: Elsevier Science B. V.

Sinha, V. R., Srivastava, S., Goel, H., and Jindal, V. (2011). Solid Lipid Nanoparticles (SLN´s) - Trends and Implications in Drug Targeting. *International Journal of Advances in Pharmaceutical Sciences,* 1, 212-238.

Sivaramakrishnan, R., Nakamura, C., Mehnert, W., Korting, H. C., Kramer, K. D., and Schäfer-Korting, M. (2004). Glucocorticoid entrapment into lipid carriers — characterisation by parelectric spectroscopy and influence on dermal uptake. *Journal of Controlled Release,* 97(3), 493-502.

Sjöström, B., and Bergenstahl, B. (1992). Preparation of submicron drug particles in lecithin-stabilized o/w emulsions I. Model studies of the precipitation of cholestreryl acetate. *International Journal of Pharmaceutics,* 88, 53-62.

Souto, E. B., and Doktorovova, S. (2009). Chapter 6 - Solid lipid nanoparticle formulations pharmacokinetic and biopharmaceutical aspects in drug delivery. *Methods in Enzymology,* 464, 105-129.

Souto, E. B., Doktorovova, S., and Boonme, P. (2011). Lipid-based colloidal systems (nanoparticles, microemulsions) for drug delivery to the skin: materials and end-product formulations. *Journal of Drug Delivery Science and Technology,* 21(1), 43-54.

Souto, E. B., Mehnert, W., and Müller, R. H. (2006). Polymorphic behaviour of Compritol 888 ATO as bulk lipid and as SLN and NLC. *Journal of Microencapsulation,* 23(4), 417-433.

Souto, E. B., and Muller, R. H. (2006). Investigation of the factors influencing the incorporation of clotrimazole in SLN and NLC prepared by hot high-pressure homogenization. *Journal of Microencapsulation,* 23(4), 377-388.

Souto, E. B., and Muller, R. H. (2010). Lipid nanoparticles: effect on bioavailability and pharmacokinetic changes. *The Handbook* of Experimental *Pharmacology,* (197), 115-141.

Souto, E. B., and Muller, R. H. (2011). Solid Lipid Nanoparticles and Nanostructures Lipid Carriers - Lipid Nanoparticles for Medicals and Pharmaceuticals. *Encyclopedia of Nanoscience and Nanotechnology,* 23, 313-328.

Souto, E. B., and Müller, R. H. (2005). The use of SLN® and NLC® as topical particulate carriers for imidazole antifungal agents. *Die Pharmazie,* 61(5), 431-437.

Souto, E. B., and Müller, R. H. (2007). Lipid Nanoparticles (SLN and NLC) for Drug Delivery. In J. Domb, Y. Tabata, M. N. V. R. Kumar and S. Farber (Eds.), *Nanoparticles for Pharmaceutical Applications* (Vol. 5, pp. 103-122): American Scientific Publishers.

Souto, E. B., Severino, P., Basso, R., and Santana, M. H. (2013). Encapsulation of antioxidants in gastrointestinal-resistant nanoparticulate carriers. *Methods in Molecular Biology,* 1028, 37-46.

Souto, E. B., Wissing, S. A., Barbosa, C. M., and Muller, R. H. (2004a). Comparative study between the viscoelastic behaviors of different lipid nanoparticle formulations. *Journal of Cosmetic Science,* 55, 463-471.

Souto, E. B., Wissing, S. A., Barbosa, C. M., and Müller, R. H. (2004b). Evaluation of the physical stability of SLN and NLC before and after incorporation into hydrogel formulations. *European Journal of Pharmaceutics and Biopharmaceutics,* 58(1), 83-90.

Sznitowska, M., Gajewska, M., Janicki, S., Radwanska, A., and Lukowski, G. (2001). Bioavailability of diazepam from aqueous-organic solution, submicron emulsion and solid lipid nanoparticles after rectal administration in rabbits. *European Journal of Pharmaceutics and Biopharmaceutics,* 52(2), 159-163.

Tabatt, K., Kneuer, C., Sameti, M., Olbrich, C., Müller, R. H., Lehr, C.-M., and Bakowsky, U. (2004). Transfection with different colloidal systems: comparison of solid lipid nanoparticles and liposomes. *Journal of Controlled Release,* 97(2), 321-332.

Venishetty, V. K., Chede, R., Komuravelli, R., Adepu, L., Sistla, R., and Diwan, P. V. (2012). Design and evaluation of polymer coated carvedilol loaded solid lipid nanoparticles to improve the oral bioavailability: A novel strategy to avoid intraduodenal administration. *Colloids and Surfaces B: Biointerfaces,* 95, 1-9.

Videira, M., Almeida, A. J., and Fabra, À. (2011). Preclinical evaluation of a pulmonary delivered paclitaxel-loaded lipid nanocarrier antitumor effect. *Nanomedicine: Nanotechnology, Biology and Medicine,* 8(7), 1208-1215.

Videira, M. A., Botelho, M. F., Santos, A. C., Gouveia, L. F., de Lima, J. J., and Almeida, A. J. (2002). Lymphatic uptake of pulmonary delivered radiolabelled solid lipid nanoparticles. *Journal of Drug Targeting,* 10(8), 607-613.

Vieira, V., Fangueiro, J. F., Silva, A. M., and Souto, E. B. (2012). *Characterization of the physicochemical performance of nimesulide-loaded lipid nanoparticulates.* Paper presented at the 3rd Scientific Meeting of the Institute for Biotechnology and Bioengineering, Lisbon, Portugal.

Vighi, E., Ruozi, B., Montanari, M., Battini, R., and Leo, E. (2007). Re-dispersible cationic solid lipid nanoparticles (SLNs) freeze-dried without cryoprotectors: Characterization and ability to bind the pEGFP-plasmid. *European Journal of Pharmaceutics and Biopharmaceutics,* 67(2), 320-328.

Vighi, E., Ruozi, B., Montanari, M., Battini, R., and Leo, E. (2010). pDNA condensation capacity and in vitro gene delivery properties of cationic solid lipid nanoparticles. *International Journal of Pharmaceutics,* 389(1-2), 254-261.

Westesen, K., Bunjes, H., and Koch, M. H. J. (1997). Physicochemical characterization of lipid nanoparticles and evaluation of their drug loading capacity and sustained release potential. *Journal of Controlled Release,* 48(2-3), 223-236.

Westesen, K., Siekmann, B., and Koch, M. H. J. (1993). Investigations on the physical state of lipid nanoparticles by synchrotron radiation X-ray diffraction. *International Journal of Pharmaceutics,* 93(1-3), 189-199.

Wiechers, J., and Souto, E. B. (2010). Solid Lipid Nanoparticles (SLNs) and Nanostructured Lipid Carriers (NLCs) as Novel Delivery Systems for Cosmetic Actives. Part I. *Cosmetics and Toiletries,* 10, 22-30.

Wissing, S. A., Kayser, O., and Muller, R. H. (2004). Solid lipid nanoparticles for parenteral drug delivery. *Advanced Drug Delivery Reviews,* 56(9), 1257-1272.

Yang, W., Peters, J. I., and Williams Iii, R. O. (2008). Inhaled nanoparticles—A current review. *International Journal of Pharmaceutics,* 356(1-2), 239-247.

Yoo, J.-W., Doshi, N., and Mitragotri, S. (2011). Adaptive micro and nanoparticles: Temporal control over carrier properties to facilitate drug delivery. *Advanced Drug Delivery Reviews,* 63(14-15), 1247-1256.

Zhang, Q., Yie, G., Li, Y., Yang, Q., and Nagai, T. (2000). Studies on the cyclosporin A loaded stearic acid nanoparticles. *International Journal of Pharmaceutics,* 200(2), 153-159.

Zhang, S.-h., Shen, S.-c., Chen, Z., Yun, J.-x., Yao, K.-j., Chen, B.-b., and Chen, J.-z. (2008). Preparation of solid lipid nanoparticles in co-flowing microchannels. *Chemical Engineering Journal*, 144(2), 324-328.

CHAPTER 1.2 - CURRENT NANOTECHNOLOGY APPROACHES FOR THE TREATMENT AND MANAGEMENT OF DIABETIC RETINOPATHY

Joana F. Fangueiro[1,2], Amélia M. Silva[3,4], Maria L. Garcia[5,6], Eliana B. Souto[7*]

[1]CEBIMED, Researh Centre for Biomedicine, FP-ENAS, Fernando Pessoa University, Praça 9 de Abril, 349, 4249-004 Porto, Portugal

[2]Faculty of Health Sciences, Fernando Pessoa University (UFP-FCS), Rua Carlos da Maia, 296, 4200-150 Porto, Portugal

[3]Centre for Research and Technology of Agro-Environmental and Biological Sciences, CITAB, University of Trás-os-Montes e Alto Douro, UTAD, Quinta de Prados, 5000-801 Vila Real, Portugal

[4]Department of Biology and Environment, University of Trás-os-Montes e Alto Douro, UTAD, Quinta de Prados, 5000-801 Vila Real, Portugal

[5]Department of Physical Chemistry, Faculty of Pharmacy, University of Barcelona, Av. Joan XXIII s/n, 08028 Barcelona, Spain

[6]Institute of Nanoscience and Nanotechnology, University of Barcelona, Av. Joan XXIII s/n, 08028 Barcelona, Spain

[7] Faculty of Pharmacy, University of Coimbra (FFUC), Pólo das Ciências da Saúde, Azinhaga de Santa Comba, 3000-548 Coimbra, Portugal

Published in *European Journal of Pharmaceutics and Biopharmaceutics*, 2015, 95(Pt B):307-22.

CHAPTER 1.2 - Current nanotechnology approaches for the treatment and management of Diabetic Retinopathy

Abstract

Diabetic Retinopathy (DR) is a consequence of diabetes mellitus at the ocular level, leading to vision loss, and contributing to the decrease of patient's life quality. The biochemical and anatomic abnormalities that occurs in DR are discussed in this review to better understand and manage the development of new therapeutic strategies. The use of new drug delivery systems based on nanoparticles (e.g. liposomes, dendrimers, cationic nanoemulsions, lipid and polymeric nanoparticles) is discussed along with the current traditional treatments, pointing out the advantages of the proposed nanomedicines to target this ocular disease. Despite the multifactorial nature of DR, which is not entirely understood, some strategies based on nanoparticles are being exploited for a more efficient drug delivery to the posterior segment of the eye. On the other hand, the use of some nanoparticles also seems to contribute to the development of DR symptoms (e.g. retinal neovascularization), which are also discussed in the light of an efficiently management of this ocular chronic disease.

1.2.1.Introduction

Diabetes mellitus is a chronic disease that affects billions of people all over the world, and results from the body's inability to either produce or use insulin. This disease is mainly associated with high levels of glucose in the blood, i.e. hyperglycemia. It can be classified in two chronic forms, namely: (i) Type 1, which is diagnosed earlier usually in children and youth, and is characterized by the deficiency in the production of insulin. In this case, there is a destruction of islet beta cells mostly attributed to auto-immune etiology; or (ii) Type 2, which has higher incidence (≈90-95% of the cases) and it is characterized by the reduced production of insulin and/or by insulin resistance, affecting mainly muscle, liver and adipose tissue, resulting on inappropriate levels of circulating

glucose. There is a third form of diabetes, the gestational diabetes, which is observed during pregnancy in a small number of women caused by interference of placental hormones interference with insulin receptor resulting in inappropriate elevated glucose levels (Madsen-Bouterse and Kowluru, 2008).

The inability of the body to use glucose resulting from the deficiency of the hormone responsible for its use (i.e. insulin), leads to constant hyperglycemia which results in many chronic effects, such as macro- and microvascular complications associated with heart disease, stroke and peripheral arterial diseases. The constant hyperglycemia causes damage in the small blood vessels, which affects the ocular, nervous and renal system. That is why it is of utmost relevance to control diabetes and its consequences, to prevent retinopathy, neuropathy and nephropathy complications (Madsen-Bouterse and Kowluru, 2008).

Diabetic retinopathy (DR) is one of the major consequences of diabetes and it is characterized by microvascular complications having a significant impact on patient´s life quality, in particular, in visual acuity, eventually leading to blindness (Ciulla et al., 2003). Diabetic patients, both type 1 and 2, are regularly screened for retinopathy with an initial dilated and comprehensive eye examination by an ophthalmologist. Even patients with a very rigorous control of diabetes, are not free from developing DR (Zhu and Zou, 2012).

In order to prevent and reverse diabetic side effects, such as retinopathy, several strategies have been used to prevent the chronic disease with modern and innovative systems based on nanoparticles which are addresses in this review. Nanoparticles may be applied for several clinical purposes. When applying this concept in medicine, it is called nanomedicine. In drug delivery, nanoparticles (1-1000 nm) are used for the treatment and/or prevention of diseases, with the finally goal to spam patient's life-time. Regarding these goals, nanoparticles offer numerous advantages, compared to treatments with drugs alone or even with classic delivery systems. The majority of the drugs show problems including (i) low solubility in solvents; (ii) high toxicity; (iii) need of high doses to exhibit therapeutic effect; (iv) aggregation; (v) enzymatic and chemical degradation and (vi) reduced half-time. Thus, the loading of drugs into nanoparticles could overcome

these limitations and additionally provide (i) sustained delivery; (ii) targeted delivery to specific cells or tissues; (iii) improved delivery of both water-insoluble drugs and large biomolecule drugs, and (iv) reduced side effects minimizing toxicological reactions (Fangueiro et al., 2013; Souto et al., 2013a).

This paper reviews the diabetes-induced mechanisms involved in the course of DR, a knowledge that is fundamental in the design of new therapeutic strategies. The contribution of nanomedicine to treat and manage DR and its microvascular changes is also discussed.

1.2.2.Diabetic Retinopathy

1.2.2.1. Concepts

DR is potentially caused by sustained hyperglycemia and the consequences occurring in the minor vascular retinal vessels (Porta and Bandello, 2002). DR is also characterized by the abnormal growth of new blood vessels resulting from a hypoxic retina, in order to improve the supply of oxygen (Rechtman et al., 2007).

According to the international classification system, DR is divided into two broad categories, namely, the non-proliferative DR (NPDR) and the proliferative DR (PDR) (Wilkinson et al., 2003). NPDR is further subdivided into mild, moderate, and severe. This classification system considers the number and severity of anatomical abnormalities, which include: (i) microaneurysms; (ii) hemorrhages; (iii) venous beading, and (iv) intra-retinal microvascular abnormalities (IRMA), when attributing to the eyes a particular level of severity (Davidson et al., 2007). The international classification of DR is summarized in Table 1.2.1. An ophthalmologist could detect the DR by the analysis of these symptoms, in parallel with additional exams, such as visual acuity test, dilated eye exam and tonometry, which measures the intraocular pressure (IOP) (Ciulla et al., 2003).

Table 1.2.1. International Clinical DR disease severity scale (Wilkinson et al., 2003).

Proposed disease Severity Level	Dilated Ophthalmoscopy Findings
No apparent retinopathy	*No abnormalities*
Mild non-proliferative DR	*Microaneurysms only*
Moderate non-proliferative DR	*More than just microaneurysms, but less than severe NPDR*
Severe non-proliferative DR	*No signs of PDR, with any of the following:* – More than 20 intra-retinal hemorrhages in each of – four quadrants – Definite venous beading in two or more – quadrants – Prominent intra-retinal microvascular anomalies in one or more quadrants
PDR	*One or more of the following:* – Neovascularization – Vitreous or preretinal hemorrhage

Retina is the anatomical structure of the eye affected in the DR. Physiologically it is the light-sensitive tissue located at the back of the eye, it is characterized by a thin transparent structure composed by several layers comprising the light-sensitive structures. It is enriched in polyunsaturated fatty acids and is metabolically very active having high glucose oxidation and oxygen uptake (Anderson et al., 1984). The schematic structure of the human eye and the ocular globe is shown in Figure 1.2.1. The cells figuring in retina are divided in three major groups, namely, (i) the neuronal component, which includes photoreceptors, interneurons, and ganglion cells, responsible for retinal visual function

which converts light into electrical signals; (ii) the glial components, Muller cells, astrocytes and resident macrophages (microglia), which are responsible for retina support (e.g., nutritional, regulatory); and (iii) the vascular components, which consist of the central retinal artery, supplying the inner and outer retina by diffusion from choroidal circulation. The retinal vessels are responsible for the maintenance of blood-retinal barrier (BRB) and are composed of endothelial cells with tight junctions between them (Kowluru, 2005; Rechtman et al., 2007). Pericytes or mural cells are another type of contractible cells surrounding the capillaries endothelial cells. The main function of these cells is the regulation of retinal capillary perfusion and its loss is associated with DR. Diabetes will affect both neuronal and vascular components of the retina and will influence some cells and extracellular proteins (Ciulla et al., 2003; Crawford et al., 2009).

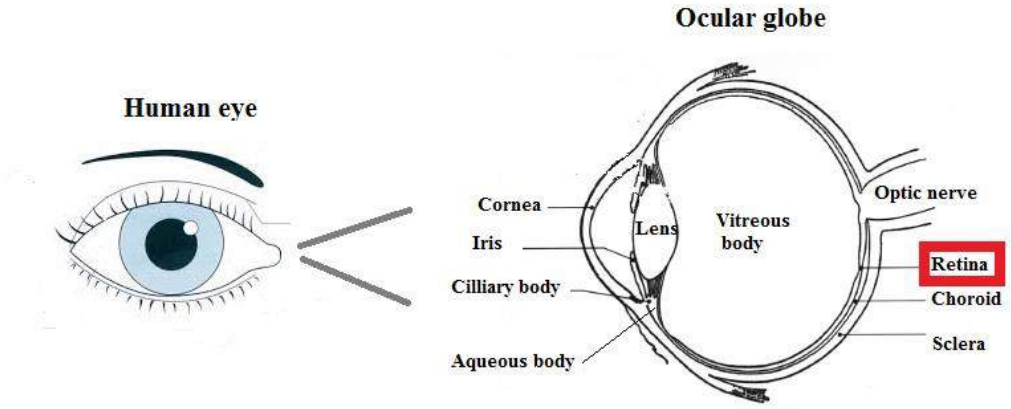

Figure 1.2.1. Schematic illustration of the human eye and its main physiological structures. Retina is the ocular structure affected by the development of DR and is located in the posterior segment of the eye.

1.2.2.2. Pathophysiology

The major symptom in diabetes is hyperglycemia, which causes both acute and reversible changes in cellular metabolism and long-term irreversible changes in stable macromolecules. The metabolism of the cells starts to response to the hyperglycemic environment even before disease pathology is detectable (Kalishwaralal et al., 2010; Porta and Bandello, 2002).

In an advanced stage, the ischemia is the major factor responsible for the growth of abnormal retinal blood vessels (neovascularization) which grow in an attempt to supply oxygen to the hypoxic retina (Ciulla et al., 2003). In addition, the loss of some retinal cells is also detected in DR patients (Kalishwaralal et al., 2010). Additionally to hyperglycemia, there are other factors that contribute to the development of DR, such as hyperlipidemia and hypertension (Cetin et al., 2013; Klein et al., 1998; Klein et al., 1988; Vitale et al., 1995). Despite the acknowledgment of hyperglycemia consequences at the ocular level, the mechanisms causing the vascular disruption in retinopathy are not well known, and, not surprisingly, several pathways have been pointed out as being implicated. However, it is crucial the understanding of the mechanism of capillary loss due to biochemical mechanisms to clarify the disease pathogenesis. Thus, good glycemic control is a very important strategy to inhibit/prevent the development of DR additionally with early intervention to prevent the progression of retinopathy in diabetes (Ciulla et al., 2003). However, the challenging in maintaining good glycemic levels for this chronic disease could be a hard task, since other factors also contribute to the development of DR, including pregnancy, age and hypertension (Madsen-Bouterse and Kowluru, 2008). In order to find a better and more efficient therapeutic option, it is essential to ascertain intracellular and molecular mechanisms that lead to the development and prevalence of DR.

During the development of DR, the sustained hyperglycemic milieu in diabetes leads to a breakdown of the BRB. The tight junctions of the endothelial cells figuring in the BRB become loose, enabling passage of certain macromolecules that leak out and the basement membranes of the capillary thickness resulting in structural rigidity of the blood vessels (Madsen-Bouterse and Kowluru, 2008). Diabetic macular edema (DME) occurs following this breakdown of BRB increasing vascular permeability of retinal capillaries, leading to thickening of the macular area. DME appears as a primary signal of DR and causes blurred vision with consequent disturbing of the architecture of the retina (Rechtman et al., 2007).

The function of endothelial cells is the maintenance of the BRB, by multiplication from the inner part of the wall, is strongly affected in DR patients in which this growth is initially exacerbated. When these cells suffer any damage or pathological multiplication,

vascular permeability is altered resulting in capillaries blockage, appearance of small hemorrhages and yellow deposits (hard exudates) (Ciulla et al., 2003; Madsen-Bouterse and Kowluru, 2008).

Other cells affected by hyperglycemia are the pericytes. The damage caused in these cells in diabetic patients, leads to a change in retinal hemodynamics, including abnormal auto-regulation of retinal blood flow (Ciulla et al., 2002). Loss of these cells occurs in DR, leading to microaneurysm formation and acellular capillaries. Thus, endothelial cells and pericytes of retinal microvasculature suffer apoptosis, and this contributes to the development of acellular capillaries and pericyte ghosts (Yanoff, 1969).

In DR there is an increased leukostasis, which seems to play an important role in the pathogenesis of the disease (Chibber et al., 2007). The leukocytes have a tendency to adhere to the vascular endothelium affecting its function resulting in retinal perfusion, angiogenesis and vascular permeability (Miyamoto and Ogura, 1999). Also, their capacity to generate superoxide radicals and proteolytic enzymes leads to endothelial cell damage and vascular leakage in the retinal microcirculation (Chibber et al., 2007; Miyamoto and Ogura, 1999).

These are the major complications observed in NPDR, being the capillary occlusion more evident and the development of abnormal capillaries without blood flow, and finally ischemia. The evolution to pre-PDR is determined by the development of neovascularization, resulting from the retinal ischemia and hypoxia (Frank, 2004).

Neovascularization, also called angiogenesis, is a significant phenomenon involved in PDR, and is a consequence of an imbalance of the growth factors which contributes to the development of other several diseases including macular edema and retinal inflammatory diseases (Kalishwaralal et al., 2010). The activation of endothelial cells located within normal vessels leads to the initiation of angiogenesis process (Carmeliet, 2000). The new capillary formation involves several steps, being the first the creation of new endothelial cells tubes, which are stabilized and spatially oriented. However, these new vessels formed will be functionally and anatomically incompetent, mainly due to the constant hyperglycemia which affects the retinal blood flow (Praidou et al., 2010).

Other complications associated to oxidative stress at retinal level are implied in the DR. The oxidative stress developed by some biochemical changes contributing to the functional and structural alterations in the retinal microvasculature. Thus, oxidative stress is responsible for the formation of reactive oxygen species (ROS) and mitochondrial dysfunction (Barot et al., 2011). Consequently, mitochondrial changes and formation of acellular retinal capillaries are prevented by an overexpression of the enzyme responsible for scavenging mitochondrial superoxide, the superoxide dismutase (SOD), which is elevated in DR leading to dysfunctional mitochondria prior to apoptosis (Al-Shabrawey et al., 2013; Kowluru, 2005).

Despite the current scientific developments, the mechanisms through which hyperglycemia results in retinal pathology, remain inconclusive. It is noteworthy that DR has a multifactorial nature and it is known that some of the major implied pathways contribute to the development of this pathology. The main biochemical pathways that influence DR are: the (i) polyol pathway; (ii) protein kinase C (PKC) activation; (iii) advanced glycation end-products (AGEs) pathway provoked by their accumulation; (iv) activation of the hexosamine pathway; (v) oxidative stress, and (vi) expression of growth factor, such as vascular endothelial growth factors (VEGFs) (Aiello et al., 1997; Gardiner et al., 2003; Kowluru, 2005; Kowluru et al., 2006; Kowluru et al., 2001; Madsen-Bouterse and Kowluru, 2008). Due to hyperglycemia, excess of intracellular glucose is converted into other molecules, activating specific pathways. The polyol pathway begins by the conversion (reduction) of glucose to sorbitol, mediated by aldose reductase using nicotinamide adenine dinucleotide phosphate (NADPH) as a cofactor. The reactions are depicted in Figure 1.2.2. The need of NADPH in the initial conversion of glucose to sorbitol leads to a deficiency for its availability for the activity of glutathione reductase (GR) that maintains the adequate levels of reduced glutathione (GSH), an important cellular antioxidant. The depletion of GSH may lead to increased levels of ROS leading to oxidative stress (Miwa et al., 2003; Naruse et al., 2000).

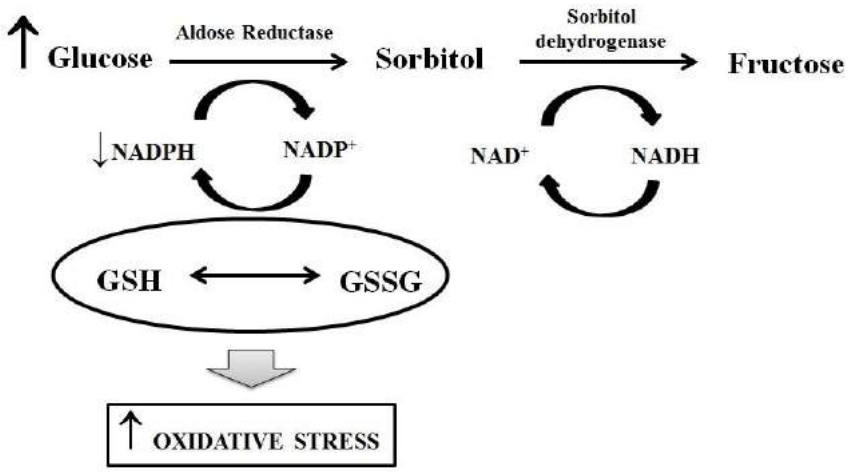

Figure 1.2.2. The polyol pathway is started by the conversion of glucose to sorbitol mediated by the enzyme aldose reductase, using NADPH as a hydrogen donor. Sorbitol is further converted in fructose by sorbitol dehydrogenase using NAD^+ as a hydrogen donor.

The PKC pathway is associated to DR since the PKC activity is increased in diabetes. Activation of some isoforms of PKC have been shown to increase vascular permeability, change blood flow (decreasing blood flow by increasing endothelin-1 levels) and development of neovascularization (Koya and King, 1998). Additionally, PKC induces the expression of endothelin-1 and growth factors, such as platelet-derived growth factors (PDGFs) and VEGFs. VEGFs contributes largely for the development of retinal neovascularization (Hoshi et al., 2002; Yokota et al., 2003).

In hyperglycemic conditions, glucose and other carbohydrates react with amino-acids, proteins, lipids and nucleic acids, which results in AGEs formation. These glycation products usually accumulate in the basement membranes of retinal cells, making the anchoring of perycites difficult and thus contributing for its loss and microvascular alterations in retinal capillaries (Friedman, 1999; Gardiner et al., 2003).

The hexosamine pathway is activated when there is an excess of intracellular glucose that cannot be drained by glycolysis. The overproduction of fructose-6-phospate (Figure 1.2.3) begins with the convertion to glucosamine 6-phosphate by glutamine-fructose-6-phosphate amidotransferase which is the first step for the accumulation of glucosamines. Glucosamine 6-phosphate is rapidly metabolized leading to the formation of uridine

diphosphat (UDP)-*N*-acetylglucosamine and UDP-*N*-acetylgalactosamine, serving as substrates for glycosilation which seems to be responsible for alterations on protein function, that can reduce cell protection and at the end induce cell apoptosis, namely on retinal neurons and endothelial cells (Nakamura et al., 2001).

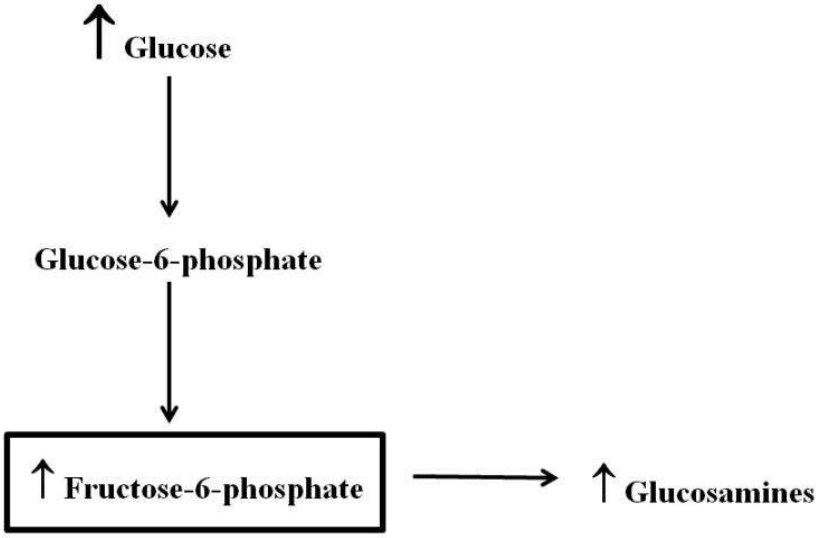

Figure 1.2.3. The overproduction of fructose-6-phosphate resulting from the high levels of glucose leads to the glucosamines accumulation.

Thus, understanding the significant biochemical mechanisms, which contributes to DR pathogenesis, is useful towards the development of new drug delivery systems and strategies to prevent and manage this ocular chronic disease. A summary illustration is depicted in Figure 1.2.4 to highlight the most important pathways and factors leading to retinal neovascularization, the primary and most important problem in DR.

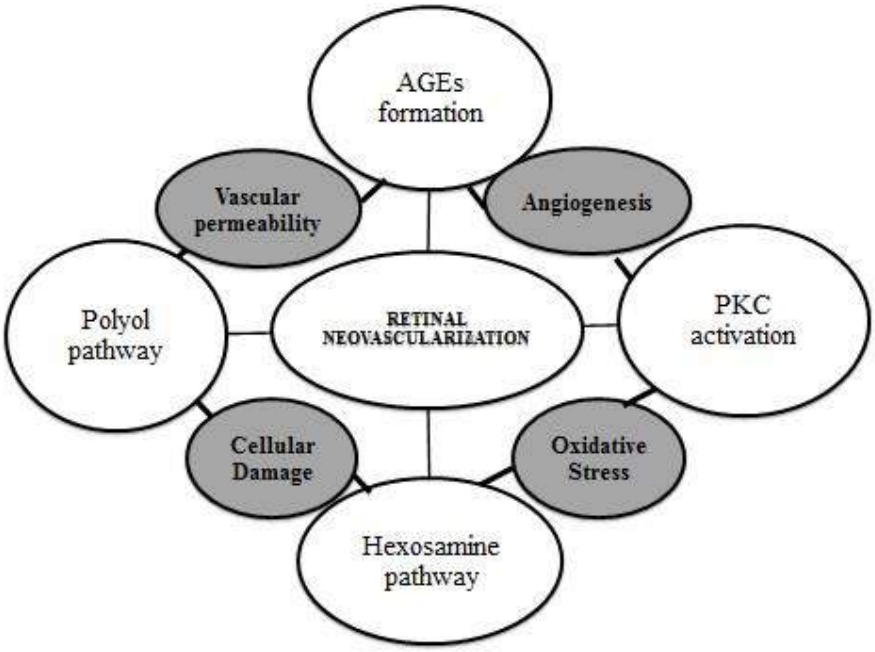

Figure 1.2.4. Schematic illustration of the main biochemical abnormalities in DR. The four pathways and some physiological changes in retinal cells, vessels and retinal blood flow, favoring retinal neovascularization.

1.2.3.Nanotechnology applied to ocular delivery

The use of nanotechnology-based approaches for ocular delivery is an interesting challenging due to the several limitations that this route represents from the pharmaceutical point of view. The delivery of several drugs is limited by the anatomy and physiology of the human eye. Thus, nanoparticles seem to be a promising alternative over the classic systems, which are generally related to a very low bioavailability (5-10%) of the administered drugs (Fangueiro et al., 2014a).

Regarding the anatomy of the human eye, this is an isolated organ divided into anterior and posterior segments. The topical delivery of drugs by using eye-drops is limited to treat diseases affecting the anterior segment of the eye. The delivery of drugs into the posterior segment of the eye is possible by topical administration (i) through conjunctiva/sclera; (ii) from the cornea and aqueous humor. Other routes including intravitreal injection and implants are more invasive. Additionally, it is possible to reach the posterior segment through the systemic circulation after topical, parenteral, oral, or

other administration routes that deliver the drug directly into the blood circulation (Al-Halafi, 2014).

The most studied nanomedicines for posterior segment of the eye are summarized in Figure 1.2.5.

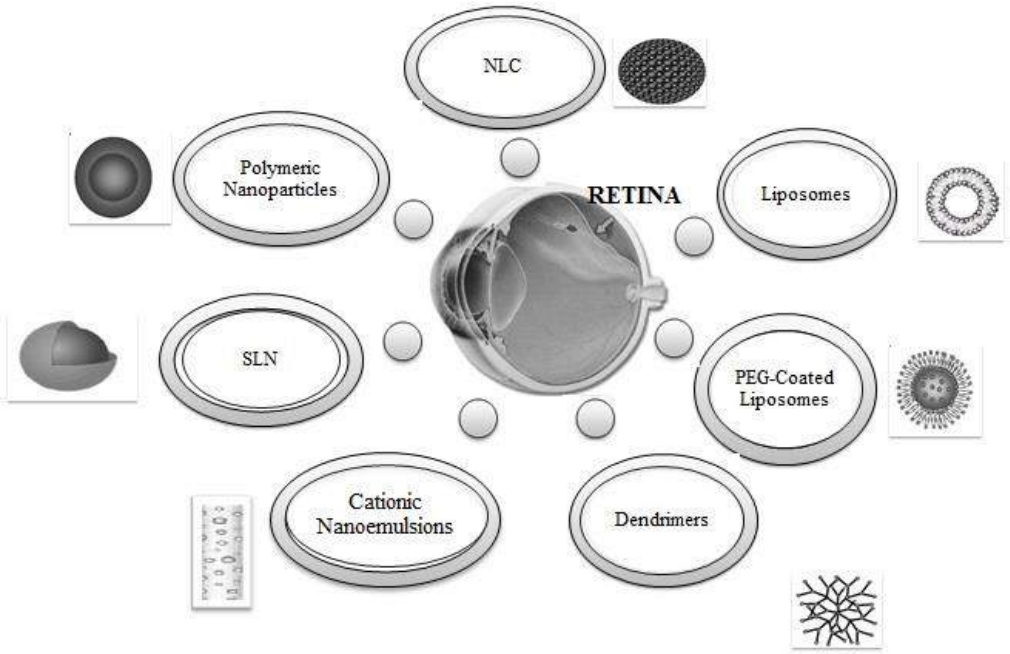

Figure 1.2.5. Schematic illustration of the most common nanoparticles used to reach the posterior segment of the eye.

Polymeric nanoparticles can be composed of several polymers, such as *poly(lactic-co-glycolic acid)* (PLGA), *poly(lactic acid)* (PLA), chitosan, polyvinyl alcohol (PVA) and poly(methyl methacrylate) (PMMA). These materials are approved by Food and Drug Administration (FDA) due to their biodegradability and biocompatibility (Kompella et al., 2013). Lipid nanoparticles, such as solid lipid nanoparticles (SLN), nanostructured lipid carriers (NLC) and liposomes, have been proposed for ocular delivery (Araujo et al., 2012; Araujo et al., 2010; Araujo et al., 2011; Gonzalez-Mira et al., 2010; Gonzalez-Mira et al., 2011; Souto et al., 2010). Their composition is mainly based on physiological lipids, such as phospholipids, ceramides, acylglycerols, being recognized as biocompatible and without or with minimal toxicity (Fangueiro et al., 2014a; Souto et al., 2013a). To further enhance the ocular bioavailability of drugs loaded in such

nanoparticles, and to avoid the mucosal irritation and ocular rejection, the use of polyethylene glycols coating the surface of nanoparticles is considered a suitable alternative to deliver drugs into the posterior segment of the eye (Kompella et al., 2013).

Dendrimers derive from polymers, such as polyamidoamine (PAMAM), which are usually water soluble (Svenson and Tomalia, 2012). These systems are useful due to their tunable chemistry and surface modification. Drugs can be entrapped in the dendrimer network composed of the functional groups. The most common material used for the production of dendrimers is PAMAM (Holden et al., 2012; Yang et al., 2012). Although these systems seem to promote a sustained drug delivery in the posterior segment of the eye, their cytotoxicity is a limitation, since it depends on the functional group (Holden et al., 2012).

Cationic nanoemulsions are being exploited for ocular drug delivery due to the capacity to electrostatically interact with human ocular mucosa, as this latter is of anionic nature (Fangueiro et al., 2014a). They are usually produced by high-energy emulsification methods and can load several types of drugs since they can be oil-in-water (o/w) or water-in-oil (w/o) (Lallemand et al., 2012; Solans et al., 2005). These systems have been successfully taken by Novagali Pharma, which has launched a marketed formulation Novasorb®. The major challenge in formulating was the selection of a cationic agent with an acceptable safety profile that would ensure a sufficient ocular surface retention time (Kim and Chauhan, 2008; Lallemand et al., 2012).

The anatomical barriers limit the penetration of drugs from the front to the posterior segments of the eye (vitreous humor, retina and choroid). The tight junctions that compose the corneal epithelium, corneal endothelium, retinal endothelial cells and retinal pigmented epithelium limit the diffusion of drugs and the BRB limits the drug delivery by systemic circulation (Xu et al., 2013). Nanoparticles may improve the bioavailability of some drugs in the posterior segment of the eye decreasing the frequency of injections and adverse side effects. In addition, it is fundamental to improve patient compliance, particularly in chronic diseases.

1.2.4. Classical vs nanotechnological strategies for the treatment and management of DR

DR is an ocular disease that should be managed by an ophthalmologist and/or endocrinologist, and it should be directed towards both systemic and ocular aspects of the disease (Nathan, 2014). The current treatment strategies need to include the management of the hyperglycemia values, blood pressure and serum lipids (Nathan, 2014; Porta and Bandello, 2002). The traditional and current strategies used in the management of DR involve laser surgery, vitrectomy, and the pharmacological therapy. For a better management, it is usual the combination of several strategies, since there is no cure for DR, but these strategies could delay and attenuate some of the major symptoms, avoiding the earlier blindness. The management of NPDR and early PDR are common in the pharmacological treatment, and sometimes associated with surgical treatment. In PDR, there is no option unless the surgery by laser, and according to the specific problems in the retina, it could include focal laser, scatter laser or vitrectomy.

1.2.4.1. Surgery treatments

Focal laser, or laser photocoagulation, is usually applied in PDR, and it is based on a focused laser beam of a discrete wavelength onto specified parts of the retina. Its application can stop or slow down the leakage of blood from the microaneurysms and fluid in the eye. The laser beam absorption causes a local rise temperature inducing protein denaturation and coagulative necrosis. Only one session is usually required (Rechtman et al., 2007). The main adverse effects associated with this and other laser surgery imply the visual field constriction, night blindness, color vision changes, and accidental laser burn of the macula (Singh et al., 2008).

Scatter laser, or pan-retinal photocoagulation, is also applied on PDR, and it is used to ablate ischemic areas of the peripheral retina and thus, reducing the induction of angiogenic growth factors. The main goal is to induce the regression of neovascularization without vitreous hemorrhage or fibrovascular proliferation. Although photocoagulation is applied once, this treatment could require more sessions, usually two

or more. The same adverse effects mentioned above for the photocoagulation treatment is also applied in pan-retinal photocoagulation (Singh et al., 2008).

Vitrectomy is applied to prevent blindness and/or severe visual loss in advanced cases of DR, specifically those with tractional retinal detachment or severe non-clearing vitreous hemorrhage (Mason et al., 2006a). This procedure is used to remove blood from the vitreous body. A possible side effect of this procedure is the acceleration of cataract formation, which can lead to the development of endophthalmitis and retinal detachment (Cohen et al., 1995; Doft et al., 2000).

The choice of the treatment is adapted for the type of DR, and the surgery is mainly used in an advanced stage followed by the risk of blindness. Laser photocoagulation, pan-retinal photocoagulation and/or vitrectomy will continue to have a relevant role in the management of DR, to improve the patient's quality life, and to reduce the cost of the therapy.

Despite the benefits that surgery could offer to diabetic patients, this is not a first choice for NPDR and early PDR treatment, since adverse side effects of these procedures are present and the other DR symptoms still remain. Several innovative pharmacological therapies, particularly based on nanoparticles, are being considered.

1.2.4.2. Pharmacological therapies

Several pharmacological therapies are available to manage the DR. According to the type of DR and the acknowledgement of the mechanisms responsible for the development and progression of the disease, there are several approaches being considered. This section discusses the traditional therapies already applied in the management of DR and the new therapies involving nanoparticles.

1.2.4.2.1. Corticosteroids

Corticosteroids are a class of drugs with high anti-inflammatory activity. These drugs also provide the ability to reduce vascular permeability and reduce the blood-retinal barriers breakdown, to down-regulate VEGF expression and/or production, and the capacity to inhibit matrix metalloproteinases (Bhavsar, 2006; Rechtman et al., 2007). The

administration of corticosteroids in the management of DR includes the peribulbar, sub-tenon and intravitreal injections (Jonas, 2007; Singh et al., 2008). The main corticosteroids used in the management of DR will be discussed in this section.

1.2.4.2.2. Triamcinolone acetonide

Triamcinolone acetonide is the most common corticosteroid used in the management of DR by intravitreal injection, since it is the most efficient approach to deliver the drug to the posterior segment of the eye. The common dose is 4.0mg/0.1mL, however higher doses of 20-25mg/0.2mL have also been reported (Jonas, 2007). The management of DR with this drug has gained interest in the past years with improvement of visual acuity (Jonas and Sofker, 2001).

Since the 70s, triamcinolone acetonide is being used for intravitreal injection to achieve a higher intraocular concentration in the post-segment of the eye. Firstly proposed in an animal model, triamcinolone acetonide was used as a pharmacological adjuvant to prevent the formation of proliferative scar tissue in order to improve outcomes following retinal detachment surgery (Machemer et al., 1979). The current marketed formulation of this drug is Kenalog®40 (Bristol-Myers-Squibb, Princeton, NJ) (Danis et al., 2000; Jonas et al., 2003; Penfold et al., 1995).

In a study carried out by Bressler and co-workers (Bressler et al., 2009), 840 eyes with macular edema were chosen to receive laser photocoagulation, injections of triamcinolone at 1 mg or 4 mg. The authors obtained fundus photographs at baseline as well as at one-, two- and three-year follow-up. At two-year follow-up, retinopathy progression has been documented in 31% of 330 eyes treated with photocoagulation; 29% of 256 eyes treated with 1 mg doses of triamcinolone; and 21% of 254 eyes treated with 4 mg doses of triamcinolone.

Also, Gillies and co-workers reported the effect of intravitreal triamcinolone injections (4mg/0.1mL) in a double-masked, placebo-controlled, randomized clinical trial over 2 years (Gillies et al., 2006). Improvement of visual acuity was found in 56% of the patient eyes treated with intravitreal injection of triamcinolone compared with 26% of the eyes treated with the placebo. Despite the relative success of triamcinolone acetonide

injections, its use also causes an increase in IOP (68%) and glaucoma medication was required in 44% of the patients, being a cataract surgery required in 54% of the patients. Additionally, other complications, such as trabeculectomy and endophthalmitis, were observed in the treated group.

Additionally, a study conducted by Robinson and co-workers showed the main ocular barriers to the transscleral delivery of triamcinolone acetonide (Robinson et al., 2006). The results suggested that the conjunctival lymphatics/blood vessels may be an important barrier to the delivery of triamcinolone acetonide to the vitreous in this rabbit model. The barrier location and clearance abilities of the ocular tissues are important to consider when developing a successful transscleral drug delivery system.

Araújo and co-workers encapsulated triamcinolone acetonide in NLC with adequate physicochemical properties for ocular delivery for anti-angiogenic purposes (Araujo et al., 2011). Additional studies revealed that these nanoparticles were able to provide a prolonged drug release followed by one-order kinetics, and permeability studies confirmed that triamcinolone acetonide was able to diffuse across rabbit sclera in sustained profile, following zero-order kinetics (Araujo et al., 2012).

A different type of particles composed of PLA was tested for trans-scleral delivery (Kadam et al., 2012). Two nanosized particles were produced, nano (≈551nm) and micro (≈2090 nm) loading triamcinolone acetonide. Beside the satisfactory parameters of both particles, only the microparticles were able to provide a sustained effective level of the drug in the retina. Other study reporting the encapsulation of triamcinolone acetatonide for retinal purposes has been published by Suen and Chau (Suen and Chau, 2013). The authors loaded the drug into nanoparticles synthetized by the functionalization of folate and poly(ethylene glycol)-β-polycaprolactone (folate-PEG-β-PCL). These nanoparticles were taken up by arising retinal pigment epithelia (ARPE)-19 cells (human RPE cell line) via receptor-mediated endocytosis. Results seem promising, since a high encapsulation efficiency was achieved (>97%) and enhanced uptake and controlled release was observed resulting in prolonged anti-angiogenic gene expression of RPE cells. Additionally, the down-regulation of VEGF and up-regulation of pigment epithelium derived factor (PEDF) was observed for 3 weeks.

1.2.4.2.3. Dexamethasone

Dexamethasone is another corticosteroid with ocular therapeutic benefits, well-known for its anti-inflammatory effects in the treatment of acute and chronic posterior segment eye diseases such as uveitis (Phillips and Katz, 2005). Among the corticosteroids, dexamethasone is one of the most potent, with an anti-inflammatory activity that is six-fold greater than that of triamcinolone and 30-fold greater than cortisol (Goldfien, 1995). The typical dose for the treatment with dexamethasone is instillation of 0.1% dexamethasone during 3-4 times per day. However, continuous application for extended periods of time could result in cases of glaucoma followed by optic nerve damage, defects in visual acuity and fields of vision, and posterior sub-capsular cataract formation and thinning of the cornea or sclera (Kim and Chauhan, 2008).

There are market formulations currently being used with dexamethasone, namely Posurdex® and Ozurdex® both from Allergan, Irvine, CA. Posurdex®, is still in phase III clinical trials, was developed to address the challenges of intravitreal corticosteroid therapy. Kuppermann and co-workers suggest that this new drug delivery system is well tolerated and provides benefits in the treatment of persistent macular edema (Kuppermann et al., 2007). The incision of the implant is simple and well tolerated. One single dose seems to have potential to treat macular edema. Ozurdex® was initially approved by the FDA in 2009 as the first drug therapy for the treatment of macular edema following retinal vein occlusion (RVO), received FDA approval for the treatment of non-infectious ocular inflammation, or uveitis, affecting the posterior segment of the eye in 2010. In 2014, the FDA approved Ozurdex® as the first intravitreal implant corticosteroid indicated for the treatment of DME in adult patients (OZURDEX®, 2014). Clinical studies demonstrated that Ozurdex® provide a sustained-release of dexamethasone with potentially reduced adverse effects (Herrero-Vanrell et al., 2011). Clinical studies have shown that this dexamethasone implant is a promising new treatment option for patients with persistent macular edema resulting from retinal vein occlusion, DR, and uveitis or Irvine-Gass syndrome.

There are some studies concerning the loading of dexamethasone in polymeric nanoparticles. Gómez-Gaete and co-workers used PLGA as a polymer and preliminary

results revealed a controlled release of dexamethasone from the nanoparticles (Gómez-Gaete et al., 2007). Another study reported by da Silva and co-workers loaded dexamethasone into biodegradable polyurethane containing clay nanoparticles (da Silva et al., 2011). The nanoparticles demonstrated to have similar mechanical properties with ocular soft tissues, which reduce their potential irritancy and toxicity. Dexamethasone was incorporated in 6.0 wt% in the polyurethane implants. *In vitro* and *in vivo* results in ARPE-19 cells show a good tolerance of the nanoparticles and additionally suggested that these degradable polyurethane and nanocomposites may act as temporary supports for transplanted RPE cells as an initial attempt of replacing dysfunctional RPE for macular reconstitution of age-related macular degeneration patients.

1.2.4.2.4. Fluocinolone acetonide

Fluocinolone acetonide is one of the most potent corticosteroid applied in post segment eye complications (Campochiaro et al., 2011). Usually, it is used to manage DME, one of the most complications of DR.

There is a marketed formulation of this drug in an implant presentation, Retisert® (Lomb, 2009). This is a non-biodegradable implant designed to release 0.59 μg/day of fluocinolone acetonide in the post segment of the eye (Driot et al., 2004). Retisert® was approved for the treatment of chronic noninfectious posterior uveitis (Jaffe et al., 2006). Preclinical studies have demonstrated that the implant is well tolerated, with no measurable systemic drug absorptions (Jaffe et al., 2000). However, in a study concerning DME patients, results from clinical trials (Pearson et al., 2011) indicate a significant reduction in ocular edema, however after 2 years a high percentage of the patients (80-90%) showed cataracts and required surgery due to the enhanced ocular pressure. Iluvien® (pSivida Corp. Watertown, MA) is another formulation with this corticosteroid, an injectable non-erodible implant used for the treatment of chronic DME. A study made by Sanford (Sanford, 2013) in patients with DME, previously treated with macular laser photocoagulation, showed that this intravitreal implant 0.2 μg/day was significantly more efficient than sham injection in improving visual acuity. The treatment showed to have more benefits in the subgroup of patients whose DME duration was ≥3 years. However, adverse effects occurred, namely cataracts, in 82% of Iluvien® treated patients and 51%

of sham injection recipients, and increase in IOP, in 37% (Iluvien® treated) and 12% (sham injection recipients) of the patients.

There are no reports describing the loading of fluocinolone acetonide in nanoparticles, however some studies have demonstrated that the formulation of this drug in polymeric implants is a promising approach for intraocular long-term delivery (Campochiaro et al., 2011; Haesslein et al., 2006; Jain et al., 2012).

1.2.4.3. Anti-angiogenic factors

VEGF is a 35-45 kDa homodimeric protein, highly conserved that exists in several isoforms. VEGF is an endothelial-cell-specific angiogenic factor and a vascular permeability factor whose production is increased by hypoxia, thus VEGF have gained much attention for the treatment of DR. The use of monoclonal antibodies to neutralize VEGFs are currently being administered via intravitreal injection for the treatment of ocular diseases, such as PDR, age-related macular degeneration (AMD) and choroidal neovascularization. VEGFs have the ability to increase the permeability of blood-tissue barriers and in DR are overexpressed due to hypoxia that occurs in the retinal cells, which is a major stimulus for the development of retinal neovascularization (Figure 1.2.6). The expression of VEGFs seems to increase in patients as they progress from NPDR to PDR (Aiello et al., 1994; Miller et al., 1997). Some of the complications occurring in PDR, e.g. reduced retinal blood flow and posterior hypoxia followed by loss of capillary pericytes and endothelial cells, are associated to an increase in the synthesis and secretion of VEGF (Crawford et al., 2009; Singh et al., 2008).

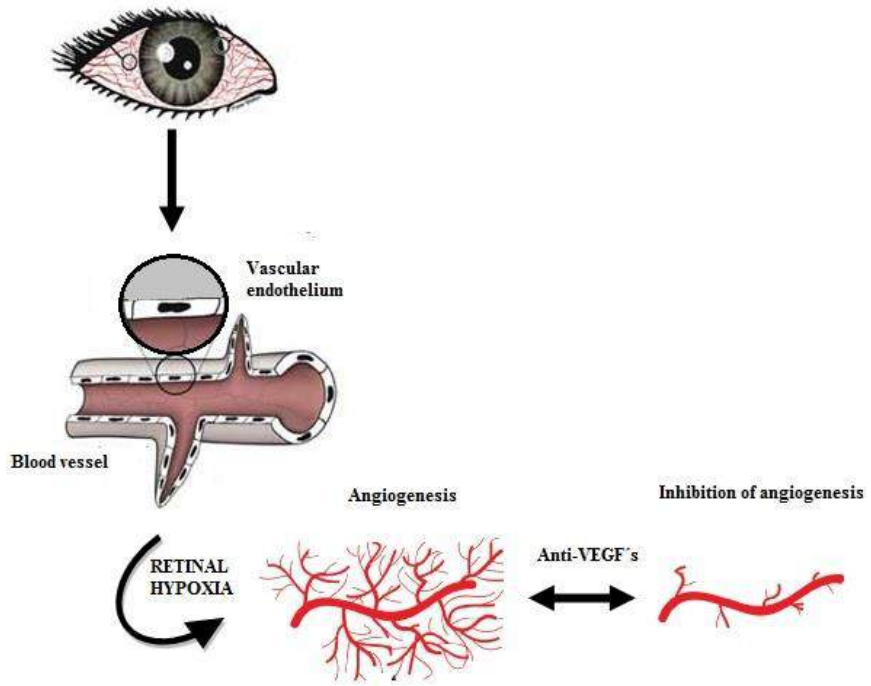

Figure 1.2.6. Schematic illustration of VEFGs action in the development of angiogenesis, a leading cause of DR.

1.2.4.3.1. Bevacizumab

Bevacizumab is a recombinant humanized antibody, showing activity against all isoforms of VEGF-A (Abu El-Asrar and Al-Mezaine, 2011). This monoclonal antibody demonstrated to be an efficient treatment for DR, DME and iris neovasculatization (Abdallah and Fawzi, 2009; Khurana et al., 2009; Mason et al., 2006b). The marketed formulation of this drug belongs to Genentech, namely Avastin® (Genentech, California, US). Several studies (Fang et al., 2008; Lam et al., 2009; Roh et al., 2008; Solaiman et al., 2013; Wu et al., 2009) regarding the use of 1.25 mg of bevacizumab for DME therapy demonstrated beneficial effects, although several injections were required. Clinical studies with Avastin® (Jorge et al., 2006) reported that a single intravitreal 1.5 mg injection reduced the leakage in persistent new vessels associated to PDR patients. A recent study (Cintra et al., 2013) also published similar results, with additional

improvement of the visual acuity in patients unresponsive to pan-retinal photocoagulation.

Studies involving the use of bevacizumab loaded into nanoparticles are being carried out, with the aim to improve the drug's bioavailability and exploit alternative administration pathways.

One the major problems encountered when loading these drugs into nanoparticles is related to the limited physicochemical stability of the monoclonal antibodies during the production process, and also during their release and *in vivo* performance. The selection of a particular type of nanoparticles will reflect its *in vitro* long-term stability and *in vivo* therapeutic efficacy. Polymeric nanoparticles are interesting systems that seem to dominate the field of ophthalmic drug delivery. Reasons for that are the adequate physicochemical properties of polymeric nanoparticles, biocompatibility, non-toxicity and diversity (Bysell et al., 2011; Varshochian et al., 2013). Varshochian and co-workers developed PLGA nanoparticles to encapsulate the bevacizumab (Varshochian et al., 2013). PLGA is considered to be safe and has been extensively used in drug delivery (Danhier et al., 2012). The authors proved that PLGA nanoparticles were able to protect protein inactivation and aggregation in the presence of albumin. *In vivo* and *ex vivo* release of bevacizumab followed a sustained profile and seemed to be effective in the protection of the antibody integrity (Varshochian et al., 2013). Other study describing the same type of nanoparticles was published by Li and co-workers (Li et al., 2012), who proved the ability of PLGA nanoparticles to load bevacizumab and to promote a prolonged release by adjusting the drug/polymer ratio.

Lu and co-workers studied the effects of an intravitreal injection of bevacizumab-chitosan nanoparticles in pathological morphology of the retina and the expression of VEGF protein and VEGF messenger ribonucleic acid (mRNA) in the retina of diabetic rats (Lu et al., 2014). The results showed that chitosan nanoparticles were able to provide a sustained release of bevacizumab and this alternative was useful to inhibit the choroidal neovascularization. Additionally, the expression of VEGF was effectively inhibited and the nanoparticles containing the anti-VEGF agent provided a prolonged action.

1.2.4.3.2. Ranibizumab

Ranibizumab is a fragment of bevacizumab with specificity for all isoforms of human VEGF-A (Abu El-Asrar and Al-Mezaine, 2011), which is already being studied for DR and DME as an anti-VEGF agent. It was shown that intravitreal ranibizumab applications reduced the progression of these pathologies and their severity (Ip et al., 2012). The marketed formulation is Lucentis® (Genentech, California, US) and is being used for the treatment of AMD and DME, in patients with DR. Lucentis® was approved for the treatment of AMD in 2006, receiving later approval for DME in 2012 (Genentech, California, US). Clinical studies revealed that intravitreal ranibizumab (0.5 or 0.3 mg) rapidly and sustainably improved vision, reducing the risk of further vision loss. Additionally, improvement of the macular edema in patients with DME was achieved. There are no reports describing the loading of ranibizumab in nanoparticles for ocular drug delivery.

1.2.4.3.3. Pegaptanib

Pegaptanib is an aptamer that binds to all isoforms of VEGF-A (Sanford, 2013). Pegaptanib has a marketed formulation named Macugen® (Pfizer / Eyetech Pharmaceuticals, New York, USA) accepted since 2004 by the FDA for the treatment of AMD. Clinical studies with intravitreal Pegaptanib showed a regression of neovascularization suggesting a direct effect upon retinal neovascularization in patients with DR (Group, 2006; Querques et al., 2009). A phase II study in patients with DME involving Macugen® (0.3, 1.0 or 3.0 mg) found that this drug specifically blocks the 165 amino-acid isoform of VEGF (V_{165}), resulting in a better visual acuity, reducing the central retinal thickness, and reducing the need for additional therapy with photocoagulation when compared with sham injections (Group, 2005). Gonzalez and co-workers showed that intravitreal injection of Pegaptanib produced short-term marked and rapid regression in diabetic retinal neovascularization (Gonzalez et al., 2009). To our knowledge there are no reports describing the loading of Pegaptanib for ocular drug delivery. Nanoparticles loading Pegaptanib could be useful to avoid intravitreal injections and increase patient's compliance.

1.2.4.4. VEGF Trap eye

VEGF Trap eye, also known as aflibercept, is a recombinant fusion protein consisting of the binding domains of VEGF receptors 1 (VEGFR1; 2nd binding domain) and 2 (VEGFR2; 3rd binding domain) and Fc fragment of a human immunoglobulin G1 (IgG1) backbone, being widely studied for DR applications. Similar to ranibizumab and bevacizumab, aflibercept, the VEGF Trap eye binds to all isomers of the VEGF-A family (Moradi et al., 2013). Currently named as Eylea® (Regeneron Pharmaceuticals, Inc., New York, USA and Bayer Healthcare Pharmaceuticals, Berlin, Germany), aflibercept was firstly approved for DME and AMD treatment in 2011 by FDA.

Aflibercept has shown a higher affinity for VEGF-A along with a longer duration of action as compared to other anti-VEGF antibodies, since the receptor sequences of aflibercept provides powerful binding to VEGF, creating a one-month intravitreal binding activity exceeding both ranibizumab and bevacizumab (Yung, 2008). Preliminary studies reveal the benefits of this treatment in improvement visual acuity in patients with DME (Do et al., 2012; Do et al., 2011). To our knowledge, there are no reports describing the loading of aflibercept for ocular drug delivery.

1.2.4.5. Protein Kinase C inhibitors

The sustained hyperglycemia, in diabetes, induces increased levels of diacylglycerol and activation of PKC. These features lead to biochemical and metabolic abnormalities, mainly due to the increased production of extracellular matrix and cytokines, induction of cytosolic phospholipase A2 activation, and inhibition of Na^+-K^+-ATPase, that enhance contractility, permeability, and vascular cell proliferation (Koya and King, 1998). PKC isoforms, β and δ, play an important role in modulating the expression and production of VEGF affecting growth and permeability of retinal endothelium (Porta and Allione, 2004; Porta and Bandello, 2002).

Ruboxistaurin, a selective inhibitor of PKC-β, is being studied for the management of DR and DME. The oral administration of this drug reveals promising results in the

improvement of visual acuity, and reducing vision loss, need for laser treatment, and macular edema progression (Aiello et al., 2006; Aiello et al., 2011; PKC-DRS2 Group et al., 2005; Sheetz et al., 2013). It has also been reported that ruboxistaurin is able to delay the progression of DME (Group, 2007) and inhibit the effect of VEGF on retinal permeability and endothelial cell growth (Aiello et al., 1997). In addition, the prevention and reversion of microvascular complications in animal models of diabetes by ruboxistaurin was reported by Ishii and co-workers (Ishii et al., 1996) and other authors also reported its ability to block neovascularization associated with retinal ischemia (Danis et al., 1998).

The commercial formulation of ruboxistaurin, designated Arxxant®, synonym LY333531 (Eli Lilly and Company, Indiana, USA) is not yet approved by FDA for the treatment of DR due to the requirement of more evidences that this drug could be safely use for this chronic disease. There are no updated studies describing the loading of PKC inhibitors for ocular drug delivery.

1.2.4.6. Growth hormone inhibitors

The effect of growth hormone (GH) in the pathogenesis of DR was firstly supported by clinical observation of regression of severe PDR in 1953 (Poulsen, 1953). Somatostatin, also known as growth hormone-inhibiting hormone (GHIH) or somatotropin release-inhibiting factor (SRIF), is a hormone that regulates the endocrine system. The use of synthetic analogues of somatostatin as therapeutic agents for DR is being exploited. Their role in the management of DR is directly linked with the inhibition of angiogenesis through somatostatin receptors present on endothelial cells. Also, there is an inhibition of post-receptor signaling events of peptide growth factors such as insulin-like growth factor 1 (IGF-1) and VEGF (Grant and Caballero, 2005).

Octreotide, a somatostatin analogue, acts as GH inhibitor, is being used for the management of DR. Results have described this drug as safe and effective, acting by blocking the local and systemic production of GH and IGF-1 associated with angiogenesis and endothelial cell proliferation (Chantelau and Frystyk, 2005; Dal Monte et al., 2009; Grant and Caballero, 2005). The use of octreotide and other somatostatin

analogues seems to regulate angiogenic responses to the retinal hypoxic environment through a modulation of retinal levels of VEGF and its receptors (Dal Monte et al., 2009).

The first clinical studies with octreotide for treating DR reported oscillating results in clinical trials for DR (Kirkegaard et al., 1990). However, later studies provided evidences about the role of octreotide in DR, retarding the progression of advanced retinopathy and delaying the need for laser surgery (Boehm and Lustig, 2002; Grant et al., 2000).

The mechanism of action of octreotide could be associated with paracrine effect. Thus, the therapeutic effects of octreotide are hypothesized to be mediated by somatostatin receptor (SSTR) activation directly on the ocular target tissue. Besides, this paracrine effect potentially involves several SSTR subtypes, selective for octreotide, which mediate GH inhibition. At least, it seems that the peptide octreotide is not able to cross the blood-brain barrier, limiting the amount of drug reaching the retinal target tissue. Furthermore, this could result in a higher dose requirement of octreotide to be efficient in DR (Palii et al., 2008). Due to the limitations mentioned above, the loading of this peptide in nanoparticles could be a suitable alternative to reach the retina in adequate concentrations, bringing benefits for the management of DR.

There is a variety of nanoparticles associated with this peptide, namely gold nanoparticles (Surujpaul et al., 2008), conjugates with amphiphilic molecules for imaging purposes (Accardo et al., 2011), polymeric nanoparticles (Dubey et al., 2012; Hong et al., 2014; Huo et al., 2012; Niu et al., 2012), polymeric hydrogels (Dorkoosh et al., 2002), polymeric microspheres (Wang et al., 2004), NLC (Su et al., 2013), nanocapsules (Damge et al., 1997), liposomes (Helbok et al., 2012). Despite reporting the loading of octreotide into new therapeutic/imaging delivery systems, these studies do not focus on the formulation of nanoparticles for ocular delivery, in particular, for the management of DR.

Recently, a novel class of SSTR agonists with nanomolar potency at SSTR2 and varying potency at SSTR3, a highly active non-peptide imidazolidine-2,4-dione (NISA) has been described and tested on DR. The effects of subtype selectivity and lipophilicity on the somatostatinergic ocular antiangiogenic function have been investigated in *in vitro* and *in vivo* ocular model systems showing that the antiangiogenic effect of NISA and octreotide

was mediated via SSTR2 receptor and, although the downstream mechanisms seems less efficient than dose of GH, one should consider the direct ocular administration of these drugs to treat DR (Palii et al., 2008).

1.2.4.7. Advanced glycation end products inhibitors

In a hyperglycemic environment, carbohydrates (e.g. glucose, fructose) interact with proteins forming covalent adducts by a non-enzymatic reaction to form AGEs (Brownlee et al., 1984; Friedman, 1999). AGEs are proposed as a contributing mechanism in the pathogenesis of diabetic clinical complications accelerating their synthesis and tissue deposition, both extracellular and intracellularly (Friedman, 1999). These complications lead to the microvascular alterations in DR (Ciulla et al., 2003).

The use of AGEs inhibitors such as aminoguanidine has been investigated to prevent some of the diabetic vascular abnormalities (Hammes et al., 1994; Hammes et al., 1991; Kern et al., 2000; Luo et al., 2012). The results suggest the inhibition of the accumulation of AGEs in the retinal capillaries with the use of aminoguanidine associated with acellular capillaries and perycite loss (Gardiner et al., 2003; Hammes et al., 1991; Kern and Engerman, 2001). Other AGEs producing inhibitor is carnosine, a natural occurring dipeptide, which seems to have potential vasoprotective effect on retinal capillaries by oral administration (Pfister et al., 2011). The main limitation for the therapeutic use of carnosine is its rapid hydrolysis mostly by plasma carnosinase (Bellia et al., 2013). Thus, new types of nanoparticles have been developed to provide high stability to this drug, e.g. functionalizing avidin- and streptavidin-gold nanoparticles with the carnosine-biotin conjugate (Bellia et al., 2013).

Examples of studies reporting the formulation of AGEs in nanocarriers include magnetic nanoparticles (Li et al., 2013), iron oxide nanoparticles (Durmus et al., 2011) and silver nanoparticles (Thomas et al., 2010).

A study carried out by Singha and co-workers (Singha et al., 2009) reported the prevention of glycation of α-crystallin (the major component of the eye lens) by conjugation with gold nanoparticles, suggesting a possible role of these particles against protein glycation reaction in ocular pathologies. Other study published by Yang and co-

workers (Yang et al., 2014) reported the use of silica-based cerium (III) chloride nanoparticles in the inhibition of AGEs formation and reduction of oxidative stress. Results seem to be promisors, suggesting these particles as a novel agent for the prevention of cataractogenesis. Moreover, these nanoparticles could be an alternative against the use of AGEs production inhibitors, such as aminoguanidine and carnosine.

1.2.4.8. Antioxidants

Hyperglycemia-induced oxidative stress is considered an important connection between high glucose levels and other metabolic abnormalities relevant in the development of DR complications. It results from the overproduction of ROS and reactive nitrogen species (RNS) and/or from the inability to suppress ROS/RNS by antioxidant defense system and thus creating an imbalance between production and destruction (Kowluru and Chan, 2007). The major ROS generated are the free radicals superoxide ($^{\bullet}O_2^-$), hydroxyl ($^{\bullet}OH$), peroxyl ($^{\bullet}RO_2$), hydroperoxyl ($^{\bullet}HRO_2^-$) and the non-radical hydrogen peroxide (H_2O_2) (Johansen et al., 2005). And the major RNS species are nitric oxide ($^{\bullet}NO$), considered vasoprotective, however, $^{\bullet}NO$ reacts easily with superoxide producing the highly reactive molecule $ONOO^-$ (peroxynitrit), and subsequently triggering a cascade of harmfulness (Johansen et al., 2005).The formation of these ROS/RNS can be mediated by both enzymatic and non-enzymatic mechanisms (Figure 1.2.7).

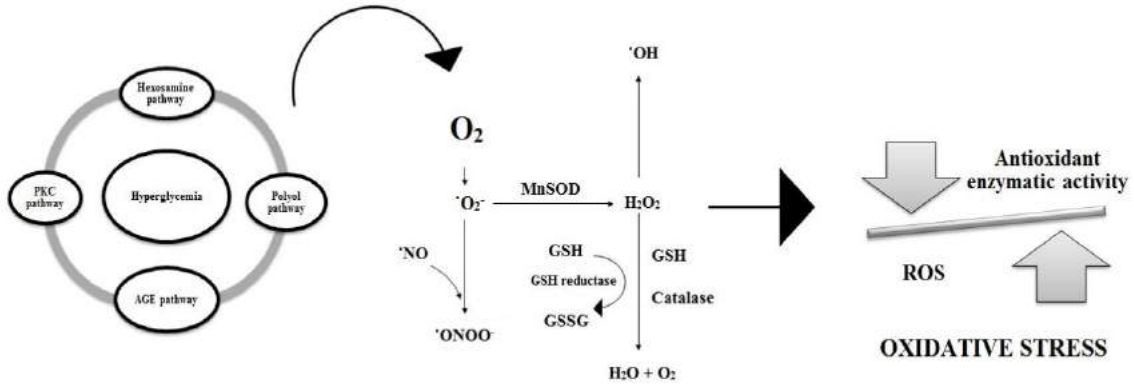

Figure 1.2.7. The oxidative stress is triggered by the constant hyperglycemia in the retinal vessels. The four pathways are influenced, since it generates ROS and AGEs

contributing to the inefficient activity of enzymatic antioxidant enzymes such as GSH, catalase, SOD and GSH redutase. This imbalance leads to the existence of retinal oxidative stress.

The main damage caused by ROS is at mitochondrial level, namely in the DNA and membrane proteins, leading to imbalances in the electron transport chain; but also can affect lipids and proteins at other organelles. Excess of ROS results in the mitochondrial release of cytochrome C, mitochondrial membrane damage and ultimately induces cellular apoptosis (Anuradha et al., 2001). It seems that overexpression of manganese superoxide dismutase (MnSOD) is enable to protect the increasing oxidative stress result from the DR (Kowluru, 2005). Additionally, it has been reported that MnSOD decrease hyperglycemia in streptozotocin (STZ)-induced diabetic rats (Kowluru et al., 2006; Obrosova et al., 2000). Thus, the use of antioxidants could be a useful approach to manage DR and to avoid some of its complications.

The antioxidants are molecules present in the human diet, such as vitamins A, C, E, some flavonoids and carotenoids, which sometimes are insufficient to prevent the oxidative stress.

Vitamin E (tocopherols) and C (ascorbic acid) are potent antioxidants that prevent lipid peroxidation (Huang et al., 2002). Their main functions are the (i) free radical scavenging and (ii) inhibition of retinal GR and SOD activity (Kowluru et al., 2001). For DR management, a short-term high-dose vitamin E therapy could help to normalize retinal hemodynamics (Bursell et al., 1999; Kunisaki et al., 1995). Also, resveratrol provides protection against oxidative stress in retinal pigment epithelial cells (Pintea et al., 2011; Sheu et al., 2010).

The use of α-tocopherol showed to be efficient in the prevention of diabetes-induced abnormal retinal blood flow (Kunisaki et al., 1998). Despite the evidences that antioxidants could have protective effects, some studies provide no association of the intake of antioxidants with improvement of DR (Haritoglou et al., 2011; Mayer-Davis et al., 1998; Millen et al., 2003). These studies have some limitations and do not translate the real situation, such as medication, severity of the disease, gene and environmental

factors (Wu et al., 2014). Despite that, it is evident that oxidative stress and the formation of ROS have an important role in the development of DR and the use of antioxidants could be a good strategy to overcome these biochemical features. The profile of these substances could be improved by the use of nanoparticles since antioxidants are highly susceptible to oxidation presenting limited absorption profiles, and thus low bioavailability (Souto et al., 2013b).

Table 1.2.2 describes the antioxidant mechanism of the most common antioxidants molecules investigated. The description of their loading in nanoparticles is also provided, however the available examples are mainly employed for oral delivery, to be introduced in the diet.

Table 1.2.2. Examples of some of the most important antioxidants used in nano- and microencapsulation indicating their antioxidant mechanism and the describing the variety nanocarriers that have being currently studied.

Antioxidant	Mechanism	Nanocarrier	References
Vitamin C/ascorbic acid	• Free radical scavenging • Stimulates the inhibition of retinal GSH reductase, and SOD activities • Prevention of lipid peroxidation • Reduction of retinal cell loss	Polymeric nanoparticles	(Alishahi et al., 2011; Desai and Park, 2005; Esposito et al., 2002; Jiménez-Fernández et al., 2014)
		Liposomes	(Wechtersbach et al., 2012; Zhou et al., 2014)
		SLN/NLC	(Comunian et al., 2014; Guney et al., 2014; Teeranachaideekul et al., 2007)
		Dendrimers	(Ghosh et al., 2010)
Vitamin E/α-tocopherol		Liposomes	(Marsanasco et al., 2011)
		Polymeric nanoparticles	(Anais et al., 2009; Byun et al., 2011; Luo et al., 2011; Murugeshu et al., 2011; Zhang and Feng, 2006)
		Nanoemulsions	(Hatanaka et al., 2010; Laouini et al., 2012)
		SLN/NLC	(de Carvalho et al., 2013; Fangueiro et al., 2012)
		Nanocapsules	(Khayata et al., 2012)
Resveratrol	• Free radical scavenging	Liposomes	(Vanaja et al., 2013)

	• Reduction of retinal oxidative stress • Reduction of retinal cell loss	Polymeric nanoparticles	(da Rocha Lindner et al., 2013; Lu et al., 2009; Shao et al., 2009)
		SLN/NLC	(Gokce et al., 2012; Jose et al., 2014; Neves et al., 2013; Pandita et al., 2014)
		Gelatin nanoparticles	(Karthikeyan et al., 2013)
		Nanoemulsions	(Davidov-Pardo and McClements, 2015; Sessa et al., 2014)
		Self-emulsifying drug delivery systems (SEDDS)	(Amri et al., 2014; Pund et al., 2014)
α-lipoic acid	• Inhibition of cell apoptosis • Reduction of retinal oxidative stress • Reduction of GSH and GPx levels • Reduction of VEGFs expression	Nanoemulsions	(Ruktanonchai et al., 2009)
		SLN/NLC	(Ruktanonchai et al., 2009; Souto et al., 2005)
		Polymeric nanoparticles	(Park et al., 2010)
		Nanocapsules	(Nishiura et al., 2013)
Curcumin	• Reduction of retinal oxidative stress • Inhibition of VEGFs production	Microcapsules and nanocapsules	(Wang et al., 2009; Zanotto-Filho et al., 2013)
		Liposomes	(Chen et al., 2012; Li et al., 2005; Ranjan et al., 2013)
		Polymeric nanoparticles	(Bisht et al., 2007; Sanoj Rejinold et al., 2011; Yallapu et al., 2010)
		Nanoemulsions	(Anuchapreeda et al., 2012; Rachmawati et al., 2014)
		SLN/NLC	(Chen et al., 2013; Puglia et al., 2012; Sun et al., 2013)

Epigalocatechin gallate (EGCG)	• Reduction of retinal oxidative stress • Activation of antioxidant enzymatic activity • Free radical scavenging	Polymeric nanoparticles	(Dube et al., 2010; Rocha et al., 2011)
		SLN/NLC	(Fangueiro et al., 2014b; Smith et al., 2010)
		Microcapsules	(Shutava et al., 2009)

The use of gold nanoparticles showed to control the activity of some enzymes, such as GR, SOD, glutathione peroxidase (GPx) and catalase (CAT) in diabetic mice (Barathmanikanth et al., 2010), also demonstrating some antioxidant activity in hyperglycemic rats. Gold nanoparticles were reported to inhibit lipid peroxidation and ROS generation, promoting a control over hyperglycemia. Thus, gold nanoparticles could represent a potential therapeutic treatment for DR management (Barathmanikanth et al., 2010) as well as natural antioxidants, such as vitamins and polyphenols (either alone or encapsulated).

1.2.4.9. Gene delivery

The management and treatment of DR is limited due to the multifactorial origin of this disease. Thus, gene delivery has gained much attention due to the exploration of genetic features that affects oxidation of retinal cells and the activation of the four main biochemical pathways (polyol, AGEs, hexosamine and PKC) (Ting and Martin, 2006). Some of the genes involved in these pathways have been treated as potential candidate genes for the management of DR. These genes include (Ng, 2010) angiotensin-I converting enzyme (*ACE*), angiotensin II type 1 receptor (*AGTR1*), angiotensinogen (*AGT*), *VEGF*, aldose reductase (*AR2*), receptor for AGEs (*RAGEs*), glucose transporter 1 (*GLUT1*), inducible and constitutive nitric oxide synthases (*NOS2A*, *NOS3*), transforming growth factor beta (*TGFbeta*), endothelin isoforms, and its cellular receptors (Beranek et al., 2002; Kumaramanickavel et al., 2002; Liu et al., 2014; Ray et al., 2004; Wang et al., 2003).

Xu and co-workers (Xu et al., 2014) studied and developed a gene-based intraocular erythropoietin (EPO) therapy for DR. The results show to be safe, feasible and exert long-term protective effects in DR patients. Studies involving nanoparticle-mediated gene delivery have been published by Park and co-workers (Park et al., 2009), using PLGA to load a plasmid, namely plasminogen kringle 5 (K5), a natural angiogenic inhibitor. Retinal neovascularization was evaluated in rats with oxygen-induced retinopathy by an intravitreal injection of the nanoparticles. The nanoparticles with the plasmid were able to mediate a sustained and efficient expression of K5 in the retina, reducing the retinal vascular leakage and retinal neovascularization.

1.2.5.Nanomaterials and diabetic retinopathy

The use of nanoparticles-based approaches to improve the prevention and treatment of DR is emerging in ocular administration. Despite the loading of some drugs that could avoid the progression of DR, nanoparticles seem to be promising, simply by the use of materials such as silver, gold, silica and titanium dioxide (Jo et al., 2011).

As mentioned above, retinal neovascularization is the most typical and risky factor occurring in DR pathogenesis. Jo and co-workers developed silicate (SI) nanoparticles and tested their anti-angiogenic effects on retinal neovascularization induced by VEGF (Jo et al., 2012). SI nanoparticles are biodegradable and safe, and were administered to mice via intravitreal injection. The results of this study demonstrated that SI nanoparticles have no toxic effect on retinal tissues by histological analysis and were shown to inhibit retinal neovascularization. Additionally, *in vitro* migration and tube formation of retinal microvascular endothelial cells was also observed. Thus, SI nanoparticles showed to be efficient in the treatment of VEGF-induced retinal neovascularization without acute toxicity, and can be applied in patients with DR.

Another study involving gold nanoparticles was reported by Kin and co-workers who demonstrated the nanoparticles ability to inhibit retinal neovascularization (Kim et al., 2011). The particles were administered in a mouse model by intravitreal injection. The results were shown to be promising and the gold nanoparticles effectively suppressed VEGF-induced *in vitro* angiogenesis of retinal microvascular endothelial cells including proliferation, migration and capillary-like networks formation. In addition, these particles showed to be safe and did not affect the cellular viability of retinal microvascular endothelial cells and induced no retinal toxicity. These could be useful for DR proliferative mediated by VEGF.

From the available studies, it is possible to conclude that several types of nanoparticles are being employed in the treatment of retinal neovascularization. Other types of nanoparticles reported by Jo and co-workers were bare titanium dioxide (TiO_2) nanoparticles (Jo et al., 2014). These nanoparticles were applied topically onto the eye surface of a mouse model. The particles were effective in suppressing *in vitro*

angiogenesis without showing any toxicity effects in the retina. *In vivo* retinal neovascularization was also suppressed when particles were administered by intravitreal injection. This study demonstrated that TiO_2 nanoparticles could be used at adequate concentration levels for the treatment of retinopathy mouse models.

The properties of silver nanoparticles seem to provide beneficial effects in the inhibition of angiogenesis. A study carried out by Gurunathan and co-workers (Gurunathan et al., 2009) showed that these particles could inhibit the formation of new blood microvessels induced by VEGF in mouse models.

1.2.6.Conclusions

DR is an eye disease that affects severely patient´s quality of life and leads to a high possibility of blindness. Despite the uncertain biochemical and biological mechanisms that provokes it, the multifactorial nature of the disease is evident, and thus its treatment remains a clinical challenge. The main biochemical pathways that DR affects are discussed as also the relation between them with the possible pharmacological strategies. The traditional and current strategies for the treatment and management of DR including pharmacological and surgical are discussed along with the major efforts that have been carried out using innovative drug delivery systems. Despite the maintenance of optimal glycemic levels, it seems not be sufficient to avoid DR in diabetic patients. In an early stage, pharmacological strategies can help in delaying the development of DR. In cases of DME and PDR, surgical strategies are employed, however they still an invasive strategy associated with enormous side effects. Thus, the development of new drug delivery systems for ocular drug delivery has gained much attention and became an important field of research. The development of sustained and prolonged action, non-invasive, safe and innovative drug delivery systems can overcome some of the major barriers and difficulties provided by the anatomy and physiology of the eye to the entrance of drugs. Additionally, these nanocarriers could be rationale alternative to invasive, high risk and painful treatments that have been applied for the management of DR. Thus, these nanotechnological advances have possibility to improve the efficacy and adhesion of therapeutic in DR as also provide better results comparing with the current strategies applied.

1.2.7.Bibliographic references

Abdallah, W., and Fawzi, A. A. (2009). Anti-VEGF therapy in proliferative diabetic retinopathy. I*nternational Ophthalmology Clinics,* 49(2), 95-107.

Abu El-Asrar, A. M., and Al-Mezaine, H. S. (2011). Advances in the treatment of diabetic retinopathy. *Saudi Journal of Ophthalmology,* 25(2), 113-122.

Accardo, A., Morisco, A., Gianolio, E., Tesauro, D., Mangiapia, G., Radulescu, A., Morelli, G. (2011). Nanoparticles containing octreotide peptides and gadolinium complexes for MRI applications. *Journal of Peptide Science,* 17(2), 154-162.

Aiello, L. P., Avery, R. L., Arrigg, P. G., Keyt, B. A., Jampel, H. D., Shah, S. T., et al. (1994). Vascular endothelial growth factor in ocular fluid of patients with diabetic retinopathy and other retinal disorders. *The New England Journal of Medicine,* 331(22), 1480-1487.

Aiello, L. P., Bursell, S. E., Clermont, A., Duh, E., Ishii, H., Takagi, C., King, G. L. (1997). Vascular endothelial growth factor-induced retinal permeability is mediated by protein kinase C in vivo and suppressed by an orally effective beta-isoform-selective inhibitor. *Diabetes,* 46(9), 1473-1480.

Aiello, L. P., Davis, M. D., Girach, A., Kles, K. A., Milton, R. C., Sheetz, M. J., Zhi, X. E. (2006). Effect of ruboxistaurin on visual loss in patients with diabetic retinopathy. *Ophthalmology,* 113(12), 2221-2230.

Aiello, L. P., Vignati, L., Sheetz, M. J., Zhi, X., Girach, A., Davis, M. D., Milton, R. C. (2011). Oral protein kinase c beta inhibition using ruboxistaurin: efficacy, safety, and causes of vision loss among 813 patients (1,392 eyes) with diabetic retinopathy in the Protein Kinase C beta Inhibitor-Diabetic Retinopathy Study and the Protein Kinase C beta Inhibitor-Diabetic Retinopathy Study 2. *Retina,* 31(10), 2084-2094.

Al-Halafi, A. M. (2014). Nanocarriers of nanotechnology in retinal diseases. *Saudi Journal of Ophthalmology,* 28(4), 304-309.

Al-Shabrawey, M., Elsherbiny, M., Nussbaum, J., Othman, A., Megyerdi, S., and Tawfik, A. (2013). Targeting neovascularization in ischemic retinopathy: recent advances. *Expert Review of Ophthalmology,* 8(3), 267-286.

Alishahi, A., Mirvaghefi, A., Tehrani, M. R., Farahmand, H., Shojaosadati, S. A., Dorkoosh, F. A., and Elsabee, M. Z. (2011). Shelf life and delivery enhancement of vitamin C using chitosan nanoparticles. *Food Chemistry,* 126(3), 935-940.

Amri, A., Le Clanche, S., Thérond, P., Bonnefont-Rousselot, D., Borderie, D., Lai-Kuen, R., Charrueau, C. (2014). Resveratrol self-emulsifying system increases the uptake by

endothelial cells and improves protection against oxidative stress-mediated death. *European Journal of Pharmaceutics and Biopharmaceutics,* 86(3), 418-426.

Anais, J. P., Razzouq, N., Carvalho, M., Fernandez, C., Astier, A., Paul, M., Lorino, A. M. (2009). Development of alpha-tocopherol acetate nanoparticles: influence of preparative processes. *Drug Development* and *Industrial Pharmacy,* 35(2), 216-223.

Anderson, R. E., Rapp, L. M., and Wiegand, R. D. (1984). Lipid peroxidation and retinal degeneration. *Current Eye Research,* 3(1), 223-227.

Anuchapreeda, S., Fukumori, Y., Okonogi, S., and Ichikawa, H. (2012). Preparation of Lipid Nanoemulsions Incorporating Curcumin for Cancer Therapy. *Journal of Nanotechnology*, 2012, 11.

Anuradha, C. D., Kanno, S., and Hirano, S. (2001). Oxidative damage to mitochondria is a preliminary step to caspase-3 activation in fluoride-induced apoptosis in HL-60 cells. *Free Radical Biology* and *Medicine,* 31(3), 367-373.

Araujo, J., Garcia, M. L., Mallandrich, M., Souto, E. B., and Calpena, A. C. (2012). Release profile and transscleral permeation of triamcinolone acetonide loaded nanostructured lipid carriers (TA-NLC): in vitro and ex vivo studies. *Nanomedicine: Nanotechnology, Biology and Medicine,* 8(6), 1034-1041.

Araujo, J., Gonzalez-Mira, E., Egea, M. A., Garcia, M. L., and Souto, E. B. (2010). Optimization and physicochemical characterization of a triamcinolone acetonide-loaded NLC for ocular antiangiogenic applications. *International Journal of Pharmaceutics,* 393(1-2), 167-175.

Araujo, J., Nikolic, S., Egea, M. A., Souto, E. B., and Garcia, M. L. (2011). Nanostructured lipid carriers for triamcinolone acetonide delivery to the posterior segment of the eye. *Colloids and Surfaces B: Biointerfaces,* 88(1), 150-157.

Barathmanikanth, S., Kalishwaralal, K., Sriram, M., Pandian, S. R., Youn, H. S., Eom, S., and Gurunathan, S. (2010). Anti-oxidant effect of gold nanoparticles restrains hyperglycemic conditions in diabetic mice. *Journal of Nanobiotechnology,* 8, 16.

Barot, M., Gokulgandhi, M. R., and Mitra, A. K. (2011). Mitochondrial Dysfunction in Retinal Diseases. *Current Eye Research,* 36(12), 1069-1077.

Bellia, F., Oliveri, V., Rizzarelli, E., and Vecchio, G. (2013). New derivative of carnosine for nanoparticle assemblies. *European Journal* of *Medicinal Chemistry*, 70, 225-232.

Beranek, M., Kankova, K., Benes, P., Izakovicova-Holla, L., Znojil, V., Hajek, D., Vacha, J. (2002). Polymorphism R25P in the gene encoding transforming growth factor-beta (TGF-beta1) is a newly identified risk factor for proliferative diabetic retinopathy. *American Journal of Medical Genetics,* 109(4), 278-283.

Bhavsar, A. R. (2006). Diabetic retinopathy: the latest in current management. *Retina,* 26(6 Suppl), S71-79.

Bisht, S., Feldmann, G., Soni, S., Ravi, R., Karikar, C., Maitra, A., and Maitra, A. (2007). Polymeric nanoparticle-encapsulated curcumin ("nanocurcumin"): a novel strategy for human cancer therapy. *Journal of Nanobiotechnology,* 5, 3.

Boehm, B. O., and Lustig, R. H. (2002). Use of somatostatin receptor ligands in obesity and diabetic complications. *Best Practice & Research Clinical Gastroenterology,* 16(3), 493-509.

Bressler, N. M., Edwards, A. R., Beck, R. W., Flaxel, C. J., Glassman, A. R., Ip, M. S., Stone, T. W. (2009). Exploratory analysis of diabetic retinopathy progression through 3 years in a randomized clinical trial that compares intravitreal triamcinolone acetonide with focal/grid photocoagulation. *Archives of Ophthalmology,* 127(12), 1566-1571.

Brownlee, M., Vlassara, H., and Cerami, A. (1984). Nonenzymatic glycosylation and the pathogenesis of diabetic complications. *Annals of Internal Medicine,* 101(4), 527-537.

Bursell, S. E., Clermont, A. C., Aiello, L. P., Aiello, L. M., Schlossman, D. K., Feener, E. P., King, G. L. (1999). High-dose vitamin E supplementation normalizes retinal blood flow and creatinine clearance in patients with type 1 diabetes. *Diabetes Care,* 22(8), 1245-1251.

Bysell, H., Mansson, R., Hansson, P., and Malmsten, M. (2011). Microgels and microcapsules in peptide and protein drug delivery. *Advanced Drug Delivery Reviews,* 63(13), 1172-1185.

Byun, Y., Hwang, J. B., Bang, S. H., Darby, D., Cooksey, K., Dawson, P. L., Whiteside, S. (2011). Formulation and characterization of α-tocopherol loaded poly ε-caprolactone (PCL) nanoparticles. *Food Science and Technology, 44*(1), 24-28.

Campochiaro, P. A., Brown, D. M., Pearson, A., Ciulla, T., Boyer, D., Holz, F. G., Kane, F. E. (2011). Long-term Benefit of Sustained-Delivery Fluocinolone Acetonide Vitreous Inserts for Diabetic Macular Edema. *Ophthalmology,* 118(4), 626-635.e622.

Carmeliet, P. (2000). VEGF gene therapy: stimulating angiogenesis or angioma-genesis? *Nature Medicine,* 6(10), 1102-1103.

Cetin, E. N., Bulgu, Y., Ozdemir, S., Topsakal, S., Akin, F., Aybek, H., and Yildirim, C. (2013). Association of serum lipid levels with diabetic retinopathy. *International Journal of Ophthalmology,* 6(3), 346-349.

Chantelau, E., and Frystyk, J. (2005). Progression of diabetic retinopathy during improved metabolic control may be treated with reduced insulin dosage and/or somatostatin analogue administration - a case report. *Growth Hormone & IGF Research,* 15(2), 130-135.

Chen, J., C., Dai, W. T., He, Z. M., Gao, L., Huang, X., Gong, J. M., Chen, W. D. (2013). Fabrication and evaluation of curcumin-loaded nanoparticles based on solid lipid as a new type of colloidal drug delivery system. *Indian Journal of Pharmaceutical Sciences,* 75, 178-184.

Chen, Y., Wu, Q., Zhang, Z., Yuan, L., Liu, X., and Zhou, L. (2012). Preparation of Curcumin-Loaded Liposomes and Evaluation of Their Skin Permeation and Pharmacodynamics. *Molecules,* 17, 5972-5987.

Chibber, R., Ben-Mahmud, B. M., Chibber, S., and Kohner, E. M. (2007). Leukocytes in diabetic retinopathy. *Current Diabetes Reviews,* 3(1), 3-14.

Cintra, L. P., Costa, R. A., Ribeiro, J. A., Calucci, D., Scott, I. U., Messias, A., and Jorge, R. (2013). Intravitreal bevacizumab (Avastin) for persistent new vessels in diabetic retinopathy (IBEPE study): 1-year results. *Retina,* 33(6), 1109-1116.

Ciulla, T. A., Amador, A. G., and Zinman, B. (2003). Diabetic Retinopathy and Diabetic Macular Edema: Pathophysiology, screening, and novel therapies. *Diabetes Care,* 26(9), 2653-2664.

Ciulla, T. A., Harris, A., Latkany, P., Piper, H. C., Arend, O., Garzozi, H., and Martin, B. (2002). Ocular perfusion abnormalities in diabetes. *Acta ophthalmologica Scandinavica,* 80(5), 468-477.

Cohen, S. M., Flynn, H. W., Jr., Murray, T. G., and Smiddy, W. E. (1995). Endophthalmitis after pars plana vitrectomy. The Postvitrectomy Endophthalmitis Study Group. *Ophthalmology,* 102(5), 705-712.

Comunian, T. A., Abbaspourrad, A., Favaro-Trindade, C. S., and Weitz, D. A. (2014). Fabrication of solid lipid microcapsules containing ascorbic acid using a microfluidic technique. *Food Chemistry,* 152, 271-275.

Crawford, T. N., Alfaro, D. V., 3rd, Kerrison, J. B., and Jablon, E. P. (2009). Diabetic retinopathy and angiogenesis. *Current Diabetes Reviews,* 5(1), 8-13.

da Rocha Lindner, G., Khalil, N. M., and Mainardes, R. M. (2013). Resveratrol-Loaded Polymeric Nanoparticles: Validation of an HPLC-PDA Method to Determine the Drug Entrapment and Evaluation of Its Antioxidant Activity. *The Scientific World Journal, 2013,* 9.

da Silva, G. R., da Silva-Cunha Jr, A., Behar-Cohen, F., Ayres, E., and Oréfice, R. L. (2011). Biodegradable polyurethane nanocomposites containing dexamethasone for ocular route. *Materials Science and Engineering: C,* 31(2), 414-422.

Dal Monte, M., Ristori, C., Cammalleri, M., and Bagnoli, P. (2009). Effects of somatostatin analogues on retinal angiogenesis in a mouse model of oxygen-induced

retinopathy: involvement of the somatostatin receptor subtype 2. *Investigative Ophthalmology & Visual Science,* 50(8), 3596-3606.

Damge, C., Vonderscher, J., Marbach, P., and Pinget, M. (1997). Poly(alkyl cyanoacrylate) nanocapsules as a delivery system in the rat for octreotide, a long-acting somatostatin analogue. *Journal of Pharmacology and Pharmacotherapeutics,* 49(10), 949-954.

Danhier, F., Ansorena, E., Silva, J. M., Coco, R., Le Breton, A., and Preat, V. (2012). PLGA-based nanoparticles: an overview of biomedical applications. *Journal of Controlled Release,* 161(2), 505-522.

Danis, R. P., Bingaman, D. P., Jirousek, M., and Yang, Y. (1998). Inhibition of intraocular neovascularization caused by retinal ischemia in pigs by PKCbeta inhibition with LY333531. *Investigative Ophthalmology & Visual Science,* 39(1), 171-179.

Danis, R. P., Ciulla, T. A., Pratt, L. M., and Anliker, W. (2000). Intravitreal triamcinolone acetonide in exudative age-related macular degeneration. *Retina,* 20(3), 244-250.

Davidov-Pardo, G., and McClements, D. J. (2015). Nutraceutical delivery systems: Resveratrol encapsulation in grape seed oil nanoemulsions formed by spontaneous emulsification. *Food Chemistry,* 167, 205-212.

Davidson, J. A., Ciulla, T. A., McGill, J. B., Kles, K. A., and Anderson, P. W. (2007). How the diabetic eye loses vision. *Endocrine, 32*(1), 107-116.

de Carvalho, S. M., Noronha, C. M., Floriani, C. L., Lino, R. C., Rocha, G., Bellettini, I. C., Barreto, P. L. M. (2013). Optimization of α-tocopherol loaded solid lipid nanoparticles by central composite design. *Industrial Crops and Products,* 49, 278-285.

Desai, K. G. H., and Park, H. J. (2005). Encapsulation of vitamin C in tripolyphosphate cross-linked chitosan microspheres by spray drying. *Journal of Microencapsulation,* 22(2), 179-192.

Do, D. V., Nguyen, Q. D., Boyer, D., Schmidt-Erfurth, U., Brown, D. M., Vitti, R., Heier, J. S. (2012). One-year outcomes of the da Vinci Study of VEGF Trap-Eye in eyes with diabetic macular edema. *Ophthalmology,* 119(8), 1658-1665.

Do, D. V., Schmidt-Erfurth, U., Gonzalez, V. H., Gordon, C. M., Tolentino, M., Berliner, A. J., Heier, J. S. (2011). The DA VINCI Study: phase 2 primary results of VEGF Trap-Eye in patients with diabetic macular edema. *Ophthalmology,* 118(9), 1819-1826.

Doft, B. M., Kelsey, S. F., and Wisniewski, S. R. (2000). Retinal detachment in the endophthalmitis vitrectomy study. *Archives of Ophthalmology,* 118(12), 1661-1665.

Dorkoosh, F. A., Coos Verhoef, J., Ambagts, M. H. C., Rafiee-Tehrani, M., Borchard, G., and Junginger, H. E. (2002). Peroral delivery systems based on superporous hydrogel

polymers: release characteristics for the peptide drugs buserelin, octreotide and insulin. *European Journal of Pharmaceutical Sciences,* 15(5), 433-439.

Driot, J. Y., Novack, G. D., Rittenhouse, K. D., Milazzo, C., and Pearson, P. A. (2004). Ocular pharmacokinetics of fluocinolone acetonide after Retisert intravitreal implantation in rabbits over a 1-year period. *Journal of Ocular Pharmacology Therapeutics,* 20(3), 269-275.

Dube, A., Nicolazzo, J. A., and Larson, I. (2010). Chitosan nanoparticles enhance the intestinal absorption of the green tea catechins (+)-catechin and (−)-epigallocatechin gallate. *European Journal of Pharmaceutical Sciences,* 41(2), 219-225.

Dubey, N., Varshney, R., Shukla, J., Ganeshpurkar, A., Hazari, P. P., Bandopadhaya, G. P., Trivedi, P. (2012). Synthesis and evaluation of biodegradable PCL/PEG nanoparticles for neuroendocrine tumor targeted delivery of somatostatin analog. *Drug Delivery,* 19(3), 132-142.

Durmus, Z., Kavas, H., Baykal, A., Sozeri, H., Alpsoy, L., Çelik, S. Ü., and Toprak, M. S. (2011). Synthesis and characterization of l-carnosine coated iron oxide nanoparticles. *Journal of Alloys and Compounds,* 509(5), 2555-2561.

Esposito, E., Cervellati, F., Menegatti, E., Nastruzzi, C., and Cortesi, R. (2002). Spray dried Eudragit microparticles as encapsulation devices for vitamin C. *International Journal of Pharmaceutics,* 242(1–2), 329-334.

Fang, X., Sakaguchi, H., Gomi, F., Oshima, Y., Sawa, M., Tsujikawa, M., Tano, Y. (2008). Efficacy and safety of one intravitreal injection of bevacizumab in diabetic macular oedema. *Acta Ophthalmologica,* 86(7), 800-805.

Fangueiro, J. F., Andreani, T., Egea, M. A., Garcia, M. L., Souto, S. B., Silva, A. M., and Souto, E. B. (2014a). Design of cationic lipid nanoparticles for ocular delivery: development, characterization and cytotoxicity. *International Journal of Pharmaceutics,* 461(1-2), 64-73.

Fangueiro, J. F., Andreani, T., Fernandes, L., Garcia, M. L., Egea, M. A., Silva, A. M., and Souto, E. B. (2014b). Physicochemical characterization of epigallocatechin gallate lipid nanoparticles (EGCG-LNs) for ocular instillation. *Colloids and Surfaces B: Biointerfaces*, 123, 452-460.

Fangueiro, J. F., Gonzalez-Mira, E., Martins-Lopes, P., Egea, M. A., Garcia, M. L., Souto, S. B., and Souto, E. B. (2013). A novel lipid nanocarrier for insulin delivery: production, characterization and toxicity testing. *Pharmaceutical Development Technology,* 18(3), 545-549.

Fangueiro, J. F., Macedo, A. S., Jose, S., Garcia, M. L., Souto, S. B., and Souto, E. B. (2012). Thermodynamic behavior of lipid nanoparticles upon delivery of Vitamin E

derivatives into the skin: in vitro studies. *Journal of Thermal Analysis and Calorimetry,* 108(1), 275-282.

Frank, R. N. (2004). Diabetic Retinopathy. *New England Journal of Medicine,* 350(1), 48-58.

Friedman, E. A. (1999). Advanced glycosylated end products and hyperglycemia in the pathogenesis of diabetic complications. *Diabetes Care,* 22 *Suppl 2*, B65-71.

Gardiner, T. A., Anderson, H. R., and Stitt, A. W. (2003). Inhibition of advanced glycation end-products protects against retinal capillary basement membrane expansion during long-term diabetes. *Journal of Pathology,* 201(2), 328-333.

Ghosh, S., Bhattacharya, S. C., and Saha, A. (2010). Probing of ascorbic acid by CdS/dendrimer nanocomposites: a spectroscopic investigation. *Analytical and Bioanalytical Chemistry,* 397(4), 1573-1582.

Gillies, M. C., Sutter, F. K., Simpson, J. M., Larsson, J., Ali, H., and Zhu, M. (2006). Intravitreal triamcinolone for refractory diabetic macular edema: two-year results of a double-masked, placebo-controlled, randomized clinical trial. *Ophthalmology,* 113(9), 1533-1538.

Gokce, E. H., Korkmaz, E., Dellera, E., Sandri, G., Bonferoni, M. C., and Ozer, O. (2012). Resveratrol-loaded solid lipid nanoparticles versus nanostructured lipid carriers: evaluation of antioxidant potential for dermal applications. *International Journal of Nanomedicine,* 7, 1841-1850.

Goldfien, A. (1995). Adrenocorticosteroids and adrenocortical antagonists. In Katzung BG (Ed.), *Basic and Clinical Pharmacology* (pp. 592-607). London: Prentice Hall International ,

Gómez-Gaete, C., Tsapis, N., Besnard, M., Bochot, A., and Fattal, E. (2007). Encapsulation of dexamethasone into biodegradable polymeric nanoparticles. *International Journal of Pharmaceutics,* 331(2), 153-159.

Gonzalez-Mira, E., Egea, M. A., Garcia, M. L., and Souto, E. B. (2010). Design and ocular tolerance of flurbiprofen loaded ultrasound-engineered NLC. *Colloids and Surfaces B: Biointerfaces,* 81(2), 412-421.

Gonzalez-Mira, E., Egea, M. A., Souto, E. B., Calpena, A. C., and Garcia, M. L. (2011). Optimizing flurbiprofen-loaded NLC by central composite factorial design for ocular delivery. *Nanotechnology,* 22(4), 045101.

Gonzalez, V. H., Giuliari, G. P., Banda, R. M., and Guel, D. A. (2009). Intravitreal injection of pegaptanib sodium for proliferative diabetic retinopathy. *British Journal of Ophthalmology,* 93(11), 1474-1478.

Grant, M. B., and Caballero, S., Jr. (2005). The potential role of octreotide in the treatment of diabetic retinopathy. *Treatments in endocrinology,* 4(4), 199-203.

Grant, M. B., Mames, R. N., Fitzgerald, C., Hazariwala, K. M., Cooper-DeHoff, R., Caballero, S., and Estes, K. S. (2000). The efficacy of octreotide in the therapy of severe nonproliferative and early proliferative diabetic retinopathy: a randomized controlled study. *Diabetes Care,* 23(4), 504-509.

Group, M. D. R. S. (2005). A Phase II Randomized Double-Masked Trial of Pegaptanib, an Anti–Vascular Endothelial Growth Factor Aptamer, for Diabetic Macular Edema. *Ophthalmology,* 112(10), 1747-1757.

Group, M. D. R. S. (2006). Changes in Retinal Neovascularization after Pegaptanib (Macugen) Therapy in Diabetic Individuals. *Ophthalmology*, 113(1), 23-28.

Group, P.-D. S. (2007). Effect of ruboxistaurin in patients with diabetic macular edema: thirty-month results of the randomized PKC-DMES clinical trial. *Archives of Ophthalmology,* 125(3), 318-324.

Guney, G., Kutlu, H. M., and Genc, L. (2014). Preparation and characterization of ascorbic acid loaded solid lipid nanoparticles and investigation of their apoptotic effects. *Colloids and Surfaces B: Biointerfaces,* 121, 270-280.

Gurunathan, S., Lee, K. J., Kalishwaralal, K., Sheikpranbabu, S., Vaidyanathan, R., and Eom, S. H. (2009). Antiangiogenic properties of silver nanoparticles. *Biomaterials,* 30(31), 6341-6350.

Haesslein, A., Ueda, H., Hacker, M. C., Jo, S., Ammon, D. M., Borazjani, R. N., Mikos, A. G. (2006). Long-term release of fluocinolone acetonide using biodegradable fumarate-based polymers. *Journal of Controlled Release,* 114(2), 251-260.

Hammes, H. P., Brownlee, M., Edelstein, D., Saleck, M., Martin, S., and Federlin, K. (1994). Aminoguanidine inhibits the development of accelerated diabetic retinopathy in the spontaneous hypertensive rat. *Diabetologia*, 37(1), 32-35.

Hammes, H. P., Martin, S., Federlin, K., Geisen, K., and Brownlee, M. (1991). Aminoguanidine treatment inhibits the development of experimental diabetic retinopathy. *Proceedings of the National Academy of Sciences USA*, 88(24), 11555-11558.

Haritoglou, C., Gerss, J., Hammes, H. P., Kampik, A., and Ulbig, M. W. (2011). Alpha-lipoic acid for the prevention of diabetic macular edema. *Ophthalmologica,* 226(3), 127-137.

Hatanaka, J., Chikamori, H., Sato, H., Uchida, S., Debari, K., Onoue, S., and Yamada, S. (2010). Physicochemical and pharmacological characterization of alpha-tocopherol-loaded nano-emulsion system. *International Journal of Pharmaceutics,* 396(1-2), 188-193.

Helbok, A., Rangger, C., von Guggenberg, E., Saba-Lepek, M., Radolf, T., Thurner, G.,Decristoforo, C. (2012). Targeting properties of peptide-modified radiolabeled liposomal nanoparticles. *Nanomedicine: Nanotechnology, Biology and Medicine,* 8(1), 112-118.

Herrero-Vanrell, R., Cardillo, J. A., and Kuppermann, B. D. (2011). Clinical applications of the sustained-release dexamethasone implant for treatment of macular edema. *Clinical Ophthalmology,* 5, 139-146.

Holden, C. A., Tyagi, P., Thakur, A., Kadam, R., Jadhav, G., Kompella, U. B., and Yang, H. (2012). Polyamidoamine dendrimer hydrogel for enhanced delivery of antiglaucoma drugs. *Nanomedicine,* 8(5), 776-783.

Hong, Y., Zhu, H., Hu, J., Lin, X., Wang, F., Li, C., and Yang, Z. (2014). Synthesis and radiolabeling of 111In-core-cross linked polymeric micelle-octreotide for near-infrared fluoroscopy and single photon emission computed tomography imaging. *Bioorganic and Medicinal Chemistry Letters,* 24(12), 2781-2785.

Hoshi, S., Nomoto, K.-i., Kuromitsu, J., Tomari, S., and Nagata, M. (2002). High Glucose Induced VEGF Expression via PKC and ERK in Glomerular Podocytes. *Biochemical and Biophysical Research Communications,* 290(1), 177-184.

Huang, H. Y., Appel, L. J., Croft, K. D., Miller, E. R., 3rd, Mori, T. A., and Puddey, I. B. (2002). Effects of vitamin C and vitamin E on in vivo lipid peroxidation: results of a randomized controlled trial. *American Journal* of *Clinical Nutrition,* 76(3), 549-555.

Huo, M., Zou, A., Yao, C., Zhang, Y., Zhou, J., Wang, J., Zhang, Q. (2012). Somatostatin receptor-mediated tumor-targeting drug delivery using octreotide-PEG-deoxycholic acid conjugate-modified N-deoxycholic acid-O, N-hydroxyethylation chitosan micelles. *Biomaterials,* 33(27), 6393-6407.

Ip, M. S., Domalpally, A., Hopkins, J. J., Wong, P., and Ehrlich, J. S. (2012). Long-term effects of ranibizumab on diabetic retinopathy severity and progression. *Archives of Ophthalmology,* 130(9), 1145-1152.

Ishii, H., Jirousek, M. R., Koya, D., Takagi, C., Xia, P., Clermont, A., King, G. L. (1996). Amelioration of vascular dysfunctions in diabetic rats by an oral PKC beta inhibitor. *Science,* 272(5262), 728-731.

Jaffe, G. J., Martin, D., Callanan, D., Pearson, P. A., Levy, B., and Comstock, T. (2006). Fluocinolone Acetonide Implant (Retisert) for Noninfectious Posterior Uveitis: Thirty-Four–Week Results of a Multicenter Randomized Clinical Study. *Ophthalmology*, 113(6), 1020-1027.

Jaffe, G. J., Yang, C. H., Guo, H., Denny, J. P., Lima, C., and Ashton, P. (2000). Safety and pharmacokinetics of an intraocular fluocinolone acetonide sustained delivery device. *Investigative Ophthalmology & Visual Science*, 41(11), 3569-3575.

Jain, N., Stinnett, S. S., and Jaffe, G. J. (2012). Prospective Study of a Fluocinolone Acetonide Implant for Chronic Macular Edema from Central Retinal Vein Occlusion: Thirty-Six-Month Results. *Ophthalmology*, 119(1), 132-137.

Jiménez-Fernández, E., Ruyra, A., Roher, N., Zuasti, E., Infante, C., and Fernández-Díaz, C. (2014). Nanoparticles as a novel delivery system for vitamin C administration in aquaculture. *Aquaculture*, 432, 426-433.

Jo, D. H., Kim, J. H., Son, J. G., Song, N. W., Kim, Y.-I., Yu, Y. S., . . . Kim, J. H. (2014). Anti-angiogenic effect of bare titanium dioxide nanoparticles on pathologic neovascularization without unbearable toxicity. *Nanomedicine: Nanotechnology, Biology and Medicine*, 10(5), 1109-1117.

Jo, D. H., Kim, J. H., Yu, Y. S., Lee, T. G., and Kim, J. H. (2012). Antiangiogenic effect of silicate nanoparticle on retinal neovascularization induced by vascular endothelial growth factor. *Nanomedicine: Nanotechnology, Biology and Medicine*, 8(5), 784-791.

Jo, D. H., Lee, T. G., and Kim, J. H. (2011). Nanotechnology and nanotoxicology in retinopathy. *International Journal of Molecular* Sciences, 12(11), 8288-8301.

Johansen, J. S., Harris, A. K., Rychly, D. J., and Ergul, A. (2005). Oxidative stress and the use of antioxidants in diabetes: linking basic science to clinical practice. *Cardiovascular Diabetology*, 4(1), 5.

Jonas, J. B. (2007). Intravitreal triamcinolone acetonide for diabetic retinopathy. *Developments in Ophthalmology*, 39, 96-110.

Jonas, J. B., Kreissig, I., Hugger, P., Sauder, G., Panda-Jonas, S., and Degenring, R. (2003). Intravitreal triamcinolone acetonide for exudative age related macular degeneration. *British Journal of Ophthalmology*, 87(4), 462-468.

Jonas, J. B., and Sofker, A. (2001). Intraocular injection of crystalline cortisone as adjunctive treatment of diabetic macular edema. *American Journal of Ophthalmology*, *132*(3), 425-427.

Jorge, R., Costa, R. A., Calucci, D., Cintra, L. P., and Scott, I. U. (2006). Intravitreal bevacizumab (Avastin) for persistent new vessels in diabetic retinopathy (IBEPE study). *Retina*, 26(9), 1006-1013.

Jose, S., Anju, S. S., Cinu, T. A., Aleykutty, N. A., Thomas, S., and Souto, E. B. (2014). In vivo pharmacokinetics and biodistribution of resveratrol-loaded solid lipid nanoparticles for brain delivery. *International Journal of Pharmaceutics*, 474(1–2), 6-13.

Kadam, R. S., Tyagi, P., Edelhauser, H. F., and Kompella, U. B. (2012). Influence of choroidal neovascularization and biodegradable polymeric particle size on transscleral sustained delivery of triamcinolone acetonide. *International Journal of Pharmaceutics, 434*(1-2), 140-147.

Kalishwaralal, K., Barathmanikanth, S., Pandian, S. R., Deepak, V., and Gurunathan, S. (2010). Silver nano - a trove for retinal therapies. *Journal of Controlled Release,* 145(2), 76-90.

Karthikeyan, S., Rajendra Prasad, N., Ganamani, A., and Balamurugan, E. (2013). Anticancer activity of resveratrol-loaded gelatin nanoparticles on NCI-H460 non-small cell lung cancer cells. *Biomedicine and Preventive Nutrition,* 3(1), 64-73.

Kern, T. S., and Engerman, R. L. (2001). Pharmacological inhibition of diabetic retinopathy: aminoguanidine and aspirin. *Diabetes,* 50(7), 1636-1642.

Kern, T. S., Tang, J., Mizutani, M., Kowluru, R. A., Nagaraj, R. H., Romeo, G., Lorenzi, M. (2000). Response of capillary cell death to aminoguanidine predicts the development of retinopathy: comparison of diabetes and galactosemia. *Investigative Ophthalmology & Visual Science,* 41(12), 3972-3978.

Khayata, N., Abdelwahed, W., Chehna, M. F., Charcosset, C., and Fessi, H. (2012). Preparation of vitamin E loaded nanocapsules by the nanoprecipitation method: From laboratory scale to large scale using a membrane contactor. *International Journal of Pharmaceutics,* 423(2), 419-427.

Khurana, R. N., Do, D. V., and Nguyen, Q. D. (2009). Anti-VEGF therapeutic approaches for diabetic macular edema. *International Ophthalmology Clinics,* 49(2), 109-119.

Kim, J., and Chauhan, A. (2008). Dexamethasone transport and ocular delivery from poly(hydroxyethyl methacrylate) gels. *International Journal of Pharmaceutics,* 353(1-2), 205-222.

Kim, J. H., Kim, M. H., Jo, D. H., Yu, Y. S., Lee, T. G., and Kim, J. H. (2011). The inhibition of retinal neovascularization by gold nanoparticles via suppression of VEGFR-2 activation. *Biomaterials,* 32(7), 1865-1871.

Kirkegaard, C., Norgaard, K., Snorgaard, O., Bek, T., Larsen, M., and Lund-Andersen, H. (1990). Effect of one year continuous subcutaneous infusion of a somatostatin analogue, octreotide, on early retinopathy, metabolic control and thyroid function in Type I (insulin-dependent) diabetes mellitus. *Acta Endocrinologica (Copenhagen),* 122(6), 766-772.

Klein, R., Klein, B. E., Moss, S. E., and Cruickshanks, K. J. (1998). The Wisconsin Epidemiologic Study of Diabetic Retinopathy: XVII. The 14-year incidence and progression of diabetic retinopathy and associated risk factors in type 1 diabetes. *Ophthalmology,* 105(10), 1801-1815.

Klein, R., Klein, B. E., Moss, S. E., Davis, M. D., and DeMets, D. L. (1988). Glycosylated hemoglobin predicts the incidence and progression of diabetic retinopathy. *Journal of American Medical Association,* 260(19), 2864-2871.

Kompella, U. B., Amrite, A. C., Pacha Ravi, R., and Durazo, S. A. (2013). Nanomedicines for back of the eye drug delivery, gene delivery, and imaging. *Progress in Retinal* and *Eye Research,* 36, 172-198.

Kowluru, R. A. (2005). Diabetic retinopathy: mitochondrial dysfunction and retinal capillary cell death. *Antioxidants & Redox Signaling,* 7(11-12), 1581-1587.

Kowluru, R. A., Atasi, L., and Ho, Y. S. (2006). Role of mitochondrial superoxide dismutase in the development of diabetic retinopathy. *Investigative Ophthalmology & Visual Science,* 47(4), 1594-1599.

Kowluru, R. A., and Chan, P. S. (2007). Oxidative stress and diabetic retinopathy. *Experimental diabetes research,* 2007, 43603, doi: 10.1155/2007/43603.

Kowluru, R. A., Tang, J., and Kern, T. S. (2001). Abnormalities of retinal metabolism in diabetes and experimental galactosemia. VII. Effect of long-term administration of antioxidants on the development of retinopathy. *Diabetes,* 50(8), 1938-1942.

Koya, D., and King, G. L. (1998). Protein kinase C activation and the development of diabetic complications. *Diabetes,* 47(6), 859-866.

Kumaramanickavel, G., Ramprasad, V. L., Sripriya, S., Upadyay, N. K., Paul, P. G., and Sharma, T. (2002). Association of Gly82Ser polymorphism in the RAGE gene with diabetic retinopathy in type II diabetic Asian Indian patients. *Journal of Diabetes Complications,* 16(6), 391-394.

Kunisaki, M., Bursell, S. E., Clermont, A. C., Ishii, H., Ballas, L. M., Jirousek, M. R., King, G. L. (1995). Vitamin E prevents diabetes-induced abnormal retinal blood flow via the diacylglycerol-protein kinase C pathway. *American Journal of Physiology,* 269(2 Pt 1), E239-246.

Kunisaki, M., Bursell, S. E., Umeda, F., Nawata, H., and King, G. L. (1998). Prevention of diabetes-induced abnormal retinal blood flow by treatment with d-alpha-tocopherol. *Biofactors,* 7(1-2), 55-67.

Kuppermann, B. D., Blumenkranz, M. S., Haller, J. A., Williams, G. A., Weinberg, D. V., Chou, C., and Whitcup, S. M. (2007). Randomized controlled study of an intravitreous dexamethasone drug delivery system in patients with persistent macular edema. *Archives of Ophthalmology,* 125(3), 309-317.

Lallemand, F., Daull, P., Benita, S., Buggage, R., and Garrigue, J. S. (2012). Successfully improving ocular drug delivery using the cationic nanoemulsion, novasorb. *Journal of Drug Delivery,* 2012, 604204, doi: 10.1155/2012/604204.

Lam, D. S., Lai, T. Y., Lee, V. Y., Chan, C. K., Liu, D. T., Mohamed, S., and Li, C. L. (2009). Efficacy of 1.25 MG versus 2.5 MG intravitreal bevacizumab for diabetic macular edema: six-month results of a randomized controlled trial. *Retina,* 29(3), 292-299.

Laouini, A., Fessi, H., and Charcosset, C. (2012). Membrane emulsification: A promising alternative for vitamin E encapsulation within nano-emulsion. *Journal of Membrane Science,* 423–424, 85-96.

Li, D.-P., Zhang, Y.-R., Zhao, X.-X., and Zhao, B.-X. (2013). Magnetic nanoparticles coated by aminoguanidine for selective adsorption of acid dyes from aqueous solution. *Chemical Engineering Journal,* 232, 425-433.

Li, F., Hurley, B., Liu, Y., Leonard, B., and Griffith, M. (2012). Controlled release of bevacizumab through nanospheres for extended treatment of age-related macular degeneration. *Open Ophthalmology Journal,* 6, 54-58.

Li, L., Braiteh, F. S., and Kurzrock, R. (2005). Liposome-encapsulated curcumin: in vitro and in vivo effects on proliferation, apoptosis, signaling, and angiogenesis. *Cancer,* 104(6), 1322-1331.

Liu, L., Jiao, J., Wang, Y., Wu, J., Huang, D., Teng, W., and Chen, L. (2014). TGF-beta1 gene polymorphism in association with diabetic retinopathy susceptibility: a systematic review and meta-analysis. *PLoS One,* 9(4), e94160.

Lomb, B. a. (2009). Retisert [package insert]. Retrieved 15/09/2014, 2014 *in* http://www.retisert.com/.

Lu, X., Ji, C., Xu, H., Li, X., Ding, H., Ye, M., Guo, X. (2009). Resveratrol-loaded polymeric micelles protect cells from Aβ-induced oxidative stress. *International Journal of Pharmaceutics,* 375(1–2), 89-96.

Lu, Y., Zhou, N., Huang, X., Cheng, J.-W., Li, F.-Q., Wei, R.-L., and Cai, J.-P. (2014). Effect of intravitreal injection of bevacizumab-chitosan nanoparticles on retina of diabetic rats. *International Journal of Ophthalmology,* 7(1), 1-7.

Luo, D., Fan, Y., and Xu, X. (2012). The effects of aminoguanidine on retinopathy in STZ-induced diabetic rats. *Bioorganic & Medicinal Chemistry Letters,* 22(13), 4386-4390.

Luo, Y., Zhang, B., Whent, M., Yu, L., and Wang, Q. (2011). Preparation and characterization of zein/chitosan complex for encapsulation of α-tocopherol, and its in vitro controlled release study. *Colloids and Surfaces B: Biointerfaces,* 85(2), 145-152.

Machemer, R., Sugita, G., and Tano, Y. (1979). Treatment of intraocular proliferations with intravitreal steroids. *Transactions of the American Ophthalmological Society*, 77, 171-180.

Madsen-Bouterse, S. A., and Kowluru, R. A. (2008). Oxidative stress and diabetic retinopathy: pathophysiological mechanisms and treatment perspectives. *Reviews in Endocrine and Metabolic Disorders*, 9(4), 315-327.

Marsanasco, M., Márquez, A. L., Wagner, J. R., del V. Alonso, S., and Chiaramoni, N. S. (2011). Liposomes as vehicles for vitamins E and C: An alternative to fortify orange juice and offer vitamin C protection after heat treatment. *Food Research International*, 44(9), 3039-3046.

Mason, J. O., 3rd, Colagross, C. T., and Vail, R. (2006a). Diabetic vitrectomy: risks, prognosis, future trends. *Current Opinion on Ophthalmology*, 17(3), 281-285.

Mason, J. O., 3rd, Nixon, P. A., and White, M. F. (2006b). Intravitreal injection of bevacizumab (Avastin) as adjunctive treatment of proliferative diabetic retinopathy. *American Journal of Ophthalmology*, 142(4), 685-688.

Mayer-Davis, E. J., Bell, R. A., Reboussin, B. A., Rushing, J., Marshall, J. A., and Hamman, R. F. (1998). Antioxidant nutrient intake and diabetic retinopathy: the San Luis Valley Diabetes Study. *Ophthalmology*, 105(12), 2264-2270.

Millen, A. E., Gruber, M., Klein, R., Klein, B. E., Palta, M., and Mares, J. A. (2003). Relations of serum ascorbic acid and alpha-tocopherol to diabetic retinopathy in the Third National Health and Nutrition Examination Survey. *American Journal of Epidemiology*, 158(3), 225-233.

Miller, J. W., Adamis, A. P., and Aiello, L. P. (1997). Vascular endothelial growth factor in ocular neovascularization and proliferative diabetic retinopathy. *Diabetes/Metabolism: Research and Reviews*, 13(1), 37-50.

Miwa, K., Nakamura, J., Hamada, Y., Naruse, K., Nakashima, E., Kato, K., Hotta, N. (2003). The role of polyol pathway in glucose-induced apoptosis of cultured retinal pericytes. *Diabetes Research and Clinical Practice*, 60(1), 1-9.

Miyamoto, K., and Ogura, Y. (1999). Pathogenetic potential of leukocytes in diabetic retinopathy. *Seminars in Ophthalmology*, 14(4), 233-239.

Moradi, A., Sepah, Y. J., Sadiq, M. A., Nasir, H., Kherani, S., Sophie, R., Nguyen, Q. D. (2013). Vascular endothelial growth factor trap-eye (Aflibercept) for the management of diabetic macular edema. *World Journal of Diabetes*, 4(6), 303-309.

Murugeshu, A., Astete, C., Leonardi, C., Morgan, T., and Sabliov, C. M. (2011). Chitosan/PLGA particles for controlled release of alpha-tocopherol in the GI tract via oral administration. *Nanomedicine (London),* 6(9), 1513-1528.

Nakamura, M., Barber, A. J., Antonetti, D. A., LaNoue, K. F., Robinson, K. A., Buse, M. G., and Gardner, T. W. (2001). Excessive hexosamines block the neuroprotective effect of insulin and induce apoptosis in retinal neurons. *Journal of Biological Chemistry,* 276(47), 43748-43755.

Naruse, K., Nakamura, J., Hamada, Y., Nakayama, M., Chaya, S., Komori, T., . . . Hotta, N. (2000). Aldose reductase inhibition prevents glucose-induced apoptosis in cultured bovine retinal microvascular pericytes. *Experimental Eye Research,* 71(3), 309-315.

Nathan, D. M. (2014). The diabetes control and complications trial/epidemiology of diabetes interventions and complications study at 30 years: overview. *Diabetes Care,* 37(1), 9-16.

Neves, A. R., Lucio, M., Martins, S., Lima, J. L., and Reis, S. (2013). Novel resveratrol nanodelivery systems based on lipid nanoparticles to enhance its oral bioavailability. *International Journal of Nanomedicine,* 8, 177-187.

Ng, D. P. K. (2010). Human Genetics of Diabetic Retinopathy: Current Perspectives. *Journal of Ophthalmology,* doi: 10.1155/2010/172593.

Nishiura, H., Sugimoto, K., Akiyama, K., Musashi, M., Kubota, Y., Yokoyama, T., Yamaguchi, Y. (2013). A Novel Nano-Capsule of α-Lipoic Acid as a Template of Core-Shell Structure Constructed by Self-Assembly. *Journal of Nanomedicine* & *Nanotechnology*, 4(1), 1-7.

Niu, J., Su, Z., Xiao, Y., Huang, A., Li, H., Bao, X., Ping, Q. (2012). Octreotide-modified and pH-triggering polymeric micelles loaded with doxorubicin for tumor targeting delivery. *European Journal of Pharmaceutical Sciences,* 45(1–2), 216-226.

Obrosova, I. G., Fathallah, L., and Greene, D. A. (2000). Early changes in lipid peroxidation and antioxidative defense in diabetic rat retina: effect of DL-alpha-lipoic acid. *European Journal of Pharmacology,* 398(1), 139-146.

OZURDEX®. (2014). OZURDEX®. Retrieved 30/09/2014, 2014 *in* http://www.ozurdex.com/ .

Palii, S. S., Afzal, A., Shaw, L. C., Pan, H., Caballero, S., Miller, R. C., Grant, M. B. (2008). Nonpeptide Somatostatin Receptor Agonists Specifically Target Ocular Neovascularization via the Somatostatin Type 2 Receptor. *Investigative Ophthalmology and Visual Science,* 49(11), 5094-5102.

Pandita, D., Kumar, S., Poonia, N., and Lather, V. (2014). Solid lipid nanoparticles enhance oral bioavailability of resveratrol, a natural polyphenol. *Food Research International*, 62, 1165-1174.

Park, C. H., Lee, K. U., Park, J. Y., Koh, E. H., Kim, H. S., and Lee, J. (2010). Lipoic acid nanoparticles: effect of polymeric stabilizer on appetite suppression. *Pharmazie*, 65(8), 580-584.

Park, K., Chen, Y., Hu, Y., Mayo, A. S., Kompella, U. B., Longeras, R., and Ma, J. X. (2009). Nanoparticle-mediated expression of an angiogenic inhibitor ameliorates ischemia-induced retinal neovascularization and diabetes-induced retinal vascular leakage. *Diabetes*, 58(8), 1902-1913.

Pearson, P. A., Comstock, T. L., Ip, M., Callanan, D., Morse, L. S., Ashton, P., Eliott, D. (2011). Fluocinolone acetonide intravitreal implant for diabetic macular edema: a 3-year multicenter, randomized, controlled clinical trial. *Ophthalmology*, 118(8), 1580-1587.

Penfold, P. L., Gyory, J. F., Hunyor, A. B., and Billson, F. A. (1995). Exudative macular degeneration and intravitreal triamcinolone. A pilot study. *Australian and New Zealand journal of Ophthalmology*, 23(4), 293-298.

Pfister, F., Riedl, E., Wang, Q., vom Hagen, F., Deinzer, M., Harmsen, M. C., Hammes, H. P. (2011). Oral carnosine supplementation prevents vascular damage in experimental diabetic retinopathy. *Cellular Physiology and Biochemistry*, 28(1), 125-136.

Phillips, K., and Katz, H. R. (2005). A Comparison of the Efficacy of Dexamethasone and Loteprednol on Endotoxin-Induced Uveitis in Rodents Following Topical Ocular Administration. *Investigative Ophthalmology & Visual Science*, 46(5), 983.

Pintea, A., Rugina, D., Pop, R., Bunea, A., Socaciu, C., and Diehl, H. A. (2011). Antioxidant effect of trans-resveratrol in cultured human retinal pigment epithelial cells. *Journal of Ocular Pharmacology and Therapeutics*, 27(4), 315-321.

PKC-DRS2 Group, Aiello LP, Davis MD, Girach A, Kles KA, Milton RC, XE., Z. (2005). The effect of ruboxistaurin on visual loss in patients with moderately severe to very severe nonproliferative diabetic retinopathy: initial results of the Protein Kinase C beta Inhibitor Diabetic Retinopathy Study (PKC-DRS) multicenter randomized clinical trial. *Diabetes*, 54(7), 2188-2197.

Porta, M., and Allione, A. (2004). Current approaches and perspectives in the medical treatment of diabetic retinopathy. *Pharmacology & Therapeutics*, 103(2), 167-177.

Porta, M., and Bandello, F. (2002). Diabetic retinopathyA clinical update. *Diabetologia*, 45(12), 1617-1634.

Poulsen, J. E. (1953). Recovery from retinopathy in a case of diabetes with Simmonds' disease. *Diabetes*, 2(1), 7-12.

Praidou, A., Androudi, S., Brazitikos, P., Karakiulakis, G., Papakonstantinou, E., and Dimitrakos, S. (2010). Angiogenic growth factors and their inhibitors in diabetic retinopathy. *Current Diabetes Reviews,* 6(5), 304-312.

Puglia, C., Frasca, G., Musumeci, T., Rizza, L., Puglisi, G., Bonina, F., and Chiechio, S. (2012). Curcumin loaded NLC induces histone hypoacetylation in the CNS after intraperitoneal administration in mice. *European Journal of Pharmaceutics and Biopharmaceutics*, 81(2), 288-293.

Pund, S., Thakur, R., More, U., and Joshi, A. (2014). Lipid based nanoemulsifying resveratrol for improved physicochemical characteristics, in vitro cytotoxicity and in vivo antiangiogenic efficacy. *Colloids and Surfaces B: Biointerfaces,* 120, 110-117.

Querques, G., Bux, A. V., Martinelli, D., Iaculli, C., and Noci, N. D. (2009). Intravitreal pegaptanib sodium (Macugen) for diabetic macular oedema. *Acta Ophthalmologica,* 87(6), 623-630.

Rachmawati, H., Budiputra, D. K., and Mauludin, R. (2014). Curcumin nanoemulsion for transdermal application: formulation and evaluation. *Drug Development* and *Industrial Pharmacy*. 41(4), 560-566.

Ranjan, A. P., Mukerjee, A., Helson, L., Gupta, R., and Vishwanatha, J. K. (2013). Efficacy of liposomal curcumin in a human pancreatic tumor xenograft model: inhibition of tumor growth and angiogenesis. *Anticancer Research,* 33(9), 3603-3609.

Ray, D., Mishra, M., Ralph, S., Read, I., Davies, R., and Brenchley, P. (2004). Association of the VEGF gene with proliferative diabetic retinopathy but not proteinuria in diabetes. *Diabetes,* 53(3), 861-864.

Rechtman, E., Harris, A., Garzozi, H. J., and Ciulla, T. A. (2007). Pharmacologic therapies for diabetic retinopathy and diabetic macular edema. *Clinical Ophthalmology,* 1(4), 383-391.

Robinson, M. R., Lee, S. S., Kim, H., Kim, S., Lutz, R. J., Galban, C., Csaky, K. G. (2006). A rabbit model for assessing the ocular barriers to the transscleral delivery of triamcinolone acetonide. *Experimental Eye Research,* 82(3), 479-487.

Rocha, S., Generalov, R., Pereira Mdo, C., Peres, I., Juzenas, P., and Coelho, M. A. (2011). Epigallocatechin gallate-loaded polysaccharide nanoparticles for prostate cancer chemoprevention. *Nanomedicine (London),* 6(1), 79-87.

Roh, M. I., Byeon, S. H., and Kwon, O. W. (2008). Repeated intravitreal injection of bevacizumab for clinically significant diabetic macular edema. *Retina,* 28(9), 1314-1318.

Ruktanonchai, U., Bejrapha, P., Sakulkhu, U., Opanasopit, P., Bunyapraphatsara, N., Junyaprasert, V., and Puttipipatkhachorn, S. (2009). Physicochemical characteristics,

cytotoxicity, and antioxidant activity of three lipid nanoparticulate formulations of alpha-lipoic acid. *Journal of the American Association of Pharmaceutical Scientists*, 10(1), 227-234.

Sanford, M. (2013). Fluocinolone Acetonide Intravitreal Implant (Iluvien®). *Drugs*, 73(2), 187-193.

Sanoj Rejinold, N., Muthunarayanan, M., Divyarani, V. V., Sreerekha, P. R., Chennazhi, K. P., Nair, S. V., Jayakumar, R. (2011). Curcumin-loaded biocompatible thermoresponsive polymeric nanoparticles for cancer drug delivery. *Journal of Colloid and Interface Science*, 360(1), 39-51.

Sessa, M., Balestrieri, M. L., Ferrari, G., Servillo, L., Castaldo, D., D'Onofrio, N., Tsao, R. (2014). Bioavailability of encapsulated resveratrol into nanoemulsion-based delivery systems. *Food Chemistry*, 147, 42-50.

Shao, J., Li, X., Lu, X., Jiang, C., Hu, Y., Li, Q., Fu, Z. (2009). Enhanced growth inhibition effect of Resveratrol incorporated into biodegradable nanoparticles against glioma cells is mediated by the induction of intracellular reactive oxygen species levels. *Colloids and Surfaces B: Biointerfaces*, 72(1), 40-47.

Sheetz, M. J., Aiello, L. P., Davis, M. D., Danis, R., Bek, T., Cunha-Vaz, J., Berg, P. H. (2013). The effect of the oral PKC beta inhibitor ruboxistaurin on vision loss in two phase 3 studies. *Investigative Ophthalmology & Visual Science*, 54(3), 1750-1757.

Sheu, S. J., Liu, N. C., and Chen, J. L. (2010). Resveratrol protects human retinal pigment epithelial cells from acrolein-induced damage. *Journal of Ocular Pharmacology and Therapeutics*, 26(3), 231-236.

Shutava, T. G., Balkundi, S. S., and Lvov, Y. M. (2009). (−)-Epigallocatechin gallate/gelatin layer-by-layer assembled films and microcapsules. *Journal of Colloid and Interface Science*, 330(2), 276-283.

Singh, R., Ramasamy, K., Abraham, C., Gupta, V., and Gupta, A. (2008). Diabetic retinopathy: an update. *Indian Journal of Ophthalmology*, 56(3), 178-188.

Singha, S., Bhattacharya, J., Datta, H., and Dasgupta, A. K. (2009). Anti-glycation activity of gold nanoparticles. *Nanomedicine : nanotechnology, biology, and medicine*, 5(1), 21-29.

Smith, A., Giunta, B., Bickford, P. C., Fountain, M., Tan, J., and Shytle, R. D. (2010). Nanolipidic particles improve the bioavailability and α-secretase inducing ability of epigallocatechin-3-gallate (EGCG) for the treatment of Alzheimer's disease. *International Journal of Pharmaceutics*, 389(1–2), 207-212.

Solaiman, K. A., Diab, M. M., and Dabour, S. A. (2013). Repeated intravitreal bevacizumab injection with and without macular grid photocoagulation for treatment of diffuse diabetic macular edema. *Retina*, 33(8), 1623-1629.

Solans, C., Izquierdo, P., Nolla, J., Azemar, N., and Garcia-Celma, M. J. (2005). Nano-emulsions. *Current Opinion in Colloid and Interface Science*, 10(3–4), 102-110.

Souto, E., Fangueiro, J., and Müller, R. (2013a). Solid Lipid Nanoparticles (SLN™). In I. F. Uchegbu, A. G. Schätzlein, W. P. Cheng and A. Lalatsa (Eds.), *Fundamentals of Pharmaceutical Nanoscience* (pp. 91-116): Springer New York

Souto, E. B., Doktorovova, S., Gonzalez-Mira, E., Egea, M. A., and Garcia, M. L. (2010). Feasibility of lipid nanoparticles for ocular delivery of anti-inflammatory drugs. *Current Eye Research*, 35(7), 537-552.

Souto, E. B., Muller, R. H., and Gohla, S. (2005). A novel approach based on lipid nanoparticles (SLN) for topical delivery of alpha-lipoic acid. *Journal of Microencapsulation*, 22(6), 581-592.

Souto, E. B., Severino, P., Basso, R., and Santana, M. H. (2013b). Encapsulation of antioxidants in gastrointestinal-resistant nanoparticulate carriers. *Methods in Molecular Biology*, 1028, 37-46.

Su, Z., Shi, Y., Xiao, Y., Sun, M., Ping, Q., Zong, L., Tian, J. (2013). Effect of octreotide surface density on receptor-mediated endocytosis in vitro and anticancer efficacy of modified nanocarrier in vivo after optimization. *International Journal of Pharmaceutics*, 447(1–2), 281-292.

Suen, W.-L. L., and Chau, Y. (2013). Specific uptake of folate-decorated triamcinolone-encapsulating nanoparticles by retinal pigment epithelium cells enhances and prolongs antiangiogenic activity. *Journal of Controlled Release*, 167(1), 21-28.

Sun, J., Bi, C., Chan, H. M., Sun, S., Zhang, Q., and Zheng, Y. (2013). Curcumin-loaded solid lipid nanoparticles have prolonged in vitro antitumour activity, cellular uptake and improved in vivo bioavailability. *Colloids and Surfaces B: Biointerfaces*, 111, 367-375.

Surujpaul, P. P., Gutiérrez-Wing, C., Ocampo-García, B., de M. Ramírez, F., Arteaga de Murphy, C., Pedraza-López, M., Ferro-Flores, G. (2008). Gold nanoparticles conjugated to [Tyr3]Octreotide peptide. *Biophysical Chemistry*, 138(3), 83-90.

Svenson, S., and Tomalia, D. A. (2012). Dendrimers in biomedical applications—reflections on the field. *Advanced Drug Delivery Reviews*, 64, *Supplement*, 102-115.

Teeranachaideekul, V., Muller, R. H., and Junyaprasert, V. B. (2007). Encapsulation of ascorbyl palmitate in nanostructured lipid carriers (NLC): effects of formulation parameters on physicochemical stability. *International Journal of Pharmaceutics*, 340(1-2), 198-206.

Thomas, S., Biswas, N., Malkar, V. V., Mukherjee, T., and Kapoor, S. (2010). Studies on adsorption of carnosine on silver nanoparticles by SERS. *Chemical Physics Letters*, 491(1–3), 59-64.

Ting, J. H., and Martin, D. K. (2006). Basic and clinical aspects of gene therapy for retinopathy induced by diabetes. *Current Gene Therapy*, 6(2), 193-214.

Vanaja, K., Wahl, M. A., Bukarica, L., and Heinle, H. (2013). Liposomes as carriers of the lipid soluble antioxidant resveratrol: evaluation of amelioration of oxidative stress by additional antioxidant vitamin. *Life Sciences*, 93(24), 917-923.

Varshochian, R., Jeddi-Tehrani, M., Mahmoudi, A. R., Khoshayand, M. R., Atyabi, F., Sabzevari, A., Dinarvand, R. (2013). The protective effect of albumin on bevacizumab activity and stability in PLGA nanoparticles intended for retinal and choroidal neovascularization treatments. *European Journal of Pharmaceutical Sciences*, 50(3–4), 341-352.

Vitale, S., Maguire, M. G., Murphy, R. P., Hiner, C. J., Rourke, L., Sackett, C., and Patz, A. (1995). Clinically significant macular edema in type I diabetes. Incidence and risk factors. *Ophthalmology*, 102(8), 1170-1176.

Wang, J., Wang, B. M., and Schwendeman, S. P. (2004). Mechanistic evaluation of the glucose-induced reduction in initial burst release of octreotide acetate from poly(d,l-lactide-co-glycolide) microspheres. *Biomaterials*, 25(10), 1919-1927.

Wang, Y., Lu, Z., Wu, H., and Lv, F. (2009). Study on the antibiotic activity of microcapsule curcumin against foodborne pathogens. *International Journal of Food Microbiology*, 136(1), 71-74.

Wang, Y., Ng, M. C., Lee, S. C., So, W. Y., Tong, P. C., Cockram, C. S., Chan, J. C. (2003). Phenotypic heterogeneity and associations of two aldose reductase gene polymorphisms with nephropathy and retinopathy in type 2 diabetes. *Diabetes Care*, 26(8), 2410-2415.

Wechtersbach, L., Poklar Ulrih, N., and Cigić, B. (2012). Liposomal stabilization of ascorbic acid in model systems and in food matrices. *LWT - Food Science and Technology*, 45(1), 43-49.

Wilkinson, C. P., Ferris, F. L., 3rd, Klein, R. E., Lee, P. P., Agardh, C. D., Davis, M., Verdaguer, J. T. (2003). Proposed international clinical diabetic retinopathy and diabetic macular edema disease severity scales. *Ophthalmology*, 110(9), 1677-1682.

Wu, L., Arevalo, J. F., Berrocal, M. H., Maia, M., Roca, J. A., Morales-Canton, V., Diaz-Llopis, M. J. (2009). Comparison of two doses of intravitreal bevacizumab as primary treatment for macular edema secondary to branch retinal vein occlusions: results of the

Pan American Collaborative Retina Study Group at 24 months. *Retina,* 29(10), 1396-1403.

Wu, Y., Tang, L., and Chen, B. (2014). Oxidative stress: implications for the development of diabetic retinopathy and antioxidant therapeutic perspectives. *Oxidative Medicine* and *Cellular Longevity,* 752387, doi: 10.1155/2014/752387.

Xu, H., Zhang, L., Gu, L., Lu, L., Gao, G., Li, W., Xu, G. T. (2014). Subretinal delivery of AAV2-mediated human erythropoietin gene is protective and safe in experimental diabetic retinopathy. *Investigative Ophthalmology & Visual Science,* 55(3), 1519-1530.

Xu, Q., Kambhampati, S. P., and Kannan, R. M. (2013). Nanotechnology approaches for ocular drug delivery. *Middle East African Journal of Ophthalmology,* 20(1), 26-37.

Yallapu, M. M., Gupta, B. K., Jaggi, M., and Chauhan, S. C. (2010). Fabrication of curcumin encapsulated PLGA nanoparticles for improved therapeutic effects in metastatic cancer cells. *Journal of Colloid and Interface Science,* 351(1), 19-29.

Yang, H., Tyagi, P., Kadam, R. S., Holden, C. A., and Kompella, U. B. (2012). Hybrid dendrimer hydrogel/PLGA nanoparticle platform sustains drug delivery for one week and antiglaucoma effects for four days following one-time topical administration. *ACS Nano,* 6(9), 7595-7606.

Yang, J., Cai, L., Zhang, S., Zhu, X., Zhou, P., and Lu, Y. (2014). Silica-based cerium (III) chloride nanoparticles prevent the fructose-induced glycation of alpha-crystallin and H(2)O(2)-induced oxidative stress in human lens epithelial cells. *Archives of Pharmacal Research,* 37(3), 404-411.

Yanoff, M. (1969). Ocular pathology of diabetes mellitus. *American Journal of Ophthalmology,* 67(1), 21-38.

Yokota, T., Ma, R. C., Park, J. Y., Isshiki, K., Sotiropoulos, K. B., Rauniyar, R. K., King, G. L. (2003). Role of protein kinase C on the expression of platelet-derived growth factor and endothelin-1 in the retina of diabetic rats and cultured retinal capillary pericytes. *Diabetes,* 52(3), 838-845.

Yung, W. K. (2008). Moving toward the next steps in angiogenesis therapy? *Neuro-Oncology*, 10(6), 939.

Zanotto-Filho, A., Coradini, K., Braganhol, E., Schröder, R., de Oliveira, C. M., Simões-Pires, A., Moreira, J. C. F. (2013). Curcumin-loaded lipid-core nanocapsules as a strategy to improve pharmacological efficacy of curcumin in glioma treatment. *European Journal of Pharmaceutics and Biopharmaceutics,* 83(2), 156-167.

Zhang, Z., and Feng, S. S. (2006). Nanoparticles of poly(lactide)/vitamin E TPGS copolymer for cancer chemotherapy: synthesis, formulation, characterization and in vitro drug release. *Biomaterials,* 27(2), 262-270.

Zhou, W., Liu, W., Zou, L., Liu, W., Liu, C., Liang, R., and Chen, J. (2014). Storage stability and skin permeation of vitamin C liposomes improved by pectin coating. *Colloids and Surfaces B: Biointerfaces*, 117, 330-337.

Zhu, X. F., and Zou, H. D. (2012). PEDF in diabetic retinopathy: a protective effect of oxidative stress. *Journal of Biomedicine and Biotechnology*, 580687. doi: 10.1155/2012/580687.

CHAPTER 2 - *Design of cationic lipid nanoparticles for ocular delivery: development, characterization and cytotoxicity*

CHAPTER 2 - DESIGN OF CATIONIC LIPID NANOPARTICLES FOR OCULAR DELIVERY: DEVELOPMENT, CHARACTERIZATION AND CYTOTOXICITY

Joana F. Fangueiro[a], Tatiana Andreani[a,b,c], Maria A. Egea[d,e], Maria L. Garcia[d,e], Selma B. Souto[f], Amélia M. Silva[b,c], Eliana B. Souto [a*]

[a] Faculty of Health Sciences, Fernando Pessoa University (UFP-FCS), Rua Carlos da Maia, 296, 4200-150 Porto, Portugal

[b] Centre for Research and Technology of Agro-Environmental and Biological Sciences (CITAB), Vila Real, Portugal

[c] Department of Biology and Environment, University of Trás-os-Montes e Alto Douro (UTAD), Vila Real, Portugal

[d] Department of Physical Chemistry, Faculty of Pharmacy, University of Barcelona, Av. Joan XXIII s/n, 08028 Barcelona, Spain

[e] Institute of Nanoscience and Nanotechnology, University of Barcelona, Av. Joan XXIII s/n, 08028 Barcelona, Spain

[f] Division of Endocrinology, Diabetes and Metabolism, Hospital de Braga, Braga, Portugal

Published in *International Journal of Pharmaceutics*, 461 (1-2): 64-73, 2014

CHAPTER 2 - Design of cationic lipid nanoparticles for ocular delivery: development, characterization and cytotoxicity

Abstract

In the present study we have developed lipid nanoparticle (LN) dispersions based on a multiple emulsion technique for encapsulation of hydrophilic drugs or/and proteins by a full factorial design. In order to increase ocular retention time and mucoadhesion by electrostatic attraction, a cationic lipid, namely cetyltrimethylammonium bromide (CTAB), was added in the lipid matrix of the optimal LN dispersion obtained from the factorial design. There are a limited number of studies reporting the ideal concentration of cationic agents in LN for drug delivery. This paper suggests that the choice of the concentration of a cationic agent is critical when formulating a safe and stable LN. CTAB was included in the lipid matrix of LN, testing four different concentrations (0.25%, 0.5%, 0.75%, or 1.0%wt) and how composition affects LN behavior regarding physical and chemical parameters, lipid crystallization and polymorphism, and stability of dispersion during storage. In order to develop a safe and compatible system for ocular delivery, CTAB-LN dispersions were exposed to Human retinoblastoma cell line Y-79. The toxicity testing of the CTAB-LN dispersions was a fundamental tool to find the best CTAB concentration for development of these cationic LN, which was found to be 0.5 wt% of CTAB.

2.1. Introduction

Lipid nanoparticles (LNs) have gained interest in recent years as drug carriers for ocular delivery, aiming a better permeation and/or prolonged drug release onto the ocular mucosa and allowing drugs reaching the post segment of the eye (Pignatello and Puglisi, 2011). Ocular drug delivery is extremely affected by eye anatomy and physiology that leads often to mechanisms that decrease bioavailability of applied drugs. These mechanisms include reflex processes, such as lacrimation and blinking

which reduces drastically the drug residence time, and difficulty to diffuse though the conjunctiva and nasolacrimal duct. In addition, the low volume of the conjunctival sac also leads to a poor corneal or scleral penetration of drugs (Diebold and Calonge, 2010). Since ocular delivery became a problem when the ultimate target is intraocular delivery, due to the ineffective drug concentrations and time residence reach the inner tissues, alternative systems for drug delivery are required (Pignatello and Puglisi, 2011; Sultana et al., 2011). New drug delivery systems based on lipids, namely liposomes, and other materials such as polymers (poly-d-l-lactic acid (PLA) nanospheres) were able to deliver an antiviral drug, acyclovir, in the inner tissues of the eye comprising the innovation of these systems (Fresta et al., 1999; Giannavola et al., 2003).

Ocular drug delivery strategies may be classified into 3 groups: noninvasive techniques, implants, and colloidal carriers. Colloidal drug delivery systems such as LNs, can be easily administered in a liquid form and have the ability to diffuse rapidly and are better internalized in ocular tissues. In addition, the interaction and adhesion of LNs ocular surface with the endothelium makes these drug delivery systems interesting as new therapeutic tools in ocular delivery (del Pozo-Rodriguez et al., 2013).

LNs based on w/o/w emulsion are versatile colloidal carriers for the administration of peptides/proteins and hydrophilic drugs (Fangueiro et al., 2012a). Droplets from the inner aqueous phase, where the drug is dissolved or/and solubilized, are supported by a solid lipid matrix surrounded by an aqueous surfactant phase. Usually LNs are composed of physiological solid lipids (mixtures of mono-, di- or triacylglycerols, fatty acids or waxes) stabilized by surfactants. In the case of a w/o/w based LN dispersion, a high hydrophilic-lipophilic balance (HLB) surfactant is added to the external aqueous phase and, a low HLB surfactant is added to the lipid phase. The two surfactants are needed to stabilize the two existing interfaces in this type of emulsion. A variety of surfactants can be applied, such as phospholipids, bile salts, polysorbates, polyoxyethylene ethers (Fangueiro et al., 2012a; Gallarate et al., 2009). Materials used for LNs production are largely used in pharmaceutical industry with proved biocompatibility (Severino et al., 2012).

Cationic LNs have been recently investigated for targeting ocular mucosa, namely the posterior segment of the eye (e.g. retina). This is a smart strategy that combines the positive surface charge of the particles and the negative surface charge of ocular mucosa by means of an electrostatic attraction. This approach could increase the drugs retention time in the eye as well as improve nanoparticles bioadhesion (Lallemand et al., 2012).

In the ocular delivery, it is especially relevant the control of the particle size since it directly influence the drug release rate, bioavailability, and patient comfort and compliance (Shekunov et al., 2007; Souto et al., 2010). In addition, it is known that the smaller the particle size, the longer the retention time and easier application (Araujo et al., 2009).

Physicochemical characterization and assessment of nanotoxicity are major issues for developing and large-scale manufacturing of nanocarriers. Furthermore, physicochemical properties of LNs such as particle size, surface and composition can significantly influence drug delivery on ocular delivery (Ying et al., 2013).

In the present work, the development and characterization of a system of LNs based on multiple emulsions using a blend of triacylglycerols as solid lipid, was carried out, in which sonication method was employed. The first aim of the work was the application of a full factorial design to achieve which dependent variables affect the LN dispersion properties. The analyzed independent variables, namely the concentration of solid lipid and both hydrophilic and lipophilic surfactants, were the mean particle size (Z-Ave), polydispersity index (PI) and zeta potential (ZP) of the produced LNs dispersions. The optimal formulation was used to evaluate the toxicity of LNs using Y-79 human retinoblastoma cells employing different cationic lipid concentrations to select the best formulation for ocular instillations.

2.2. Material and methods

2.2.1. Materials

Softisan®100 (S100, a hydrogenated coco-acylglycerols C_{10}-C_{18} fatty acid triacylglycerols) was a free sample from Sasol Germany GmbH (Witten, Germany),

Lipoid® S75, 75% soybean phosphatidylcholine was purchased from Lipoid GmbH (Ludwigshafen, Germany), Lutrol®F68 or Poloxamer 188 (P188) was a free sample from BASF (Ludwigshafen, Germany). Cetyltrimethylammonium bromide (CTAB) and uranyl acetate were acquired from Sigma-Aldrich (Sintra, Portugal). Anhydrous glycerol was purchased from Acopharma (Barcelona, Spain). Ultra-purified water was obtained from a MiliQ Plus system (Millipore, Germany). All reagents were used without further treatment. The Y-79 human retinoblastoma cell line was purchased from Cell Lines Service (CLS, Eppelheim, Germany). Reagents for cell culture were from Gibco (Alfagene, Invitrogene, Portugal).

2.2.2. Experimental factorial design

A factorial design approach using a 3^3 full factorial design composed of 3 variables which were set at 3-levels each was applied to maximize the experimental efficiency requiring a minimum of experiments. For this purpose three different variables and their influence on the physicochemical properties of the produced LNs were analyzed. The design required a total of 11 experiments. The independent variables were the concentration of solid lipid S100, concentration of lecithin (Lipoid® S75) and the concentration of hydrophilic surfactant P188. The established dependent variables were the mean particle size (Z-Ave), polydispersity index (PI) and zeta potential (ZP). For each factor, the lower, medium and higher values of the lower, medium and upper levels were represented by a (−1), a (0) and a (+1) sign, respectively (Table 2.1). The data were analyzed using the STATISTICA 7.0 (Stafsoft, Inc.) software.

Table 2.1- Initial 3-level full factorial design, providing the lower (−1), medium (0) and upper (+1) level values for each variable.

Variables	**Levels**		
	Low level (-1)	**Medium level (0)**	**High level (+1)**
S100 (wt%)	2.5	5.0	7.5
Lecithin (wt%)	0.25	0.5	0.75
P188 (wt%)	0.5	1.0	1.0

[S100, Softisan®100; P188, Poloxamer 188]

2.2.3. Lipid nanoparticles production

LN dispersions were prepared using a novel multiple emulsion (w/o/w) technique (García-Fuentes et al., 2003). Briefly, an inner w/o emulsion was initially prepared. A volume of ultra-purified water was added to the lipid phase (5%wt) composed of glycerol, S100 and Lipoid® S75 at same temperature (5-10 °C above the melting point of Softisan®100 (T≈50°C)) and homogenized 60 s with a sonication probe (6 mm diameter) by means of an Ultrasonic processor VCX500 (Sonics, Switzerland). A power output with amplitude of 40 % was applied. A few milliliters of P188 solution was added and homogenized for additional 90 s. This pre-emulsion was poured in the total volume of a P188 cooled solution under magnetic stirring for 15 min to allow the formation of the LN. The obtained LN dispersions were used for subsequent studies. The general composition of LN dispersions is described in Table 2.2.

Table 2.2. Composition of LN dispersions (wt/wt%)

Components	%(wt/wt)
Softisan®100	5.0
Glycerol	37.5
Lipoid® S75	0.5
Lutrol®F68	1.0
Water add.	100

2.2.4. Physicochemical characterization

Physicochemical parameters such as Z-Ave, PI and ZP were analyzed by dynamic light scattering (DLS, Zetasizer Nano ZS, Malvern Instruments, Malvern, UK). All samples were diluted with ultra-purified water and analyzed in triplicate. For analysis of the ZP, ultra-purified water with conductivity adjusted to 50 µS/cm was used.

2.2.5. Evaluation of the concentration of CTAB

In order to increase eye retention time and mucoadhesion onto the ocular mucosa, a cationic lipid was added to the lipid matrix. For this purpose, CTAB was used as cationic lipid maintaining the 5% of lipid matrix varying the proportions of S100 and

CTAB. Thus, in the production stage, four different concentrations (0.25, 0.5, 0.75 and 1.0 wt %) of cationic lipid (CTAB) was added in the lipid phase composed of S100 and Lipoid® S75 of the optimal formulation previously obtained from the factorial design to evaluate the influence in the physicochemical properties.

2.2.6. Stability analysis of LN by TurbiscanLab®

The TurbiscanLab® is a technique used to observe reversible (creaming and sedimentation due to fluctuation on particle size and volume) and irreversible (coalescence and segregation due to particle size variation) destabilization phenomena in the sample without the need of dilution. TurbiscanLab® is useful to detect destabilization phenomena much earlier and also in a simpler way than other methods, since it is based on the measurement of backscattering (BS) and transmission (T) signals (Araújo et al., 2009; Celia et al., 2009; Liu et al., 2011; Marianecci et al., 2010).

The physical stability of LN dispersions was assessed with an optical analyzer TurbiscanLab® (Formulaction, France). The dispersions were placed in a cylindrical glass cell, at room temperature (25°C). The equipment is composed of a near-infrared light source (λ = 880 nm), and 2 synchronous T and BS detectors. The T detector receives the light crossing the sample, whereas the BS detector receives the light scattered backwards by the sample (Araújo et al., 2009). The detection head scans the entire height of the sample cell (20 mm longitude), acquiring T and BS each 40 μm, 3 times during 10 min at different times after production (7, 15 and 30 days).

2.2.7. Thermal analysis

The crystallinity profile of LNs was assessed by differential scanning calorimetry (DSC). This technique is useful to evaluate the physical state, which directly affects the physicochemical properties and thermodynamic stability of LN dispersions. A volume of LN dispersion corresponding to 1-2 mg of lipid was scanned using a Mettler DSC 823e System (Mettler Toledo, Spain). Heating and cooling runs were performed from 25ºC to 90ºC and back to 25ºC at a heating rate of 5ºC/min, in sealed 40 μL aluminium pans. An empty pan was used as a reference. Indium (purity>99.95%; Fluka, Buchs, Switzerland) was employed for calibration purposes. DSC thermograms were recorded

for the four different CTAB concentration formulations and for the bulk lipids (CTAB and S100). The DSC parameters including onset, melting point and enthalpy were evaluated using STAR^e Software (Mettler Toledo, Switzerland).

2.2.8. X-Ray studies

X-ray diffraction patterns were obtained using the x-ray scattering (X'Pert PRO, PANalytical) using an X´Celerator as a detector. Data of the scattered radiation were detected with a blend local-sensible detector using an anode voltage of 40 kV and a current of 30 mA. For the analysis of LN dispersions and bulk materials, the samples were mounted on a standard sample holder being dried at room temperature without any previous sample treatment.

2.2.9. Alamar blue assay in Human Retinoblastoma cell line

Y-79 (Human retinoblastoma cell line) cells were used to perform the cytotoxicity assay, in which four LN dispersions containing different CTAB concentrations were tested. Each formulation was tested at four concentrations (in $\mu g.mL^{-1}$): 10, 25, 50 and 100. Y-79 cells were maintained in RPMI-1640, supplemented with 10% (v/v) fetal bovine serum (FBS), 2 mM L-glutamine, and antibiotics (100 $U.mL^{-1}$ penicillin and 100 $\mu g.mL^{-1}$ of streptomycin) in an atmosphere of 5% CO_2 in air at 37 °C. Cells were centrifuged, ressuspended in FBS-free culture media, counted and seeded, after appropriate dilution, at $1x10^5$ $cell.mL^{-1}$ density in 96-well plates (100 μL/well). The different formulations were diluted with FBS-free culture media to achieve the final concentrations, and added to cells 24 h after seeding (100 μL/well).

Cell viability was assayed with Alamar Blue (Alfagene, Invitrogene, Portugal) by adding 10% (v/v) to each well, and the absorbance at 570 nm (reduced form) and 620 nm (oxidative form) was read 24, 48 and 72 h after exposure to test compounds, data were analyzed by calculating the percentage of Alamar blue reduction (according to the manufactures recommendation) and expressed as percentage of control (untreated cells).

2.2.10. Transmission electronic microscopy analysis

Transmission electronic microscopy (TEM) is a technique useful to analyze the shape and size of LN dispersions. The chosen LN dispersion corresponding to CTAB-LN dispersion with 0.5 wt% CTAB was mounted on a grid and negative stained with a 2% (v/v) uranyl acetate solution. After drying at room temperature, the sample was examined using a TEM (Tecnai Spirit TEM, FEI) at 80 kV.

2.2.11. Statistical analysis

Statistical evaluation of data was performed using one-way analysis of variance (ANOVA). Bonferroni multiple comparison test was used to compare the significance of the difference between the groups, a p-value < 0.05 was accepted as significant. Data were expressed as the mean value ± standard deviation (Mean ± SD) (n=3).

2.3. Results and discussion

The production and optimization of LNs based on multiple emulsion requires pre-formulation studies and literature research. The stability and compatibility of the emulsifiers and the lipid matrix are essential to provide a stable and functional system (Fangueiro et al., 2012). Since the choice of the components are vital for dispersions formation, Lipoid®S75 (soybean phosphatidylcholine) was the selected lipophilic emulsifier used with a HLB value of approximately 7-9, and Poloxamer 188 was selected as hydrophilic emulsifier with a HLB value of approximately 22.

Physicochemical properties and stability of the new drug delivery systems are major issues to be considered in the formulation stage, especially those intended for ocular administration. The use of dispersions with appropriate physicochemical properties ensures adequate bioavailability of administered drugs and biocompatibility with ocular mucosa. All LN dispersions obtained by the factorial design showed an adequate macroscopically stability for their physicochemical characterization, i.e. no separation phase, flocculation or creaming processes was detected during the time of analysis. The physicochemical properties of LNs obtained from the experimental design were analyzed. The effects of the selected variables on dispersions characteristics (Z-Ave, PI and ZP) are depicted in Table 2.3. For drug ocular administration, the values of Z-Ave

and PI should be the lowest as possible, since dispersions should be well tolerated in the ocular mucosa avoiding eye irritation and the transport and uptake from the cornea is facilitated (Araujo et al., 2009)**.** The results for the 11 produced formulations is shown in Table 2.3 and varied from 164.5 ± 1.09 nm (LN 8 or LN 10) to 268.50 ± 1.47 nm (LN 2), whereas PI ranged from 0.155 ± 0.03 (LN 4) to 0.192 ± 0.02 (LN 6). The particle size distribution was very narrow in all cases since the PI was less than 0.2, corresponding to monodisperse systems. According to the literature (Zimmer and Kreuter 1995, Shekunov, Chattopadhyay et al. 2007), the Z-Ave for ocular administration should be below 1 µm with an associated narrow size distribution. Thus, all formulations revealed a Z-Ave and PI within accepted range (Fresta et al., 1999; Giannavola et al., 2003; Souto et al., 2010; Vega et al., 2008). As expected, the ZP did not vary, since all used reagents have non-ionic nature. For each of the 3 variables, analysis of variance (ANOVA) was performed. From Table 2.4 and Fig. 2.1, the only factor that was shown to have a significant effect (p-value < 0.05) on Z-Ave was the concentration of lecithin. All other evaluated factors, were not statistically significant (p-value > 0.05), neither the interactions between them. The same results were observed for the evaluation of the dependent variables on PI (Table 2.5 and Fig. 2.1). The concentration of lecithin was the only independent variable affecting the PI. The lecithin used is composed of 75% of phosphatidylcholine, which is composed by phospholipids that resemble the cellular membranes. The use of this emulsifier is reported as safe and biocompatible for several purposes, such as skin products (Fiume, 2001) and also for ophthalmic/ocular drug delivery (Bhatta et al., 2012). Their use in the development of LN dispersions is essential to decrease the interfacial tension between the oil phase and the internal and external aqueous phase, and also to facilitate the emulsification of the lipid matrix. Lecithin is used due to its higher power of emulsification able to provide a very good stabilization of the oil-in-water interfaces and has also been reported to decrease particle size in emulsions that is mainly explained by its amphiphilic character (Kawaguchi et al., 2008; Schubert et al., 2006; Trotta et al., 2002). The lipophilic portion of lecithin dissolves the lipid phase, i.e. lecithin likes to be at the edge of the lipid phase being its lipophilic tails directed to the lipid phase until the hydrophilic portion is directed to the water phase. Thus, the oil phase is totally recovered by the

lecithin promoting long time stabilization in the interface of the emulsions (Trotta et al., 2002). From the obtained results, a correlation between the concentration of lecithin and mean particle size of the particles were found, since highest concentrations leads to a decrease in Z-Ave and PI. This dependency of Z-Ave on the type of emulsifier is due to the need for the complete coverage of the interface, which is affected by the selected concentration.

The aim of this factorial design was to optimize a formulation with appropriate physicochemical parameters for the incorporation of hydrophilic drugs for ocular delivery. For this purpose, the limiting factors were the Z-Ave and PI and from the obtained results an optimal LN dispersion was found. This LN dispersion was used for the following studies.

Table 2.3. Response values (Z-Ave, PI and ZP) of the three factors depicted in Table 1 for the 11 experiment formulations.

Run	S100 (%w/t)	Lecithin (%w/t)	P188 (%w/t)	Z-Ave (nm)±SD	PI±SD	ZP (mV)
LN1	2.5	0.25	0.5	256.40±1.20	0.181±0.02	-1,04
LN2	7.5	0.25	0.5	268.50±1.47	0.173±0.04	-1,06
LN3	2.5	0.75	0.5	165.85±2.21	0.162±0.01	-1,08
LN4	7.5	0.75	0.5	171.24±1.78	0.155±0.03	-1,20
LN5	2.5	0.25	1.5	241.30±2.54	0.182±0.05	-1,22
LN6	7.5	0.25	1.5	235.40±1.87	0.192±0.02	-1,04
LN7	2.5	0.75	1.5	189.75±1.99	0.163±0.08	-1,12
LN8	7.5	0.75	1.5	164.50±1.14	0.158±0.03	-1,14
LN9	5.0	0.5	1.0	165.90±1.20	0.164±0.04	-1,18
LN10	5.0	0.5	1.0	164.50±1.09	0.183±0.05	-1,17
LN11	5.0	0.5	1.0	164.70±1.01	0.177±0.02	-1,16

Table 2.4. ANOVA statistical analysis of the Z-Ave.

Evaluated factors and their interactions	Sum of Squares	Degrees of freedom	Mean square	*F*-value	*p*-value
(1) S100 concentration	23.32	1	23.32	0.01962	0.895380
(2) Lecithin concentration	**12032.66**	**1**	**12032.66**	**10.12031**	**0.033495**
(3) P188 concentration	120.44	1	120.44	0.10129	0.766206
1 by 2	84.89	1	84.89	0.07140	0.802522
1 by 3	295.73	1	295.73	0.24873	0.644149
2 by 3	533.99	1	533.99	0.44912	0.539455
Error	4755.85	4	1188.96		
Total	17846.88	10			

Table 2.5. ANOVA statistical analysis of the PI.

Evaluated factors and their interactions	Sum of Squares	Degrees of freedom	Mean square	*F*-value	*p*-value
(1) S100 concentration	0.000072	1	0.000072	1.02591	0.368411
(2) Lecithin concentration	**0.001352**	**1**	**0.001352**	**19.26425**	**0.011791**
(3) P188 concentration	0.000032	1	0.000032	0.45596	0.536541
1 by 2	0.000032	1	0.000032	0.45596	0.536541
1 by 3	0.000072	1	0.000072	1.02591	0.368411
2 by 3	0.000032	1	0.000032	0.45596	0.536541
Error	0.000281	4	0.000070		
Total	0.001873	10			

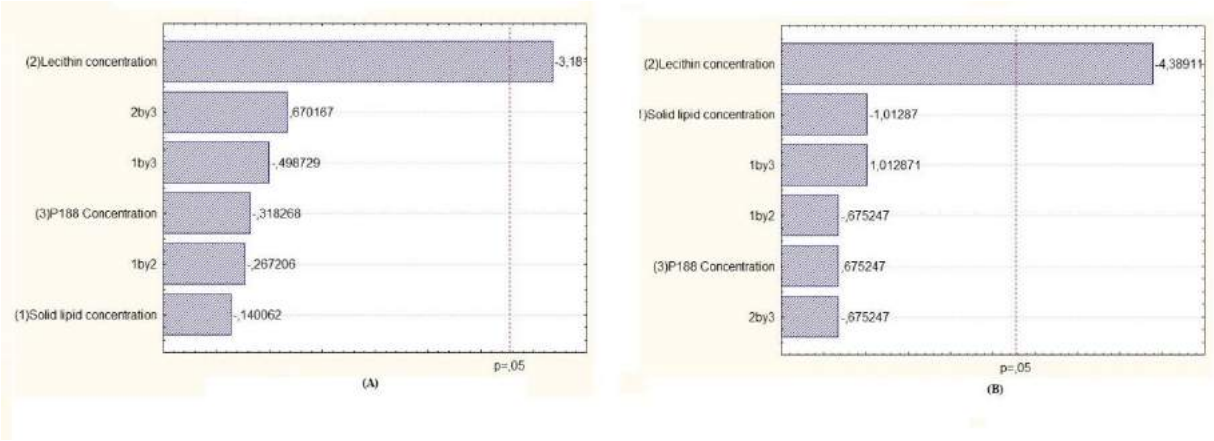

Figure 2.1. Pareto chart of the analyzed effects for the Z-Ave (A) and for the PI (B).

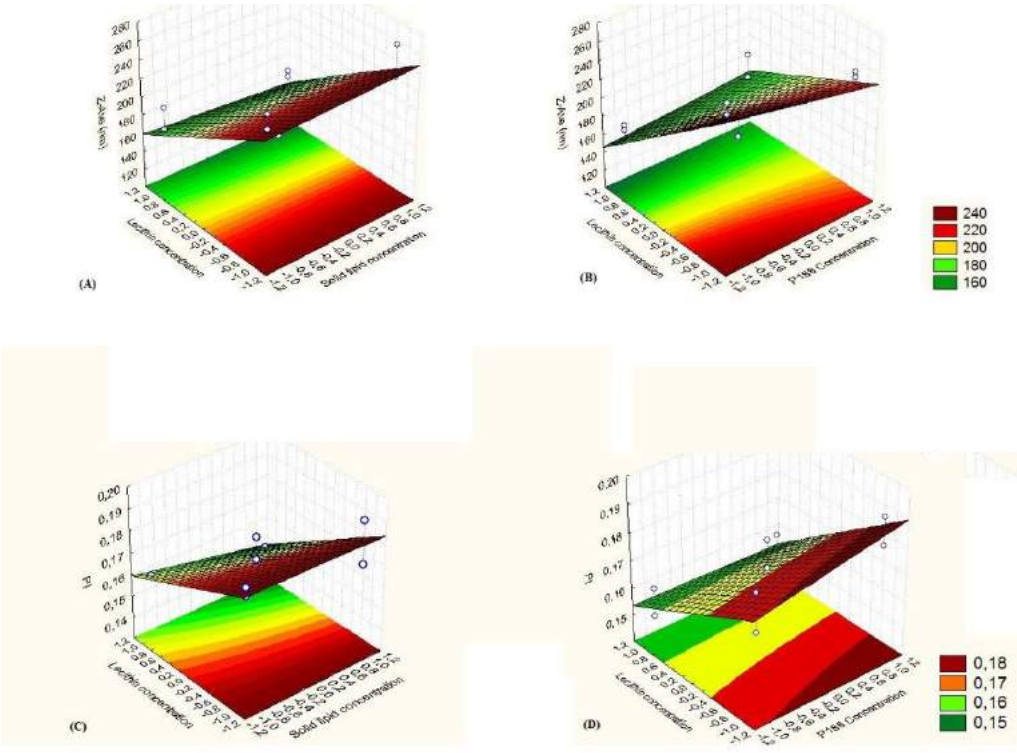

Figure 2.2. Surface response chart of the effect of the concentration of S100 and lecithin on the Z-Ave (A) and PI (C) and the effect of the concentration of lecithin and poloxamer 188 on the Z-Ave (B) and PI (D).

In order to improve LNs adhesion to ocular surface and also to improve stability of the dispersions, a cationic lipid was used. The approach of using a cationic lipid is interesting since ocular mucosa depicts slightly negative charge above its isoelectric point and also could improve some limitations related to ocular administration, such as prevent tear washout (due to tear dynamics), increase ocular bioavailability and prolong the residence time of drugs in the cul-de-sac (Araujo et al., 2009).

The study reports the use of different concentrations of a cationic lipid (CTAB) in the lipid matrix of LNs. The results of the CTAB concentration on the Z-Ave, PI and ZP of the LN dispersions optimized in the factorial design are depicted in Table 2.6. As expected, the parameter most affected by the variation on CTAB concentration is the ZP. The increase of the ZP was directly proportional to the increase on CTAB concentration. Statistical analysis of the physicochemical properties of CTAB-LN dispersions were not significant (p>0.05), indicating that the concentration of CTAB did not affect drastically the Z-Ave, PI and ZP of the formulations. All formulations properties were in agreement with the required parameters for ocular delivery. However, no statistical differences were found, the concentration of CTAB improved the ZP following a proportional relationship. This behavior was expected because of the cationic properties of CTAB and is also expected that higher ZP values contribute to higher stability of the particles due to electronic repulsion between them maintaining longer time in suspension.

Table 2.6. Physicochemical parameters from CTAB-LN dispersions at the production day and a long-term stability after 7, 15 and 30 day after production at 25°C (Mean±SD) (n=3).

Formulation	Parameters	Production day	Day 7	Day 15	Day 30
0.25% CTAB-LN	**Z-Ave (nm)**	230.70±6.71	239.5±0.61	244.9±1.17	255.2±1.32
	PI	0.308±0.09	0.267±0.01	0.261±0.03	0.266±0.01
	ZP (mV)	+24.80±2.69	+17.4±0.65	+16.7±0.56	+16.4±0.36
0.5% CTAB-LN	**Z-Ave (nm)**	194.40±0.43	199.25±0.30	201.45±0.08	213.7±0.74
	PI	0.185±0.02	0.186±0.01	0.224±0.02	0.225±0.01
	ZP (mV)	+37.20±1.27	+33.8±0.45	+32.1±0.53	+30.5±0.03
0.75% CTAB-LN	**Z-Ave (nm)**	172.10±12.64	166.25±1.20	223±0.59	236.8±1.45
	PI	0.182±0.02	0.246±0.01	0.204±0.01	0.225±0.04
	ZP (mV)	+41.70±0.71	+40.15±0.63	+38.6±0.41	+37.4±1.21
1.0% CTAB-LN	**Z-Ave (nm)**	169.10±2.51	144.7±1.61	188.3±1.52	200.7±1.65
	PI	0.222±0.022	0.211±0.01	0.236±0.02	0.245±0.04
	ZP (mV)	+48.00±0.31	+44.58±0.50	+42.0±0.05	+40.2±0.63

The BS signal is graphically reported as positive (BS increase) or negative peak (BS decrease). The migration of particles to the top of the cell leads to a concentration decrease at the bottom, translated by a decrease in the BS signal (negative peak) and vice versa for the phenomena occurred on the top of the cell. If the BS profiles have a deviation of $\leq \pm 2\%$ it can be considered that there are no significant variations in particle size. Variations up to ±10% indicate unstable formulations (Araújo et al., 2009; Celia et al., 2009). From the results depicted in Figure 2.3 it is possible to detect instability due to the variation up 10% on the CTAB-LNs composed of 0.25 wt% of CTAB, indicating that this concentration is not sufficient to promote LN dispersion stability over time. The other concentrations seem to be more stable since variations are lower than 10% during the time of analysis. This analysis could predict the good stability of the formulations with CTAB concentration ranging between 0.5 and 1.0 wt %. These results are in agreement with the ZP values recorded for the four formulations (Table 2.6), since higher ZP values could also predict a higher stability of LN dispersions as mentioned before. In order to support Turbiscan®Lab results and also to monitored particles over a period of time, zetasizer measurements were made at the same days after CTAB-LN dispersions production during storage at 25°C. All dispersions showed a milky colloidal appearance where no aggregation phenomena and no phase separation were detected during the period of analysis and storage. From the results depicted in Table 2.6 is possible to detect a slightly increase both in the Z-Ave and in the PI after 30 days of storage. During the period of analysis, CTAB-LN dispersions depicted particle sizes below 300 nm and PI≤0.3, which are acceptable values for ocular delivery (Gonzalez-Mira et al., 2010; Gonzalez-Mira et al., 2011; Souto et al., 2010; Vega et al., 2008). The long-term stability studies confirmed that concentrations of CTAB up to 0.5wt% could provide a better electrostatic repulsion between particles in suspension and from this suggestion provide better stability avoiding particle aggregation and/or flocculation.

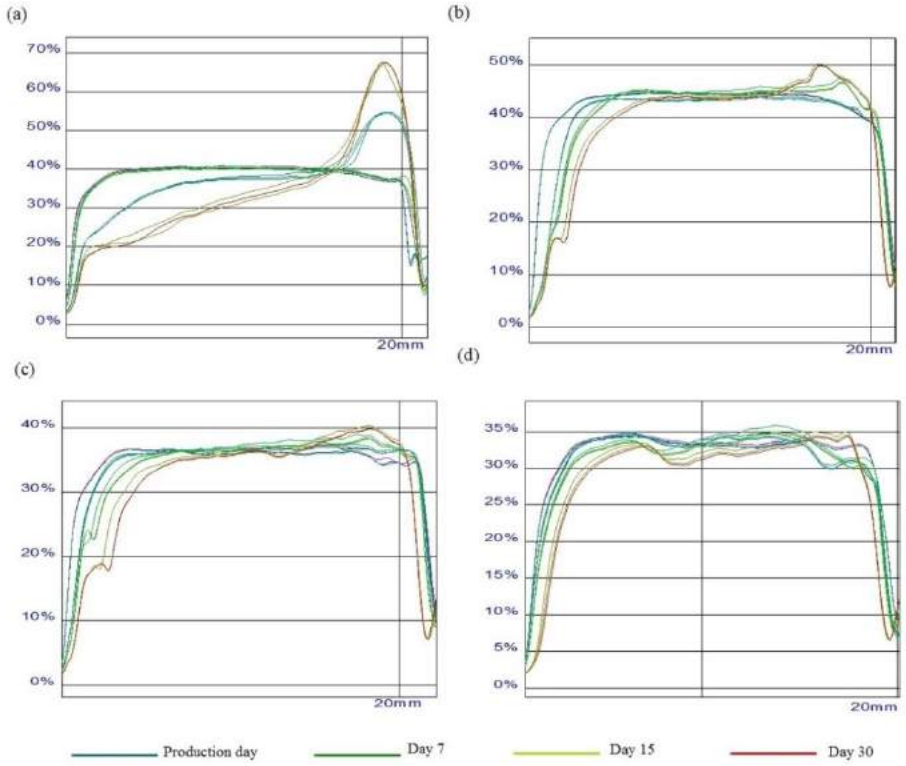

Figure 2.3. BS profiles of SLN dispersions with different CTAB concentrations, (a) 0.25%, (b) 0.50%, (c) 0.75% and (d) 1.00%. The measurement across the height of the sample cell during 10 min, on the production day, day 7, day 15 and day 30 after the production (n = 3).

The analysis of the crystallinity and polymorphism of the LN dispersions obtained was analyzed by DSC and X-Ray. The thermodynamic stability of LN depends mainly on the lipid modification that occurs after crystallization. The solid lipid used was S100, a triacylglycerol blend of vegetable fatty acids with C10-C18 (Fangueiro et al., 2013). Polymorphic transitions after crystallization of triacylglycerol based LNs are slower for longer-chain triacylglycerols than for shorter-chain triacylglycerol (Metin and Hartel, 2005). The type of emulsifier used in LN dispersions also affects their thermodynamic behavior, their storage time and degradation velocity (Han et al., 2008).

Triacylglycerols usually occur in three major polymorphic forms, namely α, β´ and β (in order of increasing thermodynamic stability) which are characterized by different sub

cell packing of the lipid chains. The β´modification is frequently observed in complex triacylglycerols such as S100 (Bunjes and Unruh, 2007).

Thermal analysis of the bulk lipid S100 (Figure 2.4) shows a single endothermic peak upon heating with a minimum of 39.12°C and an enthalpy of –44.76 Jg^{-1} (Table 2.7). Our results are in agreement with those reported by other authors (Schubert and Müller-Goymann, 2003; Thoma and Serno, 1983) for a β´modification of complex triacylglycerols mixtures. For CTAB bulk, a small melting event was observed between 40-50°C, which can be associated to the melting of acyl chains and a main transition at around 106.34°C corresponding to complete melting of CTAB and attributed to the melting of head-groups (Doktorovova et al., 2011).

Relatively to CTAB-LN dispersions (Figure 2.4) it is visible a very small endothermic event compared with the other thermograms of the bulk lipid and bulk matrix. This transition is relatively small due to the lowest values of enthalpy presented by the LN dispersions compared to the bulk lipid (Table 2.7). The peak temperature slightly decreased for all CTAB-LN dispersions confirming that polymorphism of S100. In LN dispersions, a slight decrease of enthalpy is usually observed, as well as a decrease on the peak temperature comparing to the bulk counterpart, however since this lipid has a very low melting point, it is possible to form supercooled melts. A possible explanation for the reduction of crystallinity of the LN dispersion is the coexistence of lipid being present in the α modification and also due to the colloidal particle size offering insufficient number of diffraction levels. These differences can be attributed to the high surface to volume ratio of LN dispersions (Schubert and Müller-Goymann, 2003).

The X-ray results depicted in Figure 2.5 also reveal the presence of two signals one at 0.42 nm (2Θ=21.1°) and other at 0.38 nm (2Θ=23.2°) which are both characteristic of the orthorhombic perpendicular subcell, i.e., β´ modification (Schubert and Müller-Goymann, 2003). These results are in agreement with DSC studies, since all formulations revealed a decreased crystallinity comparing with bulk lipids S100 and CTAB. Also, the melting enthalpy of CTAB-LN dispersions is increasing with increasing CTAB content, indicating higher crystallinity of the matrices containing 0.5 to 1.0wt% of CTAB. Thus, the concentration of CTAB in the lipid matrix is able to

provide higher crystallinity to the lipid matrix; however, other features such as stability and toxicity were analyzed to provide a full study in order to choose the best CTAB concentration.

Table 2.7. Differential scanning calorimetry (DSC) analysis of the SLN formulations with different CTAB.

Formulation	Onset temperature (°C)	Melting point (°C)	Integral (mJ)	Enthalpy (Jg^{-1})
Softisan100 bulk	36.68	39.12	-3111.15	-44.76
CTAB bulk	100.88	106.34	-677.30	-12.72
CTAB-LN 0.25wt%	29.58	34.12	-17.50	-0.23
CTAB-LN 0.5wt%	31.26	35.03	-116.43	-1.47
CTAB-LN 0.75wt%	31.12	34.73	-110.44	-1.41
CTAB-LN 1.0wt%	31.65	34.94	-129.98	-1.59

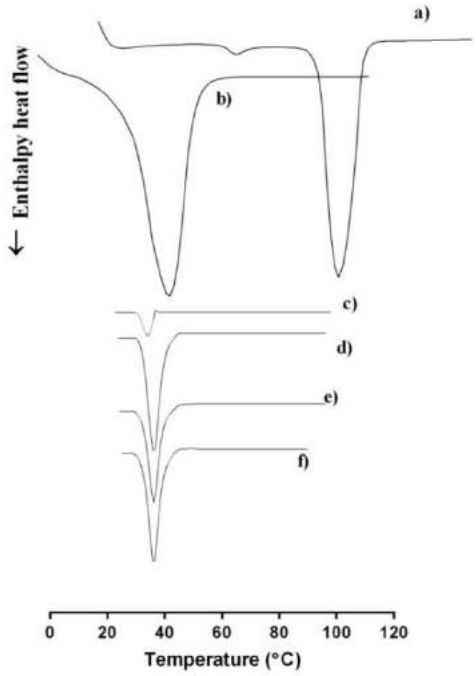

Figure 2.4. DSC thermograms of a) bulk CTAB, b) bulk S100 and CTAB-LN with different concentrations c) 0.25%wt, d) 0.50%wt, e) 0.75%wt and f) 1.0%wt.

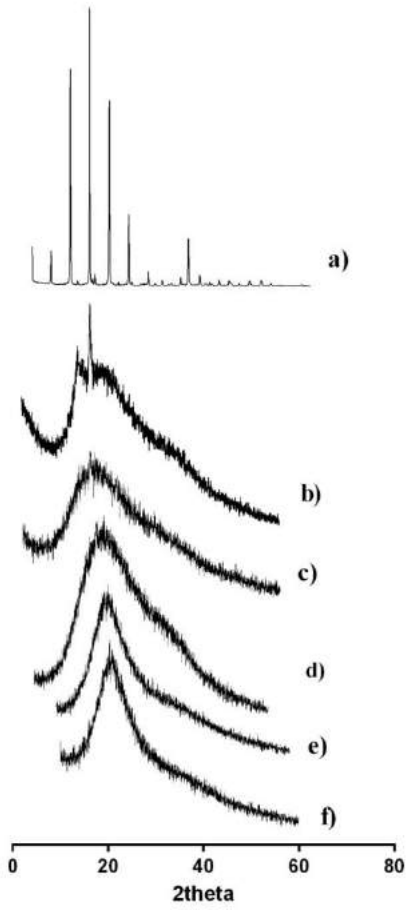

Figure 2.5. X-ray diffraction patterns of a) bulk CTAB, b) bulk S100 and CTAB-LN with different concentrations c) 0.25%wt, d) 0.50%wt, e) 0.75%wt and f) 1.0%wt.

LN toxicity is essential to design drug delivery systems able to ensure security and avoid side effects. Cytotoxicity was assessed in human retinoblastoma cell line, Y-79. The Alamar blue assay measures quantitatively the proliferation of the cells establishing cytotoxicity of tested agents/drugs and can be used as a baseline for further *in vivo* studies. This assay could predict if formulations cause cellular damage which consequently results in loss of the metabolic cell function. Alamar blue is a sensitive fluorometric/colorimetric growth indicator used to detect metabolic activity of cells. Specifically, cells incorporate an oxidation-reduction (REDOX) indicator that, when in a reducing environment of a metabolically active cell, is reduced. When reduced,

Alamar blue becomes fluorescent and changes color from blue to pink. The reduction of Alamar blue is believed to be mediated by mitochondrial enzymes (Hamid et al., 2004). However, some authors also suggest that cytosolic and microsomal enzymes also contribute to the reduction of Alamar blue (Gonzalez and Tarloff, 2001).

The evaluation of the Alamar blue assay was based on the percent viability of four concentrations for each CTAB concentration in the dispersion. This assay is important to point out the importance of the CTAB quantity in the formulation that could be administered for ocular delivery, avoiding cell damage. From figure 2.6, we can observe that 10 $\mu g.mL^{-1}$ of all CTAB-LN formulations is non-toxic to cells as cell viability is not statistically different from control (untreated cells) along the 3 time-points of exposure. The concentration of 50 $\mu g.mL^{-1}$ of CTAB-LN only reduced significantly cell viability in the CTAB-LN dispersions containing 0.75 and 1.0 wt% of CTAB, along the 3 time-points of exposure. The concentration of 100 $\mu g.mL^{-1}$ of CTAB-LN reduced significantly cell viability in all CTAB percentages. CTAB-LN formulation containing 0.25% (w/w) of CTAB is non-toxic for the range of 10 to 50 $\mu g.mL^{-1}$ (Figure 2.6a), but reduces significantly cell viability, in about 50 to 75% of control ($p<0.05$). The concentration range where cell viability is kept similar to control values is reduced increasing CTAB concentration in the formulations. In figure 2.6b (0.5% of CTAB, concentration twice that used for figure 2.6a) we can observe that 50 $\mu g.mL^{-1}$ of formulation reduces cell viability from 40 to 60% of the control while 100 $\mu g.mL^{-1}$ practically abolishes cell viability for the 3 time points of exposure. Raising CTAB concentration in the formulation to 0.75% (figure 2.6c) and to 1.0% (figure 2.6d) reduces cell tolerance to the formulation as we observe that with increasing % of CTAB in the formulation reduces the concentration that maintains cell viability. These results suggest that a higher CTAB concentration implies higher cytotoxicity which is expected since the effect of cationic agents on the human health is concentration dependent. In addition, higher CTAB-LN concentrations also imply more cytotoxicity. From our results, a safe and biocompatible LN system should be composed of, at maximum, 0.5 wt% of CTAB.

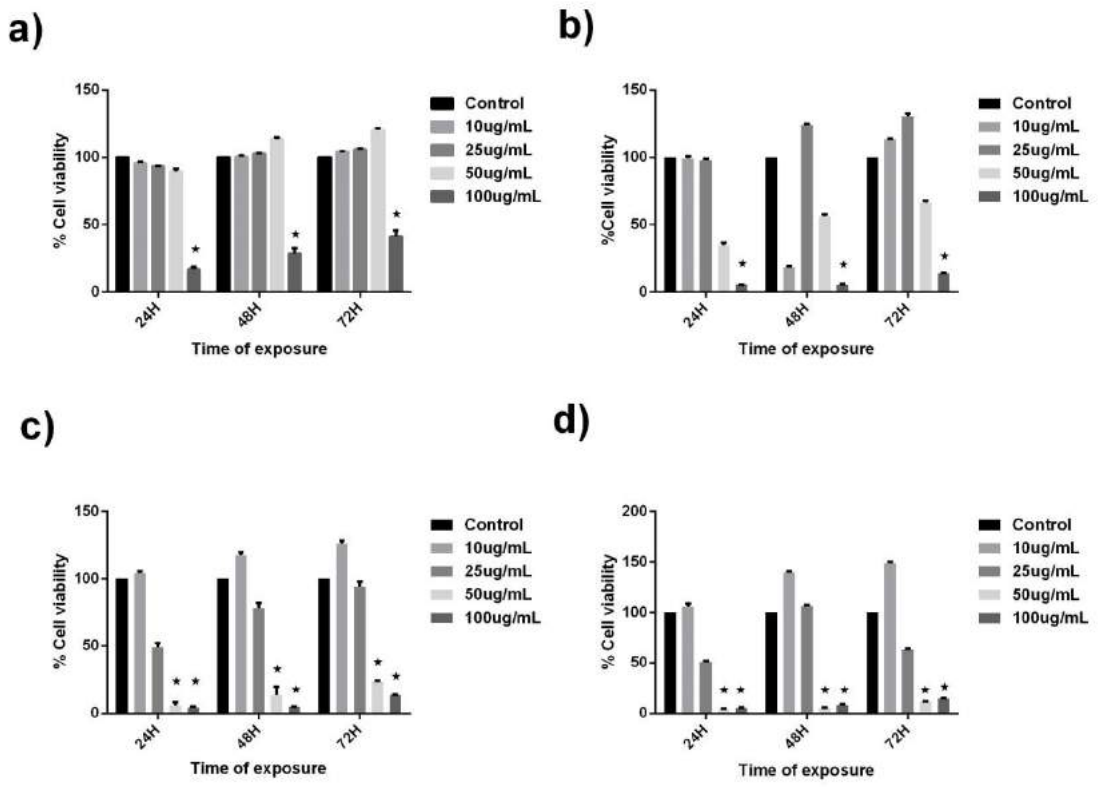

Figure 2.6. Effect of CTAB-LN a) 0.25%; b) 0.5%; c) 0.75% and d) 1.0% on Y-79 human retinoblastoma cells viability (n=4) after 24, 48 and 72 hours of exposure, *p<0.05.

TEM analysis has been performed to evaluate the particle shape and morphology of CTAB-LN dispersion. TEM image (Figure 2.7) shows particles mainly with spherical morphology. From this analysis, the absence of aggregation phenomena of CTAB-LN dispersion was also confirmed. These results are in agreement with Turbiscan® Lab results. It is possible to detect a slight polydispersity however all the particles remain within the nanometer range. All particles showed a mean diameter that varied between 190-280 nm, which is also in agreement with the zetasizer measurements. TEM analysis suggested that immediately after production CTAB-LN dispersion with 0.5 wt% CTAB contained particles no higher than 1 μm, which is useful for ocular delivery purposes.

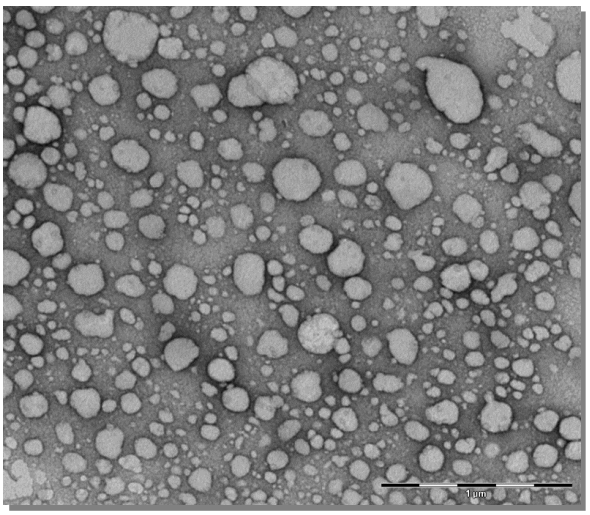

Figure 2.7. TEM micrograph of 0.5% CTAB-LN.

2.4. Conclusions

The development of LN dispersions for ocular delivery should be carried out regarding ocular morphology and biology. A full factorial design was carried out in order to find out which parameters could influence LN dispersions based on multiple emulsion technique. The size and PI of LN dispersions are highly dependent on the lecithin concentration mainly due to its higher emulsification properties and amphiphilic character able to decrease particle size in emulsions. In order to improve ocular mucoadhesion, a cationic lipid was added in the lipid matrix. The insufficient information and lack of studies regarding nanotoxicity of cationic agents for ocular or drug delivery leads us to study different CTAB concentrations on lipid matrix and its effects on the physicochemical parameters and cell toxicity of CTAB-LN dispersions.

This study demonstrated that the better CTAB concentration for the dispersion previously optimized by the factorial design was 0.5%, providing better stability and biocompatibility. Further studies encapsulating hydrophilic drugs and evaluating the *ex vivo* and *in vivo* performance of the developed CTAB-LN dispersion are required to confirm these preliminary results.

2.5. Bibliographic references

Araujo, J., Gonzalez, E., Egea, M. A., Garcia, M. L., and Souto, E. B. (2009). Nanomedicines for ocular NSAIDs: safety on drug delivery. *Nanomedicine*: *Nanotechnology, Biology, and Medicine,* 5(4), 394-401.

Araújo, J., Vega, E., Lopes, C., Egea, M. A., Garcia, M. L., and Souto, E. B. (2009). Effect of polymer viscosity on physicochemical properties and ocular tolerance of FB-loaded PLGA nanospheres. *Colloids and Surfaces. B: Biointerfaces,* 72(1), 48-56.

Bhatta, R. S., Chandasana, H., Chhonker, Y. S., Rathi, C., Kumar, D., Mitra, K., and Shukla, P. K. (2012). Mucoadhesive nanoparticles for prolonged ocular delivery of natamycin: In vitro and pharmacokinetics studies. *International Journal of Pharmaceutics,* 432(1–2), 105-112.

Bunjes, H., and Unruh, T. (2007). Characterization of lipid nanoparticles by differential scanning calorimetry, X-ray and neutron scattering. *Advanced Drug Delivery Reviews,* 59(6), 379-402.

Celia, C., Trapasso, E., Cosco, D., Paolino, D., and Fresta, M. (2009). Turbiscan lab expert analysis of the stability of ethosomes and ultradeformable liposomes containing a bilayer fluidizing agent. *Colloids and Surfaces. B: Biointerfaces,* 72(1), 155-160.

del Pozo-Rodriguez, A., Delgado, D., Gascon, A. R., and Solinis, M. A. (2013). Lipid nanoparticles as drug/gene delivery systems to the retina. *Journal of Ocular Pharmacology* and *Therapeutics,* 29(2), 173-188.

Diebold, Y., and Calonge, M. (2010). Applications of nanoparticles in ophthalmology. *Progress in Retinal and Eye Research,* 29(6), 596-609.

Doktorovova, S., Shegokar, R., Rakovsky, E., Gonzalez-Mira, E., Lopes, C. M., Silva, A. M., Souto, E. B. (2011). Cationic solid lipid nanoparticles (cSLN): Structure, stability and DNA binding capacity correlation studies. *International Journal of Pharmaceutics,* 420(2), 341-349.

Fangueiro, J. F., Andreani, T., Egea, M. A., Garcia, M. L., Souto, S. B., and Souto, E. B. (2012a). Experimental Factorial Design Applied to Mucoadhesive Lipid Nanoparticles via Multiple Emulsion Process. *Colloids and Surfaces B: Biointerfaces*, 100(1), 84-89.

Fangueiro, J. F., Gonzalez-Mira, E., Martins-Lopes, P., Egea, M. A., Garcia, M. L., Souto, S. B., and Souto, E. B. (2013). A novel lipid nanocarrier for insulin delivery: production, characterization and toxicity testing. *Pharmaceutical Development and Technology*, 18(3), 545-549.

Fiume, Z. (2001). Final report on the safety assessment of Lecithin and Hydrogenated Lecithin. *International Journal of Toxicology*, 20 Suppl 1, 21-45.

Fresta, M., Panico, A. M., Bucolo, C., Giannavola, C., and Puglisi, G. (1999). Characterization and in-vivo ocular absorption of liposome-encapsulated acyclovir. *Journal of Pharmacy and Pharmacology,* 51(5), 565-576.

Gallarate, M., Trotta, M., Battaglia, L., and Chirio, D. (2009). Preparation of solid lipid nanoparticles from W/O/W emulsions: preliminary studies on insulin encapsulation. *Journal of Microencapsulation,* 26(5), 394-402.

García-Fuentes, M., Torres, D., and Alonso, M. J. (2003). Design of lipid nanoparticles for the oral delivery of hydrophilic macromolecules. *Colloids and Surfaces B: Biointerfaces,* 27(2–3), 159-168.

Giannavola, C., Bucolo, C., Maltese, A., Paolino, D., Vandelli, M. A., Puglisi, G., Fresta, M. (2003). Influence of preparation conditions on acyclovir-loaded poly-d,l-lactic acid nanospheres and effect of PEG coating on ocular drug bioavailability. *Pharmaceutical Research,* 20(4), 584-590.

Gonzalez-Mira, E., Egea, M. A., Garcia, M. L., and Souto, E. B. (2010). Design and ocular tolerance of flurbiprofen loaded ultrasound-engineered NLC. *Colloids and Surfaces B: Biointerfaces,* 81(2), 412-421.

Gonzalez-Mira, E., Egea, M. A., Souto, E. B., Calpena, A. C., and Garcia, M. L. (2011). Optimizing flurbiprofen-loaded NLC by central composite factorial design for ocular delivery. *Nanotechnology,* 22(4), 045101.

Gonzalez, R. J., and Tarloff, J. B. (2001). Evaluation of hepatic subcellular fractions for Alamar blue and MTT reductase activity. *Toxicology In Vitro,* 15(3), 257-259.

Hamid, R., Rotshteyn, Y., Rabadi, L., Parikh, R., and Bullock, P. (2004). Comparison of alamar blue and MTT assays for high through-put screening. *Toxicology In Vitro,* 18(5), 703-710.

Han, F., Li, S., Yin, R., Liu, H., and Xu, L. (2008). Effect of surfactants on the formation and characterization of a new type of colloidal drug delivery system: Nanostructured lipid carriers. *Colloids and Surfaces A,* 315(1–3), 210-216.

Kawaguchi, E., Shimokawa, K.-i., and Ishii, F. (2008). Physicochemical properties of structured phosphatidylcholine in drug carrier lipid emulsions for drug delivery systems. *Colloids and Surfaces B: Biointerfaces,* 62(1), 130-135.

Lallemand, F., Daull, P., Benita, S., Buggage, R., and Garrigue, J. S. (2012). Successfully improving ocular drug delivery using the cationic nanoemulsion, novasorb. *Journal of Drug Delivery, 2012,* 604204. doi: 10.1155/2012/604204

Liu, J., Huang, X.-f., Lu, L.-j., Li, M.-x., Xu, J.-c., and Deng, H.-p. (2011). Turbiscan Lab® Expert analysis of the biological demulsification of a water-in-oil emulsion by two biodemulsifiers. *Journal of Hazardous Materials,* 190(1–3), 214-221.

Marianecci, C., Paolino, D., Celia, C., Fresta, M., Carafa, M., and Alhaique, F. (2010). Non-ionic surfactant vesicles in pulmonary glucocorticoid delivery: Characterization and interaction with human lung fibroblasts. *Journal of Controlled Release,* 147(1), 127-135.

Metin, S., and Hartel, R. W. (2005). Crystallization of Fats and Oils *Bailey's Industrial Oil and Fat Products*: John Wiley and Sons, Inc.

Pignatello, R., and Puglisi, G. (2011). Nanotechnology in ophthalmic drug delivery: a survey of recent developments and patenting activity. *Recent Patents* on *Nanomedicine,* 1, 42-54.

Schubert, M. A., Harms, M., and Müller-Goymann, C. C. (2006). Structural investigations on lipid nanoparticles containing high amounts of lecithin. *European Journal of Pharmaceutical Sciences,* 27(2–3), 226-236.

Schubert, M. A., and Müller-Goymann, C. C. (2003). Solvent injection as a new approach for manufacturing lipid nanoparticles – evaluation of the method and process parameters. *European Journal of Pharmaceutical Sciences,* 55(1), 125-131.

Severino, P., Andreani, T., Macedo, A., Fangueiro, J. F., Silva, A. M., Santana, M. H., and Souto, E. B. (2012). Current State-of-Art and New Trends on Lipid Nanoparticles (SLN and NLC) for Oral Drug Delivery. *Journal of Drug Delivery*. doi: 10.1155/2012/750891.

Shekunov, B. Y., Chattopadhyay, P., Tong, H. Y., and Chow, A. H. L. (2007). Particle Size Analysis in Pharmaceutics: Principles, Methods and Applications. *Pharmaceutical Research,* 24(2), 203-227.

Souto, E. B., Doktorovova, S., Gonzalez-Mira, E., Egea, M. A., and Garcia, M. L. (2010). Feasibility of lipid nanoparticles for ocular delivery of anti-inflammatory drugs. *Current Eye Research,* 35(7), 537-552.

Sultana, Y., Maurya, D. P., Iqbal, Z., and Aqil, M. (2011). Nanotechnology in ocular delivery: current and future directions. *Drugs Today (Barcelona),* 47(6), 441-455.

Thoma, K., and Serno, P. (1983). Thermoanalytischer Nachweis der Polymorphie der Suppositoriengrundlage Hartfett. *Pharmazeutische Industrie* , 45(10), 990-994.

Trotta, M., Pattarino, F., and Ignoni, T. (2002). Stability of drug-carrier emulsions containing phosphatidylcholine mixtures. *European Journal of Pharmaceutics and Biopharmaceutics,* 53(2), 203-208.

Vega, E., Gamisans, F., García, M. L., Chauvet, A., Lacoulonche, F., and Egea, M. A. (2008). PLGA nanospheres for the ocular delivery of flurbiprofen: Drug release and interactions. *Journal of Pharmaceutical Sciences,* 97(12), 5306-5317.

Ying, L., Tahara, K., and Takeuchi, H. (2013). Drug delivery to the ocular posterior segment using lipid emulsion via eye drop administration: Effect of emulsion formulations and surface modification. *International Journal of Pharmaceutics*, 453(2), 329-335.

CHAPTER 3 - Encapsulation of Epigallocatechin Gallate in cationic lipid nanoparticles

CHAPTER 3.1

Validation of a high performance liquid chromatography method for the stabilization of Epigallocatechin Gallate

CHAPTER 3.2

Physicochemical characterization of Epigallocatechin Gallate lipid nanoparticles (EGCG-LNs) for ocular instillation

CHAPTER 3.1 - VALIDATION OF A HIGH PERFORMANCE LIQUID CHROMATOGRAPHY METHOD FOR THE STABILIZATION OF EPIGALLOCATECHIN GALLATE

Joana F. Fangueiro[a,b], Alexander Parra[c], Amélia M. Silva[d,e], Maria A. Egea[f,g], Eliana B. Souto[a,b,h*], Maria L. Garcia[f,g] and Ana C. Calpena[c,g]

[a] CEBIMED, Investigation Centre of Biomedicine, Faculty of Health Sciences, Fernando Pessoa University (UFP-FCS), Rua Carlos da Maia, 296, 4200-150 Porto, Portugal

[b] Faculty of Health Sciences, Fernando Pessoa University (UFP-FCS), Rua Carlos da Maia, 296, 4200-150 Porto, Portugal

[c] Department of Pharmacy and Pharmaceutical Technology, Faculty of Pharmacy, University of Barcelona, Av. Joan XXIII s/n, 08028 Barcelona, Spain

[d] Department of Biology and Environment, University of Trás-os Montes e Alto Douro (UTAD), Quinta de Prados; 5001-801 Vila Real, Portugal

[e] Centre for Research and Technology of Agro-Environmental and Biological Sciences (CITAB-UTAD), Quinta de Prados; 5001-801 Vila Real, Portugal

[f] Department of Physical Chemistry, Faculty of Pharmacy, University of Barcelona, Av. Joan XXIII s/n, 08028 Barcelona, Spain

[g] Institute of Nanoscience and Nanotechnology, University of Barcelona, Av. Joan XXIII s/n, 08028 Barcelona, Spain

[h] Institute of Biotechnology and Bioengineering, Centre of Genomics and Biotechnology, University of Trás-os-Montes e Alto Douro, UTAD, Quinta de Prados, 5000-801 Vila Real, Portugal

Published in International Journal of Pharmaceutics, 475 (1-2): 181-190, 2014

CHAPTER 3.1 - Validation of a high performance liquid chromatography method for the stabilization of epigallocatechin gallate

Abstract

Epigallocatechin gallate (EGCG) is a green tea catechin with potential health benefits, such as anti-oxidant, anti-carcinogenic and anti-inflammatory effects. In general, EGCG is highly susceptible to degradation, therefore presenting stability problems. The present paper was focused on the study of EGCG stability in HEPES medium regarding the pH dependency, storage temperature and in the presence of ascorbic acid, a reducing agent. The evaluation of EGCG in HEPES buffer has demonstrated that this molecule is not able of maintaining its physicochemical properties and potential beneficial effects, since it is partially or completely degraded, depending on the EGCG concentration. The storage temperature of EGCG most suitable to maintain its structure was shown to be the lower values (4 or -20°C). The pH 3.5 was able to provide greater stability than pH 7.4. However, the presence of a reducing agent (i.e. ascorbic acid) was shown to provide greater protection against degradation of EGCG. A validation method based on RP-HPLC with UV-Vis detection was carried out for two media: water and a biocompatible physiological medium composed of Transcutol®P, ethanol and ascorbic acid. The quantification of EGCG for purposes, using pure EGCG, requires a validated HPLC method could be possible to apply in pharmacokinetic and pharmacodynamics studies.

3.1.1. Introduction

In the last years, extensive studies have been published about the biological and pharmacological activities of tea catechins, which are the main components of the green tea leaves (*Camellia sinensis L.*). The main component is the epigallocatechin gallate (EGCG), which is present in about 70% (Nagle et al., 2006). There are several studies reporting its effects on human health, including anti-carcinogenic (Du et al., 2013;

Rathore et al., 2012; Suganuma et al., 1999; Zhong et al., 2012a) , anti-oxidant (Henning et al., 2005; Hu and Kitts, 2001; Zhong et al., 2012c; Zhong and Shahidi, 2012) , anti-inflammatory (Cavet et al., 2011; Tedeschi et al., 2002; Zhong et al., 2012b) and anti-microbial (Du et al., 2012; Gordon and Wareham, 2010; Güida et al., 2007), based on the anti-oxidative property and inhibitory effect of tea catechins on some enzymes (Wang et al., 2006). Despite its proven health benefits, the use of EGCG for pharmaceutical purposes is not clear. The main problems that affect this catechin are related to its stability. To understand the underlying mechanisms and to study the beneficial health effects related to EGCG, it is essential to stabilize the molecule. The majority of catechins, particularly EGCG, possess certain physicochemical limitations. They are highly unstable in solution and degrade through oxidative and epimerization processes (Mochizuki et al., 2002). The catechins are hydrogen donors and the anti-oxidant capacity is dependent on the number and position of hydroxyl (-OH) groups and their conjugation. Thus, EGCG has greater beneficial health effects than other similar catechins due to the presence of the galloyl moiety, which is partly responsible for the chelating and radical scavenging properties (Heim et al., 2002). The stability of tea catechins, including EGCG, is pH and temperature dependent. The main problem is when EGCG is in aqueous solution, demonstrating limited stability when pH is below 4, and is highly unstable at pH above 6 (Chen et al., 2001; Komatsu et al., 1993; Lun Su et al., 2003; Zimeri and Tong, 1999). Thus, the *in vivo* and *in vitro* evaluation of this catechin becomes a problem regarding its dissolution on physiological buffers such as phosphate *buffered* saline (PBS) and HEPES (which is composed by 4-(2-hydroxyethyl)-1-piperazineethanesulfonic acid). In addition, storage temperature also significantly affects its stability (Chen et al., 2001; Kumamoto et al., 2001; Wang et al., 2008). The main reactions that occur with the degradation of EGCG is the epimerization, which can be caused by the temperature and leads to release of other catechins products, namely (-)-gallocatechin gallate (GCG) (Figure 3.1.1B).

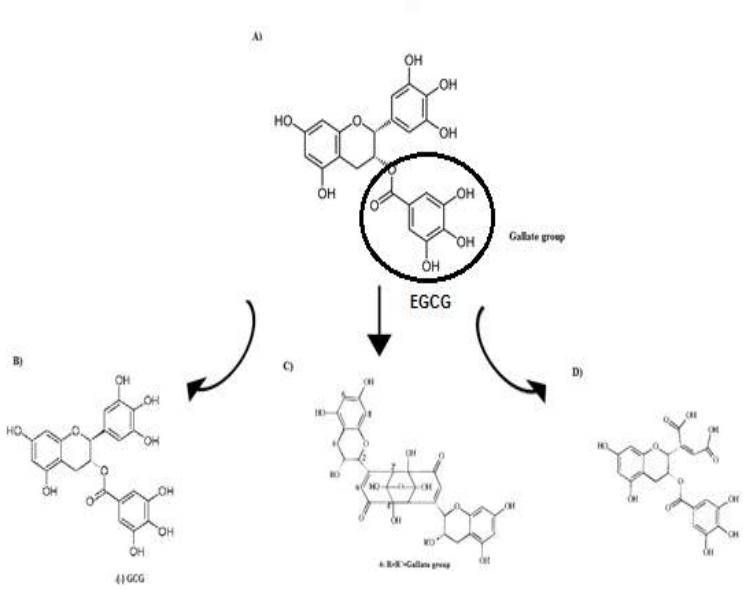

Figure 3.1.1. Degradation products of EGCG. Structure of EGCG (A), the product resulting from its epimerization –(-)GCG (B), and the products derived from its oxidation (C and D).

Some studies report that epimerization processes of catechins, including EGCG, do not significantly alter the anti-oxidant activity, absorption and metabolism of the original catechins (Xu et al., 2004). In addition, it is proven that –(-) GCG is more effective in reducing plasma cholesterol and triacylglycerol concentrations than EGCG (Ikeda et al., 2003; Lee et al., 2008). However, the epimers of the catechins revealed that stereochemistry influences radical scavenging activity of galloylated catechins (Muzolf-Panek et al., 2012). Unfortunately, there is a lack of information related to the epimerization reactions; however, some authors suggested that epimerization of catechins occurred followed by thermal degradation (Wang et al., 2008; Wang et al., 2006). Some studies already evaluated EGCG in a liquid model system, where the reaction temperature was up to 100 °C with varied pH values ranging from 4 to 7. The involved oxygen concentration was taken into account for the thermal degradation of EGCG, i.e., the conversion of EGCG to its epimer (-)- GCG and vice versa (Wang et al., 2008).

The main problems are related to the oxidation of EGCG, which leads to degradation products (Figure 3.1.1C and 3.1.1D). There are two major oxidation routes, namely: (i) the condensation with coexisting epicatechin and its gallate, yielding theaflavins, pigments with a benzotropolone moiety (Tanaka et al., 2010), and (ii) the production of some epigallocatechin dimers, such as theasinensins and oolongtheanins (Matsuo et al., 2008). The first oxidation route which leads to the formation of theaflavins, another group of polyphenols, is promoted by the enzymatic oxidation and leads to brown solutions, easily visible at naked eye (Lun Su et al., 2003). This formation could formed dimers with benzotropolone structures linked through the B-ring, namely dehydrotheaflavin and theanaphthoquinone, and is associated with the co-oxidation of the hydroxyl groups of the gallate group of EGCG, namely in the *ortho* positions (Sang et al., 2004). In the other route, EGCG degradation leads to the formation of theasinensins and oolongtheanins by the dismutation of the molecule (Tanaka et al., 2010).

Since EGCG is a potent anti-oxidant, it tends to be oxidized within the biological environment, which leads to a lower bioavailability and short half-life limiting its therapeutic efficiency. Therefore, the stability of tea catechins must be evaluated, so that reliable results can be obtained from any biopharmacokinetic or biopharmacodynamic studies. The addition of an anti-oxidant to EGCG has been reported to improve their pharmaceutical effect as also to prevent degradation of the molecule (Hatano et al., 2008). Hatano and co-workers (2008) evaluated the capacity of several food additives to maintain the EGCG in solution, and the ascorbic acid was the most potent in preserving the initial concentration (Hatano et al., 2008). In addition, some authors use ascorbic acid as reducing agent to prevent EGCG oxidation in the analysis medium (Dube et al., 2010a; Dube et al., 2010b). For this purpose, the effect of the presence of an anti-oxidant molecule, namely ascorbic acid, in the degradation of EGCG has been analyzed.

Being EGCG one of the most prevalent and biomedical interesting catechin, its stability in various media was examined in this study. In addition, a sensitive analytical method for the determination of EGCG in a mimetic biological medium has been optimized and validated, using reverse phase high performance liquid chromatography (RP-HPLC)

with UV-Vis detection. This method has been successfully applied in the analysis of EGCG in water and in a mimetic biological medium by the previous stability studies carried out at different pHs in HEPES buffer and under different storage temperatures.

3.1.2.Experimental

3.1.2.1. Materials

Epigallocatechin gallate (EGCG, 98% purity) was purchased from CapotChem (Hangzhou, China). Transcutol®P was a gift from Gattefossé (Barcelona, Spain). Acetic acid (glacial, AR grade), acetonitrile (HPLC gradient), HEPES and ascorbic acid were acquired from Sigma Aldrich (Barcelona, Spain). Ethanol absolute (AR grade) was acquired from Panreac (Barcelona, Spain). Membrane filters (0.45 µm) were acquired from Millipore (Barcelona, Spain). The water used in HPLC and for sample preparation was produced with a Super Purity Water System (Purite Ltd, England) with a resistivity over 17.5 MΩ cm.

3.1.2.2. Stability of EGCG under different mediums

The stability of EGCG was studied using six different concentrations (0.25; 0.5; 25; 100; 300 and 900 µg/mL), which covered the concentrations' range used in most pharmaceutical studies. For this purpose, EGCG was dissolved in HEPES buffer in the presence and absence of ascorbic acid (0.25 wt%) at two distinct pHs, namely 3.5 and 7.4, incubated under different conditions (4°C and 25°C). The areas under the curve (AUC) were analyzed and the percentage of EGCG represented is the AUC function since it was not possible to validate the method for HEPES medium.

3.1.2.3. HPLC instrumentation and chromatographic conditions

EGCG analysis was carried out in a RP-HPLC system and using a Waters®LC MODULE I Plus with a 1525 pump (Waters, Milford, MA) with a UV–Vis 2487 detector (Waters®) set at 280 nm. A RP column (XTerra® RP8, 5 µm 10×0.46) with a

flow rate of 1.0 mL/min was used. The mobile phase consisted of acetic acid (1%, v/v):acetonitrile (87:13, v:v). The injection volume was 15 µL and a total run of 16 minutes. The column temperature was set at 20 ± 3.0°C.

3.1.2.4. Preparation of the mobile phase

Mobile phase was prepared by mixing 87 volumes of acetic acid solution (1 %, v/v) and 13 volumes of acetonitrile with a final pH about 3.5-4.0. The mobile phase was ultrasonicated, filtered through 0.45 µm membrane filter and degassed prior to utilization.

3.1.2.5. Preparation of the standard Solutions

EGCG stock solution was prepared by dissolving 3.0 mg in 10 mL of water or the medium selected. The stock solution was further diluted to get standard solutions ranging between 9.375 and 300.000 µg/mL for water validation and 1.750 and 900.000 µg/mL for medium validation.

3.1.2.6. Validation of the analytical method

Validation of the quantitative method for EGCG has been based on the following parameters: selectivity, linearity, precision, recovery, limit of detection, limit of quantification, and stability. The stability of EGCG was tested in HEPES buffer, water and in a medium composed of ethanol (24 %, v/v), transcutol®P (20 %, v/v) and 0.25%, w/v) ascorbic acid solution.

3.1.2.6.1. Precision

Precision is expressed as a series of measurements obtained from multiple sampling of the analyte under the prescribed conditions (Hajimehdipoor et al., 2012). Precision was evaluated as relative standard deviation (RSD) and was studied by analyzing three replicate calibration samples at the low, medium and high concentrations (1.750 to 900.000 µg/mL for the medium and 9.375 to 300.000 for the water). The injections were analyzed in the same day.

3.1.2.6.2. Selectivity

Selectivity for the chromatographic method is the ability of the method to accurately measure the analyte response in the presence of all interferences (Hajimehdipoor et al., 2012). Therefore, the EGCG solutions were analyzed and the analyte peaks were evaluated for peak purity and resolution.

3.1.2.6.3. Linearity

Linearity was evaluated through the relationship between the concentration of EGCG and the absorbance obtained from the UV-HPLC detector. The correlation coefficient values (r^2) were calculated by means of the least-square analysis (Guideline, 2005). The calibration lines were achieved through three replicates of each EGCG concentration range (9.375-75.000 and 37.5-300.000 μg/mL for water and, 1.750-28.125 and 28.125-900.000 μg/mL for the medium), to identify the extent of the total variability of the response that could be explained by the linear regression model. Furthermore, linearity was determined by one-way analysis of variance (ANOVA) test to compare the ratio of peak areas versus nominal concentrations of each standard (GraphPad Prism 6.01 software) and differences were considered statistically significant when $p<0.05$.

3.1.2.6.4. Limits of detection and quantification

Detection limit (LOD) is the lowest concentration of analyte in a sample that can be detected, but not necessarily quantified, under the stated experimental conditions. Quantification limit (LOQ) is the lowest concentration of analyte in a sample that can be determined with acceptable precision and accuracy under the stated experimental conditions. Determination of LOD and LOQ was based on the standard deviation (SD) of the response and on the slope of the calibration curve (S), according to the following equations (Guideline, 2005):

$$LOD = 3.3 \times \frac{SD}{S} \quad \text{(Equation 1)}$$

$$LOQ = 10 \times \frac{SD}{S} \text{ (Equation 2)}$$

3.1.2.6.5. Accuracy/Relatively recovery

Accuracy or Relatively recovery is expressed as the closeness of the amount/weight between the actual or true value of the analyte determined as the percentage of the theoretical amount present in the medium (Hajimehdipoor et al., 2012). It ensures that no loss or uptake occurred during the process.

3.1.2.7. Statistical analysis

Statistical evaluation of data was performed using one-way analysis of variance (ANOVA). Bonferroni multiple comparison test was used to compare the significance of the differences between the groups, a *p*-value < 0.05 was accepted as significant. Data were expressed as the mean value ± standard deviation (Mean ± SD) (n=3). Non-parametric tests were used to analyze EGCG stability results in HEPES medium, with a confidence interval of 95%, a coefficient of variation (CV) >5% was defined as accepted limit.

3.1.3.Results and discussion

3.1.3.1. Analysis of EGCG stability in physiological medium

The analysis of EGCG stability has been a major challenge in pharmaceutical studies regarding this catechin. Previous studies reported its thermal stability to be acceptable at a temperature of 100°C (Lun Su et al., 2003). In the present study, the stability of EGCG in HEPES buffer was evaluated in different days and at different storage temperatures. Firstly, we prepared five EGCG solutions with distinct concentrations, ranging from 0.25 to 900 µg/mL. The storage temperature to check inter-day stability was taken into account in this study. As mobile phase, acetic acid solution (1.0 %, v/v) and acetonitrile (13:87, v/v) with a final pH between 3.5-4.0 has been used and a flow rate of 1.0 mL/min. The chosen methodology and the selection of the analytical parameters were supported by previous studies (Dube et al., 2010a; Dube et al., 2011;

Hajimehdipoor et al., 2012). Since previous studies already confirmed the susceptibility of EGCG to pH over 6, we analyze the stability in HEPES buffer at two different pHs, pH 3.5 (below its pKa) and pH 7.4 (physiological pH). As mentioned before, the addition of an anti-oxidant molecule to protect EGCG was analyzed, and for this purpose the ascorbic acid at 0.25% (w/v) was used. The use of ascorbic acid as reducing agent has been reported as effective (Dube et al., 2010a) and was chosen to develop the stability studies. As shown in Figure 3.1.2, on the first day (i.e. preparation day), EGCG solutions depicted a higher % of EGCG than on the day 2, both at room and at 4°C of storage temperature. Since it has not been possible to validate a reliable method for this quantification, the area of EGCG was set as 100% on the first day. In addition, it is possible to detect a higher degradation of EGCG in the lowest concentrations tested, i.e. 25, 0.5 and 0.25 µg/mL, for all the applied stability tests. However, the short-term stability of EGCG was shown to be limited in solutions with HEPES buffer.

Table 3.1.1. Statistical parameters of the EGCG at different conditions of evaluated media.

Conditions	Statistical Parameters	EGCG concentration (µg/mL)				
		900.0	**300.0**	**100.0**	**25.0**	**0.5**
pH 7.4 with ascorbic acid	**Geometric mean (µg/mL)**	101	99.9	98.8	92.8	79.7
	Standard error	1.4	0.9	0.7	3.6	20.3
	CV (%)	2.5	1.6	1.2	6.8(*)	36.0(*)
pH 7.4	**Geometric mean (µg/mL)**	99.1	101.8	103.0	100.1	61.1
	Standard error	0.5	0.9	1.5	2.1	22.9
	CV (%)	0.8	1.6	2.6	3.7	65.2(*)
pH 3.5 with ascorbic acid	**Geometric mean (µg/mL)**	95.3	86.4	69.5	79.5	71.7
	Standard error	7.3	14.6	26.1	20.5	28.3
	CV (%)	13.3(*)	29.3(*)	64.9(*)	36.4(*)	55.9(*)
pH 3.5	**Geometric mean (µg/mL)**	97.8	89.7	82.9	62.0	n.q.
	Standard error	1.1	5.2	8.5	18.9	n.q.
	CV (%)	1.9	10.0(*)	17.8(*)	53.0(*)	n.q.

n.q. not quantified; * Results statiscally significant , coefficient of variation (CV) >5%

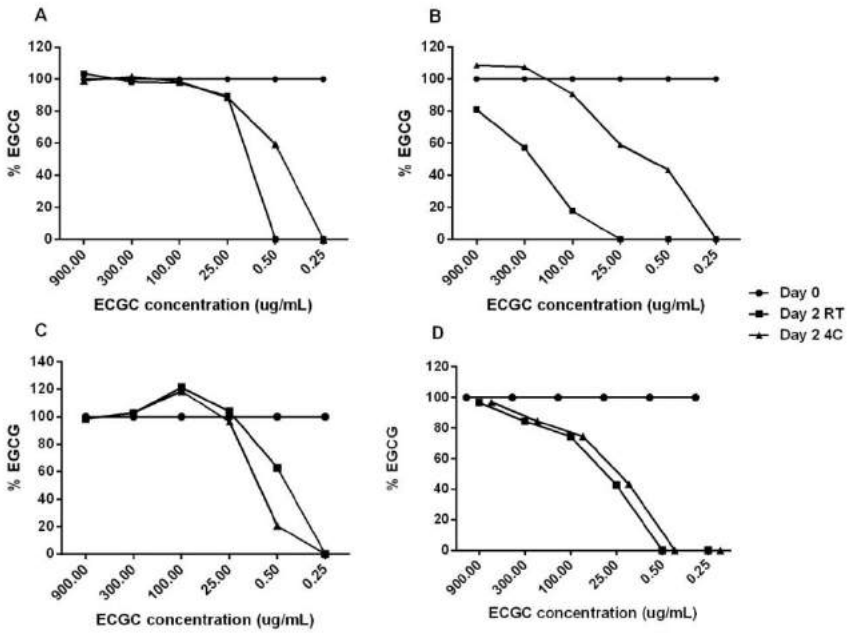

Figure 3.1.2. Stability studies of EGCG in HEPES medium: A) HEPES medium pH 7.4 with ascorbic acid; B) HEPES medium pH 7.4; C) HEPES medium pH 3.5 with ascorbic acid and D) HEPES medium pH 3.5. The presence of ascorbic acid is essential to promote a higher protection of EGCG from auto-oxidation. The pH-dependency is detected, since highest pH, greater degradation of EGCG.

With respect to the stability of EGCG at different pH values, it was shown that it was dependent on the storage temperature. In the presence of ascorbic acid at pH 7.4 (Figure 3.1.2A and Table 3.1.1), the differences were shown statistically significant (CV>5%) in concentrations below 25 µg/mL at room temperature. In the absence of ascorbic acid at pH 7.4, only the lowest concentration (0.5 µg/mL) was significantly different at both temperatures (Figure 3.1.2B and Table 3.1.1). With respect to pH 3.5, in the presence of ascorbic acid (Figure 3.1.2C and Table 3.1.1) all concentrations of EGCG revealed significant differences at both temperatures. In the absence of ascorbic acid, at pH 3.5 (Figure 3.1.2D and Table 3.1.1), EGCG solutions were stable at a maximum concentration of 300 µg/mL, being all significantly different above this concentration.

The pH seems to affect EGCG stability, where slightly differences in the lowest concentrations have been detected, demonstrating the pH-dependent stability, since the

lowest pH value of the medium, the greater the stability. For example, the storage of the solution of 25 µg/mL of EGCG at pH 7.4 (Figure 3.1.2B) led to practically 100% degradation of EGCG comparing to the lowest percentage (≈58%) at pH 3.5 (Figure 3.1.2D). The same is observed for the concentration of 0.5 µg/mL of EGCG (Figure 3.1.2A), which has been entirely degraded at pH 7.4 and at pH 3.5 degraded to almost 80%. As illustrated in Figure 3.1.3C, the chromatogram shows no peak detection for EGCG at lower concentration (25 µg/mL). In addition, there are several degradation products at peak retention times of ≈ 2, 6, 8 and 10 min. Lower concentrations were more sensitive to degradation than higher. The Figure 3.1.3A and 3.1.3B shows the analysis of EGCG in a higher concentration (100 µg/mL), indicating the peak at ≈12-13 min and revealed other degradation products (arrows) prior to this peak of EGCG. These results are in agreement with other studies (Chen et al., 2001; Lun Su et al., 2003; Mizooku et al., 2003), revealing a pH dependency of the EGCG. A hypothetical reason for the destabilization/degradation of EGCG is associated with the three hydroxyl groups at positions 3´, 4´ and 5´ in the gallate group (Figure 3.1.1), being more vulnerable to degradation. This leads to the production of semiquinone free radicals (Lun Su et al., 2003). The main goal of this work was not to identify the degradation products, but to prove that the use of some buffers, such as HEPES or PBS cannot assure EGCG stability for further biopharmacokinetic and biopharmacodynamics studies.

Another factor analyzed for stabilizing EGCG was the storage temperature. This is an important parameter for the development of a validation method, which could provide information about the incubation/storage of samples. In the stability study of EGCG in HEPES medium, only two temperatures were analyzed, at room temperature (≈25°C) and storage at 4°C. As illustrated in Figure 3.1.2, for all cases, there are slight differences between two applied temperatures, being more relevant for the EGCG in HEPES medium at pH 3.5 without ascorbic acid (Figure 3.1.2B). As illustrated in the Figure 2B, the difference is visible, since the storage at room temperature the percentage of EGCG degradation increases. In conclusion, EGCG could be more protected being stored in the freezer, at temperatures of about 4°C. EGCG degradation was expected to be higher at room temperature.

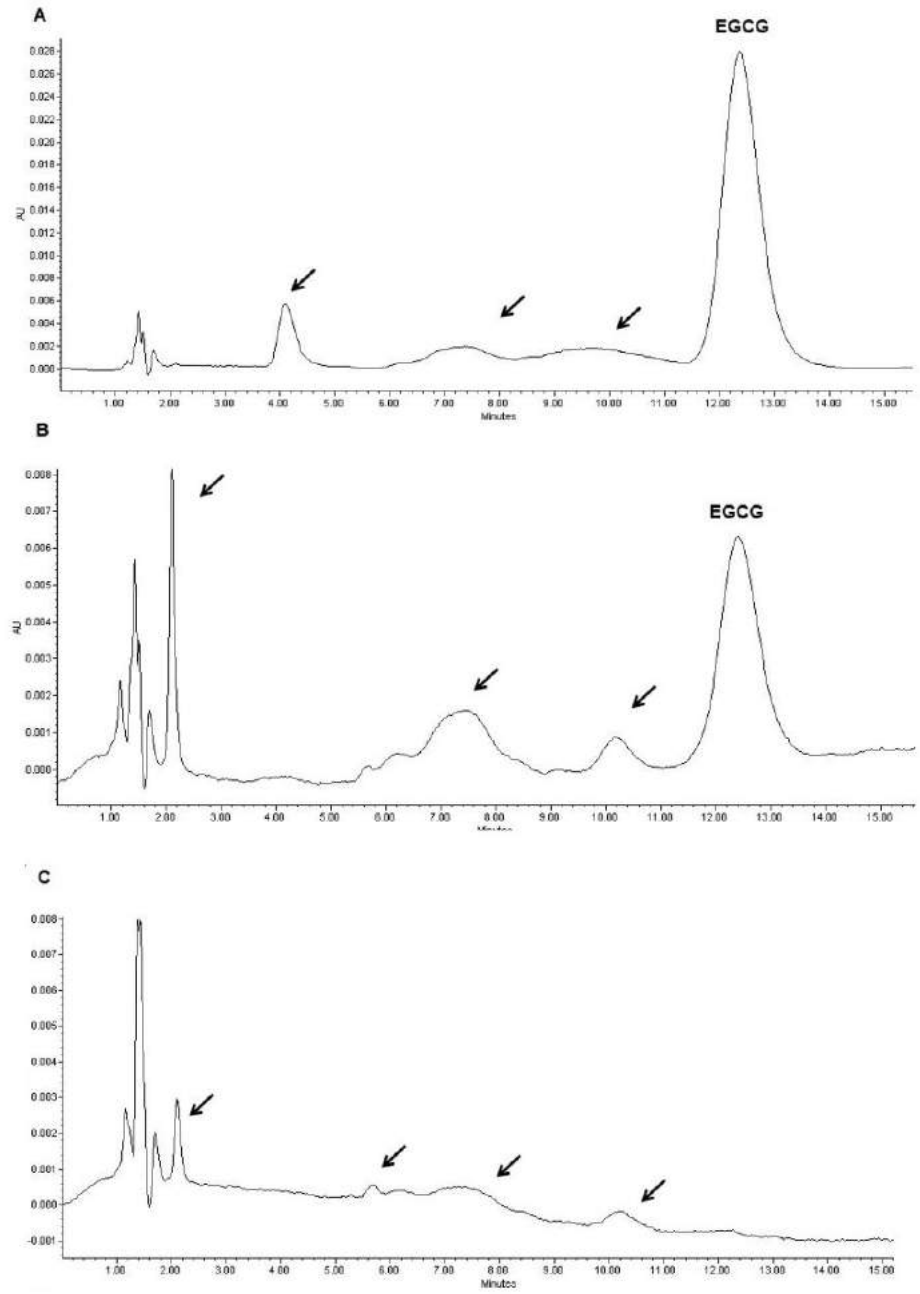

Figure 3.1.3. HPLC chromatograms of EGCG at 100 µg/mL in A) HEPES medium pH 3.5 and B) HEPES medium pH 7.4, both in the absence of ascorbic acid; C) 25 µg/mL of EGCG in HEPES medium at pH 7.4. It is noteworthy the presence of several peaks prior to EGCG peak, indicating the presence of possible degradation products. In addition, lower concentration of EGCG leads to a destruction of the product with no detection peak for EGCG at ≈12-13 min.

The adding of ascorbic acid to the EGCG solutions proved to be more efficient in the prevention of its degradation compared to the solutions without ascorbic acid. As observed for other factors, the lowest concentrations are more susceptible to degradation. Despite no statistically significant differences, in all cases the presence of ascorbic acid seems to provide a higher protection to EGCG, preventing from auto-oxidation. For example, in the presence of ascorbic acid the concentration of 25 µg/mL of EGCG (Figure 3.1.2A) was kept in the same conditions comparing to those without ascorbic acid (Figure 3.1.2B). Ascorbic acid was able to protect and to avoid almost 80% of EGCG degradation. The same results are similar for the pH 3.5 (Figures 3.1.2C and 3.1.2D), where it is possible to detect an increase degradation of EGCG in the absence of ascorbic acid from the concentration of 300 to 0.5 µg/mL, also seriously affecting the higher concentrations. This study has demonstrated that a reducing agent is essential for the stability of EGCG in solution.

From our studies, EGCG has not been stabilized in HEPES or in PBS media (data not shown). These composition media are rich in salts which, in the presence of EGCG could induce drug chelation and degradation/transformation of EGCG in other molecules with different pharmaceutical properties. Chelating groups existing in EGCG are the 3,4-dihydroxyl groups in the B ring as well the gallate group, which may neutralize several metals such as iron, for instance (Kim et al., 2012).

Thus, as EGCG suffers degradation in HEPES medium, other medium was evaluated in order to provide a good stability and no additional problems for analytical and biopharmaceutical studies. For this purpose, a medium composed of Transcutol®P, ethanol and ascorbic acid was used for further studies involving biopharmacokinetic and biopharmacodynamic analysis. The composition of the medium is not compatible with physiological fluids, however previous studies (Fernandez-Campos et al., 2013; Fernandez Campos et al., 2012) have used Transcutol®P to warrantee a biocompatible medium, following sink conditions. Despite not being a physiological medium, it is biocompatible for *ex vivo* biopharmaceutical studies, maintaining sink conditions and providing a mean to analyze EGCG. Firstly, a study comprising EGCG stability inter-day and stored at three different temperatures was carried out. As illustrated in Figure

3.1.4, EGCG exhibited excellent stability when dissolved in the selected medium. The concentrations tested varied from 900 to 25 µg/mL of ECGC, since it is the range for biopharmaceutical use. Between the day 0 and the last day of analysis (day 7) none of the EGCG concentrations are below than 90% (Figure 3.1.4), revealing that this medium is able to provide a good stability at the three different temperatures. The presence of ascorbic acid and the absence of possible quelating ions revealed to modify completely the auto-oxidation of EGCG, giving the possibility of analysis of this catechin for a period at least 7 days. However, the stock solutions were found to be stable at least two weeks when kept at three different temperatures: –20°C, 4°C and 25°C. The storage temperature is very important for *ex vivo* and *in vivo* biopharmaceutical studies since allows knowing how the samples could be stored without any problems related to stability or development of metabolites. For this reason, the three possible storage temperatures were analyzed. Thus, we developed a validated method based on HPLC with UV-Vis detection in this medium and also in water.

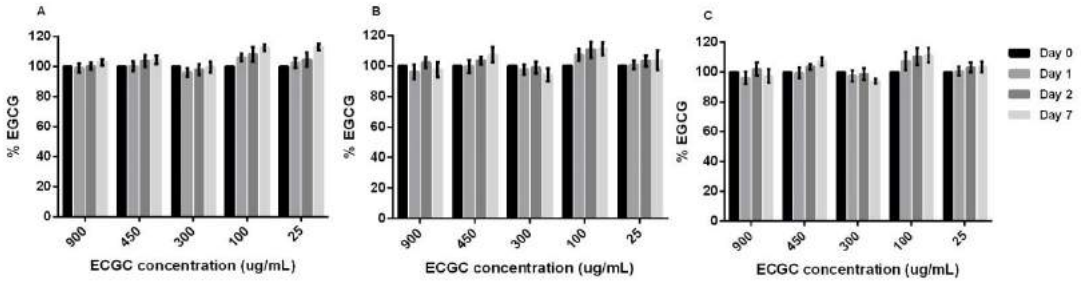

Figure 3.1.4. Stability studies of EGCG in medium composed of Ethanol, Transcutol®P and ascorbic acid at different temperatures A) 4°C; B) Room temperature (≈25°C) and C) in the freezer (-20°C) at different times of storage (day 0, 1, 2 and 7 after preparation of the standard solutions. The frozen standard solutions were kept 15 min at room temperature prior to the HPLC analysis).

3.1.3.2. HPLC method development

Method development was evaluated with sample of aqueous EGCG and in a mimetic biological medium composed of ethanol (24 %, v/v), Transcutol®P (20 %, v/v) and 0.25%, (w/v) ascorbic acid solution. Previous to method development, the stability of EGCG was analyzed in the presence and absence of 0.25 %, (w/v) ascorbic acid dissolved in HEPES medium (Figure 3.1.3). From this previous study, it is possible to ensure that EGCG is protected from auto-oxidation in the presence of ascorbic acid and that HEPES medium leads to a high degradation of EGCG in the lowest concentrations. The optimization of HPLC system led to the development of a set of conditions suitable for the analysis.

Table 3.1.2. Response factors of standard curves for EGCG quantification in the selected medium.

EGCG standards (µg/mL)	**Response factors**				
1.750	2.67×10^4	2.59×10^4	2.94×10^4	2.88×10^4	3.00×10^4
3.510	5.72×10^4	5.71×10^4	5.94×10^4	5.81×10^4	6.46×10^4
7.030	1.16×10^5	1.18×10^5	1.20×10^5	1.21×10^5	1.31×10^5
14.070	2.28×10^5	2.39×10^5	2.41×10^5	2.47×10^5	2.63×10^5
28.125	4.60×10^5	4.96×10^5	5.02×10^5	4.98×10^5	5.38×10^5
56.250	9.72×10^5	1.02×10^6	1.01×10^6	1.03×10^6	1.08×10^6
112.500	2.10×10^6	2.09×10^6	2.06×10^6	2.10×10^6	2.18×10^6
225.000	4.20×10^6	4.28×10^6	4.26×10^6	4.28×10^6	4.49×10^6
450.000	8.50×10^6	8.75×10^6	8.67×10^6	8.72×10^6	9.04×10^6
900.000	1.76×10^7	1.77×10^7	1.78×10^7	1.78×10^7	1.84×10^7

Table 3.1.3. Response factors of standard curves for EGCG quantification in water.

EGCG standards (µg/mL)	**Response factors**					
9.375	5.66×10^5	3.71×10^5	2.16×10^5	3.68×10^5	2.36×10^5	6.68×10^5
18.750	1.06×10^6	9.09×10^6	6.60×10^6	1.02×10^7	6.19×10^6	1.51×10^6
37.500	2.33×10^6	2.02×10^6	1.61×10^6	2.20×10^6	1.60×10^6	2.19×10^6
75.000	4.86×10^6	4.26×10^6	4.08×10^6	4.68×10^6	3.94×10^6	4.28×10^6
150.000	$1{,}01 \times 10^7$	9.11×10^6	8.19×10^6	9.90×10^6	8.12×10^6	1.02×10^7
300.000	$1{,}96 \times 10^7$	$1{,}82 \times 10^7$	$1{,}71 \times 10^7$	$2{,}02 \times 10^7$	$1{,}69 \times 10^7$	$2{,}08 \times 10^7$

3.1.3.3. HPLC method validation

The method was validated according to the *International Conference on Harmonisation* guidelines (ICH, Guideline 2005). Assay validation involved the determination of selectivity, linearity, precision, accuracy, LOD and LOQ. Intra-day precision values were estimated at three different concentrations of EGCG on the same day to obtain the relative standard deviation (RSD %). Accuracy was determined as the percentage of standard deviation.

3.1.3.3.1. Selectivity

The mean retention time of EGCG was found to be ≈12-13 min. The drug peak did not overlap with peaks of any of the components present in the medium, which will be used in further pharmacokinetics and pharmacodynamics studies. Representative chromatograms of samples are shown in Figure 3.1.5. The presence of ascorbic acid in the medium, which absorbs at the same wavelength (λ=280 nm) of EGCG, did not affect EGCG specificity and the drug peak remains equally detectable and specific for EGCG, as retention times are different. Thus, the method is highly specific and detects the peak of the drug in the presence of other substances, e.g. medium constituents, without any alteration to EGCG.

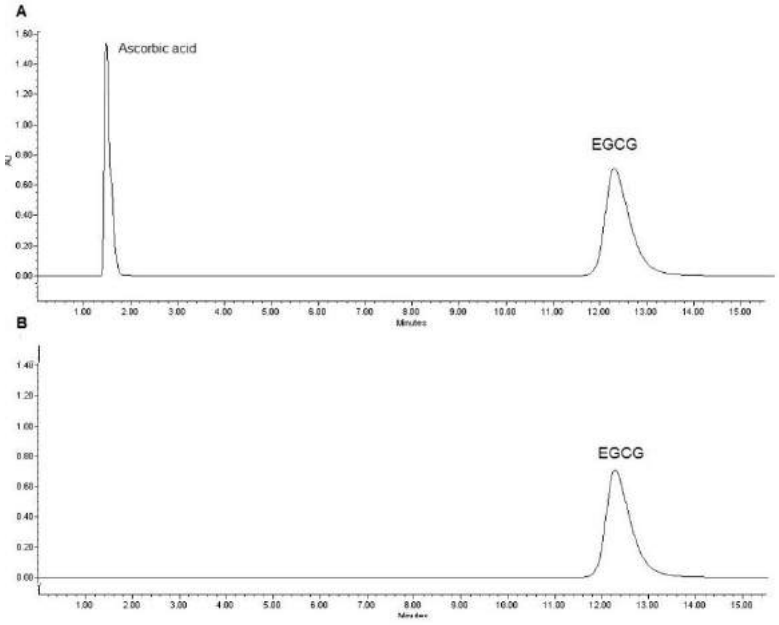

Figure 3.1.5. HPLC chromatograms of EGCG at 900µg/mL in different conditions, A) EGCG in medium with ascorbic acid and B) EGCG in water. It is possible to detect a peak at ≈12-13 min corresponding to EGCG and in the presence of ascorbic acid a peak at ≈1.8 min is detected due it also absorbs at 280nm.

3.1.3.3.2. Linearity

The linearity of the method was evaluated by the obtained equation and regression values from the calibration curves determined by least-squares linear regression analysis of the peak-area ratios of the EGCG standards solutions versus concentration (Table 3.1.2 for medium and Table 3.1.3 for water). Five and six calibration curves were made, respectively for the medium and water. For the validation of EGCG in the mimetic biological medium the calibration curves were linear in the range of 1.75-28.125 µg/mL and from 28.125-900.00 µg/mL. For the validation of EGCG in the water the linearity range was from 9.375-75.00 µg/mL and 37.50-300.00 µg/mL. The equations and the r^2 of the calibration curves are depicted in Table 3.1.4. No single calibration standard point was dropped during the validation and the data indicate good linearity of the proposed method.

Table 3.1.4. Validation parameters of the developed methods including the curve equations, r^2 and limits of detection (LOD) and of quantification (LOQ).

EGCG	Range (µg.ml^{-1})	Equation	r^2	LOD±SD (µg.ml^{-1})	LOQ±SD (µg.ml^{-1})
Medium	1.750 - 28.125	Y=17669X–4502.7	0.9999	0.31 ± 0.16	0.94 ± 0.47
	28.125 – 900.000	Y=19916X–12763 6	0.9999		
Water	9.375 – 75.000	Y=64133X–41364 3	1.000	3.67 ± 3.09	11.11 ± 9.36
	37.500 – 300.000	Y=60041X–18333 7	0.9992		

3.1.3.3.3. Precision

The precision was performed using standard solutions of EGCG in both validation media at the same concentrations used for the calibration curves. The precision was expressed as RSD (%). Statistical analysis of the results, regarding the precision results, is abridged in Tables 3.1.4 and 3.1.5. The data indicate that precision for EGCG validation in the medium (n = 5) as expressed by % RSD and % relative error ranged between 0.15–4.55 % and 0.253–(–3.906) %, respectively (Table 3.1.4). For water validation, the data indicate a range of % RSD and % relative error of 0.26–16.65 % and 0.11–(–3.94) %, respectively (Table 3.1.5).

Table 3.1.5. Statistical evaluation for EGCG quantification in the selected medium.

Theoretical concentration (µg/mL)	Experimental concentration (µg/mL)	Standard deviation	Recovery (%)	Relative Error (%)	RSD (%)
1.750	1.820	0.083	104.00	–3.91	4.55
3.510	3.560	0.044	101.43	–1.28	1.23
7.030	7.010	0.086	99.72	0.35	1.22
14.070	13.900	0.116	98.79	1.21	0.84

28.125	28.206	0.057	100.28	–0.29	0.20
56.250	57.791	0.597	102.74	–2.74	1.03
112.500	112.215	1.760	99.75	0.25	1.57
225.000	222.359	0.919	98.82	1.17	0.41
450.000	445.152	2.762	98.92	1.08	0.62
900.000	902.920	1.318	100.32	–0.32	0.15

Table 3.1.6. Statistical evaluation for EGCG quantification in water.

Theoretical concentration (µg/mL)	Experimental concentration (µg/mL)	Standard deviation	Relatively recovery (%)	Relative Error (%)	RSD (%)
9.375	9.74	1.62	103.94	–3.94	16.65
18.750	19.18	1.81	102.31	–2.03	9.45
37.500	37.42	1.89	99.79	0.21	5.06
75.000	74.44	2.85	99.26	0.74	3.83
150.000	150.97	2.25	100.65	–0.65	1.49
300.000	299.66	0.77	99.88	0.11	0.26

3.1.3.3.4. Accuracy/ Relatively recovery

The accuracy of the method is reported as Relatively recovery. The recoveries of quantification procedure of all standards were examined covering the linearity range of calibration curves. The results shown in Table 3.1.4 and 3.1.5 demonstrate that the method is accurate, ensuring reliable results, since appropriate recovery values were found. For the medium validation, all accuracy values were above of 98.79% (Table 3.1.5) and for the water validation were above of 99.26% (Table 3.1.6).

3.1.3.3.5. Limits of detection (LOD) and limits of quantification (LOQ)

The LOD and LOQ values were determined and are given in Table 3.1.3. The LOD and LOQ for EGCG in the medium are 0.31±0.16 and 0.94±0.47 μg/mL, respectively. For the validation of EGCG in water the values of LOD and LOQ are 3.67±3.09 and 11.11±9.36 μg/mL, respectively. The values for EGCG in the medium are the lowest for the water, which could be explained by the sensitivity of response to be dependent on the nature of the medium. These results indicate that the proposed HPLC method is sufficiently sensitive for the determination of EGCG in the range of the calibration curves proposed, which is suitable for biomedical applications.

3.1.4. Conclusions

EGCG has a range of beneficial effects. The present study examined the stability of this catechin in HEPES medium regarding the pH dependency, storage temperature and the presence of a reducing agent (ascorbic acid). In general, EGCG is highly susceptible to degradation. The evaluation of EGCG in HEPES buffer led to the conclusion that EGCG is not able to maintain its original properties, chemistry and potential beneficial effects, since it suffers degradation. However, this study could provide information about the storage temperature for EGCG, which is most suitably protected at lower temperature (4 or –20°C). The lowest pH (3.5 over 7.4) leads to a greater stability, and the use of a reducing agent, namely ascorbic acid (0.25%wt), provides a better chemical protection of EGCG. A validation method based on RP-HPLC with UV-Vis detection was carried out for two different media: water and a biocompatible physiological medium composed of Transcutol®P, ethanol and ascorbic acid. The methods developed showed to be precise and accurate for further analysis of EGCG in biological systems and for biopharmaceuticals, biopharmacokinetic and pharmacodynamics studies.

3.1.5. Bibliographic References

Cavet, M. E., Harrington, K. L., Vollmer, T. R., Ward, K. W., and Zhang, J. Z. (2011). Anti-inflammatory and anti-oxidative effects of the green tea polyphenol epigallocatechin gallate in human corneal epithelial cells. *Molecular Vision*, 17, 533-542.

Chen, Z., Zhu, Q. Y., Tsang, D., and Huang, Y. (2001). Degradation of green tea catechins in tea drinks. *Journal of Agricultural and Food Chemistry,* 49(1), 477-482.

Du, G. J., Wang, C. Z., Qi, L. W., Zhang, Z. Y., Calway, T., He, T. C., Yuan, C. S. (2013). The synergistic apoptotic interaction of panaxadiol and epigallocatechin gallate in human colorectal cancer cells. *Phytotherapy Research,* 27(2), 272-277.

Du, X., Huang, X., Huang, C., Wang, Y., and Zhang, Y. (2012). Epigallocatechin-3-gallate (EGCG) enhances the therapeutic activity of a dental adhesive. *Journal of Dentistry,* 40(6), 485-492.

Dube, A., Ng, K., Nicolazzo, J. A., and Larson, I. (2010a). Effective use of reducing agents and nanoparticle encapsulation in stabilizing catechins in alkaline solution. *Food Chemistry,* 122(3), 662-667.

Dube, A., Nicolazzo, J. A., and Larson, I. (2010b). Chitosan nanoparticles enhance the intestinal absorption of the green tea catechins (+)-catechin and (-)-epigallocatechin gallate. *European Journal of Pharmaceutical Sciences,* 41(2), 219-225.

Dube, A., Nicolazzo, J. A., and Larson, I. (2011). Assessment of plasma concentrations of (−)-epigallocatechin gallate in mice following administration of a dose reflecting consumption of a standard green tea beverage. *Food Chemistry,* 128(1), 7-13.

Fernandez-Campos, F., Clares Naveros, B., Lopez Serrano, O., Alonso Merino, C., and Calpena Campmany, A. C. (2013). Evaluation of novel nystatin nanoemulsion for skin candidosis infections. *Mycoses,* 56(1), 70-81.

Fernandez Campos, F., Calpena Campmany, A. C., Rodriguez Delgado, G., Lopez Serrano, O., and Clares Naveros, B. (2012). Development and characterization of a novel nystatin-loaded nanoemulsion for the buccal treatment of candidosis: ultrastructural effects and release studies. *Journal of Pharmaceutical Sciences,* 101(10), 3739-3752.

Gordon, N. C., and Wareham, D. W. (2010). Antimicrobial activity of the green tea polyphenol (−)-epigallocatechin-3-gallate (EGCG) against clinical isolates of Stenotrophomonas maltophilia. *International Journal of Antimicrobial Agents,* 36(2), 129-131.

Güida, M. C., Esteva, M. I., Camino, A., Flawiá, M. M., Torres, H. N., and Paveto, C. (2007). Trypanosoma cruzi: In vitro and in vivo antiproliferative effects of epigallocatechin gallate (EGCg). *Experimental Parasitology,* 117(2), 188-194.

Guideline., I.C.H. Validation of analytical procedures: text and methodology Q2(R1). Current Step 4 version Parent Guideline dated 27 October 1994 [complementary Guideline on Methodology dated 6 November 1996 incorporated in November; 2005].

Hajimehdipoor, H., Kondori, B. M., Amin, G. R., Adib, N., Rastegar, H., and Shekarchi, M. (2012). Development of a validated HPLC method for the simultaneous determination of flavonoids in Cuscuta chinensis Lam. by ultra-violet detection. *Daru, Journal of Pharmaceutical Sciences*, 20(1), 57.

Hatano, T., Tsugawa, M., Kusuda, M., Taniguchi, S., Yoshida, T., Shiota, S., and Tsuchiya, T. (2008). Enhancement of antibacterial effects of epigallocatechin gallate, using ascorbic acid. *Phytochemistry,* 69(18), 3111-3116.

Heim, K. E., Tagliaferro, A. R., and Bobilya, D. J. (2002). Flavonoid antioxidants: chemistry, metabolism and structure-activity relationships. *Journal of Nutritional Biochemistry,* 13(10), 572-584.

Henning, S. M., Niu, Y., Liu, Y., Lee, N. H., Hara, Y., Thames, G. D., Heber, D. (2005). Bioavailability and antioxidant effect of epigallocatechin gallate administered in purified form versus as green tea extract in healthy individuals. *Journal of Nutritional Biochemistry*, 16(10), 610-616.

Hu, C., and Kitts, D. D. (2001). Evaluation of antioxidant activity of epigallocatechin gallate in biphasic model systems in vitro. *Molecular* and *Cellular Biochemistry*, 218(1-2), 147-155.

Ikeda, I., Kobayashi, M., Hamada, T., Tsuda, K., Goto, H., Imaizumi, K., Kakuda, T. (2003). Heat-epimerized tea catechins rich in gallocatechin gallate and catechin gallate are more effective to inhibit cholesterol absorption than tea catechins rich in epigallocatechin gallate and epicatechin gallate. *Journal of Agricultural and Food Chemistry,* 51(25), 7303-7307.

Kim, J. S., Oh, E. S., and Kim, J.-M. (2012). Nitric Oxyde Synthase, Green Tea Catechins and Parkinson´s Disease. In V. R. Preedy (Ed.), *Tea in Health and Disease Prevention* (pp. 1425-1434). San Diego, USA: American Publishers

Komatsu, Y., Suematsu, S., Hisanobu, Y., Saigo, H., Matsuda, R., and Hara, K. (1993). Studies on Preservation of Constituents in Canned Drinks. Part II. Effects of pH and Temperature on Reaction Kinetics of Catechins in Green Tea Infusion. *Bioscience, Biotechnology, and Biochemistry,* 57(6), 907-910.

Kumamoto, M., Sonda, T., Nagayama, K., and Tabata, M. (2001). Effects of pH and metal ions on antioxidative activities of catechins. *Bioscience, Biotechnology,* and *Biochemistry,* 65(1), 126-132.

Lee, S. M., Kim, C. W., Kim, J. K., Shin, H. J., and Baik, J. H. (2008). GCG-rich tea catechins are effective in lowering cholesterol and triglyceride concentrations in hyperlipidemic rats. *Lipids*, 43(5), 419-429.

Lun Su, Y., Leung, L. K., Huang, Y., and Chen, Z.-Y. (2003). Stability of tea theaflavins and catechins. *Food Chemistry,* 83(2), 189-195.

Matsuo, Y., Yamada, Y., Tanaka, T., and Kouno, I. (2008). Enzymatic oxidation of gallocatechin and epigallocatechin: effects of C-ring configuration on the reaction products. *Phytochemistry,* 69(18), 3054-3061.

Mizooku, Y., Yoshikawa, M., Tsuneyoshi, T., and Arakawa, R. (2003). Analysis of oxidized epigallocatechin gallate by liquid chromatography/mass spectrometry. *Rapid Communications in Mass Spectrometry,* 17(16), 1915-1918.

Mochizuki, M., Yamazaki, S., Kano, K., and Ikeda, T. (2002). Kinetic analysis and mechanistic aspects of autoxidation of catechins. *Biochimica et Biophysica Acta,* 1569(1-3), 35-44.

Muzolf-Panek, M., Gliszczynska-Swigło, A., Szymusiak, H., and Tyrakowska, B. (2012). The influence of stereochemistry on the antioxidant properties of catechin epimers. *European Food Research* and *Technology,* 235, 1001-1009.

Nagle, D. G., Ferreira, D., and Zhou, Y. D. (2006). Epigallocatechin-3-gallate (EGCG): chemical and biomedical perspectives. *Phytochemistry,* 67(17), 1849-1855.

Rathore, K., Choudhary, S., Odoi, A., and Wang, H. C. (2012). Green tea catechin intervention of reactive oxygen species-mediated ERK pathway activation and chronically induced breast cell carcinogenesis. *Carcinogenesis,* 33(1), 174-183.

Sang, S., Tian, S., Stark, R. E., Yang, C. S., and Ho, C.-T. (2004). New dibenzotropolone derivatives characterized from black tea using LC/MS/MS. *Bioorganic and Medicinal Chemistry,* 12(11), 3009-3017.

Suganuma, M., Okabe, S., Kai, Y., Sueoka, N., Sueoka, E., and Fujiki, H. (1999). Synergistic effects of (--)-epigallocatechin gallate with (--)-epicatechin, sulindac, or tamoxifen on cancer-preventive activity in the human lung cancer cell line PC-9. *Cancer Research,* 59(1), 44-47.

Tanaka, T., Matsuo, Y., and Kouno, I. (2010). Chemistry of Secondary Polyphenols Produced during Processing of Tea and Selected Foods. *International Journal of Molecular Sciences,* 11(1), 14-40.

Tedeschi, E., Suzuki, H., and Menegazzi, M. (2002). Antiinflammatory action of EGCG, the main component of green tea, through STAT-1 inhibition. *Annals of the New York Academy of Sciences*, 973, 435-437.

Wang, R., Zhou, W., and Jiang, X. (2008). Reaction kinetics of degradation and epimerization of epigallocatechin gallate (EGCG) in aqueous system over a wide temperature range. *Journal of Agricultural and Food Chemistry,* 56(8), 2694-2701.

Wang, R., Zhou, W., and Wen, R. A. (2006). Kinetic study of the thermal stability of tea catechins in aqueous systems using a microwave reactor. *Journal of Agricultural and Food Chemistry*, 54(16), 5924-5932.

Xu, J. Z., Yeung, S. Y., Chang, Q., Huang, Y., and Chen, Z. Y. (2004). Comparison of antioxidant activity and bioavailability of tea epicatechins with their epimers. *British Journal of Nutrition,* 91(6), 873-881.

Zhong, Y., Chiou, Y.-S., Pan, M.-H., Ho, C.-T., and Shahidi, F. (2012a). Protective effects of epigallocatechin gallate (EGCG) derivatives on azoxymethane-induced colonic carcinogenesis in mice. *Journal of Functional Foods,* 4(1), 323-330.

Zhong, Y., Chiou, Y. S., Pan, M. H., and Shahidi, F. (2012b). Anti-inflammatory activity of lipophilic epigallocatechin gallate (EGCG) derivatives in LPS-stimulated murine macrophages. *Food Chemistry,* 134(2), 742-748.

Zhong, Y., Ma, C.-M., and Shahidi, F. (2012c). Antioxidant and antiviral activities of lipophilic epigallocatechin gallate (EGCG) derivatives. *Journal of Functional Foods,* 4(1), 87-93.

Zhong, Y., and Shahidi, F. (2012). Lipophilised epigallocatechin gallate (EGCG) derivatives and their antioxidant potential in food and biological systems. *Food Chemistry,* 131(1), 22-30.

Zimeri, J., and Tong, C. H. (1999). Degradation kinetics of (-)-epigallocatechin gallate as a function of pH and dissolved oxygen in a liquid model system. *Journal of. Food Sciences,* 64(5), 753-758.

CHAPTER 3.2 - PHYSICOCHEMICAL CHARACTERIZATION OF EPIGALLOCATECHIN GALLATE LIPID NANOPARTICLES (EGCG-LNS) FOR OCULAR INSTILLATION

Joana F. Fangueiro[a,b], Tatiana Andreani[b,c,d], Lisete Fernandes[e], Maria L. Garcia[f,g], Maria A. Egea[f,g], Amélia M. Silva[c,d], Eliana B. Souto [a,b,h*]

[a]CEBIMED, Research Centre for Biomedicine, Fernando Pessoa University, UFP-FCS, Praça 9 de Abril, 349, P-4249-004 Porto, Portugal

[b]Faculty of Health Sciences, Fernando Pessoa University, UFP-FCS, Rua Carlos da Maia, 296, 4200-150 Porto, Portugal

[c]Centre for Research and Technology of Agro-Environmental and Biological Sciences, CITAB, University of Trás-os-Montes e Alto Douro, UTAD, Quinta de Prados, 5000-801 Vila Real, Portugal

[d]Department of Biology and Environment, University of Trás-os-Montes e Alto Douro, UTAD, Quinta de Prados, 5000-801 Vila Real, Portugal

[e]Electron Microscopy Unit, University of Trás-os-Montes e Alto Douro, UTAD, Quinta de Prados, 5000-801 Vila Real, Portugal

[f]Department of Physical Chemistry, Faculty of Pharmacy, University of Barcelona, Av. Joan XXIII s/n, 08028 Barcelona, Spain

[g]Institute of Nanoscience and Nanotechnology, University of Barcelona, Av. Joan XXIII s/n, 08028 Barcelona, Spain

[h]Institute of Biotechnology and Bioengineering, Centre of Genomics and Biotechnology, University of Trás-os-Montes e Alto Douro, UTAD, Quinta de Prados, 5000-801 Vila Real, Portugal

Published in Colloids and Surfaces B: Interfaces, 475 (1-2): 181-190, 2014

CHAPTER 3.2. - Physicochemical characterization of Epigallocatechin Gallate lipid nanoparticles (EGCG-LNs) for ocular instillation

Abstract

The encapsulation of epigallocatechin gallate (EGCG) in lipid nanoparticles (LNs) could be a suitable approach to avoid drug oxidation and epimerization, which are common processes that lead to low bioavailability of the drug limiting its therapeutic efficacy. The human health benefits of EGCG gained much interest in the pharmaceutical field, and so far there are no studies reporting its encapsulation in LNs. The purpose of this study has been the development of an innovative system for the ocular delivery of EGCG using LN as carrier for the future treatment of several diseases, such as dry eye, age-related macular degeneration (AMD), glaucoma, diabetic retinopathy and macular edema. LN dispersions have been produced by multiple emulsion technique and previously optimized by a factorial design. In order to increase ocular retention time and mucoadhesion by electrostatic attraction, two distinct cationic lipids were used, namely, cetyltrimethylammonium bromide (CTAB) and dimethyldioctadecylammonium bromide (DDAB). EGCG has been successfully loaded in the LN dispersions and the nanoparticles analysis over 30 days of storage time predicted a good physicochemical stability. The particles were found to be in the nanometer range (< 300 nm) and all the evaluated parameters, namely pH, osmolarity and viscosity, were compatible to the ocular administration. The evaluation of the cationic lipid used was compared regarding physical and chemical parameters, lipid crystallization and polymorphism, and stability of dispersion during storage. The results show that different lipids lead to different characteristics mainly associated with the acyl chain composition, i.e. double tail lipid shows to have influence in the crystallization and stability. Despite the recorded differences between DTAB and DDAB, both cationic LNs seem to fit the parameters for ocular drug delivery.

3.2.1.Introduction

The research and application of polyphenols, namely catechins, have impacted the pharmaceutical field in a great extent (Manach, Scalbert et al. 2004, Manach, Williamson et al. 2005). Epigallocatechin gallate (EGCG) is a very know catechin which constitutes one of the most powerful metabolite of *Camelia Sinensis* L. EGCG possesses a high spectrum of potential biological activities, including antioxidant and anti-cancer, anti-inflammatory, antibacterial, and antiviral activity (Fang and Bhandari 2010, Fangueiro, Parra et al. 2014). A large body of preclinical research and epidemiological data suggests that polyphenols, specially EGCG can be applied in the treatment and prevention of certain cancers, namely breast and colorectal cancer (Surh 2003, Arts and Hollman 2005, Sen, Moulik et al. 2009, Gu, Makey et al. 2013), reduce the risks of cardiovascular disease (Arts and Hollman 2005, Li, Liu et al. 2012), neurodegenerative diseases (Mandel, Weinreb et al. 2004, Weinreb, Amit et al. 2009, Mähler, Mandel et al. 2013), diabetes (Song, Hur et al. 2003, del Pozo-Rodríguez, Delgado et al. 2008, Roghani and Baluchnejadmojarad 2010), rheumatoid arthritis (Ahmed, Pakozdi et al. 2006, Riegsecker, Wiczynski et al. 2013) or osteoporosis (Vali, Rao et al. 2007, Morinobu, Biao et al. 2008). This study comprises the encapsulation of EGCG in novel drug delivery systems, as the lipid nanoparticles (LNs). The main goal of the EGCG encapsulation is the protection from adverse environmental conditions, such as undesirable effects of light, moisture, and oxygen, thereby contributing to an increase in its shelf life and avoiding its degradation, and on other hand, providing a controlled liberation (Fang and Bhandari 2010). This could be a good alternative to protect this catechin from oxidation and epimerization processes and thus, promote its stability in order to facilitate and optimize its pharmacological effect. EGCG presents a great pharmaceutical potential mainly related to the galloyl moiety, which is partly responsible for its chelating and radical scavenging properties (Heim, Tagliaferro et al. 2002, Fangueiro, Parra et al. 2014).

LNs are a new generation of drug delivery systems being exploited for several drugs since the nineties. LNs are safe drug carriers because of their good biocompatibility and biodegradability, being composed of physiological lipids. The different types of solid

lipids include acylglycerols, waxes, and fatty acids, and particles are stabilized by a wide range of surfactants (Souto, Fangueiro et al. 2013).

For the purpose, w/o/w emulsions can be used, incorporating EGCG in the aqueous core surrounded by a lipid layer composed of physiological lipids (Fangueiro, Andreani et al. 2014). LNs are expected to improve EGCG stability, and may also enhance the drug bioavailability throughout the ocular mucosa. Their submicron size with a narrow size distribution should be non-irritant, adequately bioavailable, cause no blurred vision, and be physiological compatible with ocular tissue (Araújo, Gonzalez et al. 2009).

Barriers such as epithelial, aqueous-vitreous, blood-aqueous barrier and blood-retinal barrier limit the entry of drugs via different routes to the eye. In addition, the anatomy and physiology of human eye may also contribute to the low bioavailability of drugs. Only 7-10% of drugs administered locally onto the eye are bioavailable due to several processes, including (a) the nasolacrimal drainage and absorption to the systemic circulation; (b) pillage due to limited capacity of human cul-de-sac and (c) metabolism by enzymes (Seyfoddin, Shaw et al. 2010). The epithelium has a lipophilic nature and for this reason, represents a barrier for hydrophilic drugs, such as EGCG. Our purpose is the use of cationic LNs to promote ocular bioadhesion and increased drugs retention time in the eye by an electrostatic attraction between the anionic ocular mucosa and the cationic LN loaded with EGCG (Fangueiro, Andreani et al. 2014).

Previous studies with EGCG for ocular purposes already proved the drug's anti-inflammatory and anti-oxidant actions in human corneal epithelial cells and therefore may have therapeutic potential for ocular diseases, such as dry eye, age-related macular degeneration (AMD), glaucoma, diabetic retinopathy and macular edema (Cavet, Harrington et al. 2011). It is proven that EGCG attenuate oxidative stress-induced degeneration of the retina as occurs in these diseases (Zhang and Osborne 2006). Since there are no studies encapsulating EGCG in this type of lipid carriers, our study relate the physicochemical characterization of developed EGCG loaded LN for ocular delivery. Parameters such as particle size, distribution, polymorphic behavior and crystallization, *in vitro* stability, osmolarity, pH, viscosity were analysed to predict their biopharmaceutical properties.

3.2.2.Material and methods

3.2.2.1. Materials

Epigallocatechin gallate (EGCG, 98% purity) was purchased from CapotChem (Hangzhou, China). Softisan®100 (S100) was a free sample from Sasol Germany GmbH (Witten, Germany), Lipoid® S75, 75% soybean phosphatidylcholine was purchased from Lipoid GmbH (Ludwigshafen, Germany), Lutrol®F68 or Poloxamer 188 (P188) was a free sample from BASF (Ludwigshafen, Germany). Cetyltrimethylammonium bromide (CTAB), uranyl acetate and ascorbic acid were acquired from Sigma-Aldrich (Sintra, Portugal). Dimethyldioctadecylammonium bromide (DDAB) was acquired from Avanti Polar Lipids (Alabama, USA). Anhydrous glycerol was purchased from Acopharma (Barcelona, Spain). Ultra-purified water was obtained from a MiliQ Plus system (Millipore, Germany), home supplied. All reagents were used without further treatment.

3.2.2.2. Lipid nanoparticles production

LN dispersions were prepared based on a previous factorial design by a novel multiple emulsion (w/o/w) technique (Fangueiro, Andreani et al. 2014). Their composition is depicted on Table 3.2.1. The inner aqueous phase was prepared dissolving 15 mg of EGCG and 0.25 wt% of ascorbic acid in ultra-purified water, which was added to the lipid phase (5.0 wt%) composed of glycerol, S100, Lipoid® S75 and the cationic lipid (CTAB and DDAB) at same temperature (5-10°C above the melting point of lipid S100) and homogenized 60s with a sonication probe (6 mm diameter) by means of an Ultrasonic processor VCX500 (Sonics, Switzerland). A power output with amplitude of 40% was applied. A few millilitres of P188 solution was added and homogenized for additional 90s. This pre-emulsion was poured in the total volume of a P188 cooled solution under magnetic stirring for 15 min to allow the formation of the LN. The obtained LN dispersions were used for subsequent studies.

Table 3.2.1. Composition of the developed LN dispersions in wt%.

LN dispersion	S100	Glycerol	Lipoid® S75	CTAB	DDAB	P 188	AA	EGCG
CTAB-LN	4.5	37.5	0.5	0.5	_____	1.0	0.25	_____
EGCG CTAB-LN	4.5	37.5	0.5	0.5	_____	1.0	0.25	0.075
DDAB-LN	4.5	37.5	0.5	_____	0.5	1.0	0.25	_____
EGCG DDAB-LN	4.5	37.5	0.5	_____	0.5	1.0	0.25	0.075

S100, Softisan®100; **CTAB,** Cetyltrimethylammonium bromide; **DDAB**, Dimethyldioctadecylammonium bromide; P188, Poloxamer 188; **AA**, ascorbic acid; **EGCG**, Epigallocatechin gallate.

3.2.2.3. Physicochemical characterization

Physicochemical parameters such as Z-Ave, PI and ZP were analysed by dynamic light scattering (DLS, Zetasizer Nano ZS, Malvern Instruments, Malvern, UK). All samples were diluted with ultra-purified water to suitable concentration and analysed in triplicate. For analysis of the ZP an ultra-purified water with conductivity adjusted to 50 µS/cm was used.

3.2.2.4. Transmission electronic microscopy analysis

EGCG-LN dispersions were analysed by transmission electronic microscopy (TEM). This technique is useful to analyse the shape and to confirm the size of LN dispersions. Samples were mounted on a grid and negative stained with a 2.0% (v/v) uranyl acetate solution. After drying at room temperature, the samples were examined using a TEM (Tecnai Spirit TEM, FEI) at 80 kV. The measurement of particles was analysed using Image J Software (Version 1.47).

3.2.2.5. Thermal analysis of lipid nanoparticles

The crystallinity profile of EGCG-LN was assessed by differential scanning calorimetry (DSC). The evaluation of the physical state affects the physicochemical properties and thermodynamic stability of LN dispersions, and thus DSC was used (Fangueiro, Gonzalez-Mira et al. 2013, Fangueiro, Andreani et al. 2014). A volume of LN dispersion corresponding to 1-2 mg of lipid was scanned using a Mettler DSC 823e System (Mettler Toledo, Spain). Heating and cooling runs were performed from 25ºC

to 90ºC and back to 25 ºC at a heating rate of 5 ºC/min, in sealed 40 µL aluminium pans. An empty pan was used as a reference. Indium (purity > 99.95 %; Fluka, Buchs, Switzerland) was employed for calibration purposes. DSC thermograms were recorded and DSC parameters including onset, melting point and enthalpy were evaluated using STAR^{e} Software (Mettler Toledo, Switzerland).

3.2.2.6. X-Ray studies

X-ray diffraction patterns were obtained using the x-ray scattering (X'Pert PRO, PANalytical) using a X´Celerator as a detector. Data of the scattered radiation were detected with a blend local-sensible detector using an anode voltage of 40 kV using a current of 30 mA. The samples were mounted on a standard sample holder being dried at room temperature without any previous sample treatment.

3.2.2.7. Stability analysis of lipid nanoparticles by TurbiscanLab®

The TurbiscanLab® is a technique that is based on the measurement of backscattering (BS) and transmission (T) signals. Its application is valuable for evaluate and detect possible processes of dispersions destabilization, giving also information of the type of destabilization. Destabilizations, that detect fluctuation on particle size and volume, are commonly derived from particle migration or sedimentation causing creaming and sedimentation on the dispersions. Particle size variation usually causes flocculation or coalescence. Both processes could be evaluated and can be classified as reversible and irreversible, respectively (Araújo, Vega et al. 2009, Celia, Trapasso et al. 2009, Fangueiro, Andreani et al. 2014).

The physical stability of LN dispersions obtained was assessed with an optical analyzer TurbiscanLab® (Formulaction, France). The dispersions were placed in a cylindrical glass cell, at room temperature (25±2.0°C). The equipment is composed of a near-infrared light source (λ = 880 nm), and 2 synchronous transmission (T) and backscattering (BS) detectors. The T detector receives the light crossing the sample, whereas the BS detector receives the light scattered backwards by the sample (Araújo,

Vega et al. 2009, Fangueiro, Andreani et al. 2014). The detection head scans the entire height of the sample cell (20mm longitude), acquiring T and BS each 40µm, 3 times during 10 min at different times after production (7, 15 and 30 days).

3.2.2.8. Encapsulation efficiency and loading capacity

Encapsulation efficiency (EE) and loading capacity (LC) of EGCG in LN was assessed indirectly by filtration/centrifugation technique, determining the free EGCG (non-encapsulated) by reverse-phase high-performance liquid chromatography (RP-HPLC). The HPLC method was previous validated (Fangueiro, Parra et al. 2014). A volume of 2.0 mL of each EGCG-LN was placed in centrifugal filter devices Ultracel 100K (100.000 MWCO, Amicon Millipore Corporation, Bedford, Massachusetts) to separate the lipid and aqueous phase and centrifuged at 3000 rpm, during 20 minutes (Sigma 4K10 centrifuge, Spain). Free EGCG present in the aqueous phase was quantified by RP-HPLC. The parameters were analysed by applying the following equations:

$$\text{EE (\%)} = \frac{Total\ amount\ of\ EGCG - Free\ EGCG}{Total\ amount\ of\ EGCG} X100 \quad \text{(Equation 1)}$$

$$\text{LC (\%)} = \frac{Total\ amount\ of\ EGCG - Free\ EGCG}{Total\ amount\ of\ lipid} X100 \quad \text{(Equation 2)}$$

3.2.2.9. Determination of osmolarity

The osmolarity of LN dispersions was analysed by freezing point depression (FPD) using a Micro-Osmometer (Advanced®Model 3320, Advanced Instruments, Inc., Country). The FPD is a technique used for aqueous solutions and operates by rapidly super cooling the sample to a predetermined temperature below the expected sample freezing point**.** This freezing point is the temperature (at atmospheric pressure) at which the solid and liquid phases will co-exist in equilibrium. When a solute is dissolved in a pure solvent, the colligative properties of the solvent usually change in direct proportion to the solute concentration. Measurement of the freezing point allows concentrations to

be determined with greatest precision owing to the inherent isolation of the sample from the environment by the iced blanket generated when the sample freezes (Koumantakis and Wyndham 1989). For the analysis, 20 µL of the sample was used without any pre-treatment. The sample was introduced in a sampler tip and placed in the cooling chamber. Three measurements were made for each sample.

3.2.2.10. Determination of pH

The final pH of LN dispersions was analysed in order to evaluate the possible effects that could lead to drug absorption and also to avoid eye irritation and damage (Araújo, Gonzalez et al. 2009). The determination of pH was carried out using a pH meter InoLab®pH Level 1 (WTW GmbH and Co., Germany). The pH meter was calibrated before each use with standard pH 4, 7 and 9.2 buffer solutions. The samples were used without any pre-treatment. 5.0 mL of sample was placed in a glass beaker and the pH was read at room temperature of 25 ± 1.0 °C for 3 minutes. Three measurements were made for each sample.

3.2.2.11. Determination of viscosity

Rheological properties of LN dispersions were analysed using the Bohlin Visco 88 Viscosimeter (Malvern Instruments, Malvern, UK). The samples were measured at two distinct temperatures: 25 ± 0.5 °C and 37.0 ± 0.5 °C. Samples measured at 37 ± 0.5 °C were thermostated by a circulating bath connected to the viscometer. The shear rate was maintained at 1207 s^{-1} during the analysis. The viscosity was determined from the flow curve obtained during 5 minutes of analysis at the same shear rate. The samples were set to equilibrium prior to each measurement. All measurements were made in triplicate.

3.2.2.12. Statistical analysis

Statistical evaluation of data was performed using Student's *t*-test with a 95% level of confidence, being a *p*-value < 0.05 accepted as significant. Data were expressed as the mean value ± standard deviation (Mean ± SD), usually from three independent experiments ($n = 3$).

3.2.3.Results and discussion

The produced blank-LNs were previously optimized by a factorial design and the choice of the percentage of cationic lipid was also investigated by the analysis of the physicochemical characteristics and cytotoxicity in an ocular line cell (Fangueiro, Andreani et al. 2014). Our previous study permitted the determination of the percentage of cationic lipid that could be safely used, and could provide better physicochemical properties and long-term stability of the developed LNs. In order to evaluate if the different cationic lipids affect LN properties, and eventually the biopharmaceutical behavior of cationic LNs, DDAB was one of the selected lipids to show the difference between a single chain cationic lipid with a lowest lipophilicity, and a double chain cationic lipid with a highest lipophilicity. CTAB is a single chain and single head-group cationic lipid that is often used as surfactant (Bhattacharya and Haldar 2004). Comparing to DDAB, CTAB revealed to be more toxic (Cortesi, Esposito et al. 1996). Both lipids are currently used for gene delivery purposes due to their cationic properties. In this study, their cationic properties were exploited to provide LN stability and mucoadhesion to the ocular surface.

The samples after cooling to room temperature were divided in two portions, which were stored separately at two different temperatures, room temperature (25 °C), and 4 ℃ (freezer), respectively. All samples were stored under dark conditions and showed a milky colloidal appearance, where no aggregation phenomena and no phase separation were detected during the period of analysis and storage. The evaluated parameters were the mean particle size (Z-Ave), polydispersity index (PI) and the zeta potential (ZP) by DLS (Table 3.2.2) during 30 days of storage. These could predict the stability of LNs during storage time and information about the storage conditions that these particles support. The results depicted in Table 3.2.2 revealed a tendency for increasing the particle size over time for all tested formulations. The maximum storage time analyzed was 30 days, and during this time the temperature of 4°C showed to be more susceptible towards particles' aggregation, since both parameters (Z-Ave and PI) increased in comparison to the production day. Similar results were detected for all formulations. This could be associated with the possibility of the existence of amorphous

acylglycerols in the liquid state and thus, the lipid matrix do not form a solid amorphous phase leading to polymorphic transitions during storage time (Sato 1988).

The encapsulation of EGCG in the blank-LNs were successfully shown by the maintenance of the nanometric size, relatively narrow size distribution and high positive surface charge observed by DLS measurements (Table 3.2.2). Student's *t*-test was performed with a 95% level of confidence, to check the differences before and after encapsulation of EGCG in LNs. Student's *t*-test analysis shows that Z-Ave and PI values were statically significant ($p < 0.05$) for EGCG-CTAB LN dispersions at both temperatures analysed, while the only statistical difference found for EGCG-DDAB LN dispersion was the ZP value at 4 °C. Thus, regarding the Z-Ave and PI, it was found that encapsulation of EGCG was greatly affected by the LNs based on CTAB rather than based on DDAB, which can be explained by the highest lipophilicity of DDAB being more enclosed within the lipid matrix than CTAB, therefore more localized in the aqueous phase leading to a high destabilization of the particles. On the other hand, the encapsulation of EGCG in DDAB dispersions affects the particles' stability, represented by the significance in the ZP value at low storage temperatures. The comparison between the two cationic EGCG dispersions were also evaluated by Student's *t*-test analysis which shows that Z-Ave and PI values were statically significant ($p < 0.05$) for storage temperature at 4 °C.

In this study, nanoparticle aggregation was accelerated by low storage temperatures (Table 3.2.2). Other previous studies (Freitas and Müller 1998) also reported similar results and the reason could imply the destabilization of LN dispersions as a consequence of kinetic energy input to a level above the critical point that would favor their collision. In addition, it is proven that higher temperatures increase the kinetics of a system, in combination with a reduction on the value of ZP leading to LN aggregation and gelation (Freitas and Müller 1998). Student's *t*-test was performed with a 95% level of confidence, to test whether the differences between the two storage temperatures applied for each cationic lipid used in the lipid matrix of LN dispersions were statistically significant. Student's *t*-test analysis shows that Z-Ave and PI values were statically significant ($p < 0.05$) for CTAB-LN dispersions. On the other hand, DDAB-

LN dispersions show no statistical significance for the three parameters evaluated. Thus, it seems that the temperature of storage affects significantly the CTAB-LN dispersions than DDAB-LN dispersions.

All samples present a decrease in the value of ZP, being the lower temperature (4°C) more evident than the higher temperature analyzed (25 °C) (Table 3.2.2). This proves that steric stabilization is affected at lower temperatures promoting physically stabilization of LN dispersions. The large lipid particles can approach each other due to the loss of electrostatic repulsion and form a network, possibly promoted by the stabilizer (gel formation properties of poloxamer, the hydrophilic surfactant used for LN dispersions). The change in zeta potential indicates structural changes explained by the crystalline structure of the lipid. A probably crystalline re-orientation on the lipids occurs by the changes of the particles surface charge (Nernst potential) (Sato 1988).

As previously reported in our study (Fangueiro, Andreani et al. 2014) the use of EGCG dispersions based on cationic particles was use to improve LNs stability and mucoadhesion to ocular surface. A major stability can be reach by higher ZP values, which leads to electronic repulsion between particles and maintaining longer time in suspension. Student's t-test analysis show no statistical differences for ZP value between the two cationic lipids used as also for the EGCG dispersions.

Despite the increase on Z-Ave and PI and decrease on ZP, all the measurements during storage time over 30 days comprise the nanometer range, narrow size distribution (PI < 0.3) and a cationic nature of the formulations (positive ZP) for the storage temperature of 25 °C. In the case of storage time at 4 °C, the results are similar; however the PI exceeded the acceptable values, which could lead to problems during instillation onto the ocular mucosa, namely irritation and possible inflammation. Thus, the LNs developed seems to be temperature-dependent respecting the particles' stability, which suggests that storage temperature of 4 °C leads to aggregation/flocculation phenomena.

Table 3.2.2. Mean particle size (Z-Ave), polydispersity index (PI) and zeta potential (ZP) analysis of LNs dispersions, monitored for 30 days at 4°C and 25°C. The results are expressed as mean± S.D. (n = *3*).

Formulation	T (°C)	Parameters	Day 0	Day 7	Day 15	Day 30
CTAB-LN	**4**	Z-Ave (nm)	135.1 ± 0.22	158.3 ± 0.20	159.6 ± 1.42	163.8 ± 0.72
		PI	0.196 ± 0.018	0.201 ± 0.012	0.205 ± 0.004	0.231 ± 0.009
		ZP (mV)	28.2 ± 1.33	27.6 ± 1.73	23.9 ± 1.97	19.3 ± 2.11
	25	Z-Ave (nm)	115.1 ± 0.29	121.7 ± 0.50	126.8 ± 1.66	124.8 ± 0.81
		PI	0.158 ± 0.013	0.170 ± 0.014	0.185 ± 0.003	0.170 ± 0.008
		ZP (mV)	28.7 ± 1.78	27.8 ± 2.45	23.5 ± 2.07	19.8 ± 1.50
EGCG CTAB-LN	**4**	Z-Ave (nm)	183.9 ± 0.66	187.2 ± 3.60	181.6 ± 2.75	199.2 ± 1.35
		PI	0.298 ± 0.029	0.300 ± 0.026	0.363 ± 0.012	0.365 ± 0.022
		ZP (mV)	28.8 ± 0.89	17.9 ± 1.42	19.8 ± 3.50	17.5 ± 2.40
	25	Z-Ave (nm)	149.1 ± 1.78	145.9 ± 1.28	138.2 ± 1.26	144.9 ± 1.63
		PI	0.240 ± 0.008	0.222 ± 0.011	0.239 ± 0.006	0.233 ± 0.012
		ZP (mV)	20.8 ± 0.89	26.3 ± 1.76	24.0 ± 1.36	22.7 ± 2.38
DDAB-LN	**4**	Z-Ave (nm)	134.2 ± 1.12	150.7 ± 1.53	159.3 ± 0.18	239.8 ± 3.06
		PI	0.179 ± 0.067	0.181 ± 0.011	0.197 ± 0.021	0.297 ± 0.004
		ZP (mV)	28.2 ± 2.29	29.5 ± 2.94	27.9 ± 2.36	23.7 ± 2.38
	25	Z-Ave (nm)	154.8 ± 1.53	158.7 ± 1.14	157.5 ± 0.78	164.2 ± 1.77

	PI	0.159 ± 0.022	0.141 ± 0.015	0.196 ± 0.017	0.201 ± 0.001
	ZP (mV)	25.2 ± 2.29	26.5 ± 1.98	25.6 ± 1.79	22.8 ± 2.98
EGCG DDAB-LN	Z-Ave (nm)	155.4 ± 1.16	156.7 ± 0.95	160.0 ± 2.89	178.2 ± 0.89
4	PI	0.190 ± 0.013	0.205 ± 0.016	0.214 ± 0.012	0.221 ± 0.013
	ZP (mV)	25.4 ± 1.42	16.4 ± 3.20	15.0 ± 0.66	14.2 ± 2.75
	Z-Ave (nm)	143.7 ± 0.45	147.1 ± 1.70	186.1 ± 5.01	203.7 ± 2.30
25	PI	0.160 ± 0.015	0.169 ± 0.009	0.274 ± 0.006	0.299 ± 0.006
	ZP (mV)	25.7 ± 1.42	20.7 ± 1.70	18.5 ± 2.72	17.7 ± 1.42

TEM analysis has been performed to evaluate the particle shape and morphology of EGCG-LN dispersions. TEM micrographs are depicted in Figure 3.2.1. From this analysis, no aggregation of particles or presence of drug crystals was detected. The majority of particles showed a spherical shape. It was possible to detect a slight polydispersity however all the particles remained within the nanometer range, i.e., all particles were lower than 1 μm. This is in agreement with other authors (Zimmer and Kreuter 1995, Shekunov, Chattopadhyay et al. 2007) for the limits for ocular drug delivery, in order to avoid eye irritation or damage. EGCG-CTAB LN dispersion (Figure 3.2.1A)) presents particles with a mean diameter varying from 90 to 300 nm and EGCG-DDAB LN dispersions (Figure 3.2.1B)) presents particles between 130 and 380 nm. These results are in agreement with DLS measurements (Table 3.2.2) which detect smaller particles for the EGCG-LN dispersion composed of CTAB than the particles composed of DDAB.

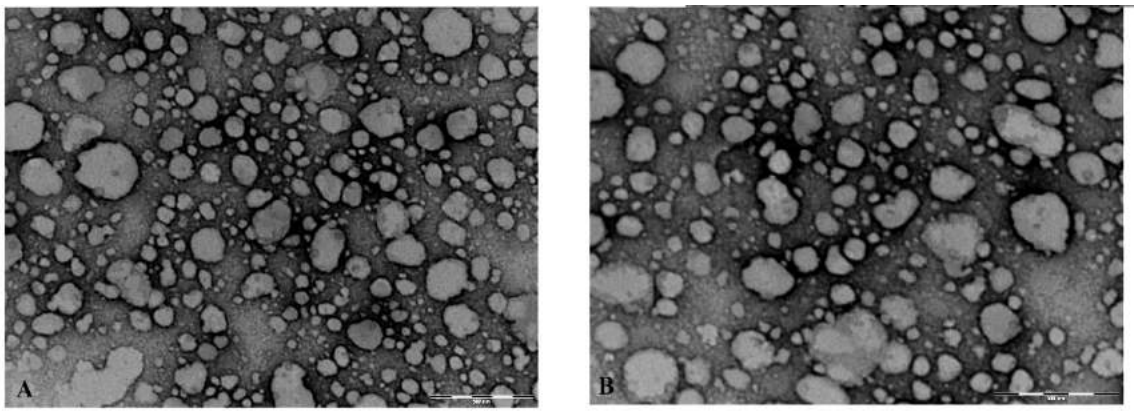

Figure 3.2.1. TEM micrographs of A) EGCG-CTAB LNs and B) EGCG-DDAB LN dispersions.

DSC and X-Ray studies were performed to evaluate the physical state of the LN dispersions developed and the polymorphic behavior of the particles' matrices. The solid lipid used was S100, a triacylglycerol blend of vegetable fatty acids with C10-C18 (Fangueiro, Gonzalez-Mira et al. 2013, Fangueiro, Andreani et al. 2014). For this study, only this solid lipid was used to compare with the LN dispersions. The cationic lipids

were not analyzed given the high temperatures required for these testings (> 100 °C), which promote disruption of the particles by removing the internal water from the double emulsion system, where the drug is encapsulated. Typically, complex triacylglycerol mixtures present a lower supercooling tendency in colloidal state. This leads to the conclusion that the longer-chain fraction acts as nucleation center and thus induces crystallization of the supercooled triacylglycerol already at higher temperatures (Westesen, Bunjes et al. 1997, Bunjes, Drechsler et al. 2001). The addition of other compounds, such as drugs, can also influence the supercooling tendency (Bunjes, Drechsler et al. 2001). Triacylglycerols usually occur in three major polymorphic forms, namely α, β` and β (in order of increasing thermodynamic stability). The β` modification is frequently observed in complex triacylglycerols such as S100 (Bunjes and Unruh 2007, Fangueiro, Andreani et al. 2014). Thermal analysis of the bulk lipid S100 (Figure 3.2.2a)) shows a single endothermic peak upon heating with a minimum of 39.12°C and an enthalpy of −44.76 Jg^{-1} (Table 3.2.3). According with our previous work (Fangueiro, Andreani et al. 2014), this is reported as a β` modification typically found in complex triacylglycerols mixtures as S100. For the LN dispersions, a single endothermic peak was also recorded, however it is noteworthy that the enthalpy event is lower than in the bulk lipid (Figure 3.2.2 and Table 3.2.3). Additionally, all LN dispersions presented a peak with a lower melting point than the bulk lipid (Table 3.2.3), which is expected for dispersions composed by triacylglycerols (Sato 1988).

Comparing the dispersions with distinct cationic lipids, the LN dispersion composed by CTAB presents more crystallinity than the dispersion composed by DDAB (enthalpy of - 1.17 Jg^{-1} versus - 0.52 Jg^{-1}, respectively, Table 3.2.3). Both cationic lipids present crystallinity profile according with X-.ray studies (Figure 3.2.3c) and 3.2.3d)). This behavior could be due not only to the different lipophilicity but also to the different chemical structure, i.e. DDAB has an aliphatic double chain directly linked to the amine and CTAB as a single chain. This could determine different packing of the surfactant molecules at the interface between the oil phase and the external aqueous phase leading to nanoparticles with a different crystallinity profile (Carbone, Tomasello et al. 2012). Results from X-Ray and DSC studies suggest that different interactions occurred

between the selected cationic lipid and the oil phase components, namely the solid lipid S100 and the lipophilic surfactant lecithin and also with the external aqueous phase.

Table 3.2.3. Differential scanning calorimetry (DSC) analysis of the LNs dispersions developed and the bulk lipid S100.

Formulation	Onset temperature (°C)	Melting point (°C)	Integral (mJ)	Enthalpy (Jg^{-1})
S100 bulk	36.68	39.12	–3111.15	–44.76
CTAB-LN	31.26	35.03	–116.43	–1.47
EGCG-CTAB LN	28.25	33.50	–39.05	–0.55
DDAB-LN	27.60	34.90	–39.09	–0.52
EGCG-DDAB LN	28.13	34.83	–56.05	–0.73

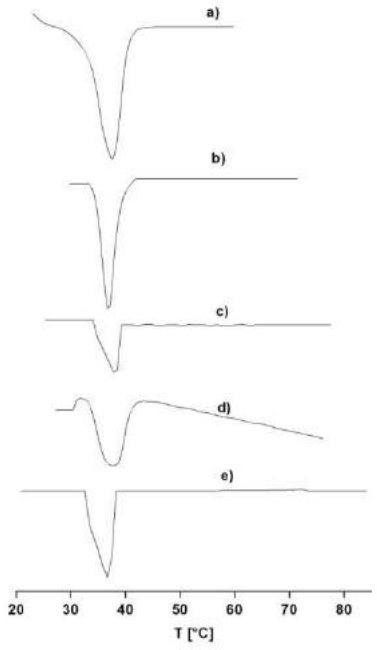

Figure 3.2.2. DSC thermograms of a) bulk CTAB, b) CTAB-LN, c) EGCG-CTAB LN , d) DDAB-LN, and e) EGCG-DDAB LN.

With respect to the encapsulation of the drug, EGCG, CTAB-LN suffers a decrease in the required enthalpy for the endothermic process, i.e. decreases from - 1.17 Jg^{-1} to - 0.55 Jg^{-1} (Table 3.2.3). A contrary fact was evaluated for the EGCG-DDAB LN where the required enthalpy was higher in the presence of the drug than in the blank DDAB particles. In this case, the enthalpy required increase from - 0.52 Jg^{-1} to - 0.73 Jg^{-1} (Table 3.2.3).

In order to complete the study regarding LNs crystallinity and polymorphism, X-ray studies were carried out for the bulks and LNs. Figure 3.2.3 depicts the bulk materials for the development of the LN dispersions. It is noteworthy the crystallinity profile for the lipids, Softisan®100 (Figure 3.2.3b)), CTAB (Figure 3.2.3c)) and DDAB (Figure 3.2.3d)). The drug EGCG also presents a crystallinity profile (Figure 3.2.3a)). EGCG depicted two well defined signals, one at 2Θ≈15.0° and the other at 2Θ ≈20.0°.

X-ray results for S100 are in agreement with our previous results (Fangueiro, Andreani et al. 2014), revealing the presence of two signals, one at 0.42 nm (2Θ =21.1°) and other at 0.38 nm (2Θ =23.2°), which are both characteristic of the orthorhombic perpendicular subcell, i.e., β´ modification (Schubert and Müller-Goymann 2003). Four strong diffraction peaks between 2Θ = 15.0° and 2Θ = 27.0° are the diffraction peaks of the crystal structure of CTAB (Figure 3.2.3c)). DDAB crystal structure showed several diffraction peaks between 2Θ = 15.0° and 2Θ = 30.0°. These cationic lipids were previous reported to present a lamellar phase structure. The basal spacings between CTAB and DDAB are much wider than that of S100 since the alkyl chains of CTAB and DDAB are much longer.

The cationic LN dispersions presented diffraction peaks similar to S100 bulk, indicating a β´ modification, as the bulk material. The basal spacings of EGCG-CTAB and EGCG-DDAB are proximally equals. These results indicate that the basal spacings of the LN dispersions are greatly influenced by the length of the alkyl chain and by volume of the cationic lipid used (Meguedad and Benharrats 2012). Thus, from DSC and X-ray studies, is possible to detect a higher crystallinity of CTAB-LN dispersion than the DDAB-LN dispersion. Additionally, the encapsulation of EGCG also provides higher crystallinity to LN dispersions, being more detectable for CTAB-LN dispersion.

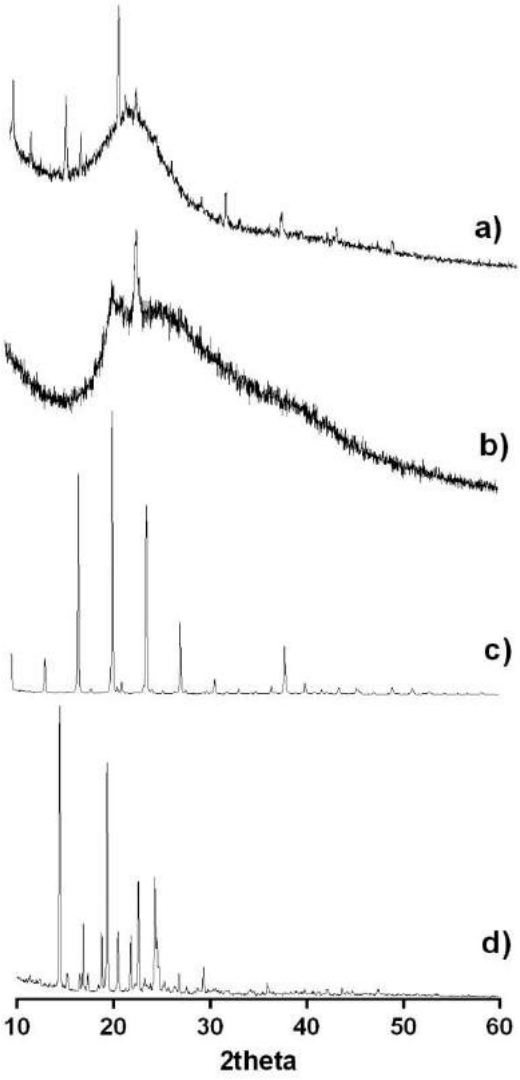

Figure 3.2.3. **X**-ray diffraction patterns of the drug and the bulks that compose the lipid matrix, namely a) EGCG, b) S100, c) CTAB and d) DDAB.

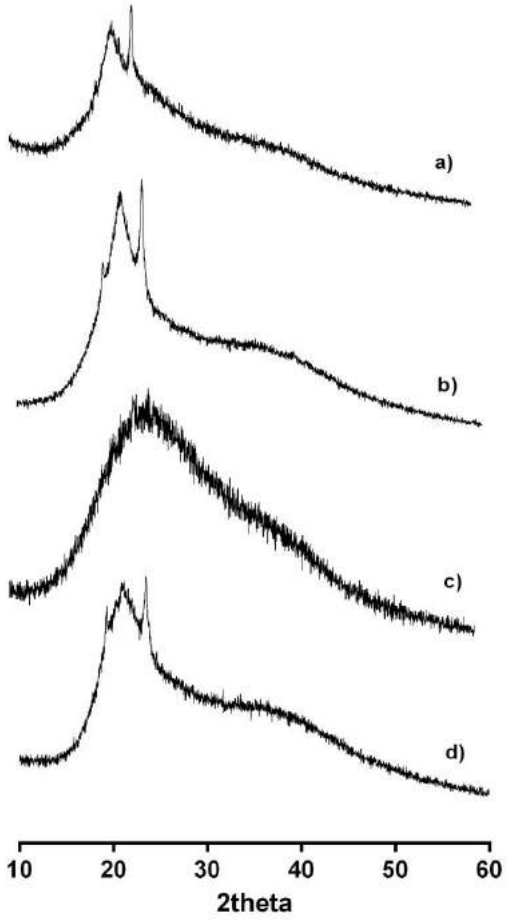

Figure 3.2.4. **X**-ray diffraction patterns of the cationic LNs dispersions a) DDAB-LN, b) EGCG-DDAB LN, c) CTAB-LN, d) EGCG-CTAB LN.

The physical stability of LN dispersions is one of the major concerns for the final product characteristics. LNs are heterogeneous systems and thermodynamically unstable, and therefore, they have a significant tendency to lose physical stability during storage (Souto and Muller 2010, Araujo, Nikolic et al. 2011). Techniques, such as microscopy, spectroscopy, turbidity and particle size analysis, are used to detect destabilization in nanoparticulate systems. However, Turbiscan® Lab analysis could detect physical destabilization much earlier and faster than these techniques mentioned (Mengual, Meunier et al. 1999). The analysis of the stability of the LN dispersions is depicted in Figure 3.2.5. The modification of a BS signal can occur as a function of time and particle migration and is graphically reported in the form of positive (BS increase) or negative peaks (BS decrease). Namely, the migration of particles from the bottom to

the top of a sample leads to a progressive concentration decrease at the bottom of the sample and as a consequence a decrease in the BS signal (negative peak) and an increase in the intensity of the T (positive peak) (Araujo, Nikolic et al. 2011, Fangueiro, Andreani et al. 2014). The opposite is true at the top of the sample. If the BS profiles have a deviation of ≤ ± 2% it can be considered that there are no significant variations in particle size. Variations up to ± 10% indicate unstable formulations (Araújo, Vega et al. 2009, Celia, Trapasso et al. 2009).

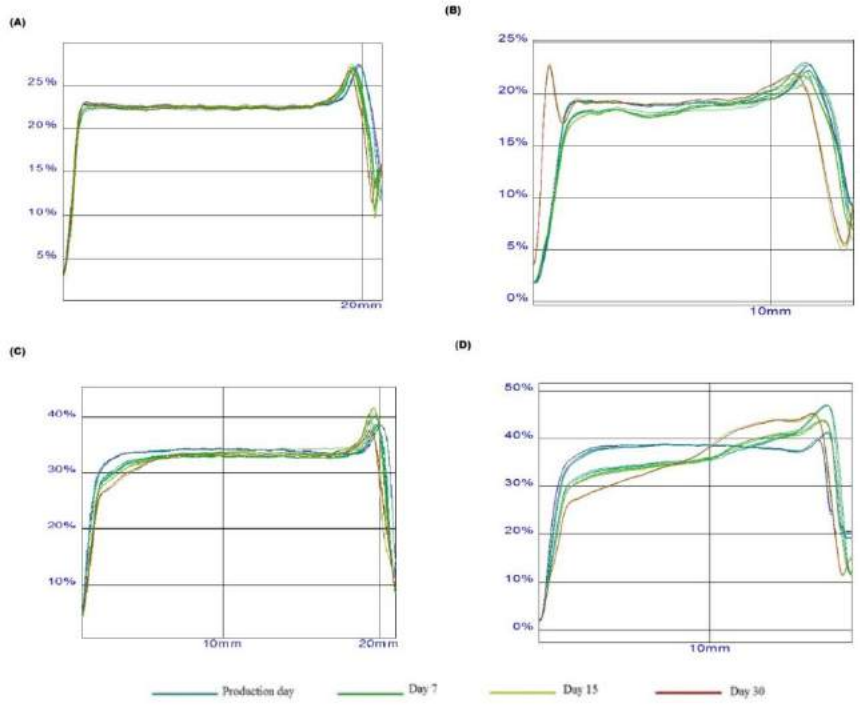

Figure 3.2.5. BS profiles of LNs dispersions, (a) CTAB-LNs, (b) CTAB-EGCG LNs, (c) DDAB-LNs and (d) EGCG-DDAB LNs, measured across the height of the sample cell for 10 min, on the production day, and on day 7, day 15 and day 30 after the production (n = 3).

From the results depicted in Figure 3.2.5, it is possible to detect higher instability in the formulations encapsulating EGCG. The blank LN dispersions (Figure 3.2.5a) and 3.2.5c)) showed less variations on BS and T signals, showing variations lower than 10% during the time of analysis. The cationic EGCG-LN dispersions, shows a higher variation on BS and T signals, being more detectable for the EGCG-DDAB LN

dispersion (Figure 3.2.5d)). This variation is higher than 10%, indicating a variation on particle size during storage time resulting from flocculation (top of the cell) and sedimentation/aggregation (bottom of the cell) phenomena. These results indicate that CTAB provide higher stability than DDAB on EGCG-LN dispersions, indicating an influence in the type of cationic lipid used. These results are in agreement with the DLS results recorded for the LN dispersions (Table 3.2.2). As mentioned before, the values of ZP of the dispersions decreased during storage time, which leads to a lower stability and capacity of the particles remains in suspension. Additionally, it is noteworthy that particle size also increases during storage time, which is confirmed by Turbiscan results by the variations on BS signal, however only the EGCG-DDAB LN showed significant variations (>10%).

The EE of EGCG was high in both LN dispersions. For the CTAB-LN dispersions the EE was 98.99 ± 0.19% and for DDAB-LN dispersions was 96.86 ± 1.88% (Table 3.2.4). EGCG is a hydrophilic drug which was encapsulated in the inner aqueous phase of LN dispersions based on the double emulsion technology. Usually, hydrophilic drugs have tendency to diffuse from the inner aqueous phase to the external aqueous phase. This event is undesirable due to the incapacity of the lipid layer entraps and protects the drug diffusion and leads to future degradation, especially for products such as catechins. A high EE was achieved for both LN dispersions, regardless of the difference in the cationic lipid used. The LC of LN dispersions was 14.85 ± 0.19% and 14.53 ± 1.88%, respectively for CTAB and DDAB-LN dispersions (Table 3.2.4).

Table 3.2.4. EE and LC of the cationic EGCG-LNs dispersions. The results are expressed as mean± S.D. (*n = 3*).

	EE (%)	**LC (%)**
EGCG-CTAB LN	98.99 ± 0.19	14.85 ± 0.19
EGCG-DDAB LN	96.86 ± 1.88	14.53 ± 1.88

The administration of pharmaceutical formulations onto the ocular surface requires the maintenance of tear film's health and function. The adequate production, retention, and balanced elimination of tears are necessary for this process. The disequilibrium of any of these functions could lead to biophysical and biochemical imbalances that affects

osmolarity (Tomlinson, Khanal et al. 2006). In the normal eye, the tear fluid osmolarity varies from 302 to 350 mOsm/kg. Its buffering ability is determined by bicarbonate ions, proteins and mucins. This is an important parameter that needs to be supervised in all ocular formulations to avoid ocular complications. When hypertonic solutions are applied to the eye, water flow passes from the aqueous layer through the cornea to the eye surface; whereas in the case of hypotonic solution, the permeability of the epithelium is increased considerably and water flows into the cornea (Reddy and Ganesan 1995). The drug uptake by the cornea also depends on viscosity of the vehicle, pH, and osmolarity. The evaluation of the osmolarity of LN dispersions showed the following values: 383.33 ± 1.15 mOsm/kg for EGCG-CTAB LN and 366.67 ± 1.15 mOsm/kg for EGCG-DDAB LN (Table 3.2.5). According to (Reddy and Ganesan 1995) ocular solutions which produce osmolarity lower than 266 mOsm/Kg or higher than 640 mOsm/kg are irritating to the eye. Thus, the EGCG-LN dispersions developed showed to be in the interval range, which avoid irritation and possible inflammation of the eye.

The pH of the final dispersions was also evaluated. This is also an important factor in the development of ocular formulations. The average pH of the ocular mucosa is around 7.2-7.4, however due to the buffer capacity of the tear film, eyes can tolerate pH of 6.5-8.0 without much discomfort (Ahuja, Singh et al. 2008). The evaluation of both EGCG-loaded LN dispersions presented a tolerable pH for human eye, namely 7.2-7.5 (Table 3.2.5).

Table 3.2.5. Evaluation of the osmolality, final pH and viscosity at two different temperatures of EGCG-LNs dispersions developed. The results are expressed as mean± S.D. (*n = 3*).

Formulation	Osmolality (mOsm/kg)	Final pH	Viscosity (mPas)	
			25.0 ± 0.5 °C	**37.0 ± 0.5 °C**
EGCG-CTAB LN	383.33 ± 1.15	7.2 ± 0.7	6.76 ± 0.0001	5.60 ± 0.0001
EGCG-DDAB LN	366.67 ± 1.15	7.5 ± 0.2	6.67 ± 0.0001	5.20 ± 0.0001

Regarding the viscosity of the EGCG-LN dispersions, is also an important physicochemical factor that should be evaluated prior to biological *in vivo* tests. Usually, human eye viscosity is ~3.00 mPas, with a non-Newtonian rheological behavior (Zambito and Di Colo 2011). The viscosity of the LN dispersions was analysed at two temperatures, at 25.0 ± 0.5 °C, which is the best storage temperature and at 37.0 ± 0.5 °C, the *in vivo* temperature of ocular mucosa. The evaluation of the temperature effect in the viscosity of the systems (Table 3.2.5) showed a decrease of viscosity with an increase of temperature from 25 to 37.0 ± 0.5 °C. The behavior of LN dispersions showed that the viscosity decreases with increasing temperature. Overall, both LN dispersions presented a low viscosity which do not compromises ocular delivery. The evaluation of viscosity is a parameter that should comprise the formulation and stability studies of the dispersions developed.

3.2.4.Conclusions

Although significant progress has been made, ocular drug delivery still is a main challenge. The physiological protective mechanisms in the eye in combination with the anatomical barrier prevent the free access of the foreign substances, including drugs, to inner eye. Cationic EGCG-LN dispersions were successfully produced and investigated, being all parameters that could affect their bioavailability and physical stability analysed. The data provided by the stability studies show that lower temperature has an important role to play. LN dispersions kept at 25 °C revealed higher stability comparing with those stored at 4 °C. In both cases, the size was kept in the nanometric range during time of analysis. The DSC and X-ray studies proved that different cationic lipids provide different crystallinity profiles. In this study, DDAB shows higher crystallinity than CTAB-LN dispersions. The encapsulation of EGCG in the inner aqueous phase of double emulsion also affected the crystal structure of LN dispersions, contributing to a decrease in the degree of crystallinity to CTAB and an increase for DDAB, respectively.

The results obtained from this study evidence the possibility of lipid based systems for EGCG ocular drug delivery, making these nanoparticles a promising approach to avoid drug stability problems and to provide a selective and prolonged drug concentration of EGCG in the eye.

3.2.5. Bibliographic references

Ahmed, S., Pakozdi, A., and Koch, A. E. (2006). Regulation of interleukin-1β–induced chemokine production and matrix metalloproteinase 2 activation by epigallocatechin-3-gallate in rheumatoid arthritis synovial fibroblasts. *Arthritis and Rheumatism,* 54(8), 2393-2401.

Ahuja, M., Singh, G., and Majumdar, D. K. (2008). Effect of Formulation Parameters on Corneal Permeability of Ofloxacin. *Scientia Pharmaceutica*, 76, 505-514.

Araújo, J., Gonzalez, E., Egea, M. A., Garcia, M. L., and Souto, E. B. (2009a). Nanomedicines for ocular NSAIDs: safety on drug delivery. *Nanomedicine : nanotechnology, biology, and medicine,* 5(4), 394-401.

Araujo, J., Nikolic, S., Egea, M. A., Souto, E. B., and Garcia, M. L. (2011). Nanostructured lipid carriers for triamcinolone acetonide delivery to the posterior segment of the eye. *Colloids and Surfaces B: Biointerfaces,* 88(1), 150-157.

Araújo, J., Vega, E., Lopes, C., Egea, M. A., Garcia, M. L., and Souto, E. B. (2009b). Effect of polymer viscosity on physicochemical properties and ocular tolerance of FB-loaded PLGA nanospheres. *Colloids and Surfaces B: Biointerfaces,* 72(1), 48-56.

Arts, I. C., and Hollman, P. C. (2005). Polyphenols and disease risk in epidemiologic studies. *American Journal of Clinical Nutrition,* 81(1 Suppl), 317s-325s.

Bhattacharya, S., and Haldar, J. (2004). Thermodynamics of micellization of multiheaded single-chain cationic surfactants. *Langmuir,* 20(19), 7940-7947.

Bunjes, H., Drechsler, M., Koch, M. H. J., and Westesen, K. (2001). Incorporation of the model drug ubidecarenone into solid lipid nanoparticles. *Pharmaceutical Research,* 18, 287-293.

Bunjes, H., and Unruh, T. (2007). Characterization of lipid nanoparticles by differential scanning calorimetry, X-ray and neutron scattering. *Advanced Drug Delivery Reviews, 59*(6), 379-402.

Carbone, C., Tomasello, B., Ruozi, B., Renis, M., and Puglisi, G. (2012). Preparation and optimization of PIT solid lipid nanoparticles via statistical factorial design. *European Journal* of *Medicinal Chemistry,* 49, 110-117.

Cavet, M. E., Harrington, K. L., Vollmer, T. R., Ward, K. W., and Zhang, J. Z. (2011). Anti-inflammatory and anti-oxidative effects of the green tea polyphenol epigallocatechin gallate in human corneal epithelial cells. *Molecular Vision, 17,* 533-542.

Celia, C., Trapasso, E., Cosco, D., Paolino, D., and Fresta, M. (2009). Turbiscan lab expert analysis of the stability of ethosomes and ultradeformable liposomes containing a bilayer fluidizing agent. *Colloids and Surfaces B: Biointerfaces,* 72(1), 155-160.

Cortesi, R., Esposito, E., Menegatti, E., Gambari, R., and Nastruzzi, C. (1996). Effect of cationic liposome composition on in vitro cytotoxicity and protective effect on carried DNA. *International Journal of Pharmaceutics,* 139(1–2), 69-78.

del Pozo-Rodríguez, A., Delgado, D., Solinís, M. A., Gascón, A. R., and Pedraz, J. L. (2008). Solid lipid nanoparticles for retinal gene therapy: Transfection and intracellular trafficking in RPE cells. *International Journal of Pharmaceutics,* 360(1–2), 177-183.

Fang, Z., and Bhandari, B. (2010). Encapsulation of polyphenols – a review. *Trends in Food Science and Technology,* 21(10), 510-523.

Fangueiro, J. F., Andreani, T., Egea, M. A., Garcia, M. L., Souto, S. B., Silva, A. M., and Souto, E. B. (2014a). Design of cationic lipid nanoparticles for ocular delivery: Development, characterization and cytotoxicity. *International Journal of Pharmaceutics, 461*(1-2), 64-73.

Fangueiro, J. F., Gonzalez-Mira, E., Martins-Lopes, P., Egea, M. A., Garcia, M. L., Souto, S. B., and Souto, E. B. (2013). A novel lipid nanocarrier for insulin delivery: production, characterization and toxicity testing. *Pharmaceutical Development and Technology,* 18(3), 545-549.

Fangueiro, J. F., Parra, A., Silva, A. M., Souto, E. B., Garcia, M. L., and Calpena, A. C. (2014b). Validation of a high performance liquid chromatography method for the stabilization of epigallocatechin gallate. *International Journal of Pharmaceutics*, 475(1-2), 181-190.

Freitas, C., and Müller, R. H. (1998). Effect of light and temperature on zeta potential and physical stability in solid lipid nanoparticle (SLN™) dispersions. *International Journal of Pharmaceutics,* 168(2), 221-229.

Gu, J. W., Makey, K. L., Tucker, K. B., Chinchar, E., Mao, X., Pei, I., Miele, L. (2013). EGCG, a major green tea catechin suppresses breast tumor angiogenesis and growth via inhibiting the activation of HIF-1alpha and NFkappaB, and VEGF expression. *Vascular Cell,* 5(1), 9.

Heim, K. E., Tagliaferro, A. R., and Bobilya, D. J. (2002). Flavonoid antioxidants: chemistry, metabolism and structure-activity relationships. *Journal of Nutritional Biochemistry,* 13(10), 572-584.

Koumantakis, G., and Wyndham, L. E. (1989). An evaluation of osmolality measurement by freezing point depression using micro-amounts of sample. *Journal of Automatic Chemistry,* 11(2), 80-83.

Li, M., Liu, J. T., Pang, X. M., Han, C. J., and Mao, J. J. (2012). Epigallocatechin-3-gallate inhibits angiotensin II and interleukin-6-induced C-reactive protein production in macrophages. *Pharmacological Reports,* 64(4), 912-918.

Mähler, A., Mandel, S., Lorenz, M., Ruegg, U., Wanker, E., Boschmann, M., and Paul, F. (2013). Epigallocatechin-3-gallate: a useful, effective and safe clinical approach for targeted prevention and individualised treatment of neurological diseases? *The European Association for Predictive, Preventive and Personalized Medicine Journal*, 4(1), 1-17.

Manach, C., Scalbert, A., Morand, C., Remesy, C., and Jimenez, L. (2004). Polyphenols: food sources and bioavailability. *American Journal of Clinical Nutrition*, 79(5), 727-747.

Manach, C., Williamson, G., Morand, C., Scalbert, A., and Remesy, C. (2005). Bioavailability and bioefficacy of polyphenols in humans. I. Review of 97 bioavailability studies. *American Journal of Clinical Nutrition*, 81(1 Suppl), 230s-242s.

Mandel, S., Weinreb, O., Amit, T., and Youdim, M. B. (2004). Cell signaling pathways in the neuroprotective actions of the green tea polyphenol (-)-epigallocatechin-3-gallate: implications for neurodegenerative diseases. *Journal of Neurochemistry*, 88(6), 1555-1569.

Meguedad, A., and Benharrats, N. (2012). Thermal Degradation Behavior of Polythiophene-modified Montmorillonite Nanocomposite. *Journal of Analytical Science and Technology*, 3(2), 193-201.

Mengual, O., Meunier, G., Cayré, I., Puech, K., and Snabre, P. (1999). TURBISCAN MA 2000: multiple light scattering measurement for concentrated emulsion and suspension instability analysis. *Talanta*, 50(2), 445-456.

Morinobu, A., Biao, W., Tanaka, S., Horiuchi, M., Jun, L., Tsuji, G., . . . Kumagai, S. (2008). (-)-Epigallocatechin-3-gallate suppresses osteoclast differentiation and ameliorates experimental arthritis in mice. *Arthritis & Rheumatology*, 58(7), 2012-2018.

Reddy, I. K., and Ganesan, M. G. (1995). Ocular Therapeutics and Drug Delivery: An Overview. In I. K. Reddy (Ed.), *Ocular Theraputics and Drug Delivery* (pp. 3-23). Pennsylvania, USA: Technomic Publishing Company, Inc.

Riegsecker, S., Wiczynski, D., Kaplan, M. J., and Ahmed, S. (2013). Potential benefits of green tea polyphenol EGCG in the prevention and treatment of vascular inflammation in rheumatoid arthritis. *Life Sciences*, 93(8), 307-312.

Roghani, M., and Baluchnejadmojarad, T. (2010). Hypoglycemic and hypolipidemic effect and antioxidant activity of chronic epigallocatechin-gallate in streptozotocin-diabetic rats. *Pathophysiology*, 17(1), 55-59.

Sato, K. (1988). Crystallization of fats and fatty acids. In N. Garti and K. Sato (Eds.), *Crystallisation and Polymorphism of Fats and Fatty Acids* (pp. 227-262). New York: Marcel Dekker

Schubert, M. A., and Müller-Goymann, C. C. (2003). Solvent injection as a new approach for manufacturing lipid nanoparticles – evaluation of the method and process parameters. *European Journal of Pharmaceutical Sciences,* 55(1), 125-131.

Sen, T., Moulik, S., Dutta, A., Choudhury, P. R., Banerji, A., Das, S., Chatterjee, A. (2009). Multifunctional effect of epigallocatechin-3-gallate (EGCG) in downregulation of gelatinase-A (MMP-2) in human breast cancer cell line MCF-7. *Life Sciences,* 84(7–8), 194-204.

Seyfoddin, A., Shaw, J., and Al-Kassas, R. (2010). Solid lipid nanoparticles for ocular drug delivery. *Drug Delivery,* 17(7), 467-489.

Shekunov, B. Y., Chattopadhyay, P., Tong, H. Y., and Chow, A. H. L. (2007). Particle Size Analysis in Pharmaceutics: Principles, Methods and Applications. *Pharmaceutical Research,* 24(2), 203-227.

Song, E.-K., Hur, H., and Han, M.-K. (2003). Epigallocatechin gallate prevents autoimmune diabetes induced by multiple low doses of streptozotocin in mice. *Archives of Pharmacal Research,* 26(7), 559-563.

Souto, E. B., Fangueiro, J. F., and Müller, R. H. (2013). Solid Lipid Nanoparticles (SLN™). In I. F. Uchegbu, A. G. Schätzlein, W. P. Cheng and A. Lalatsa (Eds.), *Fundamentals of Pharmaceutical Nanoscience* (pp. 91-116): Springer New York.

Souto, E. B., and Muller, R. H. (2010). Lipid nanoparticles: effect on bioavailability and pharmacokinetic changes. *Handbookk of Experimental Pharmacology* (197), 115-141.

Surh, Y. J. (2003). Cancer chemoprevention with dietary phytochemicals. *Nature Reviews Cancer,* 3(10), 768-780.

Tomlinson, A., Khanal, S., Ramaesh, K., Diaper, C., and McFadyen, A. (2006). Tear film osmolarity: determination of a referent for dry eye diagnosis. *Investigative Ophthalmology & Visual Science,* 47(10), 4309-4315.

Vali, B., Rao, L. G., and El-Sohemy, A. (2007). Epigallocatechin-3-gallate increases the formation of mineralized bone nodules by human osteoblast-like cells. *Journal of Nutricional Biochemistry,* 18(5), 341-347.

Weinreb, O., Amit, T., Mandel, S., and Youdim, M. B. (2009). Neuroprotective molecular mechanisms of (-)-epigallocatechin-3-gallate: a reflective outcome of its antioxidant, iron chelating and neuritogenic properties. *Genes & Nutrition,* 4(4), 283-296.

Westesen, K., Bunjes, H., and Koch, M. H. J. (1997). Physicochemical characterization of lipid nanoparticles and evaluation of their drug loading capacity and sustained release potential. *Journal of Controlled Release,* 48 (2-3), 223-236.

Zambito, Y., and Di Colo, G. (2011). Polysaccharides as Excipients for Ocular Topical Formulations,. In P. R. Pignatello (Ed.), *Biomaterials Applications for Nanomedicine* (pp. 253-280).

Zhang, B., and Osborne, N. N. (2006). Oxidative-induced retinal degeneration is attenuated by epigallocatechin gallate. *Brain Research,* 1124(1), 176-187.

Zimmer, A., and Kreuter, J. (1995). Microspheres and nanoparticles used in ocular delivery systems. *Advanced Drug Delivery Reviews,* 16(1), 61-73.

CHAPTER 4 - Biopharmaceutical evaluation of epigallocatechin gallate loaded cationic lipid nanoparticles (EGCG-LNs): in vivo, in vitro and ex vivo studies

CHAPTER 4 - BIOPHARMACEUTICAL EVALUATION OF EPIGALLOCATECHIN GALLATE LOADED CATIONIC LIPID NANOPARTICLES (EGCG-LNS): IN VIVO, IN VITRO AND EX VIVO STUDIES

Joana F. Fangueiro[a,b], Ana C. Calpena[c,d], Beatriz Clares[e], Tatiana Andreani[b,f,g], Maria A. Egea[d, h], Francisco Veiga[a,i], Amélia M. Silva[b,j], Maria L. Garcia[d,h], Eliana B. Souto[a,j]

aFaculty of Pharmacy, University of Coimbra (FFUC), Pólo das Ciências da Saúde, Azinhaga de Santa Comba, 3000-548 Coimbra, Portugal

bCentre for Research and Technology of Agro-Environmental and Biological Sciences (CITAB-UTAD), Quinta de Prados; 5001-801 Vila Real, Portugal

cDepartment of Pharmacy and Pharmaceutical Technology, Faculty of Pharmacy, University of Barcelona, Av. Joan XXIII s/n, 08028 Barcelona, SpaindInstitute of Nanoscience and Nanotechnology, University of Barcelona, Av. Joan XXIII s/n, 08028 Barcelona, Spain

eDepartment of Pharmacy and Pharmaceutical Technology, School of Pharmacy, University of Granada, Campus of Cartuja street s/n, 18071 Granada, Spain

gFaculty of Sciences, University of Porto (FCUP), Department of Chemistry and Biochemistry, Campo Alegre 4160-007 Porto, Portugal

hDepartment of Physical Chemistry, Faculty of Pharmacy, University of Barcelona, Av. Joan XXIII s/n, 08028 Barcelona, Spain

iCNC - Center for Neuroscience and Cell Biology, University of Coimbra (FFUC), Coimbra, Portugal

jDepartment of Biology and Environment, University of Trás-os Montes e Alto Douro (UTAD), Quinta de Prados; 5001-801 Vila Real, Portugal

***Published in International Journal of Pharmaceutics*, 502(1-2):161-169, 2016.**

CHAPTER 4- Biopharmaceutical evaluation of epigallocatechin gallate loaded cationic lipid nanoparticles (EGCG-LNs): in vivo, in vitro and ex vivo studies

Abstract

Cationic lipid nanoparticles (LNs) have been tested for sustained release and permeation of epigallocatechin gallate (EGCG), a potential polyphenol with improved pharmacological profile for the treatment of ocular pathologies, such as age-related macular edema, diabetic retinopathy, and inflammatory disorders. Cationic EGCG-LNs were produced by double-emulsion technique and characterized for *in vitro* release by dialysis bag following the analysis by a previously validated RP-HPLC method. *In vitro* Hen's Egg Test Chorioallantoic Membrane (HET-CAM) study was carried out using chicken embryos to determine the potential risk of irritation of the developed formulations. *Ex vivo* permeation profile was assessed using rabbit cornea and sclera isolated and mounted in Franz diffusion cells. The results showed that the use of cationic LNs provide a prolonged EGCG release following a Boltzmann sigmoidal profile. In addition, EGCG was successfully quantified in both tested ocular tissues, demonstrating the ability of these formulations to reach both anterior and posterior segment of the eye. The pharmacokinetic study of the corneal permeation showed a first order kinetics for both cationic formulations, while EGCG-cetyltrimethylammonium bromide (CTAB) LNs followed a Boltzmann sigmoidal profile and EGCG-dimethyldioctadecylammonium bromide (DDAB) LNs a first order profile. Our studies also proved the safety and non-irritant nature of the developed LNs. Thus, loading EGCG in cationic LNs is recognized as a promising strategy for the treatment of ocular diseases related to anti-oxidant and anti-inflammatory pathways.

4.1. Introduction

The anatomical and physiological barriers that eye provides to the entrance of drugs are a challenge that could be overcome by the use of nanoparticles for drug delivery (Wadhwa et al., 2009; Zhou et al., 2013). The main barriers encountered in ocular drug delivery are the physical barriers (cornea, sclera and retina), the blood aqueous and blood-retinal barriers, and the physiological barriers (blood flow, lymphatic clearance, enzymatic degradation, protein binding and the tear dilution and renovation) compromising the deliver of drugs specially targeted to the posterior segment of the eye (Gaudana et al., 2010).

Topical application of drugs in the ocular mucosa is usually used to reach the anterior or/and posterior segment of the eye. The anterior segment of the eye is anatomically composed of the cornea, conjunctiva, sclera and anterior uvea. Usually, the most commonly applied formulations to reach these structures are the eye drops, which are rapidly drained from the ocular surface reducing drastically drug residence time (Urtti, 2006). The posterior segment of the eye is composed of retina, vitreous and choroid (Thrimawithana et al., 2011). The pathologies that affect these structures are difficult to treat due to their anatomic position, and thus are invasive and painful routes, such as intravitreal injection which is often used to delivery high drug doses. However, intravitreal injection can cause complications, such as endophthalmitis and due to the high doses, systemic absorption may be compromised (Kim et al., 2014). These pathologies include age-related macular degeneration (AMD), retinitis pigmentosa, diabetic retinopathies (DR), and neural consequences caused by glaucoma (Kim et al., 2014; Urtti, 2006).

Designing non-invasive and sustained delivery nanoparticles for targeting drugs to the anterior and posterior segment of the eye is an ultimate objective of our research study. Cationic lipid nanoparticles (LNs) for ocular delivery have been reported by our research group to be safe, and long-term stable (Fangueiro et al., 2014a; Fangueiro et al., 2014b). The use of physiological lipids is being documented as a safe, biocompatible and biodegradable approach (Souto et al., 2013). However, the main concern is the toxicity related to the surfactants and in this particularly case, to the use

of cationic molecules. Our research group produced biocompatible and biodegradable cationic epigallocatechin gallate LNs (EGCG-LNs) (Fangueiro et al., 2014a; Fangueiro et al., 2014b), composed of natural and physiological lipids, cationic lipid, surfactants, EGCG and water. LNs have been widely investigated for targeted drug delivery because of their nanometer size, long-term physicochemical stability, biocompatibility and biodegradability, controlled release of drugs, low cytotoxicity and easily scale-up production (Mishra et al., 2010; Müller et al., 2000; Sinha et al., 2011; Souto and Muller, 2011; Souto and Müller, 2007; Souto et al., 2011; Wissing et al., 2004). It is therefore anticipated that LNs could overcome some of the disadvantages of ocular drug delivery and could provide a controlled/prolonged release of drugs and sustained therapeutic levels over an extended period of time (Araujo et al., 2009).

The topical administration of drugs provides a short period of residence time in the mucosa (usually 1-2 minutes), and these are efficiently removed via the lacrimal fluid renovation (Araujo et al., 2009). Cationic LNs seem to provide high capacity to increase the bioavailability of topical drugs when administered onto the ocular mucosa since they promotes electrostatic interaction between the cationic particles' surface and the anionic ocular mucosa, with a considerable improvement of the drug residence time (Fangueiro et al., 2014a).

The polyphenol EGCG with antioxidant properties has been successfully formulated in cationic LNs by our group (Fangueiro et al., 2014b). Currently, there are no studies involving the topical use of this drug to treat ocular diseases such as DR, diabetic macular edema (DME), glaucoma or AMD. Some of the biological mechanisms involved in the development of these ocular pathologies are related to the increased oxidative stress due to the inability of the organism to suppress the production of reactive oxygen species (ROS) (Kowluru and Chan, 2007; Madsen-Bouterse and Kowluru, 2008; Wakamatsu et al., 2008). It is well-known that polyphenols have potential human health benefits (Heim et al., 2002), and recently EGCG is being reported as one of the most potent polyphenols (Du et al., 2012; Yamauchi et al., 2009). Our group stabilized EGCG in biological medium for further characterization of the physicochemical stability and release/permeation profile under physiological conditions (Fangueiro et al., 2014b; Fangueiro et al., 2014c).

Our efforts have been driven towards the development of cationic LNs formulations that should maximize the EGCG ocular drug absorption via prolonged drug residence time in the cornea and conjunctival sac, as well as to enhance the transcorneal and transscleral drug penetration. In the present paper, the *ex vivo* transcorneal and transscleral permeation profiles of the EGCG-LNs has been evaluated, in parallel with the *in vitro* profile release of EGCG from the LNs. Pharmacokinetic parameters for each tissue were determined to establish the mechanism for transcorneal and transscleral permeation of the EGCG. In order to assess the local LNs toxicity and irritancy, an *in vitro* test Hen's Egg Test Chorioallantoic Membrane (HET-CAM test) and an *in vivo* test (Draize test) have been carried out.

4.2. Materials and Methods

4.2.1. Materials

Epigallocatechin gallate (EGCG, 98% purity, molecular weight 458.7 g/mol and pKa 7.59–7.75) was purchased from CapotChem (Hangzhou, China). Softisan®100 (S100) was a free sample from Sasol Germany GmbH (Witten, Germany), Lipoid® S75, 75% soybean phosphatidylcholine was purchased from Lipoid GmbH (Ludwigshafen, Germany), Lutrol®F68 or Poloxamer 188 (P188) was a free sample from BASF (Ludwigshafen, Germany). Transcutol®P was a gift from Gattefossé (Barcelona, Spain). Acetic acid (glacial, AR grade), acetonitrile (HPLC gradient), Cetyltrimethylammonium bromide (CTAB), sodium lauryl sulfate and ascorbic acid were acquired from Sigma-Aldrich (Sintra, Portugal). Dimethyldioctadecylammonium bromide (DDAB) was acquired from Avanti Polar Lipids (Alabama, USA). Anhydrous glycerol was purchased from Acopharma (Barcelona, Spain). Ethanol absolute (AR grade) was acquired from Panreac (Barcelona, Spain). The water used for sample preparation and for HPLC analysis was produced with a Super Purity Water System (Purite Ltd, England) with a resistivity over 17.5 MΩ cm. Ultra-purified water was obtained from a MiliQ Plus system (Millipore, Germany). All reagents were used without further treatment.

4.2.2. Cationic LNs production

Cationic LN dispersions were prepared based on a previous developed multiple emulsion (w/o/w) technique described by our group (Fangueiro et al., 2014a; Fangueiro et al., 2014b). Their composition is depicted on Table 4.1. EGCG and ascorbic acid were dissolved in ultra-purified water, which was added to the lipid phase at same temperature (5-10°C above the melting point of lipid S100) and homogenized 60s with a sonication probe (6 mm diameter) by means of an Ultrasonic processor VCX500 (Sonics, Switzerland). A power output with amplitude of 40% was applied. The poloxamer solution was added and homogenized for additional 90s. This pre-emulsion was poured in the total volume of poloxamer cooled solution under magnetic stirring for 15 min to allow the formation of the LN. The obtained LN dispersions were used for subsequent studies.

Table 4.1. Composition of the developed cationic LNs dispersions in wt%.

LN dispersion	S100	Glycerol	Lipoid® S75	CTAB	DDAB	P 188	A.A.	EGCG
CTAB-LN drug free	4.5	37.5	0.5	0.5	_____	1.0	0.25	_____
EGCG CTAB-LN	4.5	37.5	0.5	0.5	_____	1.0	0.25	0.075
DDAB-LN drug free	4.5	37.5	0.5	_____	0.5	1.0	0.25	_____
EGCG DDAB-LN	4.5	37.5	0.5	_____	0.5	1.0	0.25	0.075

S100- Softisan®100; P188 – Poloxamer 188; A.A. – Ascorbic acid

4.2.3. Physicochemical characterization

The physicochemical parameters mean particle size (Z-Ave), polydispersity index (PI) and zeta potential (ZP) were determined by dynamic light scattering (DLS, Zetasizer Nano ZS, Malvern Instruments, Malvern, UK). All samples were diluted with ultra-purified water to suitable concentration and analyzed in triplicate. For the determination of the ZP an ultra-purified water with conductivity adjusted to 50 µS/cm was used. Laser diffraction (LD) was performed for particle size analysis by a Mastersizer Hydro 2000 MU (Malvern Instruments, Malvern, UK). Data was evaluated using the volume distribution method to detect even few large particles and characterization parameters

were d10, d50, and d90 (*i.e*, a diameter d90 of 1 μm means that 90% of all particles have 1 μm or less).

4.2.4. *In vitro* EGCG release

The release study of EGCG from the LNs was carried out over 48 hours using the dialysis bag method (Chidambaram and Burgess, 1999). For the assay, 2.0 mL of sample corresponding to 15 mg/mL of EGCG was separated from 10.0 mL of a simulated biological study (ethanol (24%, v/v), transcutol®P (20%, v/v) and ascorbic acid solution (0.25%. w/v)) by means of a membrane (cellulose membrane MW cutoff 12,000-14,000 Da, Iberlabo, Spain). The system was mounted at 37°C to mimic *in vivo* conditions, stirred continuously, and at selected time intervals 300 μL of sample were analyzed by a RP-HPLC method validated by our group (Fangueiro et al., 2014c). The samples withdrawn were replaced by 300 μL of medium maintaining sink conditions.

The kinetic release profile of EGCG was evaluated according to the Akaike's approach (Doménech et al., 1998). The empirical models were selected based on the Akaike Information Criteria (AIC). The model associated to the smallest value of AIC is considered as giving the best fit of the set of data (Andreani et al., 2014). The AIC was calculated according to the following equation:

$$AIC = n \ln SSQ + 2p$$

where n is the number of pairs of experimental values, SSQ is the residual sum of squares and p is the number of parameters of the model. The mean release time (MRT) of EGCG from the LNs was also arithmetically assessed from experimental data using the following equation:

$$MRT = \frac{\sum t_i \times \Delta Q}{Q_\infty}$$

where Q_∞ is the asymptote of the dissolved amount of drug and $\sum t_i \times \Delta Q$ is the area between the cumulative release.

The release efficiency ($E_R\%$) was calculated according to the equation:

$$E_R\% = \frac{AUC_0^t}{Q_\infty \times t} \times 100$$

where AUC_0^t is the area under the curve, Q_∞ is the asymptote of the dissolved amount of drug, the *t* is the time of the cumulative release.

The other parameters evaluated, V50 and AUC, were extracted from the software. V50 is a modelistic parameter from the Boltzmann Sigmoidal model which corresponds to the time that the release of the drug is half of the maximum that can be achieved. AUC is a non modelistic parameter, which corresponds to the area under the curve of the curve presented by the release of the drug.

4.2.5. Transcorneal and Transscleral permeation studies

Six adult New Zealand male rabbits (Panlab, Spain) weighting between 2 and 2.5 kg were used. Rabbits were anesthetized with intramuscular administration of ketamine HCl (35 mg/kg) and xylazine (5 mg/kg). Animals were euthanized by an overdose of sodium pentobarbital (100 mg/kg) administered through marginal ear vein under deep anesthesia. Eyes were removed carefully, then excised, and the anterior and posterior segment were separated by cutting along the corneal/scleral limbus junction. To obtain bare cornea and sclera, the rest of the tissues were removed, including conjunctiva, and muscles, whereas the tissue was kept moist by placing it in balanced salt solution (BSS). The cornea and sclera were carefully cleaned using a cotton swab, stored in moist chambers at 4°C, and used within 24 hours of explantation. Experiments were performed according to the "*Association for Research in Vision and Ophthalmology"* (ARVO) resolution of the use of animals in research and were approved by the animal research ethical committee of the University of Barcelona and the normative (Directive 214/97, Gencat). The excised tissue was mounted on Franz-type diffusion cells (FDC 400, Crown Glass, Somerville, New York) with diffusion area of 0.64 cm^2. The episcleral side was placed toward the donor compartment on which 1.0 mL of each sample were placed. The receptor compartment was filled with 8 mL of the mimetic

biological medium (ethanol (24%, v/v), transcutol®P (20%, v/v) and ascorbic acid solution (0.25%. w/v)), kept at 37°C, and magnetically stirred at 450 rpm. At predetermined time intervals, an aliquot (300 µL) of the receptor solution was sampled for the determination of drug permeated and replaced with equal amounts of fresh buffer. All experiments were carried out under sink conditions. Samples were analysed in triplicate by RP-HPLC.

4.2.6. Quantification of EGCG retained in the cornea and sclera

Immediately after the 6-hour experiment, the cornea and the sclera were removed from each cell, cleaned with 0.5% of sodium lauryl sulfate and washed with distilled water, and then blotted dry with filter paper. The permeation area of sclera was then excised, weighed, and EGCG contained therein was extracted with acetonitrile:acetic acid solution (1%) (87:13, v:v) mixture during 20 minutes of sonication in an ultrasound bath. The EGCG levels (expressed as $\mu g.g^{-1}.cm^{-2}$ of cornea or sclera) were measured by RP-HPLC, yielding the amount of EGCG retained.

4.2.7. Permeation parameters

The cumulative drug amount (*Qt*) permeated through the sclera per unit area was calculated, at each time point, from the EGCG concentration in the receiving medium and plotted as a function of time. EGCG flux (*Jss*) through the cornea and sclera from each formulation was calculated by plotting the cumulative drug amount permeating the cornea and sclera against time, determining the slope of the linear portion of the curve by linear regression analysis and dividing by the diffusion area. Permeability coefficient of the drug at the steady state (k_{pss}) from solution and formulations was calculated by dividing the flux (J_{ss}) by the initial drug concentration (C_0) in the donor phase translated in the following equation:

$$k_{p\,ss} = \frac{J_{ss}}{C_0}$$

4.2.8. Ocular hydration levels

The ocular hydration level (*HL (%)*) of the cornea was assessed at the end of the corneal permeation studies. Each cornea was carefully washed, weighed and dessicated at constant weight dried at 80°C and then reweighed. HL was calculated using the following expression:

$$HL = \left[1 - \left(W_d / W_w\right)\right] x100$$

where W_d is weight of the cornea after dried and W_w is the weight before dried. Three replicates were used to determinate *HL*.

4.2.9. Ocular tolerance by HET-CAM

The risk of ocular irritation of LNs was assessed using the HET-CAM (Gilleron et al., 1996). To perform the test, the egg shell and the inner membrane of 10-day-old chicken eggs were previously removed, so that the CAM that separates the embryo from the air chamber becomes visible. After proceeding with the negative control (i.e. 2 eggs treated with 0.9% sodium chloride (NaCl)) and the positive controls (i.e. 2 eggs treated with 0.1 M sodium hydroxide (NaOH) and 2 treated with 1% sodium dodecyl sulfate (SDS)), 6 eggs were used for each tested sample. After exposing the CAM and rinsing it with PBS, 300 µL of the test solution was applied to the CAM. The intensity of the reactions was semi-quantitatively assessed on a scale from 0 (no reaction) to 3 (strong reaction). The appearance and the intensity of any reactions occurring were observed at 0s, 30s, 2min and 5min. The ocular irritation index (OII) was then calculated by the following expression:

$$\mathrm{OII} = \frac{(301 - h) \times 5}{300} + \frac{(301 - l) \times 7}{300} + \frac{(301 - c) \times 9}{300}$$

where h is the time (in seconds) of the beginning of hemorrhage, l of lysis and c of coagulation. The following classification was used: $\mathrm{OII} \leq 0.9$: slightly irritating; $0.9 < \mathrm{OII} \leq 4.9$: moderately irritating; $4.9 < \mathrm{OII} \leq 8.9$: irritating; $8.9 < \mathrm{OII} \leq 21$: severely irritating.

4.2.10. Ocular tolerance by the *in vivo* Draize test

Ocular tolerance was also assessed by the Draize test. This *in vivo* eye irritation test was performed in New Zealand white rabbits. Draize test is the official procedure for the evaluation of cosmetic and pharmaceutical products for ocular instillation by the interpretation of Kay and Calandra (Kay and Calandra, 1962). A single instillation of 50 μL of each sample was administered in one eye, using the untreated contralateral eye as a control. Readings were performed 1 hour after the sample application, then after 1, 2, 3, 4, and 7 days, respectively. The method provided an overall scoring system for grading the severity of ocular lesions involving the cornea (opacity), iris (inflammation degree), and conjunctiva (congestion, swelling, and discharge). The Draize score was determined by visual assessment of changes in these ocular structures. The mean total score (MTS) was calculated using the following equation:

$$\text{MTS} = \sum \frac{x_1(n)}{5} + \sum \frac{x_2(n)}{2} - \sum \frac{x_3\,(n)}{5}$$

where $x_1\,(n)$, $x_2\,(n)$, and $x_3\,(n)$ are the cornea, conjunctiva, and iris scores, respectively, and *n* being the number of rabbits included in the ocular tolerance assay. Three animals were used for each product, in accordance with the principles of the 3R's (reduction, refinement, and replacement) (Howard et al., 2004).

4.2.11. Statistical evaluation

Statistically evaluation of data was performed using a one-way analysis of variance (ANOVA) test. Bonferroni's multiple comparison test was carried out to compare the significance between the different groups. A *p*-value <0.0001 was considered statistically significant. Fitting of release profile was evaluated by GraphPad Prism version 6.01.

4.3. Results and Discussion

Cationic LNs were previous optimized by a factorial design study (Fangueiro et al., 2014a) and then physicochemically characterized for ocular delivery (Fangueiro et al.,

2014b). The DLS studies showed cationic LNs with a mean particle size for both EGCG-LNs below 150 nm and a PI below 0.25 (Table 4.2).

However, further studies employing other techniques were carried out since ocular delivery requires a narrow control in the particle size, to avoid possible irritations and lesions to the eye (Araujo et al., 2011). LD was used to provide more information about the polydispersity present in the LNs dispersions. The results of LD are summarized in Table 4.2, showing the nanometer size of all formulations (over 200 nm), except for the formulation EGCG CTAB-LN. From the tested formulations, EGCG DDAB-LN did not show Z-Ave values above 200 nm, which is ideal for ocular administration. CTAB-LN reveals a higher Z-Ave, which could predict that different cationic lipids follow different behavior when encapsulating EGCG.

Table 4.2. Physicochemical characterization of the EGCG-LN dispersions developed using dynamic light scattering (DLS) and Laser diffraction (LD). The results are expressed as mean± S.D. (*n = 3*).

Formulation	DLS			LD		
	Z-Ave (nm)	**PI**	**ZP (mV)**	**d10 (nm)**	**d50 (nm)**	**d90 (nm)**
EGCG CTAB-LN	149.1±1.779	0.24±0.008	20.80±0.896	70.0±0.00	153.0±0.01	368.0±0.02
EGCG DDAB-LN	143.7±0.450	0.16±0.015	25.70±1.42	74.0±0.00	115.0±0.00	191.0±0.01

The EGCG release profile from the solution and from the different LNs in the biological medium at 37°C is represented in Figure 4.1. EGCG experimental results from the release profiles showed similar trends for both LN formulations, however EGCG solution releases faster when comparing with EGCG-LNs. The initial release of EGCG was statistically different between the three formulations (p-value<0.0001), being more evident for the EGCG solution since this formulation released almost 50% of EGCG within the first 4 hours. Despite the different initial EGCG release, after 24 hours the three formulations achieved a similar level of EGCG release, i.e. with no statistical differences. Regarding the evaluated parameters, *V50, MRT, AUC* and E_R*%* (Table 4.3), statistical significant differences (p-value<0.0001) were found between the three

formulations. However, Bonferroni test showed a major difference between the EGCG solutions and both LNs formulations. The *MRT* obtained with EGCG free is markedly lower than EGCG encapsulated in LNs, confirming that its encapsulation in LNs modified its release profile. This is expected since EGCG in the solution has no barriers against its release, while in the case of the LNs, the drug is released only after the lipids erosion or melting takes place. This can also be proven by the E_R% values obtained for the EGCG solution and EGCG LNs, since lower values were found for the last ones, however these values were near 70% (Table 4.3).

Table 4.3. Kinetic parameters for the evaluation of EGCG release from solution and encapsulated in the cationic LNs.

Parameters	**EGCG solution**	**EGCG-CTAB LNs**	**EGCG-DDAB LNs**
$\mathbf{V_{50}}$	1.058±0.86	8.763±0.49	7.156±0.80
***MRT* (h)**	1.68±0.04	7.49±0.33	7.38±0.10
AUC	2231.49±1.31	1605.07±59.57	1672.94±16.30
$\boldsymbol{E_R}$**%**	92.98±0.17	68.78±1.37	69.23±0.39

In addition, the different cationic structure of LNs demonstrated to have no interference with the release of EGCG, since for all parameters no statistically significant differences between the two LN formulations (Bonferroni´s test, *p*-value<0.0001) were found. However, there are slightly differences between them since CTAB-EGCG LN followed a delayed release pattern of EGCG (Figure 4.1).

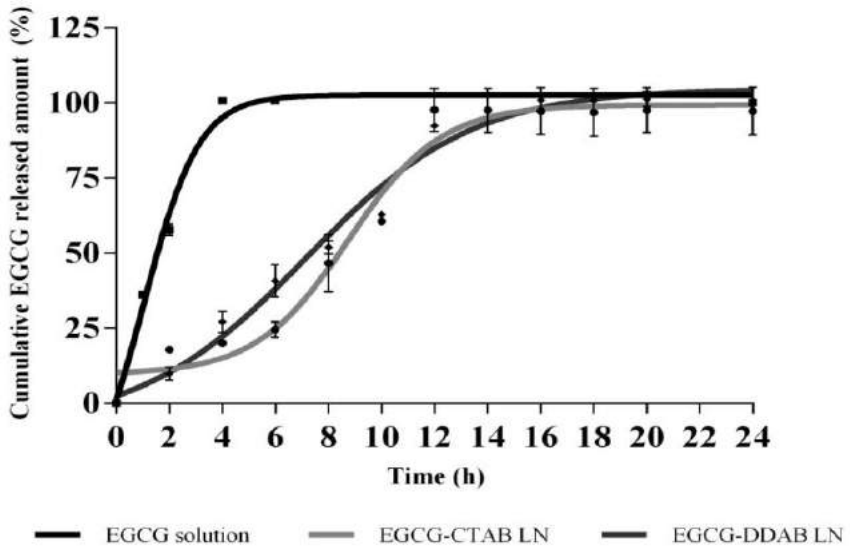

Figure 4.1. Release profile of the EGCG from solution (squares) and from the cationic EGCG-LNs, namely CTAB (lozenges) and DDAB (circles).

EGCG release from a solution and the different LNs was kinetically studied applying the Boltzmann sigmoidal, sigmoidal dose response and Gompetz models. Table 4.4 shows the models and their corresponding dissolution parameters for EGCG solution and cationic LNs. According to lower AIC and the r^2 values (Table 4.4), the best fitting for all formulations was the Boltzmann sigmoidal model, which is described by the following equation:

$$F = \frac{A_1 - A_2}{1 + e^{\frac{(x - x_0)}{dx}}} + A_2$$

where *F* is defined by the ratio of the number of samples to the number of total samples. A_1 is the low EGCG concentration released limit, A_2 is the high EGCG concentration released limit, x_0 is the inflexion (half amplitude) point and *dx* is the width.

Table 4.4. Mathematical modeling for EGCG release in solution and encapsulated in the cationic LNs.

Release profiles	**Boltzmann sigmoidal**		**Sigmoidal dose response**		**Gompetz**	
Parameters	r^2	***AIC***	r^2	***AIC***	r^2	***AIC***
EGCG solution	0.9967	17.39	n.d.	n.d.	0.9961	17.55
EGCG-CTAB LNs	0.9923	24.85	0.9784	25.88	0.9898	25.13
EGCG-DDAB LNs	0.9952	24.36	0.9626	26.42	0.9940	24.59

n.d. – not determinated

LNs has gained much attention for ocular drug delivery and recent studies have shown improved drug permeation across the cornea and sclera (Araujo et al., 2012; Elsaid et al., 2014; Li et al., 2013). The use of an *ex vivo* model was used and results showed that LNs enhanced drug delivery. The permeated amount per unit area through excised cornea and sclera was analyzed and the resulting J_{ss} and K_{pss} obtained for both EGCG-LNs, are shown in Table 4.5. These two parameters were evaluated in the steady state and gave distinct information, since the first is dependent from the drug concentration in opposition to the other. The intrinsic permeation of EGCG solution was not tested due to the problems of ocular adherence, as also the high solubility of EGCG in water and its hypertonicity. The permeation and absorption of topical ocular drugs is strongly dependent on the physicochemical properties of the nanoparticles. Thus, smallest and uniformly distributed LNs has higher tendency to present efficient results (Pade and Stavchansky, 1997). The LNs developed in this study showed a mean particle size smaller than 200 nm and PI below 0.3 (Table 4.2). Furthermore, previous morphological studies by transmission electronic microscopy (TEM) (Fangueiro et al., 2014b) revealed spherical LNs, and this property was referred by some authors to be crucial for permeation properties (Albanese et al., 2012; Kobayashi et al., 2014). According to Srikantha and co-workers (Srikantha et al., 2012) the shape, size and PI, influence the transscleral permeation and that spherical particles optimize permeation properties. The results shown in Table 4.5, revealed that permeability and flux of EGCG-CTAB LNs were 3-fold higher than EGCG-DDAB LNs in the cornea. However,

for the transscleral permeation, the EGCG-DDAB LNs permeated 3-fold higher than EGCG-CTAB LNs. The transccleral permeation is usually higher than the transcorneal due to the tightest stractum corneum of this tissue (Bu et al., 2007; Malhotra and Majumdar, 2001). Additionally, the cornea divided in the epithelium, stroma, and endothelium offers a different polarity due to these layers as also a limiting structure for drug permeation. The topically hydrophilic drug administered, such as EGCG, has a higher resistance associated with the tight junctions of corneal epithelium (Gaudana et al., 2010). In the other hand, sclera is composed by collagen fibers and proteoglycans and is been reported that permeability through this tissue depends on various parameters, namely molecular weight, hydrophilicity, molecular radius and charge of the molecule (Nicoli et al., 2009; Prausnitz and Noonan, 1998). Furthermore, the sclera is not the only barrier against drug penetration, but the bilayer choroid-Bruch's, although very thin, may also add an important contribution to the overall resistance [34]. Regarding the molecular weight of EGCG (458.7 g/mol), it seems to be able to permeate ocular tissues.

Table 4.5. Permeation parameters, namely permeation coefficient (k_{pss} (cm.h^{-1})) and flux (J_{ss} (µg.h.cm^{-2})) of tanscorneal and transscleral permeation of EGCG-CTAB and EGCG-DDAB LNs during 6 h (*n=3*±*S.D*).

Permeation parameters	**Corneal permeation**		**Scleral permeation**	
	EGCG-CTAB LNs	**EGCG-DDAB LNs**	**EGCG-CTAB LNs**	**EGCG-DDAB LNs**
K_{pss} (cm.h^{-1})	0.0313 ± 0.0037	0.0130 ± 0.0017	0.0142 ± 0.0013	0.0387 ± 0.0029
J_{ss} (µg.h.cm^{-2})	4.7006 ± 0.5559	1.9565 ± 0.2551	2.1265 ± 0.2010	5.8087 ± 0.4291

The analysis of EGCG permeation by kinetic models is summarized in Table 4.6. For the transcorneal permeation, both formulations followed a first order kinetics, in which the rate of permeation is directly proportional to the concentration of EGCG in the particles. For transccleral permeation, EGCG-CTAB LNs followed a Boltzmann sigmoidal profile and EGCG-DDAB LNs followed a first order, as same observed for the corneal permeation.

Table 4.6. Kinetic models and parameters evaluated for EGCG release in the cornea and sclera encapsulated in the cationic EGCG-LNs. LNs.

Formulation	Corneal permeation		Scleral permeation	
	Kinetic model	r^2	**Kinetic model**	r^2
EGCG-CTAB LNs	First order	0.9982	Boltzmann Sigmoidal	0.9911
EGCG-DDAB LNs	First order	0.9908	First order	0.9946

The concentration of EGCG permeated was very low compared to the initial concentration of EGCG (750 µg/mL). The differences were explained by the need of drug diffusion from the inner aqueous phase through the lipid matrix that divided this phase from the outer aqueous phase. Thus, there is a reduction of EGCG available for diffusion. Another reason of this lower concentration was the 6 h time of analysis, after which the sink conditions could not be maintained. According to Araújo and co-workers (Araujo et al., 2012), the flux to the receptor compartment is blocked and sink conditions are not respected after this period.

Results of EGCG transcorneal and transscleral permeation from LNs demonstrated that these particles deliver the encapsulated drug at a constant rate with enhanced accumulation into the corneal and scleral tissue (Figure 4.2). This study provides clear evidence of EGCG permeation in ocular tissues and also a prolonged release during the time of analysis (6 h). Although both formulations achieved the anterior and posterior segment of the eye, there is statistical evidence that CTAB-based particles are expected to be used to deliver EGCG to the anterior segment of the eye, while DDAB-LNs are mostly appropriated for the delivery of EGCG to the posterior segment. Both cornea and sclera are permeable to many drugs and can potentially act as a drug reservoir for extended-release delivery (Ambati et al., 2000), however some drugs are not able to reach the posterior segment. From our studies, EGCG was able to reach both tissues, cornea and sclera.

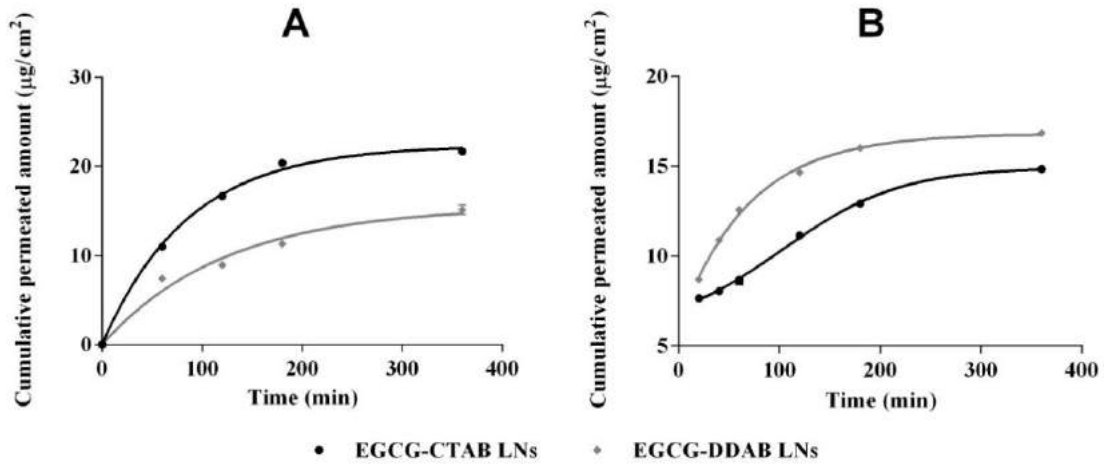

Figure 4.2. Transcorneal (A) and transscleral (B) permeation profile of EGCG-CTAB LNs (■) and EGCG-DDAB LNs (♦).

The amount of EGCG retained (Q_r) and permeated (Q_p) in the cornea and sclera were determined at the end of the assay and the results are shown in Table 4.7. From the results, EGCG presented higher permeation than retention in the cornea and sclera when delivered by EGCG-CTAB LNs. For EGCG-DDAB LNs the opposite has been observed, i.e. the retention on both tissues, cornea and sclera was higher than the permeated amount. The diffusion and retention of drugs deposited in the cornea and sclera of the eye is influenced by the drug molecule's size and/or its binding characteristics to the tissues (Edelhauser et al., 2010; Kim et al., 2014). Thus, the cationic structure of LNs developed could improve drug residence time and consequently improve bioavailability.

There are no statistically differences between both tissues and formulations for the amount retained, however the formulation composed of DDAB is expected to retain more time the drug in the ocular tissues. Overall, LNs showed excellent properties to deliver efficiently EGCG in the eye, such as very similar size, narrow size distribution, shape and stability properties (Fangueiro et al., 2014a; Fangueiro et al., 2014b). Additionally, the ocular hydration level of the cornea (Table 4.7) warrantees the good conditions of the cornea during the assay, proving that no damage was made due to the optimal values ranging 78.83-82.50%.

Table 4.7. Quantities of EGCG permeated (Q_p) and retained (Q_r) in the cornea and sclera and corneal hydration level (HL) of the EGCG-LNs after 6h of assay.

Parameters	Corneal permeation		Scleral permeation	
	EGCG-CTAB LNs	**EGCG-DDAB LNs**	**EGCG-CTAB LNs**	**EGCG-DDAB LNs**
Q_p (%.cm^2.g)	21.69±0.54	15.13±0.94	14.84±0.14	16.84±0.26
Q_r (%.cm^2.g)	15.88±1.01	39.24±0.29	9.45±0.14	45.39±1.04
HL (%)	78.83±1.890	82.5±2.150	n.d.	n.d.

n.d. not determinated

LNs are usually well tolerated by ocular and other mucosa due to their physiological composition, reducing the risk of toxicological reactions (Souto and Doktorovova, 2009). Additionally, they have the ability to target specific tissues and cells, with improved penetration and enhanced drug bioavailability into ocular barriers, increase the therapeutic effectiveness and minimize the undesirable side effects (Fangueiro et al., 2014a). However, the developed LNs have cationic nature due to the need for ocular bioadhesion and prolonged release time of EGCG onto the eye surface. The cationic lipids selected for the study (CTAB and DDAB) may raise toxicological concerns therefore HET-CAM and Draize tests were carried out.

The HET-CAM can provide information about the conjunctiva ocular effects that formulations may develop. Due to its vascularized mucosa similar to human eye, the irritation with risk of vascular damage (hemorrhage, lysis and coagulation) can be predicted for ocular formulations (Abdelkader et al., 2012; Vargas et al., 2007).

The HET-CAM test was performed in the CAM of 10-day-old chicken eggs. For the test one negative control has been used. The possible injuries, i.e. hemorrhage, lysis and coagulation, were observed 0 s, 30 s, 2 min and 5 min after the exposure of the formulations or solutions. The negative control was done applying 0.9% NaCl onto the surface of the CAM and no injuries were found after the total time of analysis (5 min) (Figure 4.3A). Concerning the positive controls, 0.1 M NaOH and 1% SDS, the initial

injuries were observed in the first 30 s i.e. the hemorrhage and the rosette-like coagulation (Figures 4.3B and 4.3C). The average cumulative score of the positive control of 0.1 M NaOH was higher than for SDS (17.37 versus 19.87, respectively) (Table 4.8). These compounds proved to be adequate for quality control because they were shown to be severely irritant (Table 4.8).

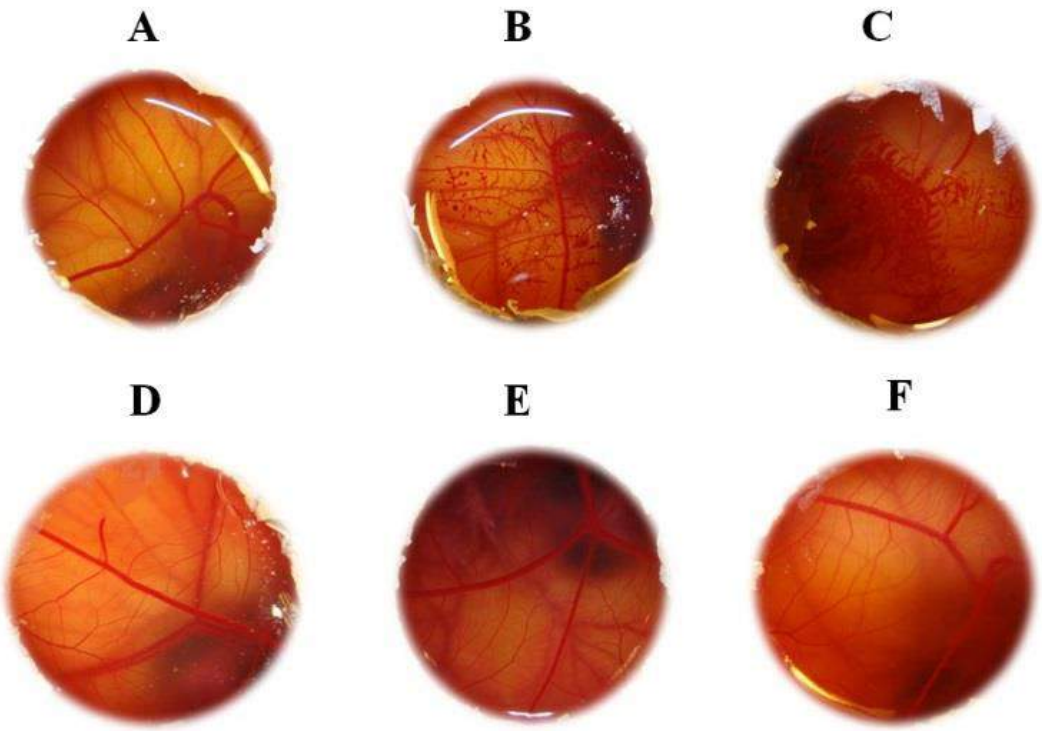

Figure 4.3. Stereomicrographs of the CAM after 5 minutes of exposure to (A) 0.9% NaCl (negative control); (B) 0.1 M NaOH solution (positive control); (C) 1% SDS (positive control); (D) EGCG solution (750 µg/mL); (E) EGCG-CTAB LNs and (F) EGCG-DDAB LNs.

The EGCG solution at the same concentration figuring in the LNs (750 µg/mL), and also the tested formulations (EGCG-CTAB LNs and EGCG-DDAB LNs) showed no signs of vascular response (Figure 4.3D–4.3F), and the average cumulative scores calculated for the tested LNs and EGCG free were found to be <0.9, which categorized these substances as slightly irritant or non-irritant (Table 4.8). These results revealed that the test substances were practically non-irritant when applied onto the surface of the CAM.

Table 4.8. Ocular irritation index (OII) scores for the tested EGCG and LN dispersions. The score was calculated according with the equation mentioned above and the correspondent classification. The results are expressed as mean± S.D. (n = *6*).

Tested solution/dispersion	OII±SD	Irritancy classification
0.9% NaCl	≤0.9±0.0	NI*
0.1 M NaOH	17.37±0.9	SI*
1% SDS	18.97±1.2	SI
EGCG solution	≤0.9±0.0	**NI**
EGCG-CTAB LNs	≤0.9±0.0	**NI**
EGCG-DDAB LNs	≤0.9±0.0	**NI**

*NI- Non-irritant or slightly irritant; *SI- Severely irritant

Despite the non-irritancy of EGCG-LNs in HET-CAM test, the Draize test was also performed to complement the full understanding of ocular tolerance. As expected, no sign of ocular inflammation, congestion, swelling and lacrimation was observed in both EGCG-LN formulations and in EGCG solution (scores were zero, data not shown). The corneas were observed to be crystal clear with intact ocular surface. No damage was observed on cornea, iris and conjunctiva in all time of analysis (total time = 7 days). Results showed the acceptable tolerability of both EGCG-LN formulations and also of EGCG solution in the rabbit eye.

4.4. Conclusion

The cationic EGCG-LNs for ocular delivery revealed promising results and may be an innovative approach for the treatment of several eye disorders, such as AMD, DR and glaucoma. Despite the previous studies reporting the good physicochemical parameters, this study complement the information related to the release of EGCG. The LNs provide a prolonged drug release of EGCG, following the Boltzmann sigmoidal release profile. The *ex vivo* permeation of EGCG was achieved in the cornea and in the sclera, which could predict an absorption in the anterior and posterior segment of the eye. The corneal permeation followed a first order permeation for both formulations, while EGCG-CTAB LNs followed a Boltzmann sigmoidal profile and EGCG-DDAB-LNs a first order profile. The *in vitro* HET-CAM and *in vivo* Draize test studies classified both formulations as safe and non-irritant. Cationic LNs may provide higher drug residence

time, higher drug absorption and consequently higher bioavailability of EGCG in the ocular mucosa. Despite the chemical difference of the cationic lipids, there are no statistical differences between them.

4.5. Bibliographic References

Abdelkader, H., Ismail, S., Hussein, A., Wu, Z., Al-Kassas, R., and Alany, R. G. (2012). Conjunctival and corneal tolerability assessment of ocular naltrexone niosomes and their ingredients on the hen's egg chorioallantoic membrane and excised bovine cornea models. *International Journal of Pharmaceutics,* 432(1-2), 1-10. d

Albanese, A., Tang, P. S., and Chan, W. C. W. (2012). The Effect of Nanoparticle Size, Shape, and Surface Chemistry on Biological Systems. *Annual Review of Biomedical Engineering,* 14(1), 1-16.

Ambati, J., Canakis, C. S., Miller, J. W., Gragoudas, E. S., Edwards, A., Weissgold, D. J., Adamis, A. P. (2000). Diffusion of high molecular weight compounds through sclera. *Investigative Ophthalmology & Visual Science,* 41(5), 1181-1185.

Andreani, T., Souza, A. L. R. d., Kiill, C. P., Lorenzón, E. N., Fangueiro, J. F., Calpena, A. C., Souto, E. B. (2014). Preparation and characterization of PEG-coated silica nanoparticles for oral insulin delivery. *International Journal of Pharmaceutics,* 473(1–2), 627-635.

Araujo, J., Garcia, M. L., Mallandrich, M., Souto, E. B., and Calpena, A. C. (2012). Release profile and transscleral permeation of triamcinolone acetonide loaded nanostructured lipid carriers (TA-NLC): in vitro and ex vivo studies. *Nanomedicine: Nanotechnology, Biology and Medicine,* 8(6), 1034-1041.

Araujo, J., Gonzalez, E., Egea, M. A., Garcia, M. L., and Souto, E. B. (2009). Nanomedicines for ocular NSAIDs: safety on drug delivery. *Nanomedicine: Nanotechnology, Biology and Medicine,* 5(4), 394-401.

Araujo, J., Nikolic, S., Egea, M. A., Souto, E. B., and Garcia, M. L. (2011). Nanostructured lipid carriers for triamcinolone acetonide delivery to the posterior segment of the eye. *Colloids and Surfaces B: Biointerfaces,* 88(1), 150-157.

Bu, H. Z., Gukasyan, H. J., Goulet, L., Lou, X. J., Xiang, C., and Koudriakova, T. (2007). Ocular disposition, pharmacokinetics, efficacy and safety of nanoparticle-formulated ophthalmic drugs. *Current Drug Metabolism,* 8(2), 91-107.

Chidambaram, N., and Burgess, D. J. (1999). A novel in vitro release method for submicron sized dispersed systems. *American Association of Pharmaceutical Sciences, 1*(3), E11.

Doménech, J., Martínez, J., and Plá, J. (1998). *Biofarmacia y Farmacocinética. Volumen II: Biofarmacia*. Síntesis Editor. Madrid, Spain.

Du, G. J., Zhang, Z., Wen, X. D., Yu, C., Calway, T., Yuan, C. S., and Wang, C. Z. (2012). Epigallocatechin Gallate (EGCG) is the most effective cancer chemopreventive polyphenol in green tea. *Nutrients,* 4(11), 1679-1691.

Edelhauser, H. F., Rowe-Rendleman, C. L., Robinson, M. R., Dawson, D. G., Chader, G. J., Grossniklaus, H. E., Wong, W. T. (2010). Ophthalmic Drug Delivery Systems for the Treatment of Retinal Diseases: Basic Research to Clinical Applications. *Investigative Ophthalmology and Visual Science,* 51(11), 5403-5420.

Elsaid, N., Somavarapu, S., and Jackson, T. L. (2014). Cholesterol-poly(ethylene) glycol nanocarriers for the transscleral delivery of sirolimus. *Experimental Eye Research,* 121, 121-129.

Fangueiro, J. F., Andreani, T., Egea, M. A., Garcia, M. L., Souto, S. B., Silva, A. M., and Souto, E. B. (2014a). Design of cationic lipid nanoparticles for ocular delivery: development, characterization and cytotoxicity. *International Journal of Pharmaceutics,* 461(1-2), 64-73.

Fangueiro, J. F., Andreani, T., Fernandes, L., Garcia, M. L., Egea, M. A., Silva, A. M., and Souto, E. B. (2014b). Physicochemical characterization of epigallocatechin gallate lipid nanoparticles (EGCG-LNs) for ocular instillation. *Colloids and Surfaces B: Biointerfaces,* 123,452-460.

Fangueiro, J. F., Parra, A., Silva, A. M., Egea, M. A., Souto, E. B., Garcia, M. L., and Calpena, A. C. (2014c). Validation of a high performance liquid chromatography method for the stabilization of epigallocatechin gallate. *International Journal of Pharmaceutics,* 475(1-2), 181-190.

Gaudana, R., Ananthula, H. K., Parenky, A., and Mitra, A. K. (2010). Ocular drug delivery. *American Association of Pharmaceutical Sciences Journal,* 12(3), 348-360.

Gilleron, L., Coecke, S., Sysmans, M., Hansen, E., Van Oproy, S., Marzin, D., Vanparys, P. (1996). Evaluation of a modified HET-CAM assay as a screening test for eye irritancy. *Toxicology in Vitro,* 10(4), 431-446.

Heim, K. E., Tagliaferro, A. R., and Bobilya, D. J. (2002). Flavonoid antioxidants: chemistry, metabolism and structure-activity relationships. *Journal of Nutritional Biochemistry*, 13(10), 572-584.

Howard, B., van Herck, H., Guillen, J., Bacon, B., Joffe, R., and Ritskes-Hoitinga, M. (2004). Report of the FELASA Working Group on evaluation of quality systems for animal units. *Laboratory Animals,* 38(2), 103-118.

Kay, J. H., and Calandra, J. K. (1962). Interpretation of eye irritation test. *Journal of the Society* of *Cosmetic Chemists,* 13, 281-289.

Kim, Y. C., Chiang, B., Wu, X., and Prausnitz, M. R. (2014). Ocular delivery of macromolecules. *Journal of Controlled Release,* 190, 172-181.

Kobayashi, K., Wei, J., Iida, R., Ijiro, K., and Niikura, K. (2014). Surface engineering of nanoparticles for therapeutic applications. *Polymer Journal,* 46(8), 460-468.

Kowluru, R. A., and Chan, P. S. (2007). Oxidative stress and diabetic retinopathy. *Experimental Diabetes Research,* 43603, doi: 10.1155/2007/43603.

Li, J., Wu, L., Wu, W., Wang, B., Wang, Z., Xin, H., and Xu, Q. (2013). A potential carrier based on liquid crystal nanoparticles for ophthalmic delivery of pilocarpine nitrate. *International Journal of Pharmaceutics,* 455(1-2), 75-84.

Madsen-Bouterse, S. A., and Kowluru, R. A. (2008). Oxidative stress and diabetic retinopathy: pathophysiological mechanisms and treatment perspectives. *Reviews in Endocrine and Metabolic Disorders,* 9(4), 315-327.

Malhotra, M., and Majumdar, D. K. (2001). Permeation through cornea. *Indian Journal of Experimental Biology,* 39(1), 11-24.

Mishra, B., Patel, B. B., and Tiwari, S. (2010). Colloidal nanocarriers: a review on formulation technology, types and applications toward targeted drug delivery. *Nanomedicine: Nanotechnology, Biology and Medicine,* 6(1), 9-24.

Müller, R. H., Mäder, K., and Gohla, S. (2000). Solid lipid nanoparticles (SLN) for controlled drug delivery – a review of the state of the art. *European Journal of Pharmaceutics and Biopharmaceutics,* 50(1), 161-177.

Nicoli, S., Ferrari, G., Quarta, M., Macaluso, C., Govoni, P., Dallatana, D., and Santi, P. (2009). Porcine sclera as a model of human sclera for in vitro transport experiments: histology, SEM, and comparative permeability. *Molecular Vision,* 15, 259-266.

Pade, V., and Stavchansky, S. (1997). Estimation of the relative contribution of the transcellular and paracellular pathway to the transport of passively absorbed drugs in the Caco-2 cell culture model. *Pharmaceutical Research,* 14(9), 1210-1215.

Prausnitz, M. R., and Noonan, J. S. (1998). Permeability of cornea, sclera, and conjunctiva: A literature analysis for drug delivery to the eye. *Journal of Pharmaceutical Sciences,* 87(12), 1479-1488.

Sinha, V. R., Srivastava, S., Goel, H., and Jindal, V. (2011). Solid Lipid Nanoparticles (SLN´s) - Trends and Implications in Drug Targeting. *International Journal of Advances in Pharmaceutical Research,* 1, 212-238.

Souto, E. B., and Doktorovova, S. (2009). Chapter 6 - Solid lipid nanoparticle formulations pharmacokinetic and biopharmaceutical aspects in drug delivery. *Methods in Enzymology*, 464, 105-129.

Souto, E. B., Fangueiro, J. F., and Müller, R. H. (2013). Solid Lipid Nanoparticles (SLN™). In I. F. Uchegbu, A. G. Schätzlein, W. P. Cheng and A. Lalatsa (Eds.), *Fundamentals of Pharmaceutical Nanoscience* (pp. 91-116). New York: Springer New York.

Souto, E. B., and Muller, R. H. (2011). Solid Lipid Nanoparticles and Nanostructures Lipid Carriers - Lipid Nanoparticles for Medicals and Pharmaceuticals. *Encyclopedia of Nanoscience and Nanotechnology*, 23, 313-328.

Souto, E. B., and Müller, R. H. (2007). Lipid Nanoparticles (SLN and NLC) for Drug Delivery. In J. Domb, Y. Tabata, M. N. V. R. Kumar and S. Farber (Eds.), *Nanoparticles for Pharmaceutical Applications* (Vol. 5, pp. 103-122): American Scientific Publishers.

Souto, E. B., Teeranachaideekul, V., Boonme, P., Muller, R. H., and Junyapraset, V. B. (2011). Lipid-Based Nanocarriers for Cutaneous Administration of Pharmaceutics. *Encyclopedia of Nanoscience and Nanotechnology*, 15, 479-491.

Srikantha, N., Mourad, F., Suhling, K., Elsaid, N., Levitt, J., Chung, P. H., Jackson, T. L. (2012). Influence of molecular shape, conformability, net surface charge, and tissue interaction on transscleral macromolecular diffusion. *Experimental Eye Research*, 102, 85-92.

Thrimawithana, T. R., Young, S., Bunt, C. R., Green, C., and Alany, R. G. (2011). Drug delivery to the posterior segment of the eye. *Drug Discovery Today*, 16(5-6), 270-277.

Urtti, A. (2006). Challenges and obstacles of ocular pharmacokinetics and drug delivery. *Advanced Drug Delivery Reviews*, 58(11), 1131-1135.

Vargas, A., Zeisser-Labouèbe, M., Lange, N., Gurny, R., and Delie, F. (2007). The chick embryo and its chorioallantoic membrane (CAM) for the in vivo evaluation of drug delivery systems. *Advanced Drug Delivery Reviews*, 59(11), 1162-1176.

Wadhwa, S., Paliwal, R., Paliwal, S. R., and Vyas, S. P. (2009). Nanocarriers in ocular drug delivery: an update review. *Current Pharmaceutical Design*, 15(23), 2724-2750.

Wakamatsu, T. H., Dogru, M., and Tsubota, K. (2008). Tearful relations: oxidative stress, inflammation and eye diseases. *Arquivos Brasileiros de Oftalmologia*, 71(6 Suppl), 72-79.

Wissing, S. A., Kayser, O., and Muller, R. H. (2004). Solid lipid nanoparticles for parenteral drug delivery. *Advanced Drug Delivery Reviews*, 56(9), 1257-1272.

Yamauchi, R., Sasaki, K., and Yoshida, K. (2009). Identification of epigallocatechin-3-gallate in green tea polyphenols as a potent inducer of p53-dependent apoptosis in the human lung cancer cell line A549. *Toxicology In Vitro*, 23(5), 834-839.

Zhou, H. Y., Hao, J. L., Wang, S., Zheng, Y., and Zhang, W. S. (2013). Nanoparticles in the ocular drug delivery. *International Journal of Ophthalmology*, 6(3), 390-396.

CHAPTER 5 - Evaluation of cytotoxicity and the antioxidant activity of Epigallocatechin gallate loaded cationic lipid nanoparticles in Y-79 human retinoblastoma cells

CHAPTER 5 - EVALUATION OF CYTOTOXICITY AND THE ANTIOXIDANT ACTIVITY OF EPIGALLOCATECHIN GALLATE LOADED CATIONIC LIPID NANOPARTICLES IN Y-79 HUMAN RETINOBLASTOMA CELLS

Joana F. Fangueiro[a,b], Dario L. Santos[a, c], Tatiana Andreani[a,d], Francisco Veiga[b,e], Maria L. Garcia[f,g], Maria A Egea[f,g], Eliana B. Souto[b,e] Amélia M. Silva[a,c,*]

[a] Centre for Research and Technology of Agro-Environmental and Biological Sciences (CITAB-UTAD), Quinta de Prados; 5001-801 Vila Real, Portugal

[b] Faculty of Pharmacy, University of Coimbra (FFUC), Pólo das Ciências da Saúde, Azinhaga de Santa Comba, 3000-548 Coimbra, Portugal

[c]Department of Biology and Environment, University of Trás-os Montes e Alto Douro (UTAD), Quinta de Prados; 5001-801 Vila Real, Portugal

[d]Faculty of Sciences, University of Porto (FCUP), Department of Chemistry and Biochemistry, Campo Alegre 4160-007 Porto, Portugal

[e] Center for Neuroscience and Cell Biology (CNC), University of Coimbra, Coimbra, Portugal

[f]Institute of Nanoscience and Nanotechnology, University of Barcelona, Av. Joan XXIII s/n, 08028 Barcelona, Spain;

[g]Department of Physical Chemistry, Faculty of Pharmacy, University of Barcelona, Av. Joan XXIII s/n, 08028 Barcelona, Spain

Submitted to Nanotoxicology, September 2015

CHAPTER 5 - Evaluation of cytotoxicity and the antioxidant activity of Epigallocatechin gallate loaded cationic lipid nanoparticles in Y-79 human retinoblastoma cells

Abstract

The use of epigalocatechin gallate (EGCG) for ocular purposed was firstly purposed by our research group in order to investigate its ability to prevent and manage diabetic retinopathy (DR) encapsulated in lipid nanocarriers. Due to the antioxidant capacity of EGCG comproved in various types of human cells, the capacity of reversing the oxidative stress environment present in the diabetic eye was investigated in Y-79 human retinoblastoma cells. Thus, encapsulation of EGCG was carried out in cationic lipid nanoparticles (LNs) and according with viability results the most harmful formulations were composed by cetyl trimethylammonium bromide (CTAB). Additionally, the influence of the LNs developed and EGCG in the antioxidant enzymatic activity of superoxide dismutase, catalase, glutathione reductase and glutathione-S-transferase seems to decreased their activity, indicating the inability to neutralize the reactive oxygen species (ROS) formation and thus, leading to oxidative stress. Also, the lipids and proteins oxidation was increased which is related with decreased enzymatic activity, since they are the primary defense to avoid these events. The dimethyldioctadecylammonium bromide (DDAB)-LNs was the only formulation with improved enzymatic protection regarding the cell viability, antioxidant enzymatic activity and protection against lipids and proteins oxidation. This could be associated with the chelating effect of EGCG with the enzymatic co-factors of the enzymes, leading to a lower availability of the drug for exercising their proven antioxidant effects. Also, the EGCG seems not prevent lipid peroxidation but seems to be more efficient preventing proteins oxidation. Overall, the use of the developed cationic loaded EGCG LNs and EGCG in the clinical treatment and management of DR stills unclear, sand more studies are needed to analyze the interference of EGCG with the enzymatic activity.

5.1. Introduction

The encapsulation of the major and powerful polyphenol found in green tea, epigallocatechin gallate (EGCG), in nanotechnology based lipid systems is rarely described particularly for ocular instillation. EGCG is being widely investigated due to the several effects on human health with proven beneficial effects, including anti-inflammatory (Cavet et al., 2011), anti-carcinogenic (Farabegoli et al., 2011; Hsu and Liou, 2011), antioxidant (Cavet et al., 2011), anti-angiogenic (Piyaviriyakul et al., 2011; Yamakawa et al., 2004), anti-diabetic (Chen et al., 2009; Wolfram et al., 2006), arthritis (Akhtar and Haqqi, 2011), cardiovascular (Wolfram, 2007) and neurodegenerative protector (Lee et al., 2015b). Despite the investigation of this drug is mainly associated with the oral administration, our purpose is the use of EGCG encapsulated in LN for ocular administration to prevent diabetic retinopathy (DR) by the antioxidant ability of this drug. The encapsulation of this drug is used with two major purposes; first, the stabilization of the drug to prevent its auto-oxidation and conversion in its degradation products with no equal pharmacologic activity (Fangueiro et al., 2014c) and second, the improvement of its bioavailability, which seems to be the great problem for its *in vivo* efficiency (Fangueiro et al., 2014b).

The use of EGCG to treat and manage DR is our strategy due to the oxidative stress environment present in the diabetic eye. DR is one of the diabetes mellitus consequences affecting the visual acuity due to the constant and sustained hyperglycemia causing damage to the vascular retinal vessels (Fangueiro et al., 2014d; Stitt et al., 2015).

EGCG is known as a powerful antioxidant with scavenger properties of reactive oxygen species (ROS), such as superoxide radical anion, peroxyl and hydroxyl radicals, singlet oxygen, nitric oxide and peroxynitrite, among others (Zhong et al., 2012). Some of these reactive species are implicated in the development of ocular diseases (Kowluru et al., 2006). The ROS are oxygen species with unpaired electron that can be generated during mitochondrial oxidative metabolism as well as in some cellular responses to external factors. The levels of ROS in cells are important and must be regulated since they are responsible for processes such as, regulation of apoptosis (Chandra et al., 2000) and cell signaling and proteins disulphide bond formation (Filomeni et al., 2002). Oxidative stress

happens due to the incapacity of the enzymatic and non-enzymatic antioxidant defense system to reverse ROS production resulting in an imbalance due to the excess of ROS (Calabrese et al., 2012). When the overproduction and consequent accumulation of ROS is not neutralized, several cellular consequences occurs, including the damage of molecules such as lipids and nucleic acids (deoxyribonucleic acid, DNA) which can lead to alteration of proteins expression (Cutler, 2005). The antioxidant defense system is comprised of intracellular antioxidants and enzymes, including superoxide scavenging enzymes, glutathione peroxidase and reductase (Kowluru and Mishra, 2015) (Figure 5.1). The increased oxidative stress developed in the retina in DR is consequence of some biochemical changes which leads to the functional and structural alterations in the retinal microvasculature (Fangueiro et al., 2014d). Thus, the use of antioxidant molecules could avoid some steps involving the oxidative stress developed in retinal cells and thus help to manage DR (Kowluru and Chan, 2007). Furthermore, since diabetes is a chronic disease, the constant metabolic stress leading to tissue damage stimulates the continuous free radical production (Shah, 2008). The several mechanisms that lead to this feature in the retina include the auto-oxidation of glucose, mitochondrial dysfunction, increased levels of ROS and insufficient capacity of the antioxidant defense system (Barot et al., 2011; Kowluru and Mishra, 2015). However, it is still not clear how these mechanisms lead to increased oxidative stress and to the development of DR.

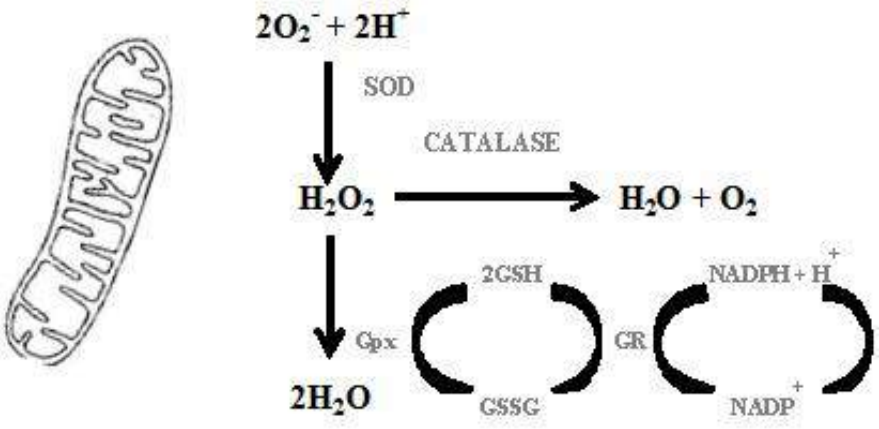

Figure 5.1. Schematic illustration of the mechanism by which the most important antioxidant enzymes contribute to the neutralization of free radicals in the cell's mitochondria (e.g. superoxide anion). SOD: superoxide dismutase; GSH: Glutathione

reduced; GSSG: Glutathione oxidized; GR: Glutathione reductase and Gpx: Glutathione peroxidase.

The decreasing intracellular antioxidant and increasing production of ROS in DR could be caused by the activation of the polyol pathway (that reduces glucose to sorbitol), which increases the NADPH (β-nicotinamide adenine dinucleotide 2'-phosphate reduced tetrasodium salt hydrate) consumption by aldose reductase, and consequently is associated with a decrease on reduced glutathione (GSH) levels leading to the increased formation of ROS (De Mattia et al., 1994). Also, the formation and accumulation of advanced glycation end-products (AGEs) caused by non-enzymatic glycation of biological proteins in retinal capillary induce permanent abnormalities in its extra- and intracellular function and, via their recognition by receptors, causes oxidative stress by depleting of GSH (Miller et al., 2006) and formation of ROS (Wu et al., 2010). Other mechanisms of AGEs are the activation of nuclear translocation factor-*k*B (NF-*k*B) and caspase-3, leading to apoptosis of the retinal capillaries (Cowell and Russell, 2004).

The formation of ROS can activate the protein kinase C (PKC) resulting in the loss of thiols and contribute to redox-mediated events (Gopalakrishna and Jaken, 2000). Additionally, the increased formation of ROS also interferes with many inflammatory mediators and leukocyte adhesion (Kern, 2007), since stimulate release of inflammatory cytokines via activation of NF-*k*B, increasing its levels in the retina and vitreous of patients with DR (Romeo et al., 2002). It has been suggested a bidirectional mechanism in the relation between ROS and cytokines, since cytokines stimulates the formation and are a source of ROS and ROS are a strong stimulus for the release of the cytokines (Chang and LoCicero, 2004; Padgett et al., 2013; Yang et al., 2007).

Overall, oxidative stress appears to be inter-related with the development of DR and its major metabolic abnormalities and the approach to reduce the metabolic stress in the retina with cationic EGCG-loaded LNs is our purpose for this study. There a lot of pharmacological strategies (Rechtman et al., 2007), however involves an intravitreal injection, which is an invasive route and also could cause some complications including vitreous hemorrhage, retinal detachment, or infections such as endophthalmitis (Sampat and Garg, 2010). Thus, the cationic EGCG-loaded LNs were produced to increased ocular

mucoadhesion due to their cationic nature by electrostatic attraction to anionic ocular mucosa and characterized to verify their physicochemical properties for ocular delivery. Further, cytotoxicity studies were carried out in retinoblastoma cell line, Y-79 and the activity of the most important enzymes involved in oxidative stress were analyzed, namely, superoxide dismutase (SOD), glutathione reductase (GR), glutathione-S-transferase (GST) and catalase (CAT).

5.2. Materials and methods

5.2.1. Materials

Epigallocatechin gallate (EGCG, 98% purity, molecular weight 458.7 g/mol and pKa 7.59–7.75) was purchased from CapotChem (Hangzhou, China). Softisan®100 (S100) was a free sample from Sasol Germany GmbH (Witten, Germany), Lipoid® S75, 75% soybean phosphatidylcholine was purchased from Lipoid GmbH (Ludwigshafen, Germany), Lutrol®F68 or Poloxamer 188 (P188) was a free sample from BASF (Ludwigshafen, Germany). Cetyltrimethylammonium bromide (CTAB) and ascorbic acid were acquired from Sigma-Aldrich (Sintra, Portugal). Dimethyldioctadecylammonium bromide (DDAB) was acquired from Avanti Polar Lipids (Alabama, USA). Anhydrous glycerol was purchased from Acopharma (Barcelona, Spain). Ultra-purified water was obtained from a MiliQ Plus system (Millipore, Germany). All reagents were used without further treatment.

The Y-79 human retinoblastoma cell line was purchased from Cell Lines Service (CLS, Eppelheim, Germany). Reagents for cell culture were from Gibco (Alfagene, Invitrogene, Portugal). Alamar Blue from Invitrogen Alfagene, Portugal was used for cell viability estimation.

Trichloroacetic acid was from AppliChem. All other reagents (for determination of enzyme activity, oxidized lipids content and oxidized proteins were obtained from Sigma: NADPH, GSH, GSSH (oxidized glutathione), NBT **(**3,3′-(3,3′-Dimethoxy-4,4′-biphenylene)bis[2-(4-nitrophenyl)-5-phenyl-2*H*-tetrazolium chloride]**),** CDNB (1-chloro-2,4-dinitrobenzene), hypoxanthine, glutathione reductase, xanthine oxidase, thiobarbituric

acid (TBA), BHT (2,6-di-tert-butyl-4-methylphenol/ butylatedhydroxytoluene), DTNB (5,5'-ditiobis(2-nitrobenzoate), sulfosalicilyc acid, BSA (bovine serum albumin) and salts for buffer solutions.

5.2.2. Cationic LNs production

Cationic LN dispersions were prepared based on a previous developed multiple emulsion (w/o/w) technique described by our group (Fangueiro et al., 2014a; Fangueiro et al., 2014b). EGCG and ascorbic acid were dissolved in ultra-purified water, which was added to the lipid phase at same temperature (5 ºC to 10 °C above the melting point of lipid S100) and homogenized 60 s with a sonication probe (6 mm diameter) by means of an Ultrasonic processor VCX500 (Sonics, Switzerland). A power output with amplitude of 40 % was applied. The poloxamer solution was added and homogenized for additional 90 s. This pre-emulsion was poured in the total volume of poloxamer cooled solution under magnetic stirring for 15 min to allow the formation of the LN. The obtained LN dispersions were used for subsequent studies.

5.2.3. Physicochemical characterization

The physicochemical parameters Z-Ave (mean particle size), PI (polydispersity index) and ZP (zeta potential) were determined by dynamic light scattering (DLS, Zetasizer Nano ZS, Malvern Instruments, Malvern, UK). All samples were diluted with ultra-purified water to suitable concentration and analysed in triplicate. For the determination of the ZP an ultra-purified water with conductivity) adjusted to 50 µS/cm was used. Laser diffraction (LD) was performed for particle size analysis by a Mastersizer Hydro 2000 MU (Malvern Instruments, Malvern, UK).

5.2.4. Equipment

The equipment used for absorbance readings were a spectrophotometer Varian Cary 50 using Kinetics mode for enzyme kinetics (Varian). Absorbance reading for protein quantification, thiobarbituric acid reactive substances (TBARS) quantification and cell viability evaluation were recorded using a Multiskan EX microplate reader (MTX LabSystems, USA). For estimation of oxidized proteins, absorbance was recorded using a BioTekPowerWave X52 microplate reader.

5.2.5. Cell viability determination by Alamar blue assay

Y-79 (Human retinoblastoma cell line) cells were used to perform the viability assay, as previously reported (Fangueiro et al., 2014a), in which five different samples were tested. The five samples were i) CTAB-LNs, ii) DDAB-LNs, iii) EGCG solution, iv) CTAB-loaded EGCG LNs, and v) DDAB-loaded EGCG LNs. Each formulation was tested at four concentrations (in $\mu g.mL^{-1}$ for EGCG concentration, respectively): 10, 25, 50 and 100. Y-79 cells were maintained in RPMI-1640, supplemented with 10% (v/v) fetal bovine serum (FBS), 2 mM l-glutamine, and antibiotics (100 $U.mL^{-1}$ penicillin and 100 $\mu g.mL^{-1}$ of streptomycin) in an atmosphere of 5% CO_2 in air at 37 ºC. As Y-79 cells are non-adherent cells, we performed the experiments on previously coated 96-well plates. Briefly, a solution of 100 $\mu g.mL^{-1}$ of poly-L-lysine (Sigma, Portugal) in borate buffer (0.15 M, pH 8.4) was prepared, an amount of 30 µL was added per well and, after 1 h, this solution was removed and the 96-well plates was washed with autoclaved deionized water. After drying, the 96-well plates (or T75 flasks) were ready to receive the cells. The entire procedure was performed in the laminar flow cabinet. Y-79 cells that grow in aggregates were gently dispersed, using a Pasteur pipette, then counted and diluted to a density of $1x10^5$ $cell.mL^{-1}$ and plated (100 µL per well). After 24 hours of culture, the culture media was removed and replaced by FBS-free culture media containing the different samples to test at the selected concentrations. Exposure of 24 h and 48 h was performed, before assaying the cell viability with Alamar Blue.

Cell viability was assayed with Alamar Blue (Invitrogene, Alfagene, Portugal), as previously reported (Andreani et al., 2014). Briefly, after 24 h or 48 h of exposure, the incubating media was removed and replaced by FBS-free culture media supplemented with Alamar Blue 10% (v/v), 100 µL to each well. The absorbance at 570 nm (reduced form) and 620 nm (oxidative form) was read 4 h after addition of the Alamar Blue solution. Data were analysed by calculating the percentage of Alamar blue reduction (according to the manufactures recommendation and as previously reported (Andreani et al., 2014; Fangueiro et al., 2014a), and expressed as percentage of control (untreated cells).

5.2.6. Determination of enzyme activity

Y-79 cells were seeded on previously poly-L-lysine coated culture flasks (75 cm^2, Orange Scientific). The coating was as described above, but using 3 mL of poly-L-lysine solution per flask. Y-79 cells were added to the flasks ($8x10^6$ cells per flask) and allowed to adhere for at least 24 h, and then were exposed to the samples in appropriate concentration. After 24 h of exposure, the media was removed, cells were washed twice with PBS and then the cells were harvested, lysed in 3.0 mL RiPa buffer (150 mM NaCl, 50 mM Tris, 0.1% (w/v) SDS, 1.0% (v/v) Triton, 0.5% (w/v) deoxycholic acid; pH 7.4), on ice, and the pellet was separated from the supernatant by centrifugation (3500 rpm, 15 min, Sigma 2-6E centrifuge). Activity of enzymes was determined in the supernatant, as described before (Doktorovova et al., 2014). All activities were determined in triplicate for each treatment. Five samples at two different concentration were tested (*n=3,* for each condition).

5.2.6.1. Superoxide dismutase activity

Activity of superoxide dismutase (SOD) was determined indirectly by nitroblue tetrazolium-formazan (NBT-diformazan) reduction after xanthine conversion by xanthine oxidase (Payá et al., 1992). Xanthine-xanthine oxidase is used to generate O_2 and NBT reduction is used as an indicator of O_2 production. SOD will compete with NBT for O_2. (Weydert and Cullen, 2010). Quantity of NBT-formazan was estimated by monitoring changes in absorbance at 560 nm during 2 min. The values are expressed as % inhibition of NBT-diformazan formation, represent a relative % of inhibition of NBT-diformazan formation, values were calculated using the following equation:

$$\left[\left(\frac{\left(A_{control} - A_{\ test}\right)}{A_{control}} x100\right)\right]$$

Where A is the rate of NBT-diformazan formation during the assay. Test values were always normalized for the quantity of protein present (*Δ*Abs/ min/mg of protein) (Doktorovova et al., 2014).

5.2.6.1.1. Glutathione reductase activity

The activity of glutathione reductase (GR) evaluated using the consumption of NADPH (GR substrate) was determined by measuring the absorbance of the reaction media at 340 nm, in the presence of excess GSSG (Carlberg and Mannervik, 1985).

5.2.6.1.2. Glutathione *S*-transferase activity

Activity of glutathione S-transferase (GST) was estimated by monitoring the production of Gs-CDNB (CDNB, 1-chloro-2,4-dinitrobenzene) conjugate, catalyzed by GST, at A340 (Hayes et al., 2005). Enzyme activity was normalized to protein content.

5.2.6.1.3. Catalase activity

Catalase (CAT) activity was based in a direct assay with pseudo-first order kinetics measuring peroxide removal by a spectrophotometric procedure. This method is based on Beers and Sizer method (Beers and Sizer, 1952). The rate of peroxide removal by CAT is exponential and H_2O_2 is consumed. CAT activity was measured by monitoring the absorbance of the reaction at 240 nm.

5.2.7. Determination of protein content

Protein content, in the samples, was analyzed by the Bradford method (Bradford, 1976), using BSA as standard for calibration. Thus, 100 µl of Bradford reagent (containing 0.01% (w/v) Coomassie brilliant blue, 4.7% (v/v) ethanol (95%) and 8.5% (w/v) phosphoric acid) was added to 100 µl diluted samples. Protein quantification was determined using absorbance at 590 nm.

5.2.8. Determination of thiobarbituric acid reactive species

Determination of quantity of species reactive with thiobarbituric acid (thiobarbituric acid reactive species, TBARS) was used to estimate lipid peroxidation following a modified method by Buege and Aust (Buege and Aust, 1978). Lipid peroxidation lead to alterations in membranes contributing to cells disorders regarding their permeability, by changing the ionic flow, resulting in the loss of selectivity for input and/or output of nutrients and substances toxic to the cell. Other disorders include alterations on the genetic material,

oxidation of lipoproteins (low density proteins) and involvement of extracellular matrix components such as proteoglycans, collagen and elastin (Yajima et al., 2009). In the technique performed 300 µL of sample was mixed with 2.50 mL of reagent mixture consisting of 0.375% (w/v) of TBA, 15% (w/v) of trichloroacetic acid and 0.25 M hydrochloric acid. The 2,6-di-*tert*-butyl-4-methylphenol (butylatedhydroxytoluen, BHT) was added to the reagent immediately before use in final concentration of 0.01% (w/v). The mixture was heated to 95 °C during 15 min, let cool down to room temperature and submitted to centrifuge. Quantity of malondialdehyde (MDA)-TBA complex was determined from the absorbance reading at 540 nm in the supernatant. The results are expressed as nmol TBARS per milligram protein. TBARS were quantified in triplicates for each treatment and cell passage (*n=4*) (Doktorovova et al., 2014).

5.2.9. Determination of oxidized proteins

Quantity of sulfhydryl groups was estimated by a method originally described by Ellman with further modifications (Sedlak and Lindsay, 1968; Suzuki et al., 1990). 400 µL of sample was mixed with 1.0 mL of 4% sulfosalicylic acid followed by vigorous shaking. The dispersion was centrifuged (4500 rpm, 30 min, 20 °C, Hettich Universal 320R Centrifuge), the supernatant was discarded and the pellet was re-suspended in 1.0 mL of phosphate buffer. 350 µL of re-suspended pellet was mixed with 50 µL DTNB. Absorbance at 412 nm was read after 20 min of mixture incubation in the dark. The results are expressed as nmol protein thiol content per mg protein. Sulfhydryl groups were quantified in duplicate for each treatment and cell passage (*n*=4 independent experiments, for each condition) (Doktorovova et al., 2014).

5.2.10. Statistical analysis

Statistical evaluation of data was performed using one-way analysis of variance (ANOVA). The Bonferroni and Tukey multiple comparison test was used to compare the significance of the difference between the groups, a p-value < 0.05 was accepted as significant. Data were expressed as the mean value ± standard deviation (Mean ± SD) of *n* experiments as indicated.

5.3. Results and discussion

The production of blank-LNs were based in a previous 3^3 full factorial design (Fangueiro et al., 2014a) and the encapsulation of EGCG revealed to not alter significantly the physicochemical properties of the LNs (Fangueiro et al., 2014b), see (Table 5.1). The analysis by DLS revealed particles under 150 nm with a relatively narrow distribution (>0.25). The use of cationic lipids, such as CTAB and DDAB, contributed to the high positive ZP values. This strategy is not only to promote particles stability as also to induce mucoadhesion of the LN dispersions in the ocular mucosa by electrostatic attraction (Fangueiro et al., 2014b). The results of LD also revealed a mean particle size in the nanometre range varying between 115 nm and 153 nm (Table 5.1). Thus, the results of LD and DLS are concordant, since revealed practically the same data by different techniques. The use of these techniques is very important to control the size of nanoparticles produced for ocular delivery, due to the sensible route of administration that requires a very controlled production.

Table 5.1. Analysis by dynamic light scattering (DLS) indicating the mean particle size (Z-Ave), polydispersity index (PI) and zeta potential (ZP) and by laser diffraction (LD) of LN dispersions. The results are expressed as mean ± S.D. (n = 3).

Formulation	DLS			LD
	Z-Ave (nm)	PI	ZP (mV)	d50 (nm)
CTAB-LN	135.1 ± 0.22	0.196 ± 0.018	28.20 ± 1.33	118.3 ± 0.04
EGCG CTAB-LN	149.1 ± 1.779	0.24 ± 0.008	20.80 ± 0.896	153.0 ± 0.01
DDAB-LN	134.2 ± 1.12	0.179 ± 0.067	28.20 ± 2.29	119.8 ± 0.01
EGCG DDAB-LN	143.7 ± 0.450	0.16 ± 0.015	25.70 ± 1.42	115.0 ± 0.00

LN dispersions cytotoxicity was assessed in human retinoblastoma cell line, Y-79, and observed during 24 h and 48 h of exposure (Figure 5.2). This evaluation is an important parameter during the development and optimization of drug delivery systems. The technique used was the Alamar blue assay, it evaluates the cellular damage caused by the loss of the metabolic cell function measuring quantitatively the proliferation of the cells (cell viability) by the establishment of the toxicity of tested agents/drugs (Fangueiro et al.,

2014a). From Figure 5.2, we can observe that all formulations revealed to induce a decrease on cell viability, revealing a degree of toxicity, for all formulations and also for all EGCG concentrations, that a statistically difference ($p < 0.05$) relatively to the control (untreated cells), along the 2 time-points of exposure (24 h and 48 h). It is noteworthy that LNs containing CTAB (both encapsulated (figure 5.2A) and non-encapsulated (figure 5.2D) are more toxic than DDAB containing particles (figure 5.2B and 5.2E). The CTAB-LNs (figure 5.2A and 5.2D) reduces cell viability in about 70-80% of the control, while the DDAB made LNs (Figure 5.2B and 5.2E) varies its effects in about 20 to 80%. In other studies, delivery systems containing CTAB proved to be more toxic than DDAB (Cortesi et al., 1996; Tabatt et al., 2004). The different structure of both cationic lipids could be associated with the related toxicity expressed. CTAB is a single-tail lipid while DDAB is a double-tail lipid, and according with literature the single-tail cationic agents/lipids are more toxic than the others (Pinnaduwage et al., 1989; Tabatt et al., 2004).

Comparing the same concentration, at 24 h and 48 h of exposure, there are no statistical differences ($p < 0.05$) concerning to exposure time, however the results showed that increasing concentration of blank-LNs (either CTAB or DDAB containing particles) reduces cell tolerance, revealing the harmful effects of cationic agents in these ocular cell lines. CTAB and DDAB are detrimental for cell survival, and seems to increase the cytotoxicity of these lipid-based delivery systems (Marcato and Durán, 2014). In other previous study performed by our group (Fangueiro et al., 2014a), it was detectable the dependency of CTAB concentration in Y79 cells viability, revealing that higher concentrations leads to higher toxicity. Additionally, it is important to refer that CTAB-LNs (figure 5.2D) are more toxic than EGCG-CTAB LNs (figure 5.2A) for concentration of 10 and 25 $\mu g.mL^{-1}$, which for the DDAB based LNs is the maximum concentration used (100 $\mu g.mL^{-1}$). Somehow, the EGCG seems to protect the effects of CTAB on cells and it is visible from the figure 5.2A that EGCG-CTAB LNs produced a decrease on cell toxicity with the increase EGCG concentration (as is shown by an increase on cell viability). The same results are found in EGCG-DDAB LNs (figure 5.2B), which means that EGCG seems to protect the cell against cellular damage promoted by the LNs formulations containing cationic lipids. Thus, attending to our results it seems that EGCG

increases retinoblastoma cell survival in a stress environment promoted by these cationic lipids promoting a protective effect.

The EGCG solution (figure 5.2C) was the less toxic to Y79 cells. Although the cell viability decreases to the higher concentrations, the decrease is lower than the rest of the formulations, EGCG showed increasing toxicity with the highest concentrations tested (50 and 100 $\mu g.mL^{-1}$), namely reduction in about 50-70% compared with untreated cells. It is possible to detect a concentration-dependency of EGCG, since higher EGCG concentration presents higher cytotoxicity, which is in accordance with other studies (Collins et al., 2007; Farabegoli et al., 2007). Thus, an antioxidant effect of EGCG is detected for lower concentrations and pro-oxidant activity for higher concentrations. Also, a study reported the use of high concentrations (>50 μM) of EGCG seems to have cytotoxic effects due to the formation of ROS, namely hydroxyl radicals (Nakagawa et al., 2004; Nakagawa et al., 2002). This could be associated with the anti-proliferative and apoptotic effects in human cells, highlighting its potential anti-carcinogenic effect, already described in several cells, such as neuroblastoma (Chung et al., 2007), oral carcinoma (Babich et al., 2005; Lee et al., 2015a; Weisburg et al., 2004), colon cancer cells (Saldanha et al., 2014), HepG2-cells, liver hepatocellular carcinoma cell line (Shan et al., 2014), A549 cells, human lung cancer cell line (Yamauchi et al., 2009), MCF-7 breast cancer cells (Ranzato et al., 2014), among others.

It is noteworthy that cancerous cells are more sensitive to oxidative stress than the normal cells (Weisburg et al., 2004). In order to evaluate the effect of exposure to these formulations, in terms of antioxidant defense; we also evaluated the enzymatic activity of the main enzymes of cellular stress defense, using Y-79 cells pre-exposed to the formulations developed and to EGCG solution.

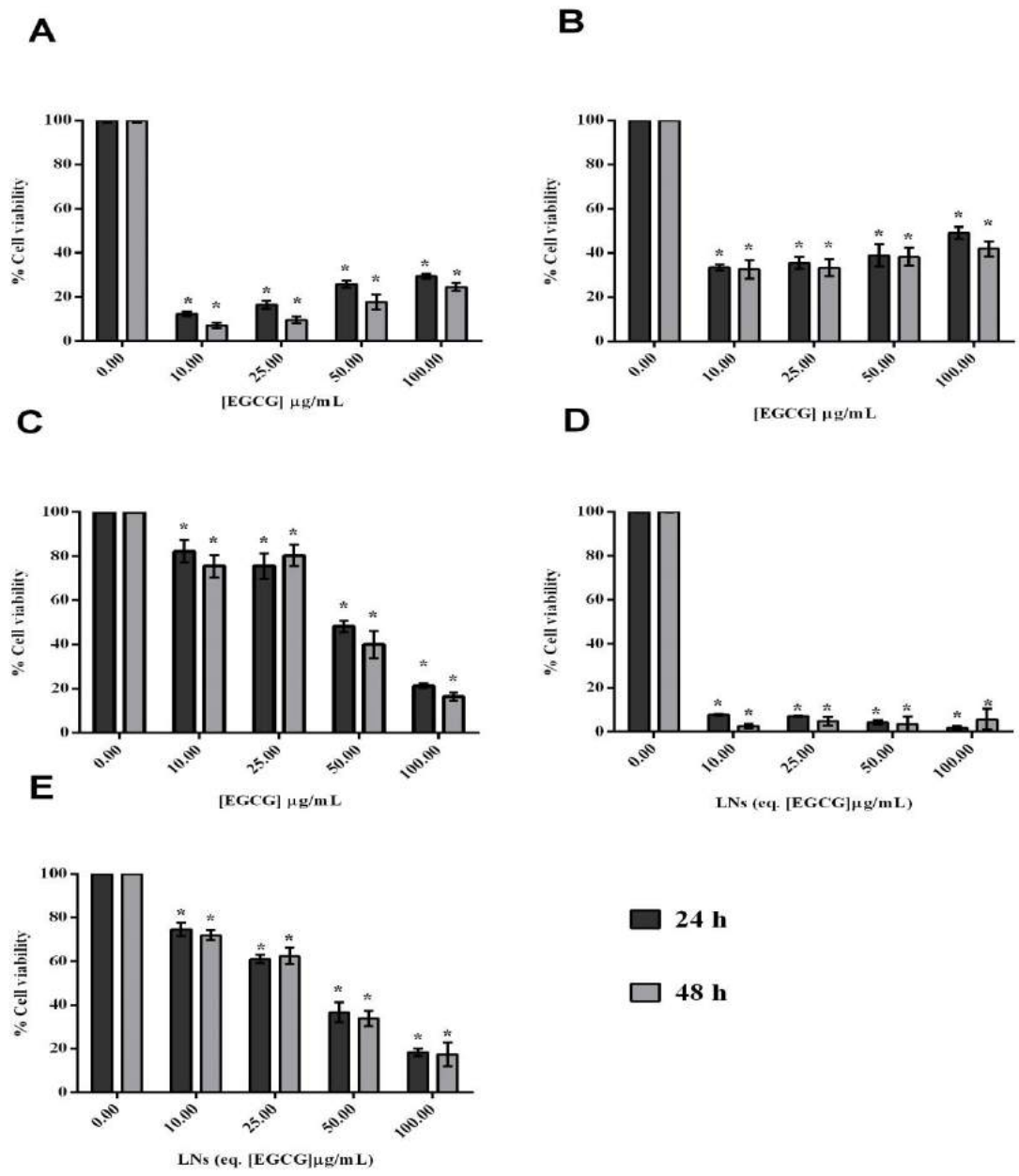

Figure 5.2. Effect of LN dispersions on Y-79 human retinoblastoma cells viability (*n = 6*) after 24 h and 48 h of exposure. Concentrations are given as the content of EGCG in NPs formulation, (A) EGCG-CTAB LNs and (B. EGCG-DDAB LNs; or in solution (C) EGCG solution. For the empty LNs, the amount is given as the equivalent of A and B for the respective formulations, being (D) CTAB-LNs and (E) DDAB-LNs. Results were compared with the control (untreated cells), being **p-value* < 0.05.

The influence of LN dispersions developed and EGCG on selected enzymes is graphically depicted in Figure 5.3. Due to the lack of information regarding these nanocarriers in Y-79 human retinoblastoma cells, our goal was to observe how the LNs dispersions and EGCG solution affects the most important enzymes of the antioxidant defense system against the oxidative stress. Briefly, SOD activity (Figure 5.3A) was decreased in about 50% for all conditions, except for DDAB-LNs at two tested concentrations (10 and 50 μg/mL). The ANOVA analysis also indicates that the effect of these formulations were the only that were not statistically significant, in relation to the control. SOD is one of the most important enzymatic defenses against the formations of ROS and acts protecting the cell from superoxide toxicity. Thus, the decreased SOD activity is a signal of oxidative stress, namely bthe presence of superoxide anion, which induces cell damage regarding its DNA, lipids and proteins (Alam et al., 2013). The CTAB, as expected, is an inducer of oxidative stress since the formulations based on CTAB also decreased cell viability (Figure 5.2). Other studies revealed the same results in other type of cells for CTAB (Nakata et al., 2011) and LNs based on CTAB (Doktorovova et al., 2014).

Regarding to the CAT activity (Figure 5.3B), the most concentrated formulations (50 μg/mL) produce statically significant results and were able to interfere more with its activity causing its decrease. As showed for SOD, the DDAB-LNs at the two tested concentrations (10 and 50 μg/mL) were the only that seems not to interfere so much with CAT activity. The primary enzymatic defenses against ROS production are SOD and CAT and if these two enzymes have a decreased activity it seems that the production of ROS is occurring in the cells but at lower levels, as these enzymes have the capacity to neutralize those molecules or that these formulations have the capacity to alter the structure of the enzyme leading to a decreased activity. The biochemical alterations induced by high level of ROS leads to cell death by apoptosis (Michiels et al., 1994).

The GR activity (Figure 5.3C), in general, also decreased for all conditions tested, however the same formulations (DDAB-LNs 10 and 50 μg/mL) were those less affected on its activity. ANOVA analysis indicate differences between the conditions tested and the control (Figure 5.3C*). The decreased GR activity also comprises the GSSG accumulation and decreases the GSH/GSSG ratio (Figure 5.1). This event leads to the accumulation of ROS and induction of apoptosis to the cells (Circu and Aw, 2012). Thus,

the decreased activity detected in retinoblastoma cells can be a sign of evident oxidative stress, mostly detected after exposure to CTAB based LNs.

The GST activity (Figure 5.3D), in general, also decreased for all conditions tested, being more evident at the higher concentrations for all conditions. GST is mainly involved in conjugation of lipophilic electrophilic compounds with sulfhydryl groups preventing the interaction of ROS with proteins and nucleic acids (Habig et al., 1974). Thus, the most concentrated LNs and EGCG solution decreased the activity of this enzyme which could induce an increased oxidation of lipids and proteins leading to cell damage and consequent death.

Overall, it is possible to observe that EGCG affects the antioxidant activity of the majority of enzymes (Figure 5.3) and, according with the cell viability results (Figure 5.2C), there is also a concentration dependency. This means that higher EGCG concentrations lead to higher cytotoxicity and also higher inhibition of enzymatic activity. As explained above, this could be related with the cytostatic effect of this polyphenol, which leads to the death of cancerous cells. Also, EGCG is a hydrophilic molecule with many hydroxyl groups in its structure, that easily chelates with metal ions (Hatcher et al., 2009) and somehow this could interact with the enzymatic co-factors of the enzymes (Cu^{2+} and Zn^{2+}, for SOD, and Fe^{2+} for CAT) and interact with the activity of these enzymes. Despite the mechanisms of action of EGCG is not completely understood, there is a clearly evidence of its potential effect in cancer cells mainly associated with its antioxidant properties and for human retinoblastoma cells is also observed (Figure 5.3). A recent study revealed the possibility of EGCG destabilizes the membrane by direct pore formation (Lorenzen et al., 2014). More recent findings suggest many additional mechanisms of action for EGCG including the deregulation of $[Ca^{2+}]$ in cells (Ranzato et al., 2014), interactions with plasma membrane proteins (Zhang et al., 2012), activation of second messengers and signal transduction pathways (Kim et al., 2007; Song et al., 2014; Valenti et al., 2013a; Valenti et al., 2013b), modulation of metabolic enzymes (Kumazoe et al., 2013), and autophagy (Kim et al., 2013).

Additionally, it is possible to detect the difference between the two cationic lipids on these cells. Regarding the viability and enzymatic activity, DDAB is less toxic and

inhibitor of activity than CTAB. CTAB cytotoxicity could be associated with the interaction with the phospholipid bilayer leading to the cell membranes destabilization and death. Another possibility is the formation of CTA^+ cation, one of CTAB's dissociation products from the catalytic action, might cause the quenching of the enzyme adenosine triphosphate- (ATP)-synthase and thus lead to energy deprivation and death of the cell (Schachter, 2013). DDAB cytotoxicity seems to be dependent in the capacity to induce cell apoptosis in several cancer lines, such as leukemia, intestinal and liver cells, suggesting that DDAB can induce caspase-mediated apoptosis triggering caspase-3-mediated apoptosis through the extrinsic caspase-8 pathway and cytotoxic pore formation in cell membrane (Kusumoto and Ishikawa, 2010).

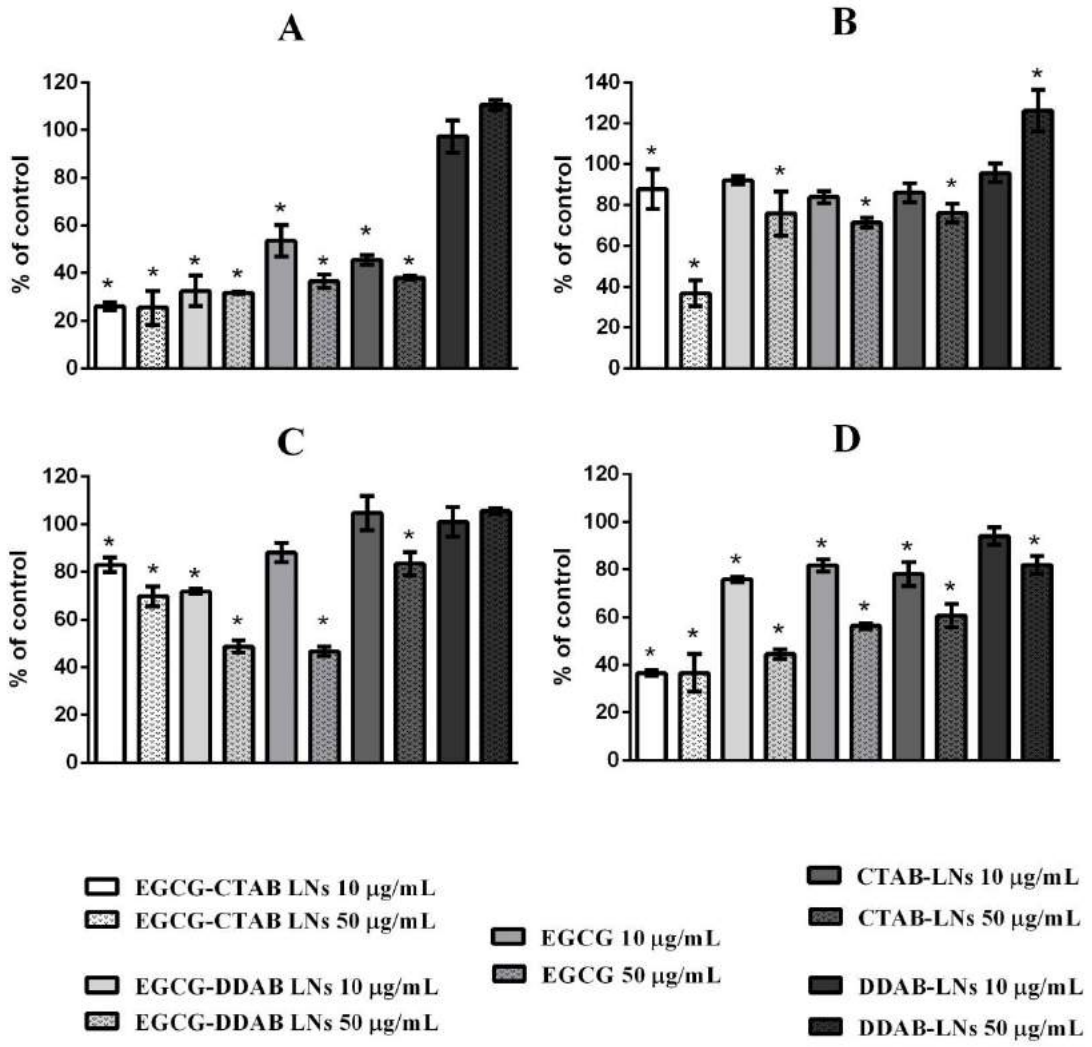

Figure 5.3.. Effect of LN dispersions and EGCG on the activity of the antioxidant enzymes SOD (A), CAT (B), GR (C) and GST (D). Data are presented as % of activity of respective enzyme on untreated control, with standard error of the mean, calculated from various measurements (min. 2) per each passage of cells (*n = 4*). **p-value* < 0.05 means results that are significantly different from control.

The analysis of TBARS and sulfhydryl groups on Y-79 human retinoblastoma cells after exposure to LNs and EGCG is depicted on Figure 5.4A and 5.4B, respectively. These two techniques are often applied for the evaluation of oxidative stress, more specifically as a conseuquence of ROS formation. ROS have a reduced half-life and these indirect techniques are applied to detect the influence of them in cells (Pizzimenti et al., 2013).

The control corresponding to the untreated cells contained 11.63 nmol TBARS/mg protein and all conditions tested were statistically significant (*p-value < 0.05). All conditions demonstrated increased production of TBARS except for the DDAB-LNs, which showed decreased production of TBARS than the control (figure 5.4A). TBARS are end products formed by decomposition of lipid peroxidation, which indicates the destruction of cellular lipids (Pizzimenti et al., 2013). The exposure of cells to the formulations seems to interfere with the cellular lipids, enhancing its peroxidation. These results indicate that cells were subjected to oxidative stress, which is caused by a cascade of biochemical processes caused by the overproduction of ROS. This could lead to several damages to the cells, including cell death or dysfunction (Pizzimenti et al., 2013). EGCG that is a powerful antioxidant molecule seems not to be able to protect the lipid peroxidation on Y-79 cells according with the results depicted in figure 5.4A, at the tested concentrations. The effect of EGCG in other cells, such as erythrocytes (Saffari and Sadrzadeh, 2004), macular retinal pigment epithelial (RPE) cells (Li et al., 2013), human corneal cells (Cavet et al., 2011), intestinal Caco-2 cells (Peng and Kuo, 2003), has been described to protect lipid peroxidation and as being effective against oxidative stress, however our results in retinoblastoma cells seems to show the contrary of the other cells. The lack of other comparative reports in this type of retinoblastoma cells, and also with this type of nanometre formulations make the comparison difficult to assess. However, a study in this type of cells reported an enhanced lipid peroxidation in these cells treated with lipid enzymes inhibitors, causing apoptosis of these cells (Vandhana et al., 2013). Additionally, other study revealed the susceptibility of these cells to oxidative stress due to the high ROS levels founded and reduced antioxidant gene expression for tumors that invade the choroid, optic nerve and RPE (Vandhana et al., 2012).

The DDAB-LNs were the only formulation at the two tested concentrations (10 and 50 μg/mL) that were able to protect against cellular lipids against peroxidation. This could be associated with the facility of the double chain composing this cationic lipid integrates more easily with the cellular lipids and somehow can protect them. This also can be related with the high lipophilicity of this formulation than the others, since DDAB has a double chain and CTAB a single chain, is noteworthy the higher lipophilicity of this formulation. Also, as mention above, EGCG is a hydrophilic molecule, that chelates

easily with metal ions and due to its hydrophilic character, could not interact easily with the cellular lipids and is not able to protect them in this type of cells. Some strategies involving the esterification of EGCG with aliphatic fatty acids are been investigated to increase its lipophilicity (Wang et al., 2016). Regarding the sulfhydryl groups content that can be translated with the proteins oxidation, is also a technique to indirectly detect ROS formation since the oxidative damage lead to the decrease of contents of membrane protein thiol groups (Wang et al., 1999). From our results, all conditions were also statistically significant (*p-value < 0.05), with exception for EGCG solution at both concentrations tested (10 and 50 μg/mL) (Figure 5.4B). Although, the formulations EGCG-CTAB and EGCG-DDAB and CTAB-LNs recorded lower sulfhydryl groups formation comparatively to control, EGCG solution and DDAB-LNs at both concentrations tested were able to increase the sulfhydryl groups formation (Figure 5.4B). This means that EGCG was not able to prevent lipid peroxidation (Figure 5.4A) in Y-79 retinoblastoma cells, but did not affect oxidation of proteins. On the other hand, DDAB-LNs prevented oxidation of proteins and seem to be the most relevant formulation to prevent oxidative stress, despite not loaded with EGCG. Thus, it seems that DDAB-LNs seems to act as antioxidant preventing the formation of oxidized proteins. Since hyperglycemia can accelerate proteins oxidation and glycation with subsequent AGEs formation (Wu et al., 2009), the inhibitory effect of LNs and EGCG could be useful for DR treatment. A study performed by Wu and co-workers (Wu et al., 2010), revealed the ability of EGCG bind to lipoproteins and facilitates their antioxidant and antiglycation activity, which could be the explanation for the protection effect of this molecule non-encapsulated, however when encapsulated it is not able to promote a protective effect in the proteins. Thus, the enhanced ROS formation leads to the enhanced protein oxidation inhibiting the normal function of cells promoting its damage and consequent death (Squier, 2001).

Cellular lipids and proteins oxidation can be related with the activity of the enzymes since any damage to the membranes and signaling proteins will result in decrease in their activity and consequently in antioxidant protection (Circu and Aw, 2012; Wang et al., 1999). Thus, the decrease and inhibitory activity of certain enzymatic defenses, namely SOD and CAT in the LNs formulations tested seems to have a complementary effect on

lipid peroxidation, contributing to the enhanced cellular lipids damage. As the results in Figure 5.3 indicates, the activity of SOD (Figure 5.3A) was highly affected by all conditions, excepting DDAB-LNs, which affects also the lipid and proteins oxidation due to the ineffective enzymatic protection during the production of ROS. Also, the GR and GST activity (Figure 5.3C and 5.3D, respectively) was also affected increasing the interaction of GSSG with reactive cysteines of proteins to form mixed disulphides and also allowing the interaction of ROS with proteins, leading to its oxidation.

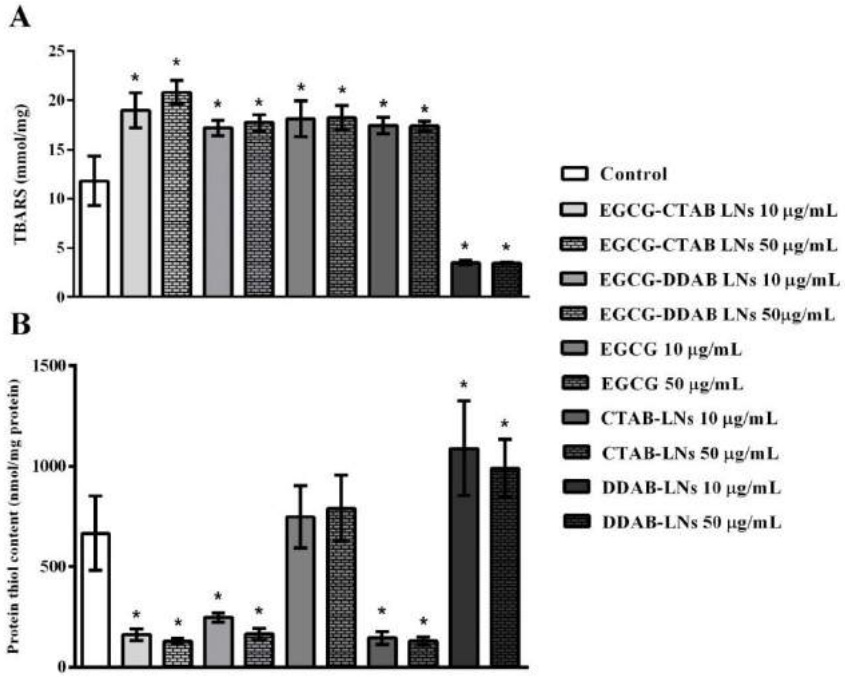

Figure 5.4. Determination of (A) TBARS and (B) of sulfhydryl groups in Y-79 cells treated with LNs developed and EGCG (the legend is ordered top to down according to with bars indicated from the left to right). Each condition was tested for two concentrations, namely 10 and 50 μg/mL of EGCG or equivalent. Data are presented as % of TBARS/Protein thiol content normalized to protein content found in untreated cells, **p-value* < 0.05.

5.4. Conclusions

Overall, the results suggest that cationic LNs developed interfere with cellular viability of y-79 human retinoblastoma cells, being the formualtions composed by CTAB able to

promote more cellular damage. The activity of EGCG is concentration dependent, being this molecule antioxidant for lower concentrations and pro-oxidant for higher concentrations used. Additionally, the cellular enzymatic defense against oxidative stress was affected by the exposure to EGCG and cationic LNs, and oxidized proteins and lipids were enhanced, with exception for DDAB-LNs. It is possible to detect a tendency in the formulations that encapsulate EGCG and the EGCG solution in being ineffective against the oxidative stress, however the DDAB-LNs which are composed of the most safe cationic lipid and without EGCG seems to have a powerful capacity of enzymatic protection regarding the cell viability, antioxidant enzymatic activity and protection against lipids and proteins oxidation. This could be associated with the chelating effect of EGCG with the enzymatic co-factors of the enzymes, leading to a lower availability of the drug for exercising their proven antioxidant effects.

Consideration of the use of the developed cationic loaded EGCG LNs and EGCG in the clinical treatment and management of DR needs to be more studied, since our preliminary studies indicate an interference with the cell viability, antioxidant enzymatic activity with consequent proteins and lipids oxidation and formation of ROS indicating oxidative stress.

5.5. Bibliographic References

Akhtar, N., and Haqqi, T. M. (2011). Epigallocatechin-3-gallate suppresses the global interleukin-1beta-induced inflammatory response in human chondrocytes. *Arthritis Research and Therapy,* 13(3), R93.

Alam, M. N., Bristi, N. J., and Rafiquzzaman, M. (2013). Review on in vivo and in vitro methods evaluation of antioxidant activity. *Saudi Pharmaceutical Journal,* 21(2), 143-152.

Andreani, T., Kiill, C. P., Souza, A. L. R. d., Fangueiro, J. F., Fernandes, L., Doktorovová, S., Silva, A. M. (2014). Surface engineering of silica nanoparticles for oral insulin delivery: Characterization and cell toxicity studies. *Colloids and Surfaces B: Biointerfaces,* 123, 916-923.

Babich, H., Krupka, M. E., Nissim, H. A., and Zuckerbraun, H. L. (2005). Differential in vitro cytotoxicity of (−)-epicatechin gallate (ECG) to cancer and normal cells from the human oral cavity. *Toxicology in Vitro,* 19(2), 231-242.

Barot, M., Gokulgandhi, M. R., and Mitra, A. K. (2011). Mitochondrial dysfunction in retinal diseases. *Current Eye Research,* 36(12), 1069-1077.

Beers, R. F., Jr., and Sizer, I. W. (1952). A spectrophotometric method for measuring the breakdown of hydrogen peroxide by catalase. *Journal of Biological Chemistry,* 195(1), 133-140.

Bradford, M. M. (1976). A rapid and sensitive method for the quantitation of microgram quantities of protein utilizing the principle of protein-dye binding. *Analytical Biochemistry,* 72(1), 248-254.

Buege, J. A., and Aust, S. D. (1978). Microsomal lipid peroxidation. *Methods in Enzymology,* 52, 302-310.

Calabrese, V., Cornelius, C., Leso, V., Trovato-Salinaro, A., Ventimiglia, B., Cavallaro, M., Castellino, P. (2012). Oxidative stress, glutathione status, sirtuin and cellular stress response in type 2 diabetes. *Biochimica et Biophysica Acta (BBA) - Molecular Basis of Disease,* 1822(5), 729-736.

Carlberg, I., and Mannervik, B. (1985). Glutathione reductase. *Methods in Enzymology,* 113, 484-490.

Cavet, M. E., Harrington, K. L., Vollmer, T. R., Ward, K. W., and Zhang, J. Z. (2011). Anti-inflammatory and anti-oxidative effects of the green tea polyphenol epigallocatechin gallate in human corneal epithelial cells. *Molecular Vision,* 17, 533-542.

Chandra, J., Samali, A., and Orrenius, S. (2000). Triggering and modulation of apoptosis by oxidative stress. *Free Radical Biology* and *Medicine,* 29(3-4), 323-333.

Chang, C. K., and LoCicero, J., 3rd. (2004). Overexpressed nuclear factor kappaB correlates with enhanced expression of interleukin-1beta and inducible nitric oxide synthase in aged murine lungs to endotoxic stress. *The Annals of Thoracic Surgery,* 77(4), 1222-1227.

Chen, N., Bezzina, R., Hinch, E., Lewandowski, P. A., Cameron-Smith, D., Mathai, M. L., Weisinger, R. S. (2009). Green tea, black tea, and epigallocatechin modify body composition, improve glucose tolerance, and differentially alter metabolic gene expression in rats fed a high-fat diet. *Nutrition Research,* 29(11), 784-793.

Chung, W. G., Miranda, C. L., and Maier, C. S. (2007). Epigallocatechin gallate (EGCG) potentiates the cytotoxicity of rotenone in neuroblastoma SH-SY5Y cells. *Brain Research,* 1176, 133-142.

Circu, M. L., and Aw, T. Y. (2012). Glutathione and modulation of cell apoptosis. *Biochimica et Biophysica Acta (BBA) - Molecular Cell Research,* 1823(10), 1767-1777.

Collins, Q. F., Liu, H. Y., Pi, J., Liu, Z., Quon, M. J., and Cao, W. (2007). Epigallocatechin-3-gallate (EGCG), a green tea polyphenol, suppresses hepatic gluconeogenesis through 5'-AMP-activated protein kinase. *Journal of Biological Chemistry,* 282(41), 30143-30149.

Cortesi, R., Esposito, E., Menegatti, E., Gambari, R., and Nastruzzi, C. (1996). Effect of cationic liposome composition on in vitro cytotoxicity and protective effect on carried DNA. *International Journal of Pharmaceutics, 139*(1–2), 69-78.

Cowell, R. M., and Russell, J. W. (2004). Nitrosative injury and antioxidant therapy in the management of diabetic neuropathy. *Journal of Investigative Medicine,* 52(1), 33-44.

Cutler, R. G. (2005). Oxidative stress profiling: part I. Its potential importance in the optimization of human health. *Annals of the New York Academy of Sciences, 1055*, 93-135.

De Mattia, G., Laurenti, O., Bravi, C., Ghiselli, A., Iuliano, L., and Balsano, F. (1994). Effect of aldose reductase inhibition on glutathione redox status in erythrocytes of diabetic patients. *Metabolism,* 43(8), 965-968.

Doktorovova, S., Santos, D. L., Costa, I., Andreani, T., Souto, E. B., and Silva, A. M. (2014). Cationic solid lipid nanoparticles interfere with the activity of antioxidant enzymes in hepatocellular carcinoma cells. *International Journal of Pharmaceutics,* 471(1-2), 18-27.

Fangueiro, J. F., Andreani, T., Egea, M. A., Garcia, M. L., Souto, S. B., Silva, A. M., and Souto, E. B. (2014a). Design of cationic lipid nanoparticles for ocular delivery: development, characterization and cytotoxicity. *International Journal of Pharmaceutics,* 461(1-2), 64-73.

Fangueiro, J. F., Andreani, T., Fernandes, L., Garcia, M. L., Egea, M. A., Silva, A. M., and Souto, E. B. (2014b). Physicochemical characterization of epigallocatechin gallate lipid nanoparticles (EGCG-LNs) for ocular instillation. *Colloids and Surfaces B: Biointerfaces,* 123, 452-460.

Fangueiro, J. F., Parra, A., Silva, A. M., Egea, M. A., Souto, E. B., Garcia, M. L., and Calpena, A. C. (2014c). Validation of a high performance liquid chromatography method for the stabilization of epigallocatechin gallate. *International Journal of Pharmaceutics,* 475(1-2), 181-190.

Fangueiro, J. F., Silva, A. M., Garcia, M. L., and Souto, E. B. (2014d). Current nanotechnology approaches for the treatment and management of diabetic retinopathy. *European Journal of Pharmaceutics and Biopharmaceutics*. doi: 10.1016/j.ejpb.2014.12.023

Farabegoli, F., Barbi, C., Lambertini, E., and Piva, R. (2007). (-)-Epigallocatechin-3-gallate downregulates estrogen receptor alpha function in MCF-7 breast carcinoma cells. *Cancer Detection and Prevention,* 31(6), 499-504.

Farabegoli, F., Papi, A., and Orlandi, M. (2011). (-)-Epigallocatechin-3-gallate down-regulates EGFR, MMP-2, MMP-9 and EMMPRIN and inhibits the invasion of MCF-7 tamoxifen-resistant cells. *Bioscience Reports,* 31(2), 99-108.

Filomeni, G., Rotilio, G., and Ciriolo, M. R. (2002). Cell signalling and the glutathione redox system. *Biochemical Pharmacology,* 64(5-6), 1057-1064.
Gopalakrishna, R., and Jaken, S. (2000). Protein kinase C signaling and oxidative stress. *Free Radical Biology and Medicine,* 28(9), 1349-1361.

Habig, W. H., Pabst, M. J., and Jakoby, W. B. (1974). Glutathione S-transferases. The first enzymatic step in mercapturic acid formation. *Journal of Biological Chemistry,* 249(22), 7130-7139.

Hatcher, H. C., Singh, R. N., Torti, F. M., and Torti, S. V. (2009). Synthetic and natural iron chelators: therapeutic potential and clinical use. *Future Medicinal Chemistry,* 1(9), 1643-1670.

Hayes, J. D., Flanagan, J. U., and Jowsey, I. R. (2005). Glutathione transferases. *The Annual Review of Pharmacology and Toxicology,* 45, 51-88.

Hsu, Y. C., and Liou, Y. M. (2011). The anti-cancer effects of (-)-epigallocatechin-3-gallate on the signaling pathways associated with membrane receptors in MCF-7 cells. *Journal of Cell Physiology,* 226(10), 2721-2730.

Kern, T. S. (2007). Contributions of inflammatory processes to the development of the early stages of diabetic retinopathy. *Experimental Diabetes Research,* 95103.

Kim, H. S., Montana, V., Jang, H. J., Parpura, V., and Kim, J. A. (2013). Epigallocatechin gallate (EGCG) stimulates autophagy in vascular endothelial cells: a potential role for reducing lipid accumulation. *Journal of Biological Chemistry,* 288(31), 22693-22705.

Kim, J. A., Formoso, G., Li, Y., Potenza, M. A., Marasciulo, F. L., Montagnani, M., and Quon, M. J. (2007). Epigallocatechin gallate, a green tea polyphenol, mediates NO-dependent vasodilation using signaling pathways in vascular endothelium requiring reactive oxygen species and Fyn. *Journal of Biological Chemistry,* 282(18), 13736-13745.

Kowluru, R. A., and Chan, P. S. (2007). Oxidative stress and diabetic retinopathy. *Experimental Diabetes Research,* 43603.

Kowluru, R. A., and Mishra, M. (2015). Oxidative Stress, Mitochondrial Damage and Diabetic Retinopathy. *Biochimica et Biophysica Acta (BBA) - Molecular Basis of Disease*. doi: http://dx.doi.org/10.1016/j.bbadis.2015.08.001

Kumazoe, M., Sugihara, K., Tsukamoto, S., Huang, Y., Tsurudome, Y., Suzuki, T., Tachibana, H. (2013). 67-kDa laminin receptor increases cGMP to induce cancer-selective apoptosis. *Journal of Clinical Investigation,* 123(2), 787-799.

Kusumoto, K.-i., and Ishikawa, T. (2010). Didodecyldimethylammonium bromide (DDAB) induces caspase-mediated apoptosis in human leukemia HL-60 cells. *Journal of Controlled Release,* 147(2), 246-252.

Lee, J.-C., Chung, L.-C., Chen, Y.-J., Feng, T.-H., Chen, W.-T., and Juang, H.-H. (2015a). Upregulation of B-cell translocation gene 2 by epigallocatechin-3-gallate via p38 and ERK signaling blocks cell proliferation in human oral squamous cell carcinoma cells. *Cancer Letters,* 360(2), 310-318.

Lee, J. H., Moon, J. H., Kim, S. W., Jeong, J. K., Nazim, U. M., Lee, Y. J., Park, S. Y. (2015b). EGCG-mediated autophagy flux has a neuroprotection effect via a class III histone deacetylase in primary neuron cells. *Oncotarget,* 6(12), 9701-9717.

Li, C.-P., Yao, J., Tao, Z.-F., Li, X.-M., Jiang, Q., and Yan, B. (2013). Epigallocatechin-gallate (EGCG) regulates autophagy in human retinal pigment epithelial cells: A potential role for reducing UVB light-induced retinal damage. *Biochemical and Biophysical Research Communications,* 438(4), 739-745.

Lorenzen, N., Nielsen, S. B., Yoshimura, Y., Vad, B. S., Andersen, C. B., Betzer, C., Otzen, D. E. (2014). How epigallocatechin gallate can inhibit alpha-synuclein oligomer toxicity in vitro. *Journal of Biological Chemistry,* 289(31), 21299-21310.

Marcato, P., and Durán, N. (2014). Cytotoxicity and Genotoxicity of Solid Lipid Nanoparticles. In N. Durán, S. S. Guterres and O. L. Alves (Eds.), *Nanotoxicology* (pp. 229-244): Springer New York, USA.

Michiels, C., Raes, M., Toussaint, O., and Remacle, J. (1994). Importance of SE-glutathione peroxidase, catalase, and CU/ZN-SOD for cell survival against oxidative stress. *Free Radical Biology and Medicine,* 17(3), 235-248.

Miller, A. G., Smith, D. G., Bhat, M., and Nagaraj, R. H. (2006). Glyoxalase I is critical for human retinal capillary pericyte survival under hyperglycemic conditions. *Journal of Biological Chemistry,* 281(17), 11864-11871.

Nakagawa, H., Hasumi, K., Woo, J. T., Nagai, K., and Wachi, M. (2004). Generation of hydrogen peroxide primarily contributes to the induction of Fe(II)-dependent apoptosis in Jurkat cells by (-)-epigallocatechin gallate. *Carcinogenesis,* 25(9), 1567-1574.

Nakagawa, H., Wachi, M., Woo, J. T., Kato, M., Kasai, S., Takahashi, F., Nagai, K. (2002). Fenton reaction is primarily involved in a mechanism of (-)-epigallocatechin-3-gallate to induce osteoclastic cell death. *Biochemical and Biophysical Research Communications,* 292(1), 94-101.

Nakata, K., Tsuchido, T., and Matsumura, Y. (2011). Antimicrobial cationic surfactant, cetyltrimethylammonium bromide, induces superoxide stress in Escherichia coli cells. *Journal of Applied Microbiology,* 110(2), 568-579.

Padgett, L. E., Broniowska, K. A., Hansen, P. A., Corbett, J. A., and Tse, H. M. (2013). The role of reactive oxygen species and proinflammatory cytokines in type 1 diabetes pathogenesis. *Annals of the New York Academy of Sciences,* 1281, 16-35.

Payá, M., Halliwell, B., and Hoult, J. R. S. (1992). Interactions of a series of coumarins with reactive oxygen species: Scavenging of superoxide, hypochlorous acid and hydroxyl radicals. *Biochemical Pharmacology,* 44(2), 205-214.

Peng, I.-W., and Kuo, S.-M. (2003). Flavonoid Structure Affects the Inhibition of Lipid Peroxidation in Caco-2 Intestinal Cells at Physiological Concentrations. *The Journal of Nutrition,* 133(7), 2184-2187.

Pinnaduwage, P., Schmitt, L., and Huang, L. (1989). Use of a quaternary ammonium detergent in liposome mediated DNA transfection of mouse L-cells. *Biochimica et Biophysica Acta (BBA),* 985(1), 33-37.

Piyaviriyakul, S., Shimizu, K., Asakawa, T., Kan, T., Siripong, P., and Oku, N. (2011). Anti-angiogenic activity and intracellular distribution of epigallocatechin-3-gallate analogs. *Biological & Pharmaceutical Bulletin,* 34(3), 396-400.

Pizzimenti, S., Ciamporcero, E., Daga, M., Pettazzoni, P., Arcaro, A., Cetrangolo, G., Barrera, G. (2013). Interaction of aldehydes derived from lipid peroxidation and membrane proteins. *Frontiers in physiology,* 4, 242.

Ranzato, E., Magnelli, V., Martinotti, S., Waheed, Z., Cain, S. M., Snutch, T. P., Burlando, B. (2014). Epigallocatechin-3-gallate elicits Ca^{2+} spike in MCF-7 breast cancer cells: Essential role of Cav3.2 channels. *Cell Calcium,* 56(4), 285-295.

Rechtman, E., Harris, A., Garzozi, H. J., and Ciulla, T. A. (2007). Pharmacologic therapies for diabetic retinopathy and diabetic macular edema. *Clinical Ophthalmology,* 1(4), 383-391.

Romeo, G., Liu, W. H., Asnaghi, V., Kern, T. S., and Lorenzi, M. (2002). Activation of nuclear factor-kappaB induced by diabetes and high glucose regulates a proapoptotic program in retinal pericytes. *Diabetes,* 51(7), 2241-2248.

Saffari, Y., and Sadrzadeh, S. M. H. (2004). Green tea metabolite EGCG protects membranes against oxidative damage in vitro. *Life Sciences,* 74(12), 1513-1518.

Saldanha, S. N., Kala, R., and Tollefsbol, T. O. (2014). Molecular mechanisms for inhibition of colon cancer cells by combined epigenetic-modulating epigallocatechin gallate and sodium butyrate. *Experimental Cell Research,* 324(1), 40-53.

Sampat, K. M., and Garg, S. J. (2010). Complications of intravitreal injections. *Current Opinion on Ophthalmology,* 21(3), 178-183.

Schachter, D. (2013). *The source of toxicity in CTAB and CTAB-stabilized gold nanorods.* Rutgers, The State University of New Jersey, Graduate School - New Brunswick Electronic Theses and Dissertations.

Sedlak, J., and Lindsay, R. H. (1968). Estimation of total, protein-bound, and nonprotein sulfhydryl groups in tissue with Ellman's reagent. *Analytical Biochemistry,* 25(1), 192-205.

Shah, C. A. (2008). Diabetic retinopathy: A comprehensive review. *Indian Journal of Medical Sciences,* 62(12), 500-519.

Shan, X., Li, Y., Meng, X., Wang, P., Jiang, P., and Feng, Q. (2014). Curcumin and (−)-epigallocatechin-3-gallate attenuate acrylamide-induced proliferation in HepG2 cells. *Food and Chemical Toxicology,* 66, 194-202.

Song, S., Huang, Y.-W., Tian, Y., Wang, X.-J., and Sheng, J. (2014). Mechanism of action of (–)-epigallocatechin-3-gallate: auto-oxidation-dependent activation of extracellular signal-regulated kinase 1/2 in Jurkat cells. *Chinese Journal of Natural Medicines,* 12(9), 654-662.

Squier, T. C. (2001). Oxidative stress and protein aggregation during biological aging. *Experimental Gerontology,* 36(9), 1539-1550.

Stitt, A. W., Curtis, T. M., Chen, M., Medina, R. J., McKay, G. J., Jenkins, A., Lois, N. (2015). The progress in understanding and treatment of diabetic retinopathy. *Progress in Retinal and Eye Research*. doi: http://dx.doi.org/10.1016/j.preteyeres.2015.08.001

Suzuki, Y., Lyall, V., Biber, T. U., and Ford, G. D. (1990). A modified technique for the measurement of sulfhydryl groups oxidized by reactive oxygen intermediates. *Free Radical Biology* and *Medicine,* 9(6), 479-484.

Tabatt, K., Sameti, M., Olbrich, C., Müller, R. H., and Lehr, C.-M. (2004). Effect of cationic lipid and matrix lipid composition on solid lipid nanoparticle-mediated gene transfer. *European Journal of Pharmaceutics and Biopharmaceutics,* 57(2), 155-162.

Valenti, D., de Bari, L., Manente, G. A., Rossi, L., Mutti, L., Moro, L., and Vacca, R. A. (2013a). Negative modulation of mitochondrial oxidative phosphorylation by epigallocatechin-3 gallate leads to growth arrest and apoptosis in human malignant pleural mesothelioma cells. *Biochimica* et *Biophysica Acta (BBA),* 1832(12), 2085-2096.

Valenti, D., De Rasmo, D., Signorile, A., Rossi, L., de Bari, L., Scala, I., Vacca, R. A. (2013b). Epigallocatechin-3-gallate prevents oxidative phosphorylation deficit and

promotes mitochondrial biogenesis in human cells from subjects with Down's syndrome. *Biochimica* et *Biophysica Acta (BBA),* 1832(4), 542-552.

Vandhana, S., Coral, K., Jayanthi, U., Deepa, P. R., and Krishnakumar, S. (2013). Biochemical changes accompanying apoptotic cell death in retinoblastoma cancer cells treated with lipogenic enzyme inhibitors. *Biochimica* et *Biophysica Acta (BBA),* 1831(9), 1458-1466.

Vandhana, S., Lakshmi, T. S., Indra, D., Deepa, P. R., and Krishnakumar, S. (2012). Microarray analysis and biochemical correlations of oxidative stress responsive genes in retinoblastoma. *Current Eye Research,* 37(9), 830-841.

Wang, M., Zhang, X., Zhong, Y. J., Perera, N., and Shahidi, F. (2016). Antiglycation activity of lipophilized epigallocatechin gallate (EGCG) derivatives. *Food Chemistry,* 190, 1022-1026.

Wang, X., Wu, Z., Song, G., Wang, H., Long, M., and Cai, S. (1999). Effects of oxidative damage of membrane protein thiol groups on erythrocyte membrane viscoelasticities. *Clinical Hemorheology and Microcirculation,* 21(2), 137-146.

Weisburg, J. H., Weissman, D. B., Sedaghat, T., and Babich, H. (2004). In vitro cytotoxicity of epigallocatechin gallate and tea extracts to cancerous and normal cells from the human oral cavity. *Basic* & *Clinical Pharmacology* & *Toxicology*, 95(4), 191-200.

Weydert, C. J., and Cullen, J. J. (2010). Measurement of superoxide dismutase, catalase and glutathione peroxidase in cultured cells and tissue. *Nature Protocols,* 5(1), 51-66.

Wolfram, S. (2007). Effects of green tea and EGCG on cardiovascular and metabolic health. *Journal of the American College of Nutrition,* 26(4), 373s-388s.

Wolfram, S., Raederstorff, D., Preller, M., Wang, Y., Teixeira, S. R., Riegger, C., and Weber, P. (2006). Epigallocatechin gallate supplementation alleviates diabetes in rodents. *Jounral of Nutrition,* 136(10), 2512-2518.

Wu, C.-H., Yeh, C.-T., and Yen, G.-C. (2010). Epigallocatechin gallate (EGCG) binds to low-density lipoproteins (LDL) and protects them from oxidation and glycation under high-glucose conditions mimicking diabetes. *Food Chemistry,* 121(3), 639-644.

Wu, C. H., Lin, J. A., Hsieh, W. C., and Yen, G. C. (2009). Low-density-lipoprotein (LDL)-bound flavonoids increase the resistance of LDL to oxidation and glycation under pathophysiological concentrations of glucose in vitro. *Journal of Agricultural and Food Chemistry,* 57(11), 5058-5064.

Yajima, D., Motani, H., Hayakawa, M., Sato, Y., Sato, K., and Iwase, H. (2009). The relationship between cell membrane damage and lipid peroxidation under the condition of

hypoxia-reoxygenation: analysis of the mechanism using antioxidants and electron transport inhibitors. *Cell Biochemistry & Function*, 27(6), 338-343.

Yamakawa, S., Asai, T., Uchida, T., Matsukawa, M., Akizawa, T., and Oku, N. (2004). (-)-Epigallocatechin gallate inhibits membrane-type 1 matrix metalloproteinase, MT1-MMP, and tumor angiogenesis. *Cancer Letters*, 210(1), 47-55.

Yamauchi, R., Sasaki, K., and Yoshida, K. (2009). Identification of epigallocatechin-3-gallate in green tea polyphenols as a potent inducer of p53-dependent apoptosis in the human lung cancer cell line A549. *Toxicology In Vitro*, 23(5), 834-839.

Yang, D., Elner, S. G., Bian, Z. M., Till, G. O., Petty, H. R., and Elner, V. M. (2007). Pro-inflammatory cytokines increase reactive oxygen species through mitochondria and NADPH oxidase in cultured RPE cells. *Experimental Eye Research*, 85(4), 462-472.

Zhang, Y., Yang, N. D., Zhou, F., Shen, T., Duan, T., Zhou, J., Shen, H. M. (2012). (-)-Epigallocatechin-3-gallate induces non-apoptotic cell death in human cancer cells via ROS-mediated lysosomal membrane permeabilization. *PLoS One*, 7(10), e46749.

Zhong, Y., Ma, C.-M., and Shahidi, F. (2012). Antioxidant and antiviral activities of lipophilic epigallocatechin gallate (EGCG) derivatives. *Journal of Functional Foods*, 4(1), 87-93.

CHAPTER 6- General Conclusions

CHAPTER 6 - General Conclusions

LNs emerged in the last decades as innovative and versatile drug delivery systems due to the many advantages they show relatively to other traditional therapies. Their physiological nature due to the composition based on solid lipids is a key point and the lipid matrix allows the delivery of many problematic drugs, such as peptides and proteins, and poorly water-soluble drugs. The constant research of these delivery systems improves the knowledge about their physicochemistry and also their biopharmaceutical profile. The ocular drug delivery still is a main challenge and the use of LNs could overcome some of the physiological and anatomic protective mechanisms in the eye allowing the delivery of drugs into the inner eye.

In the present research, was carried out the development and assessment of physicochemical and biopharmaceutical parameters of LNs developed for ocular delivery. The main goal was to treat and manage the main ocular consequence of diabetes mellitus, DR, which compromises patient´s quality of life and can lead to blindness. The multifactorial nature of the disease is evident, and thus its treatment remains a clinical challenge. The traditional and current strategies for the treatment and management of DR need to be improved and the development of new drug delivery systems seems to be a future alternative. Additionally, these nanocarriers could be rationale alternative to invasive, high-risk and painful treatments that have been applied for the management of DR.

The first stage of this research reported the development and characterization of LNs based on a multiple emulsion for ocular delivery. The results provide the best formulation based on the suitable Z-Ave, PI and ZP for ocular delivery and with the adequate safety. The formulation selected for further studies was composed by 4.5 wt% of Softisan®100, 0.5 wt% of CTAB, 0.5 wt % of Lipoid®S75, 37.5 wt % of glycerol and 1.0 wt % of Poloxamer 188. The cationic nature of LNs is used as a strategy to increase bioadhesion and thus, drug residence time in the ocular surface.

Secondly, the encapsulation of EGCG requires a previous stabilization of this drug in LNs and also in biological medium. Thus, the stabilization of EGCG was achieved in a

medium composed by ethanol (24 %, v/v), transcutol®P (20 %, v/v) and 0.25%, w/v) ascorbic acid solution. The use of ascorbic acid as reducing agent was essential to promote EGCG stability and avoids its auto-oxidation, as also the pH depend was detected, highest pH leads to higher degradation of EGCG. Additionally, two validations methods based on RP-HPLC with UV-Vis detection for different media: water and the biocompatible medium was developed.

The encapsulation of EGCG into cationic LNs was successfully obtained in the inner aqueous phase. The physicochemical parameters evaluated, such as Z-Ave, PI, ZP, DSC and X-ray studies proved that different cationic lipids provide different crystallinity profiles. DDAB shows higher crystallinity than CTAB-LN dispersions. Also, was observed a decrease in the degree of crystallinity to CTAB and an increase for DDAB, respectively. The LNs provide a prolonged drug release of EGCG, following the Boltzmann sigmoidal release profile. The *ex vivo* permeation of EGCG was achieved in the cornea and in the sclera, which could predict an absorption in the anterior and posterior segment of the eye. The corneal permeation followed a first order permeation for both formulations, while EGCG-CTAB LNs followed a Boltzmann sigmoidal profile and EGCG-DDAB-LNs a first order profile. The *in vitro* HET-CAM and *in vivo* Draize test studies classified both formulations as safe and non-irritant. The results obtained from this study evidence the possibility of cationic lipid based systems for EGCG ocular drug delivery, making these nanoparticles a promising approach to avoid drug stability problems, providing higher drug residence time, higher drug absorption and consequently higher bioavailability.

The last studies suggest that cationic LNs developed interfere with cellular enzymatic defense against oxidative stress being responsible for the enhanced oxidized proteins and lipids to LNs and EGCG exposure, with exception for DDAB-LNs. The DDAB-LNs which are composed of the most safe cationic lipid and without EGCG seems to have a powerful capacity of enzymatic protection regarding the cell viability, antioxidant enzymatic activity and protection against lipids and proteins oxidation. This could be associated with the chelating effect of EGCG with the enzymatic co-factors of the enzymes and these dispersions being composed by the safest cationic lipid, leading to a lower availability of the drug for exercising their proven antioxidant effects.

Despite the observed interference with the cell viability, antioxidant enzymatic activity with consequent proteins and lipids oxidation and formation of ROS indicating oxidative stress, our study provide valuable information and data in using the developed cationic loaded EGCG LNs and EGCG for the clinical treatment and management of DR.